# The derivation of bioprocess understanding from mechanistic models of chromatography

**A thesis submitted to University College London for the degree of DOCTOR OF ENGINEERING**

**by**

**Edward James Close**

**April 2015**

The Advanced Centre for Biochemical Engineering
Department of Biochemical Engineering
University College London
Torrington Place, London, WC1E 7JE, UK

I, Edward Close confirm that the work presented in this thesis is my own. Where information has been derived from other sources, I confirm that this has been indicated in the thesis.

---

# Abstract

This thesis, completed in collaboration with Purification Process Development of Pfizer Biotherapeutics, is concerned with how mechanistic models of chromatographic bioseparations can be applied in industry to accelerate development and increase robustness of industrial protein purification processes, whilst also realising the benefits of a systematic development approach based on fundamental process and product understanding.

The first results chapter considers the application of mechanistic models to provide a link between high throughput screening (HTS) and scouting runs conducted during early process development. The chapter focuses on an anion exchange (AEX) weak partitioning chromatography (WPC) polishing step in a platform monoclonal antibody purification process. Adsorption isotherms are formulated from experimental multicomponent batch adsorption studies of monomer – aggregate. A new approach is taken where the adsorption equilibria is characterised as a function of the product partition coefficient, enabling the model to be applied to new candidate monoclonal antibodies without additional experimental effort. Stochastic simulations conducted at an early stage of process development identify promising operating parameter ranges for challenging separations, directs optimal performance, and reduces development times. A detailed analysis of model predictions increases fundamental knowledge and understanding of the complex WPC multidimensional design space, which enables better informed process development at Pfizer.

Resin fouling over a chromatography columns lifetime can cause significant (undesired) changes in process performance. A lack of fundamental knowledge and mechanistic understanding of fouling in industrial bioseparations limits the application of mechanistic models in industry. An experimental investigation was conducted into fouling of the AEX WPC considered in the first results chapter. Analysis of fouled resin samples by batch uptake experiments, scanning electron microscopy, confocal laser scanning microscopy and scale down column studies, indicated significant blockage of the pores at the resin surface occurred that after successive batch cycles. Mass transport into resin particles was severely hindered, but saturation capacity was not affected. The increased understanding of resin fouling can direct future efforts to mitigate this detrimental phenomenon and maintain process performance, whilst providing a basis for the development of new fouling models.

The third results chapter considers an industrial hydrophobic interaction chromatography (HIC) separation at a late stage of process development. Resin lot variability, combined with

a variable feed stream, had resulted in serious performance issues during the purification of a therapeutic protein from crude feed material. The traditional approach to tackling this type of problem involves defining a design space based on an extensive experimental effort directed by factorial design of experiments conducted at great cost. The result is a fixed, inflexible manufacturing process, with a control strategy based on reproducibility rather than robustness, and little fundamental understanding of the source of the issue. In the third results chapter, the application of mechanistic models to identify robust operating conditions for the HIC is considered. A model is developed, validated experimentally, and used to generate probabilistic design spaces accounting the historical variability in the resin lots and load material. The stochastic simulation approach is extended to explore the impact of reducing variability in the load material on the design space. With historical process variability, no operating condition was found where the probability of meeting product quality specifications remained > 0.95 for all resin lots. Model simulations indicated that adopting an adaptive design space, where operating conditions are changed according to which resin lot is in use, is favorable for ensuring process robustness, which is a step change concept for bioprocessing.

The conclusions and outcomes resulting from the application of mechanistic models to the two industrial systems in this thesis, provides a basis for the next generation purification process development platform.

# Acknowledgement

I feel exceptionally fortunate to have had the privilege to undertake this Engineering Doctorate. What strikes me most is the kindness and support I have received from those I have met with along the way. This will stay with me always. I am forever grateful to those who were there for me when times were tough.

This project would not have been possible without the support from Pfizer, and the support from the Engineering and the Physical Sciences Research Council (EPSRC) under the Innovative Manufacturing Research Initiative. I would like to express my sincere thanks to both of these organisations for co-funding this Engineering Doctorate.

My deepest gratitude goes to my supervisors, Eva, Dan and Jeff.

It is impossible to describe to just how positive an impact Eva has had on my life since I joined University College London in 2006. She was responsible for first igniting my interest in process modelling during my undergraduate studies, and I have not looked back since. Her endless endurance, strength of conviction, personal touch, willingness to listen, generosity with her time, and her maddening attention to detail sets her apart from all others, and I am incredibly grateful for everything she has done and taught me over the years.

Dan has been the rock on which I have built this Engineering Doctorate. His hands-off approach has allowed me to flourish, whilst his timely intervention at key moments kept me from straying too far from the path to the finish line. He has the rare ability to see the larger picture whilst also being perfectly comfortable drilling down into the fundamentals. His support and confidence in me throughout my EngD has been instrumental to its success, and I am truly thankful for his contribution over the last 5 years.

When I started I had little appreciation for how important Jeff would become as my industrial supervisor. His generosity with his time and attention, whilst also balancing his responsibilities at Pfizer and supporting a growing young family was truly outstanding. I am forever grateful for his integrity and intellect whilst supporting me during my time at Pfizer. This EngD would not have been possible without his scientific insight and constant encouragement to consider multiple perspectives. I would not have gained the same appreciation for the practicalities of industry without his guidance, and I am forever thankful to him for all he has done for me.

I feel privileged to have been part of Purification Process Development at Pfizer, and to have had the opportunity to work and get to know so many marvellous people there. Thank you to all those who made my time in Andover so enjoyable. I am hugely grateful to Andy, Aaron, Victoria, Chris and Jenna for their training and support in the lab. In particular, I would like to thank Tim for his substantial contribution to my project in terms of material, equipment, experimental procedures and help with my first paper. Last but certainly not least, I must single out Mary for my most heartfelt thanks, not only for helping with lifts when the days grew short and the snow started to fall, but for her contribution to my work on weak partitioning chromatography, and her trust, support, advice and encouragement throughout the year. Her generosity and spirit will stay with me forever.

I am indebted to Process Systems Enterprise Ltd for their support ensuring I had access to gPROMS whist at Pfizer. Thank you also to Costas for several discussions which helped to focus my thoughts on stochastic simulation and process design spaces.

The last 5 years would not have been the same without my friends and colleagues in London. Thank you so much to all past and present members of the Chemical and Biochemical Engineering departments at UCL for making it such a rewarding experience. In particular, thank you Eddie, Bettsy, Thwaites, Roumaz, Banio, Iwan, Kristina, Udo, Leanne, Heather and Yvonne for being such a great EngD cohort. Special thanks must go to Jay, Toby and Stevie for their companionship over the years through all our adventures. Thanks for staying calm in the face of fire, for the shoulder to lean on, and for the sofa to sleep on when times were tough. To Mithila, thank you for always being there for me no matter the problem, whatever the hour. To Cyrus, thank you for all the laughs over the years, and for being there through everything. And thanks to James for making the misery of the daily commute in Andover bearable. You drove me so crazy with endless banter at work that I completely forgot about all other problems. It wouldn’t have been the same without you.

Lastly, my warmest and deepest thanks must go to my family. My dearest Yvonne, Mum and Dad, Dave and Amy, Pete, Tom, Martin and Sarah, Grannie and Granddad Hoskins, Grannie Mollie and Granddad Clive. Your example gave me the strength and motivation to get through whatever life threw at me. This Engineering Doctorate is testament to your love, support and faith. More than anything else, it was the strength and character of our family that got me through, and I couldn't have done it without you. My deepest gratitude and love to you all.

# Table of Contents

# Table of Figures

# List of Tables

# List of abbreviations

| | |
|---|---|
| AEX | Anion exchange chromatography |
| B/E | Bind and elute chromatography |
| BSA | Bovine serum albumin |
| CEX | Cation exchange chromatography |
| cGMP | Current good manufacturing practice |
| CHO | Chinese hamster ovary |
| CLSM | Confocal laser scanning microscopy |
| CQA | Critical quality attribute |
| CV | Column volume |
| DBC | Dynamic binding capacity |
| DOE | Design of experiments |
| DSP | Downstream processing |
| FDA | US Food and Drugs Administration |
| FT | Flowthrough |
| FTIR | Fourier transform infrared spectroscopy |
| HCP | Host cell protein |
| HIC | Hydrophobic interaction chromatography |
| HTS | High throughput screening |
| HMMS | High molecular mass species |
| HPLC | High performance liquid chromatography |
| IQR | Interquartile range |
| MAB | Monoclonal antibody |
| MW | Molecular weight |
| pI | Isoelectric point |
| PPD | Purification process development |
| QBD | Qualty by design |
| RSM | Response surface model |
| RP | Reverse phase |
| SEC | Size exclusion chromatography |
| SEM | Scanning electron microscopy |
| SMA | Steric mass action isotherm |
| USD | Ultra scale down |
| UV | Ultra violet |
| WPC | Weak partitioning chromatography |

# List of notation

| | |
|---|---|
| $a$ | Adsorption constant [-] |
| $b$ | Adsorption constant [-] |
| c | Adsorption constant [-] |
| d | Adsorption constant [-] |
| $C_0$ | Load concentration [mg/ml] |
| $C^m$ | Extra particular mobile phase concentration [mg/ml] |
| $C^{sp}$ | Stationary phase concentration [mg/ml] |
| $C_i^p$ | Intra particular mobile phase concentration [mg/m] |
| $C_{equil}$ | Concentration of the equilibration supernatant [mg/ml] |
| $C_{elution}$ | Concentration of the elution supernatant [mg/ml] |
| $C_{salt}$ | Concentration of salt in the mobile phase [mM] |
| $CF$ | Compression factor [-] |
| $D_A$ | Apparent axial dispersion coefficient [$cm^2/s$] |
| $D_{ax}$ | Axial dispersion coefficient [$cm^2/s$] |
| $D_m$ | Molecular diffusivity in the intra particular mobile phase [cm/s] |
| $D_{mol}$ | Molecular coefficient [-] |
| $d_m$ | Molecular diameter [cm] |
| $d_p$ | Particle macropore diameter [cm] |
| $F$ | Mobile phase flowrate [ml/s] |
| $i$ | Component identifier [-] |
| $k_a$ | Equilibrium constant [-] |
| $k'$ | Salt capacity factor [-] |
| $k$ | Film mass transfer coefficient [cm/s] |
| $K_{SMA}$ | SMA equilibrium constant [-] |
| $K_p$ | Product partition coefficient [-] |
| $L$ | Column length [cm] |
| $MW$ | Molecular weight [kg/mol] |
| $M_t$ | Total amount of protein added to the micro well (mg) |
| $N_C$ | Number of components [-] |
| $N_p$ | Number of theoretical plates [-] |
| $P_i^{load}$ | Component i percentage in load material [-] |
| $P_i^m$ | Component i percentage in equilibration supernatant [-] |
| $P_i^{elution}$ | Component i percentage in elution peak [-] |

| | |
|---|---|
| $q_s$ | Saturation capacity [mg/ml] |
| $q$ | Concentration per unit volume settled resin [mg/ml] |
| $r$ | Radial coordinate [cm] |
| $R_p$ | Particle radius [cm] |
| $Re$ | Reynolds number [-] |
| $t_0$ | Retention time [1/s] |
| $t$ | Time [s] |
| $T$ | Column temperature [K] |
| $u$ | Interstitial velocity [cm/s] |
| $V_{elution}$ | Volume of the equilibration supernatant [ml] |
| $V_{equil}$ | Volume of the elution supernatant [ml] |
| $V_{resin}$ | Settled resin volume in microwell [ml] |
| $V_{tot}$ | Total volume of liquid dispensed into each well [ul] |
| $V_0$ | Column void volume [ml] |
| $V_C$ | Column volume [ml] |
| $w_{0.5}$ | Peak width at half peak height [-] |
| $z$ | Axial coordinate [cm] |

| | |
|---|---|
| $\alpha$ | Adsorption constant [-] |
| $\beta$ | Adsorption constant [-] |
| $\gamma$ | Adsorption constant [-] |
| $\epsilon_T$ | Total column porosity [-] |
| $\varepsilon_b$ | Bed porosity [-] |
| $\varepsilon_p$ | Particle porosity [-] |
| $\eta$ | Kinematic viscosity [Pa.s] |
| $\Lambda$ | Total ionic capacity of the stationary phase [mM] |
| $\upsilon$ | Steric factor [-] |
| $v$ | Superficial velocity [cm/s] |
| $\sigma$ | Steric factor [-] |
| $\tau_{tor}$ | Resin tortuosity [-] |

# List of publications

***Original research papers***

Close, EJ, Salm, JR, Iskra, T, Sørensen E, Bracewell, DG, 2013, Fouling of an anion exchange chromatography operation in a monoclonal antibody process: Visualization and kinetic studies, Biotechnology and Bioengineering, 110: 2425 – 2435. (Relates to chapter 4)

Close, EJ, Salm, JR, T, Sørensen E, Bracewell, DG, 2013, Modelling of industrial biopharmaceutical multicomponent chromatography, Chemical Engineering Research and Design, 92: 1304 – 1314. (Relates to chapter 5)

Close, EJ, Salm, JR, T, Sørensen E, Bracewell, DG, 2014, A model based approach for identifying robust operating conditions for industrial chromatography with process variability, Chemical Engineering Science, 116: 284 – 295. (Relates to chapter 5)

***Conference presentations***

Close, E, Salm, J, Iskra, T, Sørensen, E, Bracewell, DG, 2011, Characterizing the fouling of an industrial anion exchange polishing step during the manufacturing process of a commercial therapeutic protein. 2011 AIChE Annual Meeting. Minneapolis, MN, USA. (Relates to chapter 4)

Close, E, Salm, J, Bracewell, DG, Sørensen, E. 2011, Modelling an industrial hydrophobic interaction chromatography step from a quality by design (QbD) perspective. 2011 AIChE Annual Meeting. Minneapolis, MN, USA. (Relates to chapter 5)

Close, E, Salm, J, Bracewell, DG, Sørensen, E. 2012, Mechanistic modelling of an industrial hydrophobic interaction chromatography column, from a Quality by Design (QbD) perspective, European Symposium on Computer Aided Process Engineering, 2012. (Relates to chapter 5)

Close, E, Jin, J, Salm, J, Sorensen, E, Bracewell, DG, 2012, Understanding chromatography fouling in therapeutic protein manufacture, 8th Annual Protein and Antibody Engineering Summit (PEGS), Boston, USA. (Relates to chapter 4)

Close, E, Salm, J, Sørensen, E, Bracewell, DG. 2012, Understanding chromatography fouling in therapeutic protein manufacture, IChemE Fluid Separations Special Interest Group Research Event, Basingstoke, UK. (Relates to chapter 4)

Close, E, Salm, J, Bracewell, DG, Sørensen, E. 2013, A model based approach to an adaptive design space in chromatography, European Congress on Chemical Engineering 2013. (Relates to chapter 5)

Close, E, Salm, J, Bracewell, DG, Sørensen, E. 2013, Adaptive design space in chromatography, 246th American Chemical Society Annual Meeting, division of biochemical technology, New Orleans. (Relates to chapter 5)

Close, E, Salm, J, Bracewell, DG, Sørensen, E. Design space: modelling an industrial chromatographic bioseparation in the face of process variability, Process Systems Enterprise Advanced Process Modelling Forum, 2013. (Relates to chapter 5)

Close, E, Salm, J, Bracewell, DG, Sørensen, E. Accounting for process uncertainty in industrial chromatographic separations using probabilistic design spaces, IChemE Fluid Separations Special Interest Group Research Event: "What's New in Fluid Separations", 2013. (Relates to chapter 3)

Close, E, Salm, J, Bracewell, DG, Sørensen, E. Design Space: Modelling chromatographic bioseparation in the face of process variability, Process Systems Enterprise Webinar, 2013. (Relates to chapter 5)

Close, E, Salm, J, Sørensen, E, Bracewell, DG. A Minimalist Approach to Mechanistic Modeling of Chromatography for Intermediate Purification and Polishing Steps. 247th American Chemical Society Annual Meeting, Division of Biochemical Technology, Dallas. (Relates to chapter 3)

# Chapter 1. Introduction

*Therapeutic proteins are well established as a clinically and commercially important class of therapeutics. The key consideration when bringing a product to market remains the need to launch as early as possible. There is also increasing desire in industry to move to a more systematic approach to bioprocess development and operation based on fundamental process and product understanding. Innovation and engineering approaches based on first principles modelling have been proven in a variety of processing industries (e.g. refining, oil and gas, chemicals, energy). However, mechanistic models derived from first principles are seldom utilized in the biopharmaceutical sector. There remains a need to determine how to apply mechanistic models in industry, where production of a product of consistent quality in amounts satisfying demand remains the primary concern of bioprocess engineers, rather than traditional processing objectives. This engineering doctorate thesis, completed in collaboration with Purification Process Development of Pfizer Biotherapeutics, is concerned with how mechanistic models of chromatographic bioseparations can be applied in industry to accelerate development and increase robustness of bioseparations, whilst realising benefits of an approach based on fundamental process and product understanding.*

## 1.1. Recombinant proteins market considerations

Proteins are now used in a broad range of important clinical applications (Waldmann, 2003, Descotes and Gouraud, 2008), and are recognised as a commercially important class of therapeutics. Annual revenues for 2012 estimated to total in excess of $50 billion of the $600billion global pharmaceutical market (Walsh, 2010). Increasing incidence of many diseases due to aging populations, rising living standards and fast developing geographical markets (China and India have estimated markets approaching $10 and $2 billion, respectively) have provided strong drivers for this growth, which is predicted to continue in the future (Walsh, 2010). This is evident in industry with several hundred clinical candidate proteins currently estimated in company pipelines (Kelley, 2009), of which many serve significant unmet medical needs (Shukla et al., 2007).

Until recently, the biopharmaceutical industry has relied primarily on blockbuster drug products such as Infliximab and Etanercept (Khanna, 2012). These are drugs with annual revenues in excess of $1billion which are highly desirable for companies as they provide consistent high revenues over long periods of time (>10 years). The desire to bring new blockbuster drugs to market remains strong. However, although there are numerous candidate biopharmaceuticals in development, few are predicted to reach blockbuster status as many target rare or orphan indications (Walsh, 2010). In addition, many first generation drugs have now reached or are reaching the end of patent protection, and their market value renders them attractive targets for biosimilars. This brings challenges for industry, both for companies trying to break into established markets, and for primary innovators protecting their investment in off patent products.

Traditionally, the key considerations when bringing a newly discovered molecule to market have been: (i) the need to launch as early as possible in order to maximise the period of patent protection (which lasts 20 years), and (ii) the need to get the product first to market when companies are launching similar products, since this often results in better recognition from customers and increased sales. Both are significant challenges as development is typically long and costly. The average time to market is 10 years at a cost of $1billion (Di Masi et al., 2003, Di Masi and Grabowski, 2007). There is a high risk of clinical failure (82% of newly discovered molecules are estimated to fail). New drugs must follow strict regulatory pressures, and biopharmaceutical manufacturing processes are inherently complex. In addition, the increasing prevalence of biosimilars means that manufacturing efficiency and the reduction of cost are becoming additional considerations, and companies must strive to find a competitive edge which gives them an advantage over their rivals.

## 1.2. Production of recombinant proteins

The aim of production is to consistently produce a quality product which delivers its intended performance (ICH, 2008). Protein therapeutics are typically required in amounts reaching several hundred kilograms of bulk drug substance per annum (Kelley, 2007). Consequently, compared to early biopharmaceutical products, large scale production processes are now necessary with manufacturing processes producing many tens of kilograms of product per batch (Aldington and Bonnerjea, 2007).

Although varied, therapeutic protein production processes can typically be divided into cell culture/fermentation, cell harvesting, primary recovery and purification sections, which are often grouped into the upstream processing (cell culture/fermentation) and downstream processing sections (DSP) (cell harvesting, primary recovery and purification) of the manufacturing process (Shukla and Thömmes, 2010). Each is comprised of a number of unit operations that are selected and optimised according to the product being produced.

The primary aim of cell culture and fermentation is a high productivity, low cost production of the therapeutic protein, whilst enabling a facile and inexpensive DSP (Chu and Robinson, 2001). This is achieved by a combination of cell line development and process optimisation (Wurm, 2004, Costa et al., 2010). The goal is to grow the expression system to high cell densities, thus producing a large amount of product per unit volume per unit time with minimal production of contaminants to be removed.

Material is passed from cell culture/fermentation to the primary recovery section of the manufacturing process. Here, cells and cell debris are removed from the culture broth, and cell culture supernatant that contains the product of interest is clarified for subsequent purification. Primary recovery may also involve the extraction of product from the host cell if the product is expressed intracellularly. Primary recovery is generally achieved through use of microfiltration, centrifugation, depth filtration and flocculation/precipitation (Roush and Lu, 2008).

Material is then passed to the purification section, where the objective is to achieve acceptable product purity. Other important considerations include yield/recovery, process throughput and manufacturability criteria (e.g. robustness, reliability and scalability). Membrane filtration, crystallisation and liquid extraction see some use, however, chromatographic separations are currently the dominant technology for the purification of therapeutic proteins, as their very high selectivity is well suited to separating the product

from the heterogeneous mix of impurities present in biologically derived material (Kelley, 2007).

## 1.3. Chromatography

In chromatography, a mobile phase (liquid or gas) moves through a bed of particles known as the solid or stationary phase. Species in the mobile phase are separated as they interact with the solid phase to different degrees via molecular interactions or chemical bonds. Many different configurations are available to bring the mobile phase into contact with the solid phase, including packed beds, stirred tanks and expanded beds. Radial flow packed beds and simulated moving beds are available, but most commonly the solid phase is packed into a column and the mobile phase flows along the axial dimension with material applied in batches.

### 1.3.1. **Operating modes**

Chromatographic separations can be operated in a number of different modes. The most commonly used are bind and elute mode (B/E), and flowthrough mode (FT). More recently, a third type designated weak partitioning (WPC) has been developed at Pfizer by Kelley et al. (2008). Further distinction is made between separations that occur with constant mobile phase conditions (i.e. pH, ionic strength, buffer composition) which are known as isocratic operation, or separations where the mobile phase conditions are changed during the separation either stepwise or continuously which are known as gradient elution.

The key feature of B/E mode is that the protein product is strongly bound to the solid phase and impurities flow through to waste. Each batch is divided into distinct phases, which include column equilibration (where the column mobile phase is brought to the desired conditions), column loading (where the material to be purified is applied to the column), one or more wash steps (where mobile phase buffer without protein material is applied to the column in order to push out remaining impurities), elution (where the mobile phase conditions are changed to promote desorption of any bound material for collection), sanitisation (where the column is cleaned of any remaining material) and storage (where the column is put in mobile phase which preserves the resin bed for future use).

In FT mode the opposite occurs, and the impurities are strongly bound to the solid phase, whilst the protein product flows through and is collected for further processing. The phases of FT include column equilibration, column loading, one or more wash steps, column strip

(where the mobile phase conditions are changed so that the bound impurities are eluted from the column to waste), sanitisation and storage.

In WPC, the strength of the product binding is between those observed in B/E and FT mode. Although similar to FT as impurities bind to the resin and the protein of interest flows through to be collected as product, WPC is distinct, as it is performed under mobile phase conditions where in addition to impurities a significant amount of product also binds to the resin. The more stringent binding conditions improves removal of impurities, and any loss in yield due to adsorption of the product can be restored by extending the load challenge and conducting a wash step at the end of the load phase. Typically WPC employs equilibration, load, wash, strip, sanitisation and storage phases, respectively (Kelley et al. 2008a).

### 1.3.2. **Solid phase**

The solid phase in chromatographic separations is composed of particles known as resins. Their properties are highly customisable and have important implications as summarised in Table 1.1. Resin particles are made from polymerisation of various materials (e.g. agarose, methacrylate etc), and can be porous or non-porous. Particles are often modified with the addition of specialised functional groups in order to confer additional properties such as better mechanical properties or selectivity. Functional groups that are designed to directly interact with species in the mobile phase are known as ligands.

Ligands are normally attached to the resin base matrix via covalent bonding. As molecules of interest propagate through a resin bed, the surface of the molecule interacts with the surface of the ligand, which forms the basis for separation. Many different ligands are available and can be grouped according to the type of interaction they offer as summarised in Table 1.2. This variety makes orthogonal sequences of chromatographic bioseparations possible, where species are separated according to a different type of interaction in each column, giving unmatched selectivity. The main ligands related to this work are affinity, anion exchange and hydrophobic interaction.

Table 1.1. Chromatography resin properties and their implications (Hagel et al., 2007).

| **Resin property** | **Implication** |
|---|---|
| Mechanical properties | Throughput, scale up, maximum flow rates |
| Ligand density and distribution | Binding capacity, selectivity, recovery |
| Pore size distribution | Dynamic binding capacity |
| Particle size distribution | Resolution, product recovery, impurity removal, dynamic binding capacity |
| Chemical stability | Lifetime, reusability |
| Hydrophilicity/hydrophobicity | Product recovery, cleanability |

Affinity ligands are specially designed to strongly bind to the target of interest through multiple molecular interactions giving unmatched selectivity (Fahrner et al., 1999). They are commonly utilised in the first step of chromatographic purification sequences (Ayyar et al., 2012). The chromatography is typically operated in bind and elute mode, thus, the protein of interest binds to the resin and impurities flow through to waste. The protein is released from the affinity ligand to be collected for further purification by changing the mobile phase composition (usually by lowering the pH). Affinity separations yield very pure product, however, the resins are expensive and ligand leakage and the harsh conditions used for elution can introduce additional impurities that must be removed (Pollock et al., 2013). An example of an affinity ligand is Protein A, which binds to the Fc region of monoclonal antibodies, and is used extensively throughout the biopharmaceutical industry.

Ion exchange chromatography separates molecules based on solute charge (Vermeulen et al., 1984, Yamamoto, 1988). In anion exchange chromatography, ligands are positively charged and thus bind negatively charged solutes. Conversely, in cation exchange chromatography, ligands are negatively charged and therefore bind positively charged solutes. The charge on a protein is a function of the proteins' isoelectric point (pI) and the pH of the mobile phase. At a pH below their pI, proteins carry a net positive charge. At a pH above their pI, proteins carry a net negative charge. Hence, the pH and the concentration of competing ions in the mobile phase (known as counterions) can be manipulated in order to selectively bind components in the feed material, and allow others to pass unhindered through the column. Anion exchange steps are commonly used as the second stage within chromatographic sequences, where positively charged product flows through the column unhindered, and negatively charged impurities, such as host cell proteins, nucleic acids, DNA and

endotoxins, are bound to the column (Shukla and Thömmes, 2010). Cation exchange steps are most commonly employed as polishing steps after the bulk of the purification has been completed to remove any remaining aggregated product and leached affinity ligand (Shukla and Thömmes, 2010).

Table 1.2. Types of ligand chemistries used in the purification of therapeutic proteins.

| **Type** | **Examples of ligands** | **Retention mechanism** |
|---|---|---|
| Affinity | Protein A/G<br>Glutathione<br>Heparin<br>Dye<br>Antibody<br>Recombinant protein<br>Lectin<br>Immobilised metal affinity | Biospecific interaction, cooridination complex formation |
| Anion exchange | Diethylaminoethylene (DEAE)<br>Quaternary aminoethyl (QAE)<br>Quaternary ammonium (Q) | Electrostatic interaction |
| Cation exchange | Sulfopropyl (SP)<br>Methylsulfonate (S)<br>Carboxymethyl (CM) | Electrostatic interaction |
| Hydrophobic interaction | Phenyl-<br>Butyl-<br>Octyl- | Hydrophobic complex formation |
| Hydroxyapatite | $(Ca_5(PO_4)_3OH)_2$ | Cation exchange and coordination bonds (Between $Ca^{2+}$ and carboxyl/phosphoryl groups) |
| Mixed mode | N-benzyl-N-methyl-ethanoline<br>4-mercapto-ethyl-pyridine<br>Phenylpropylamine | Hydrophobic interaction and ion exchange |
| Reversed phase | 4-carbon alkyl (C4)<br>18-carbon alkyl (C18) | Hydrophobic complex formation |
| Size exclusion | N/A (porous inert base matrix) | Size exclusion |

Hydrophobic interaction ligands contain exposed hydrophobic groups (often Butyl or phenyl groups) which interact with hydrophobic groups present on the surface of proteins. A series of publications by To and Lenhoff provide a useful introduction to hydrophobic interaction chromatography (To and Lenhoff, 2007a, 2007b, 2008). The strength of the protein – ligand interaction is a function of the salt used, and the salt concentration in the mobile phase, commonly classified according to the Hoffmeister series. A decrease in salt concentration results in an increase in the exposure of hydrophilic regions of protein molecules, which leads to solute elution based on the order of decreasing hydrophobicity. HIC is used both as an intermediate and a polishing chromatographic step. In flow through mode HIC can remove product aggregates, and in bind and elute mode both process and product related impurities can be separated from the product.

## 1.4. Purification Process Development

The development of a chromatographic bioseparation that isolates a protein of interest as part of the DSP is known as purification process development (PPD). An optimal, safe and economic purification process which consistently delivers the desired product purity and yield must be found quickly, somewhere in an extremely large parameter space (Lightfoot and Moscariello, 2004). The amount of material available to work with during process development is often limited, and the work must be completed within constricted timelines to meet time to market constraints (Steinmeyer and McCormick, 2008).

US Food and Drugs Administration (FDA) regulations require that the basic separation scheme is fixed prior to clinical trials, i.e. early on in the overall development process (ICH, 2008a, 2008b). In addition, there are further complexities that must be accounted for, such as the inherent variability in biopharmaceutical manufacturing due to the biological nature of the materials used, and the high end product purity constraints due to the sensitive therapeutic nature of the products. The purification section is also the most expensive part of the manufacturing process, and often the processing bottleneck (Kelley, 2007). Against this background, purification process development is a very challenging prospect.

The development of a chromatographic bioseparation in industry relies heavily on experienced engineers and scientists drawing from experience and heuristics to derive a skeleton process. An extensive experimental program is conducted to optimise the process which is usually conducted following a design by experiment (DOE) type approach. Process development involves experimentally testing a range of possible operating conditions using the minimal amount of time and material possible, until a combination is found which can

achieve adequate product quality. As confidence in the products clinical success grows through successful toxicology studies and clinical trials, the process is scaled up and further optimisation occurs via experimental studies conducted at laboratory and pilot scale. Final acceptance is achieved via the successful completion of three validation runs of the full sized manufacturing process (Jakobsson et al., 2005). Platform approaches, ultra scale down experimentation and statistical design of experiments are all key methodologies that are used in industry to ensure a satisfactory process is found in the limited time available for process development.

### 1.4.1. **Platform approaches**

Therapeutic proteins often have common biochemical structures, the obvious example being monoclonal antibodies which contain a fixed Fc region. This enables platform approaches, where generic purification processes are employed for similar molecules (Shukla et al., 2007, Kelley, 2007). Molecules still have different physiochemical properties. Therefore, the exact operating conditions will differ from molecule to molecule. However, the platform strategy serves as a guidance that defines the overall scheme of operations, and often provides a template for process development to use when identifying specific operating conditions.

The key advantage of a platform approach is that they greatly reduce the time and resources needed for process development (Nfor et al., 2009). Further wide ranging benefits include (i) better alignment between company business units with process development such as quality and manufacturing, where template documents can be integrated into systems to streamline communications and technology transfer, (ii) greater expertise and understanding of all parties concerned with associated benefits from extensive experience using the platform, (iii) a reduction in the number of raw materials required allows better deals can be negotiated with vendors, (iv) critical raw materials can be sourced from multiple vendors reducing organisational risk, (v) a common aligned philosophy can be adopted by multiple process development sites enabling better core focus, (vi) a site independent process can be developed that is straightforward to transfer between multiple manufacturing sites as business needs dictate, and (vii) easier planning across the entire organisation as it lays down a common set of expectations (Shukla et al., 2007). The disadvantages of using a platform approach are (i) they may hinder the long term improvement of biopharmaceutical production, as there is less desire to innovate and greater focus on utilizing the current platform for as many molecules as possible, (ii) if not guarded against, platform approaches can favour design based upon heuristic knowledge, rather than from process understanding

and fundamental knowledge, with a loss of the associated benefits, resulting in (iii) sub optimal processes, and (iv) difficulties when the platform does not perform as expected.

### 1.4.2. **Ultra scale down**

The limited availability of material and stringent time constraints during process development has given rise to ultra-scale down (USD) approaches to process characterisation (Chhatre et al., 2009, Li et al., 2012, Lau et al., 2013). Experimental data is generated with millilitre to microlitre scale devices and very small amounts of material. The data is then used to predict the performance of industrial scale unit operations (> 10 – 500 L). In addition to chromatography, USD has been successfully utilised for many different unit operations such as centrifugation and depth filtration. In chromatographic separations, the most popular USD devices are micro columns in pipette tips and micro plate technologies (Bhambure et al., 2011). However, there is a continuing effort to develop devices that require smaller volumes of material which means that new technologies continue to appear.

High throughput screening (HTS) is an approach to purification process development that makes use of USD through micro titre plates and robotic platforms (Coffman et al., 2008, Kramarczyk et al., 2008, Wensel et al., 2008, Kelley et al., 2008a). In this approach, each well in a 96 well micro titre plate represents an independent experiment. This enables a systematic exploration of many different combinations of operating conditions and processing strategies in parallel to predict trends in larger scale column performance. This approach enables unattended, rapid and automated process screening that significantly reduces material requirements and accelerates development times. Combinations and strategies that are undesirable can be quickly disregarded whilst those of interest can be taken forward to subsequent scale down column scouting runs.

### 1.4.3. **Statistical design of experiment methods**

Despite their success, significant differences still exist between USD predictions and chromatographic performance at an industrial scale. For example, USD devices by their nature have different hydrodynamic properties compared to the large scale columns they seek to predict, which results in differences in the quality of packed beds at different scales. These differences necessitate the use of qualified laboratory scale down column studies (i.e. that have been experimentally validated as representative of manufacturing scale), and the application of conventional scale up rules for final process characterisation, optimisation and validation, prior to biological license application submission. This experimental effort is

commonly conducted according to a multivariate statistical design of experiment (DOE) type approach (Ferreira et al., 2007, Dejaegher and Heyden, 2011, Hibbert, 2012), using factorial design to consider interactions between variables, in contrast with univariate studies, which are limited as they only optimise one factor at a time. The DOE approach uses a statistical regression model to generate a response surface that maps process performance over the complete range of conditions considered. Parameter estimation is based on a limited number of experiments conducted at specific combinations of variables, directed by the chosen factorial design (Ferreira et al., 2007). DOE approaches reduce experimental effort required to identify favourable operating conditions, whilst still using a system that has been qualified as representative of the large scale process. The type of factorial design and the range and number of operating variables selected for studies are important considerations, as the right balance must be found between experimental burden and the resolution and range of the generated response surface (Ferreira et al., 2007). In order to reduce the experimental effort, multiple DOE studies can be conducted in sequence, where initial scouting studies explore a wide range of process conditions in order to identify variable ranges for more detailed studies as the purification process approaches maturity.

### 1.4.4. **Key outstanding issues**

Although the modern approach to the development of chromatographic bioseparations is able to produce products of the desired quality, it is often at great time, effort and cost. Processes are developed and validated following an empirically driven experimental approach that results in a fixed, inflexible manufacturing process, a control strategy based on reproducibility rather than robustness, and end product testing via offline analysis. The approach to problems in manufacturing and/or deviations from the required product specification is reactive and done on a case by case basis. As a result, for many products, manufacturing efficiency is low, waste is high, and it is difficult to analyse and understand reasons for batch failures. The consequences of this are: (i) higher costs for products, (ii) a risk of drug shortages, (iii) a lack of improvements based on new technologies and (iv) a need for intensive regulatory oversight, resulting in (v) little flexibility in the regulatory process and thus little flexibility in manufacturing, (iv) problems with regulatory consistency, (vii) increasing and sometimes irrelevant information required in submission documentation, (viii) hindrance of innovation from manufacturers because of the need for time consuming and costly additional supplements, and (ix) slowed time to market (ICH, 2005, 2008a, 2008b).

### 1.4.5. **Proposed solution**

For these reasons, there has been a sustained effort in recent years to move to a more systematic approach based upon the principles of Quality by Design (QbD), which starts with predefined objectives, emphasise development based on product and process understanding, and encourages process control based on sound science and quality risk management. The objective of this initiative is to reach a desired state of biopharmaceutical development similar to that defined by Janet Woodcock (Director, Centre for Drug Evaluation and Research, FDA,) as, "a maximally efficient, agile, flexible pharmaceutical manufacturing sector that reliably produces high quality drug products without extensive regulatory oversight''. The recommended systematic approach can be broken into different elements. The guidance issued for industry from the FDA is as follows: (ICH, 2005, 2008a, 2008b).

***Identification of the quality target product profile (QTPP)***

As soon as a molecule has been identified as a viable candidate for commercialisation, the ideal quality characteristics of the drug product that ensure the safe implementation of the desired therapeutic effect should be established. This includes (i) dosage form, (ii) route of administration, (iii) bioavailability, (iv) pharmokinetic characteristics and (v) quality criteria such as sterility and purity. (ICH, 2005, 2008a, 2008b)

***Identification of critical quality attributes (CQA)***

Once the quality target product profile (QTPP) has been defined, the next step is to identify the physical, chemical, biological or microbiological properties or characteristics that should be within an appropriate limit, range or distribution to ensure the desired product quality, i.e. that the QTPP is met. These properties and characteristics, known as critical quality attributes (CQA), are initially derived from the QTPP and/or prior knowledge, and are used to guide process development. Commonly observed classes of CQA's and the quality attributes associated with them include (i) identity (primary amino acid sequence), (ii) potency, (iii) host cell modifications (e.g. glycosylation, phosphorylation, truncation, glycation, methylation and isomerisation), (iv) process modifications (e.g. PEGylation, aggregation, oxidisation, deamidation, C-termial lysine and misfolding), (v) host cell related impurities (e.g. host cell proteins (HCP), DNA and andotoxins), and (vi) other characteristics (e.g. appearance, colour, particles, pH, osmolarity, effector function and concentration). (ICH, 2005, 2008a, 2008b)

***Process development***

In a QbD type approach, process development is conducted with the aim of designing a manufacturing process and control strategy to consistently meet the defined critical quality attributes, thus assuring product quality (ICH, 2008a). This should follow a systematic procedure where manufacturing options are evaluated and subsequently refined based on: (i) first identifying the material attributes and process parameters associated with each manufacturing option that effects the product CQA's, (ii) determining the functional relationship that links those material attributes and process parameters to the product CQA's, and (iii) using enhanced product and process understanding combined with quality risk management to identify appropriate control strategies. Both the CQA's and manufacturing process are modified and refined as product knowledge and process understanding increase throughout development, utilizing a combination of design of experiments, mathematical models, and studies that lead to mechanistic understanding. The outcome of process development is a product design space and a process design space. (ICH, 2005, 2008a, 2008b)

***Product design space***

During the development effort, the criticality of product attributes should be determined such that a product design space can be created and documented in the regulatory filing that defines the acceptable variability in CQA's. The size of this space will depend on a range of factors including: (i) process robustness or capability, (ii) stability of the drug substance or drug product, (iii) clinical data for the product or other similar platform products, (iv) non clinical data for the product or similar platform products e.g. binding assays, cell based assays and in vitro assays, (v) the capability of analytical methods, and (vi) the level of understanding on the impact of each CQA on the safety and efficacy of the product. (ICH, 2005, 2008a, 2008b)

***Process design space***

The relationship between the material attributes and process parameters with product critical quality attributes is described in the process design space. This is defined by the International Conference on Harmonisation (ICH) guidance document as "the multidimensional combination and interaction of input variables and process parameters that have been demonstrated to provide an assurance of product quality" (ICH, 2008a). This can be shown in terms of parameter ranges, or more complex mathematical relationships, including time dependent functions, scale up factors, and combinations of variables, e.g. models. Not all process parameters and material attributes need be included in the design

space, as the increased understanding and knowledge gained during process development combined with quality risk management can provide the rational for inclusion or exclusion from the design space, which should be documented in the regulatory submission. Independent design spaces for each individual unit operation, or design spaces that span multiple unit operations, are both acceptable options. While single unit design spaces are simpler to develop, a design space that spans the entire process can provide more operational flexibility. (ICH, 2005, 2008a, 2008b)

***Control strategy***

Equally important to the development of the process is the development of how that process is controlled. The control strategy should be designed as part of the overall development of the therapeutic protein production process. Sources of variability that impact quality should be identified, appropriately understood, and subsequently controlled. Understanding the variability and its impact on product quality in combination with quality risk management can support the control of the process, such that variability is compensated for in an adaptable manner. This enables the attractive possibility that variability can be less tightly constrained, and instead, unit operations are responsive to the process input. In addition, enhanced understanding of how process performance relates to product quality can justify the use of alternative approaches to determine that process streams are meeting the desired quality attributes, supporting real time testing and resulting in an increased level of quality assurance compared to the traditional end product testing. (ICH, 2005, 2008a, 2008b)

***Process validation and filing***

After the process design space and the control strategy has been defined, process validation studies are performed to demonstrate that the process does indeed deliver a product of acceptable quality. The regulatory filing is then compiled including the acceptable operating parameter ranges specified in the process design space, in addition to the product design space, the control strategy, the outcome of the validation studies and a plan for ongoing process monitoring. (ICH, 2005, 2008a, 2008b)

### 1.4.6. **Advantages of a systematic approach**

The expected benefits of a systematic approach following QbD principles are numerous, and include: (i) better design of products, (ii) less problems in manufacturing, (iii) a reduction in the number of manufacturing supplements required for post market changes, (iv) increased understanding of the process risk bringing improved risk mitigation, (v) greater process robustness, (vi) enabling the implementation of new technologies to improve manufacturing

without regulatory scrutiny, (vii) increased process efficiencies and reduced waste resulting in reduction in the overall cost of manufacturing, (viii) continuous improvement possible in products and in manufacturing processes, (ix) manufacturing is related to the clinic through design, (x) better coordination, consistency, quality and flexibility across the full regulatory process (review, compliance and inspection) resulting in (xi) less haggle during regulatory review and (xii) quicker approvals. The key differences between the QbD and traditional approach are summarised in Table 1.3 (ICH, 2005, 2008a, 2008b).

## 1.5. Issues with QbD

Although the proposed systematic approach to process development and operation has important benefits to be released, in practice, there will be significant upfront costs, as fulfilling regulatory guidelines requires substantial additional effort by purification process development. There is a serious concern that this may hinder the effort to launch products as early as possible whilst maximising efficiency and reducing costs when bringing a product to market. This is a very important consideration in an increasingly competitive biopharmaceutical market. Therefore, approaches that can aid or provide an alternative to the existing experimental approach in a quality by design development paradigm are of increasing interest in industry.

## 1.6. First principles models for QbD

Innovation and engineering approaches based on first principles modelling have been proven in a variety of processing industries (e.g. refining, oil and gas, chemicals, energy). However, mechanistic models derived from first principles have so far been seldom utilized in the biopharmaceutical sector. Regulatory guidance regarding the implementation of Quality by Design has proposed greater use of mechanistic models (ICH, 2008a), and they have great potential for generating value and for reducing costs. Their use as an aid or an alternative to experimentation may provide a means for implementation of a Quality by Design development approach without increasing costs and development times.

One of the most straightforward ways that mechanistic models can help to implementation of a Quality by Design without increasing costs and development times is by reducing the amount of drug substance used for experimentation. A reduction can be achieved by directly replacing experiments with model simulations or by leveraging increased knowledge and fundamental understanding from the model in order that fewer but more useful experiments are conducted during process development. The model may facilitate better informed

heuristics, or be used for more advanced mathematical methods such as optimisation (Avraam et al., 1998), or experimental design.

A reduction in the amount of drug substance used for experimentation enables process development to become less dependent on the generation of material, which is usually deliberately kept small so that losses are reduced in the event that a molecule fails. This is very useful as in industry, if the amount of drug substance available for an experimental programme is insufficient, the result can be substantial costs and delay whilst new material is generated, or significant risk may be incurred by continuing development on the basis of limited information.

A reduction in the size of the required experimental programme during process development also reduces direct costs associated with laboratory facilities and personnel. This does not necessarily result in a reduction in the number of personnel employed, as reducing the number of experiments required per molecule may increase the number of drugs that can be studied. Thus, the inclusion of mechanistic models in a systematic approach to process development can bring associated benefits in the opportunities that biopharmaceutical companies can exploit.

The speed and efficiency with which model simulations can be conducted can enable the exploration of the process design space in ways that experimentation cannot, since experiments will always be limited by the amount of material and time that it takes to conduct them. Unlike experimentation, model simulations can be conducted quickly, and advances in process modelling technology mean that model deployment in industry is now straightforward (Pantelides and Urban, 2005). Models give more control when examining process sensitivity compared to experiments via techniques such as global sensitivity analysis, and the ability to quantify process risk using a model can help bring greater assurance of product quality than traditional qualitative approaches (e.g. failure mode effects analysis) can provide on their own.

Table 1.3. Key differences between the QbD and traditional approach (ICH, 2005, 2008a, 2008b)

| Aspect | Traditional approaches | Enhanced, Quality by Design approaches |
|---|---|---|
| Overall pharmaceutical development | ▪ Mainly empirical<br>▪ Development research often conducted one variable at a time | ▪ Systematic, relating mechanistic understanding of material attributes and process parameters to drug product critical quality attributes<br>▪ Multivariate experiments to understand product and process<br>▪ Establishment of design space<br>▪ Process Analytical Technology tools utilised |
| Manufacturing process | ▪ Fixed<br>▪ Validation primarily based on initial full scale batches<br>▪ Focus on optimisation and reproducibility | ▪ Adjustable within design space<br>▪ Lifecycle approach to validation and ideally, continuous process verification<br>▪ Focus on control strategy and robustness<br>▪ Use of statistical process control methods |
| Process controls | ▪ In process tests primarily for go/no go decisions<br>▪ Off line analysis | ▪ PAT tools utilised with appropriate feed forward and feedback controls<br>▪ Process operations tracked and trended to support continual improvement efforts post approval |
| Product specifications | ▪ Primary means of control<br>▪ Based on batch data available at time of registration | ▪ Part of the overall quality control strategy<br>▪ Based on desired product performance with relevant support data |
| Control strategy | ▪ Drug product quality controlled primarily by intermediates (in process materials) and end product testing | ▪ Drug product quality ensured by risk based control strategy for well understood product and process<br>▪ Quality control shifted upstream, with the possibility of real time release testing or reduced end product testing |
| Lifecycle management | ▪ Reactive (i.e. problem solving and corrective action) | ▪ Preventive action<br>▪ Continual improvement facilitated |

First principles modelling approaches surpass Design of experiments (DOE) and response surface models (RSM) for quality by design related tasks such as design space identification due to the increased process understanding gained during model development and application. Increased process understanding not only enables a reduction in the experimental programme and amount of material required during process development (which is also achieved through the use of DOE and RSM), but is very useful for answering operating questions during manufacturing. Testing hypotheses is greatly simplified with a predictive model enabling answers to be found in hours rather than days which is not possible with an empirical RSM which is limited to the data used for parameter estimation.

More advanced applications of first principle models may also allow operators to intervene before unexpected deviations occur, as models can extract more information from laboratory and plant data. Processes can be monitored for key performance indicators by using model based soft sensing tools (de Assis and Filho, 2000), so that batch processes that are likely to fail can be terminated at an early stage of the batch, reducing the impact on the manufacturing campaign. When combined with process control, soft sensing allows for adjustments to manipulated variables in order to reduce the number of batch failures.

Lastly, at a higher level, models allow companies to safeguard, develop and exploit their intellectual property to maximum advantage. Company knowledge can be captured and organised independently of employees in such a way that when key employees leave, knowledge is retained. This is can be extremely important in a biopharmaceutical sector where many companies utilise similar processes, and personnel regularly move between jobs.

***Concluding remarks***

Innovation and engineering approaches based on first principles modelling have been proven in a variety of processing industries (e.g. refining, oil and gas, chemicals, energy). However, mechanistic models derived from first principles have so far been seldom utilized in the biopharmaceutical sector. With the emergence of the quality by design initiative and the desire to move to a more systematic approach to process development, there are new opportunities for mechanistic modelling approaches in the biopharmaceutical industry. Regulatory guidance regarding the implementation of Quality by Design has proposed greater use of mechanistic models (ICH, 2008a), and they have great potential for generating value and for reducing costs, and research into this area is of great importance.

## 1.7. Summary

Therapeutic proteins are now well established as a clinically and commercially important class of therapeutics (Leader et al., 2008) and they have played a key role in major advances in healthcare over the last quarter century (Waldmann, 2003). Their high specificity and relatively low immunogenicity means they are useful as therapeutic agents in the treatment of various disorders and diseases (Walsh, 2010, Carter, 2011). Annual revenues from therapeutic protein sales are now estimated to total in excess of $50 billion, nearly 10% of the $600 billion pharmaceutical market (Walsh, 2010). Continuing growth is evident in industry, with several hundred clinical candidate proteins currently in company pipelines (Kelley, 2009), of which many serve significant unmet medical needs (Shukla et al., 2007).

The key considerations when bringing a product to market are launching as early as possible whilst maximising efficiency and reducing costs. The downstream section of the manufacturing process traditionally constitutes a significant proportion (50 – 80 %) of the total manufacturing costs (Lightfoot and Moscariello, 2004), and is now considered to be the manufacturing bottleneck (Nfor et al., 2009). Chromatographic purification is the predominant unit operation used in downstream processing, but developing a chromatographic bioseparation is a hugely complex task (Lightfoot and Moscariello, 2004). Process development must be completed within very constricted timelines (Steinmeyer et al., 2008), and is both technically and economically challenging.

The traditional approach to developing and operating biopharmaceutical processes relies heavily on empirical methods and experimentation guided by heuristics. However, in recent years, there has been a sustained effort to implement a more systematic approach based upon the principles of Quality by Design (QbD) (ICH, 2005, 2008a, 2008b). The goal is to develop a more efficient, agile, and flexible sector that can reliably produce high quality drug products without extensive regulatory oversight (Woodcock, 2005). The desired approach starts with predefined objectives, and emphasizes product and process understanding, and process control, based on sound science and quality risk management (Rathore and Winkle, 2009, Rathore, 2009).

Model based innovation and engineering approaches have been proven in a variety of processing industries (e.g. refining, oil and gas, chemicals, energy), but are seldom utilized in the biopharmaceutical sector. Regulatory guidance regarding the implementation of Quality by Design has proposed greater use of mechanistic models (ICH, 2008a). Predictive chromatography models can help increase process understanding and fundamental

knowledge, whilst the speed and efficiency with which model simulations can investigate design alternatives, means they can help accelerate process development and increase process robustness. Mechanistic models therefore have great potential for generating value, and reducing costs in biopharmaceutical industry. As a consequence, biopharmaceutical companies are now increasingly interested in the development and application of mechanistic models of industrial chromatographic bioseparations, and research into this area is of great importance.

## 1.8. Aim of this thesis

Motivated by the desire to accelerate the development and increase the robustness of *industrial* protein purification processes whilst also realising the benefits from following a systematic QbD approach to process development and operation, the aim of this thesis is to derive fundamental process understanding of specific industrial chromatographic separations currently in development or operation at Pfizer, via the development and application of mechanistic models chromatography.

## 1.9. Organisation of this thesis

An introduction to the relevance of developing mechanistic models of industrial chromatographic bioseparations has been given, and the general aim of the project has been set out. The rest of the thesis is divided into five chapters. Chapter two provides a literature review of first principles modelling of chromatographic purification of therapeutic proteins with regard to model formulation, calibration and application.

Chapter three considers the development and application of an anion exchange weak partitioning chromatography model at an early stage of process development for the purposes of; (i) increasing process understanding by providing a more informative method for exploring how process parameters can be controlled in order to raise product recovery to acceptable levels whilst maintaining impurity clearance, and (ii) accelerating process development by providing a link between high throughput screening and scale down column experiments.

Chapter four addresses a lack of fundamental knowledge on the mechanistic impact of resin fouling experienced during the purification of a monoclonal antibodies in the anion exchange weak partitioning chromatography process considered in chapter three. A selection of experimental methods are used to characterise the fouling, which include, scanning

electron microscopy, confocal laser scanning microscopy, batch adsorption and scale down column studies.

The fifth chapter considers the development and application of a model of a hydrophobic interaction chromatography process at a late stage of development for the purposes of (i) increasing process understanding by determining the mechanistic effect of resin lot to lot variability that was resulting in serious performance issues, and (ii) increasing process robustness via the application of stochastic simulation to generate probabilistic design spaces that identify prospective operating conditions that assure product quality.

The sixth chapter summarises the findings and conclusions from each part of the project. A number of areas for future work are discussed. The chapter focuses in particular on the broader implications for the use of mechanistic models of chromatography in the biopharmaceutical industry.

# Chapter 2. Literature Review

*This chapter provides a review of the current state of the art in first principles modelling of chromatographic bioseparations, categorised and discussed according to model formulation, model calibration and model applications. It will be shown that there is a fundamental lack of mathematical descriptions and approaches to characterise and calibrate relevant model parameters for describing the non-ideal phenomena and challenging feed material compositions experienced in industrial chromatographic separations. In addition, not enough consideration has been given to how to apply mechanistic models of chromatography (e.g. model calibration, optimisation, design space generation etc.) in an industrial environment with limited time and material.*

# 2.1. Introduction

The background presented in chapter 1 suggests first principles models of chromatography may have an important role to play in the systematic development and operation of industrial chromatographic bioseparations based on fundamental process understanding. However, before first principles modelling approaches are adopted by industry, a critical mass of evidence needs to be built demonstrating the unique advantages mechanistic models can give industry compared to a purely experimental approach.

# 2.2. Model formulation

Model formulation consists of deriving or selecting suitable descriptive equations that mathematically describe the physical phenomena encountered in chromatographic bioseparations, in order to meet the objectives of a modelling project. A wide range of options are available and have been presented in the literature. Two types of physical phenomena dominate chromatography; *movement of solutes* through the packed bed of porous particles via mass transfer mechanisms, and *adsorption* based on the fundamental thermodynamic interactions between migrating solutes and the stationary phase. Equations used to describe these phenomena are discussed in section 2.2.1 and 2.2.2, respectively. Chromatographic bioseparations where heat effects play a role are extremely rare, but exceptional cases are discussed in section 2.2.3. Very few chromatographic bioseparations have been designed where desired reactions occur whilst the species are separated. However, undesired isomerisation, association, aggregation of species, resin fouling and ligand leaching are commonly observed in practice, and are discussed in section 2.2.4.

### 2.2.1. **Mass conservation**

Mass conservation equations describe the movement of load material components through the packed bed. The main phenomena that can contribute to this are illustrated in Figure 2.1, and include convection, axial dispersion, diffusion through an external film surrounding resin particles, and intraparticle diffusion through the stagnant mobile phase within particle pores. Diffusion along the surface of pores may play a role in some cases, but is usually insignificant and therefore generally ignored (Guiochon et al., 2006). A range of different mass transport models have been published and are summarised in Table 2.1.

The general system of equations used to describe the main mass transfer phenomena consist of two sets of partial differential mass conservation equations. One describes the bulk fluid phase across the column axial dimension, and contains terms for accumulation in the mobile phase, accumulation in resin particles, convection, and dispersion. The other describes the

intraparticle fluid phase across the radial particle dimension, which includes terms for accumulation in the intraparticle fluid phase, accumulation in the solid phase, and intraparticle diffusion. In addition to the two partial differential mass balances, a kinetic expression is used to describe diffusion through a stagnant film surrounding resin particles (Guiochon et al., 2006). When these equations are combined with an appropriate adsorption equation (which will be discussed in section 2.2.2), the model is known as a general rate model.

The mass balance equations used in modern day general rate models are still similar to the original systems of partial differential equations derived in 1920 (Bohart and Adams, 1920), and again in 1939 (Wicke, 1939, 1940), used as a basis for the fundamental work on modelling of chromatography (Wilson, 1940, DeVault, 1943, Lapidus and Amundson, 1952, van Deemter et al., 1956). Mass transport equations almost always assume Fickian diffusion, although Maxwell – Stefan equations have also been used, in particular where surface diffusion has been found to have an important contribution to a separation (Kaczmarski et al., 2002, 2003, Sun and Yang, 2007).

The fundamental assumptions made when deriving the mass conservation equations of the general rate model are universal for all its subsequent simplifications, and have been discussed in detail by Guiochon et al., (2006). They include; the incompressibility of the mobile phase, concentration independence of the mass transfer parameters, constant mobile phase viscosity, and constant molar volumes between species in the mobile and stationary phase. The column is assumed to be one-dimensional (radially homogeneous), and evenly packed with spherical, uniformly porous, constant sized particles. As a result, the radial column dimension is usually ignored (Guiochon et al., 2006).

Table 2.1. Summary of common mechanistic mass transfer models of chromatography

| Model Name | Convection | Axial Dispersion | Mass Transfer through external film | Intra-particle diffusion |
|---|---|---|---|---|
| General Rate Model | YES | YES | YES | YES (Heterogeneous particle) |
| Lumped Kinetic Model | YES | YES | YES | NO |
| Equilibrium Dispersive Model | YES | YES | NO | NO |
| Ideal Model | YES | NO | NO | NO |

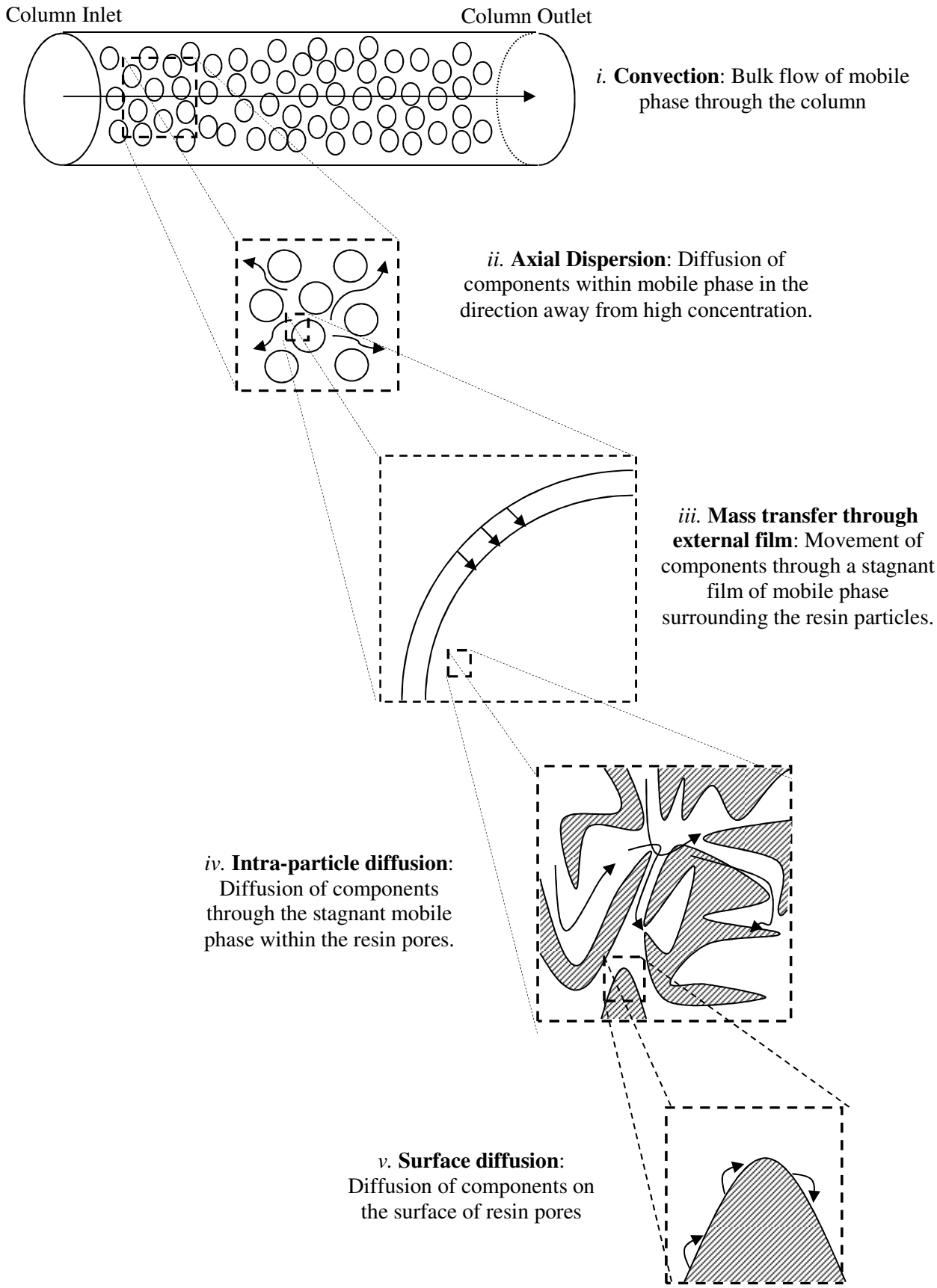


Figure 2.1. Sources of mass transfer in packed bed chromatography.

In practice, packed beds are almost always heterogeneous (Farkas et al., 1996, Shallikera et al., 2003), and particle size varies. However, it is commonly cited that any resulting radial or axial heterogeneity in concentration and velocity averages out when the ratio of column to particle diameter is high (typically greater than 30), as is true for most laboratory and manufacturing scale chromatography processes (Guiochon et al., 2006). For industrial systems, this assumption is dubious. Although bed consistency is checked by ensuring that the column asymmetry and plate height are within set ranges, often the ranges deemed acceptable are set very wide because tighter ranges result in many repacks wasting time and money. Therefore, packing quality can vary considerably. Wall effects, the low density of resin particles, variability in the particle diameter, the length of time that resin is left to settle, changes during scale up (McCue et al., 2007), and differences in the packing method can all play a role.

For microscale devices in particular, hydrodynamic effects caused by non-ideal bed properties are dominant e.g. in microfluidic columns, microcolumns and microtips (Abia et al., 2009). Using a standard model which assumes homogeneous bed and particle structure will therefore result in inaccurate model predictions. An approach for simulation of micro scale devices has been demonstrated, which utilises a model based on computational fluid dynamics that is able to account for heterogeneity in particle and packed bed structure (Gerontas et al., 2013). However, the approach is not suitable for large scale systems, as the high level of discretisation required results in extremely long solution times.

Another issue for bioseparations in particular, is assuming a uniformly porous resin structure. Chromatography resin particles are known to exhibit a range of pore sizes with normal-like distribution (dePhillips and Lenhoff, 2000, Yao and Lenhoff, 2006). This is not an issue when all species are significantly smaller than the smallest pore size, as all species have equal access to resin binding sites. However, as the size of biomolecules often falls within the pore size distribution (i.e. biomolecule and particle pore sizes are similar), pore accessibility becomes dependent on component size. This can impact mass transfer performance, as there is more competition for binding sites in the larger pores which are accessible to all components, than in smaller pores where few species can enter. In addition, as adsorbed proteins occupy a finite space, the adsorption process itself can modify the effective pore radius as bound proteins partially obstruct pores, hindering intraparticle diffusion (Boyer and Hsu, 1992, Susanto et al., 2007). This is especially true where tentacles are used within resin pores to increase resin capacity (Thomas et al., 2013). A change of tentacle orientation (which can occur when the mobile phase composition changes) can result in large changes to pore accessibility of components. If the impact of changes to

particle structure is large, then the more detailed distributed pore model can be used which accounts for the pore size distribution of the stationary phase, and pore shrinkage due to protein adsorption (de Neuville et al., 2013). Alternatively, diffusion parameters can be calculated as a function of stationary phase concentration (Susanto et al., 2007).

Despite the issues mentioned regarding model assumptions, the predictive capability of the general rate model is well proven. Older studies using the general rate model focused on increasing theoretical understanding of underlying phenomena such as displacement effects (Gu et al., 1990a), desorption (Gu et al., 1990b), restricted protein diffusion (Boyer and Hsu, 1992), scale up (Li et al., 1998), intraparticle diffusion (Susanto et al., 2006), and hydrophobic interaction mechanisms (To and Lenhoff, 2008). Later, the general rate model was applied to process development tasks such as process design (Melter et al. 2008), optimisation (Karlsson et al., 2004, Degerman et al., 2006, Lienqueo et al., 2009), design space exploration (Degerman et al., 2009) and scale up (Gerontas et al. 2010), albeit most often using well known proteins. In recent years, the general rate model has been successfully used to simulate more complex chromatographic processes that are often nonlinear and contain streams with multiple species (Nagrath et al., 2011, Guélat et al. 2012, Osberghaus et al., 2012a, 2012b, 2012c).

The problem with the general rate model is that it can be difficult to accurately estimate the large number of parameters required for simulations, and the model can take a long time to solve. This is of particular concern for industry, where minimising process development time is key, and processes are complex. In order to increase computational efficiency and the speed of model development, assumptions are commonly made to reduce model complexity by neglecting or lumping multiple phenomena into single terms. Successive simplification of the general rate model results in the lumped pore model, the lumped kinetic model, the equilibrium dispersive model and the ideal model, listed in order of decreasing model complexity (Kaczmarski et al., 2001). A summary of the main mass transport phenomena considered in each model is presented in Table 2.1.

The lumped pore model simplifies the general rate model by assuming that particles are homogeneous. The partial differential equation describing intra particular mass transport across the radial particle dimension is modified accordingly. The intraparticle mobile and stationary phase concentrations are replaced with average concentrations, and the intra particle diffusion term is replaced with a kinetic expression. The kinetic expression describes mass transfer between the column mobile phase and intra particular mobile phase via an

overall mass transfer coefficient which is related to the external and internal mass transfer coefficients (Guiochon, 2002, Guiochon et al., 2006).

Few studies have been conducted using the lumped pore model, as the lumped kinetic model provides identical solutions for experimental conditions typical of current chromatographic separations, but with greater computational efficiency, and less parameter estimation burden (Kaczmarski et al., 2001). The model achieves this by replacing the partial differential equation describing intraparticular mass transport with a kinetic expression, which links the column mobile phase concentration to the average intraparticular mobile phase concentration (Kaczmarski et al., 2001, Guiochon, 2002). Hence, intraparticular mass transport is still directly accounted for within the model, but the radial distribution domain is removed, which significantly reduces the number of equations.

As a result, the lumped kinetic model has been used in a wide range of studies, most commonly considering process development tasks. These include process design (Mollerup et al., 2007), process optimisation (Chan et al., 2008, Teeters et al., 2009), design space exploration (Degerman et al., 2009, Gétaz et al., 2012), process control (Westerberg et al., 2010), continuous chromatography (Muller – Spath et al., 2011), resin selection (Nfor et al. 2011) and process synthesis (Nfor et al., 2013). There have also been studies where the focus was on increasing process understanding in areas such as hydrophobic interaction separations (McCue et al., 2008), and chromatographic separations involving complex feedstocks (Bak et al., 2007, Gétaz et al., 2013).

Simplifications made in the equilibrium dispersive model go even further than the lumped kinetic model, and assume that the mass transfer kinetics between the mobile phase moving through the column bed and the resin particles is infinitely fast. Thus, the concentration of a component in the extraparticular mobile phase is equal to the average concentration of that component in the intraparticular mobile phase, and the mass balance over particle pores can be neglected. The kinetic expression used in the lumped kinetic model is removed, and the axial dispersion coefficient is replaced with an apparent axial dispersion coefficient, which lumps the contribution from all sources of mass transfer associated with resin particles and axial dispersion (Kaczmarski et al., 2001, Guiochon, 2002, Guiochon et al., 2006). Despite its simplicity, the model still gives useful predictions (Chan et al., 2008, Susanto et al., 2008, Gu et al. 2013), and its high computational efficiency is particularly useful when model applications are computationally expensive, such as optimization (Degerman et al., 2007, Ng et al., 2012), robustness analysis (Jakobsson et al., 2005, Westerberg et al., 2012), and exploring the effect of experimental uncertainty on parameter estimation (Borg et al., 2013).

### 2.2.2. **Adsorption**

Adsorption of proteins refers to the reversible adhesion of molecules from the liquid phase to the resin surface, dictated by the fundamental thermodynamic interactions that occur when a load material component associates with a ligand or number of ligands covalently bound to the surface of the chromatographic adsorbent (Mollerup, 2008). The exact nature of the bonding between the resin ligand and molecule depends on the details of the species involved. The conformational entropy of proteins, hydrophobic interactions and electrostatic interactions can all contribute (Norde, 1998). At a macroscopic level, the mixture components distribute themselves between the stationary and mobile phase.

Adsorption of therapeutic proteins and other molecules found in chromatography feed material is non-trivial. The application of models from theory alone is not yet possible due to many complicating factors. As explained in the review by Rabe et al., (2011):

1. Each molecule contains many electrostatic and hydrophobic groups heterogeneously distributed throughout the entire protein structure, i.e. some are on the external surface while others are located inside the molecule.
2. Proteins are typically asymmetric and so representing them as a sphere is unrealistic.
3. Proteins often simultaneously interact with multiple binding sites, using contributions from multiple groups.
4. Cooperative effects from proteins that are already adsorbed means that proteins are sometimes more likely to adsorb if there are pre-adsorbed proteins.
5. During adsorption and/or desorption proteins often unfold and change structure, potentially changing the groups exposed at the surface of the protein.
6. Due to the similar size of molecules to resin pore diameter, and the range of ionic strengths encountered, electrostatic force fields can interact causing the local conditions to vary.
7. Proteins can also self-associate (aggregate), both in solution and on the stationary phase, so interactions between components are very important.
8. Proteins often denature in extreme conditions or due to other components, e.g. proteases.
9. Overshooting adsorption kinetics due to conformational rearrangement of adsorbed proteins on the resin surface have also been observed.

The complexity of protein adsorption means that adsorption equations are primarily based on experimentally correlated equations that are sometimes derived from rigorous thermodynamic principles (Mollerup, 2008), but are most commonly empirical or semi empirical (Guiochon et al, 2006). Models are composed of a generic function known as an adsorption isotherm which describes the relationship between the concentration in the mobile phase and the stationary phase of a chemical or biochemical species. There are many different adsorption isotherms available, which can be grouped into equilibrium models and kinetic models.

***Equilibrium isotherm models***

Equilibrium models predict the equilibrium state of adsorption (e.g. the bound protein concentration at steady state) using selected parameters such as unbound protein concentration, pH and ionic strength. Common equilibrium adsorption isotherms are summarised in Table 2.2.

The simplest equilibrium model is the linear model, which assumes that the chromatography resin is under challenged and thus there are a large number of free binding sites (Guiochon et al, 2006). This is often the case in analytical chromatography where only small amounts of protein are applied to the chromatography column. However, this is rarely the case in industrial bioseparations, where columns are loaded as close to full capacity as possible in order to maximise productivity (Tugcu et al., 2007). Therefore, the ideal model has only been used in a few studies, where its simplicity was helpful in reducing the solution time of optimisation problems (Chan et al., 2008b, Ng et al., 2012).

In practice, as the resin becomes increasingly saturated, it becomes more difficult for proteins to find free binding sites. After a certain amount of protein has been loaded onto the resin, all sites will be occupied and no more protein can bind. Many different isotherm models have been developed to represent this phenomena, such as Langmuir, steric mass action and quadratic isotherms (Foo and Hameed, 2010). Each isotherm makes a range of assumptions and often aims to address specific adsorption phenomena.

The Langmuir isotherm is the most commonly used model, and assumes monolayer adsorption at a finite number of equivalent and identical binding sites, with no lateral interactions, steric hindrance, or migration of adsorbed molecules on the adsorption surface (Guiochon et al., 2006). Despite the idealistic nature of these assumptions, the Langmuir isotherm has been used in a number of different studies. Single component Langmuir isotherms are typically applied where simulation of a model chromatographic system is used

to derive understanding of a particular feature or aspect of chromatography. For example, Gu et al., (1990) used a single component Langmuir when considering optimisation of desorption chromatography, and Sun and Yang, (2007) used a single component Langmuir when studying the difference between mass transport models.

The dependence of adsorption on mobile phase modulators, such as the counter ion concentration or pH, is often included in adsorption models if the model is intended for exploring potential operating conditions during process development. The Langmuir isotherm with mobile phase modulators has been used in numerous studies where models are used for process design and optimisation, considering a range of molecules (IgG, BSA, insulin, myoglobin and lactoferrin) and retention mechanisms (affinity, ion exchange, hydrophobic interaction and reversed phase chromatography) (Karlson et al., 2004, Melter et al., 2008, Degerman et al., 2009a, Westerberg et al., 2010, Gerontas et al., 2010, Ng et al., 2012, Borg et al., 2013).

Adsorption models can also be extended to deal with more than one component, including competition between components. In general, multicomponent adsorption isotherms are less rigorous than single component isotherms, as multicomponent adsorption is not well understood (Guiochon et al., 2006). For example, the multicomponent Langmuir isotherm is only thermodynamically correct when all components have identical saturation capacities, which is rarely the case for the extremely heterogeneous, multicomponent feed streams of industrial processes. Despite this limitation, the multicomponent competitive Langmuir isotherm is useful for systems with similar components, and has been used for hydrophobic interaction chromatography of alpha chymotrypsin and alpha amylase (Lienqueo et al., 2009), IgG capture with cation exchange chromatography (Muller – Spath et al., 2011), and the separation of monoclonal antibody variants with ion exchange chromatography (Guélat et al. 2012).

Table 2.2. Common equilibrium adsorption isotherms

| Adsorption model | Equation | Notes | Reference |
|---|---|---|---|
| Linear | $q = a \cdot C$ | Simplest isotherm available. | Guiochon et al., (2006) |
| Langmuir | $q = \frac{q_s \cdot k_a \cdot C}{1 + k_a \cdot C}$ | where $q_s$ is the saturation capacity and $k_a$ is the equilibrium constant. Formulation assumes monolayer adsorption at a finite number of equivalent and identical binding sites, with no lateral interactions, steric hindrance and migration of adsorbed molecules on the adsorption surface. | Gu et al., (1990), Sun and Yang, (2007) |
| Bi – Langmuir | $q = \frac{q_{s1} \cdot k_{a,1} \cdot C}{1 + k_{a,1} \cdot C} + \frac{q_{s2} \cdot k_{a,2} \cdot C}{1 + k_{a,2} \cdot C}$ | Accounts for two different binding mechanisms. | Kaczmarski et al., (2001) |
| Competitive Langmuir | $q_i = \frac{q_s \cdot k_{a,i} \cdot C_i}{1 + \sum k_{a,i} \cdot C_i}$ | Langmuir isotherm where the adsorption of one component is influenced by all components in the system. | Lienqueo et al., (2009), Muller – Spath et al., (2011) |
| Steric mass action | $q = \frac{C}{K_{SMA}}\left(\frac{C_s}{\Lambda - (\nu + \sigma)C}\right)^{\upsilon}$ | where $K_{SMA}$ is the equilibrium constant, $\Lambda$ is the total ionic capacity of the stationary phase, $\sigma$ is the steric factor, and $\nu$ is the characteristic charge. | Brooks and Cramer, (1992), Natarajan and Cramer, (2000) |
| Preferential interaction quadratic (PIQ) | $q = \frac{k_i^{'}\left(a_i C_i + d_i C_i^2\right)}{1 + \sum_{j=1}^{N_c} k_i^{'}\left(b_i C_i + c_i C_i^2\right)}$<br>$\ln k_i^{'} = \alpha_i + \beta_i \cdot C_{salt} + \gamma_i \cdot \ln C_{salt}$ | where $i$ and $j$ denotes the solutes, $k_i^{'}$ is the capacity factor, $N_c$ is the number of components, $C_{salt}$is the salt concentration, $\alpha$, $\beta$ and $\gamma$ are retention factors, and $a$, $b$, $c$, and $d$ are isotherm parameters. The model assumes competitive binding, equilibrium parameters independent of solute and salt concentration, no aggregation of conformal change, and a constant saturation capacity. | Xia et al., (2003) |

The steric mass action (SMA) isotherm was developed based on the stoichiometric exchange of components between the stationary and mobile phase (Rounds and Regnier, 1984, Regnier and Mazsaroff, 1987), and steric hindrance of adsorption sites due to protein size (Velayudhan and Horvath, 1988, Brooks and Cramer, 1993). In the SMA model, competitive binding is described by mass-action equilibrium where electroneutrality on the stationary phase is maintained. The multipointed nature of protein binding is represented by an

experimentally determined characteristic charge, and the steric hindrance of binding sites by adsorbed molecules is represented by a steric factor for each component (Brooks and Cramer, 1993). The obvious application of the SMA isotherm is for ion exchange chromatography where salt and proteins are exchanged. The model has been successfully applied to a range of systems, including alpha chymotrypsinogen A, ribonuclease A, nyomysin sulphate on a cation exchange system (Natarajan and Cramer, 2000), BSA on a strong anion exchanger (Susanto et al., 2006), IgG, BSA and myoglobin on an anion exchanger (Jakobsson et al., 2005), and most recently Lysozyme, ribonuclease A and cytochrome C on a cation exchanger (Osberghaus et al., 2012a, 2012b, 2012c).

A more recent addition to the literature are the association isotherms (Mollerup et al, 2008a, Mollerup, 2008b), which are derived from thermodynamic principles. Association models include a primary equation used regardless of adsorption mechanism which relates the bound and unbound component concentrations. A separate equation is used to describe an initial slope term within the primary equation which varies according to retention mechanism. Protein adsorption is modelled as a reversible association between ligand and component. When the interactions are electrostatic, proteins displace counterions associated with the ligands. If the interaction is hydrophobic, then adsorption entails a reversible association of the protein with the ligand to form a complex by non-polar interactions. Mollerup et al., (2007) used the model for ion exchange chromatography, and were able to successfully simulate the gradient elution of β-Lactoglobulin A and B, and the purification of four closely related components.

***Kinetic isotherm models***

Kinetic isotherm models express the state of adsorption through rate expressions that describe relevant adsorption and desorption phenomena and mechanisms (Guiochon et al., 2006). Rate expressions can be added or removed from kinetic models as needed, to represent the different adsorption phenomena relevant to the separation in consideration. Therefore, a very large number of expressions are possible. A simplified and schematic summary of kinetic adsorption models that have been proposed has been presented by Rabe et al., (2011).

The kinetic Langmuir isotherm is the most widely used kinetic model, and has been applied for modelling affinity (Bak et al., 2007), ion exchange (Susanto et al., 2008, Gerontas et al. 2010), and reversed phase chromatography processes (Degerman et al., 2007). A second order kinetic binding expression was used when modelling IgG elution during affinity chromatography by Sandoval et al. (2012), and a kinetic expression including a term

describing conformational change on the resin surface during HIC was used by To and Lenhoff, (2008).

A useful feature of kinetic isotherms is that the kinetic parameters can include the contribution of mass transfer resistances taking place inside the pores of the adsorbents, when an explicit particle mass balance is not included in the chromatography model. Degerman et al., (2007) and Susanto et al., (2008) both took this approach when using the equilibrium dispersive mass transport model. Although these chromatography models give a good description of the experimental chromatograms, the kinetic parameters do not have physical meaning (Kaczmarski et al., 2001).

### 2.2.3. **Heat effects**

Heat effects have little consequence for conventional chromatographic columns, and no detectable influence of the heat of adsorption on the migration of species through a chromatography column has been demonstrated (Gritti and Guiochon, 2007). High mobile phase velocities can result in thermal heterogeneity due to mobile phase decompression (Gritti, and Guiochon, 2007). Therefore, a differential heat balance for the mobile and stationary phase may be useful when modelling high or ultra-performance chromatography (Guiochon et al., 2006). In general, chromatographic separations are almost always assumed isothermal and adiabatic, thus the energy balance is usually entirely neglected without loss of model accuracy.

### 2.2.4. **Aging effects**

Fouling of chromatographic resin over operational lifetimes is a serious issue associated with industrial separations, attributed to repeated or prolonged exposure to the complex mix of components commonly seen in load material. This can result in significant reductions in binding capacities, and therefore altered process kinetics (Staby et al., 1998). Although standard clean-in-place (CIP) procedures can help restore columns towards their original state, fouling by certain types of material is often irreversible under typical conditions (Jin et al., 2009), and this must be balanced by the fact that more stringent cleaning can cause degeneration of the resin pore structure and loss of ligands (Jiang et al., 2009; Muller-Spath et al., 2009). Studies have shown that the binding capacity of Protein A affinity resins can decrease between 20 – 40 % due to ligand leaching, depending on the volume of material applied to the resin over its lifetime (Pollock et al., 2013).

Against this background, aging effects are very important phenomena to consider in chromatographic models, but despite this, only one such study has been published, where a

term for irreversible binding was included in the model (McCue et al., 2008). Indeed, there are relatively few experimental investigations into chromatography column aging in the literature.

The impact of fouling on a range of performance indicators such as pressure drop profiles, dynamic capacity and breakthrough curves have been measured at University College London, where scaled down columns were repeatedly loaded with fouling material (Boushaba et al., 2011; Bracewell et al., 2008; Chau et al., 2006; Shepard et al., 2000). Rather than considering fouling directly, other studies have focused on resin lifetime issues and CIP procedures (Muller-Spath et al., 2009; Norling et al., 2005). More recently, confocal laser scanning microscopy (CLSM), a tool that can monitor adsorption processes on a particle scale by observing the distribution of a fluorescent molecule within particles (Ljunglöf and Hjorth, 1996; Ljunglöf and Thömmes, 1998; Linden et al., 1999, Hubbuch et al. 2002), has been utilized to visualize fouling at the particle level (Jin et al., 2009; Siu et al., 2006, 2007). However, despite this progress, there remains only limited understanding of the mechanistic effect of aging phenomena, for example whether fouling impacts adsorption or mass transfer. Therefore, the development of mathematical descriptions of these phenomena is currently extremely difficult, which is a serious concern that needs to be addressed if models are to be used for process development in industry without resulting in unrealistic predictions.

## 2.3. Model calibration

Before chromatographic models can simulate a particular chromatographic separation, values for model parameters must be determined. In the following section of the chapter, methods to determine adsorption isotherm parameters, mass transfer parameters, and void volumes are reviewed.

### 2.3.1. **Methods to determine mass transfer parameters**

Mass transport equations are used to describe the movement of solutes through the packed bed of porous particles via mass transfer mechanisms. These equations include mass transfer coefficients and rate constants specific to each component. The methods used to determine these mass transfer parameters can be classified into three groups, correlations, inverse methods, and experimental methods.

#### *2.3.1.1. Correlations*

Due to intensive study in classical chemical engineering mass transfer research, there are a large number of correlations (summarised in Table 2.3) available that attempt to relate dimensional groups (e.g. the Peclet number and the Biot number) and mass transfer parameters to fundamental properties of packed beds (e.g. porosity, tortuosity, pore size distribution) and/or molecules (e.g. size, structure etc). Correlations have been used to determine all the major mass transfer parameters used in rate models, such as the apparent axial dispersion coefficient (Charton et al., 1994, Ng et al., 2012), axial dispersion coefficient (Kaczmarski et al., 2001), the film mass transfer coefficient (Kaczmarski et al., 2001, Karlsson et al., 2004, Gerontas et al. 2010), and intraparticle diffusivity (Nagarath and Cramer, 2000, Gallant, 2004). The advantage of using a correlation is that it is then not necessary to determine the parameters experimentally, which is challenging and can give inaccurate values due to difficulties distinguishing between the effects of each parameter on the shape of the measured chromatograms. Conversely, values of parameters used in correlations can themselves be unavailable and so must be assumed, and mass transfer parameter values determined using correlations are less specific to the system in question than parameters that are fitted to experimental data. Correlations are sometimes used in combination with other methods to ensure a good model fit to experimental data (Nagarath and Cramer, 2000, Teoh et al., 2001), and have been used to develop models for increasing process understanding (Li et al., 1998, Melter et al., 2008, Sandoval et al., 2012, Gu et al., 2013), and assisting with process development tasks (Jakobsson et al., 2005, Degerman et al., 2006, Lienqueo et al., 2009, Nfor et al. 2011).

#### *2.3.1.2. Inverse methods*

Inverse methods can also be used to estimate the values of mass transfer parameters, and are similar to the method used when estimating adsorption isotherm parameters. An algorithm is used to minimize the error between experimental measurements and model predictions by changing the mass transfer parameter in question. The inverse method is usually applied to estimate parameters from a single phenomenon at a time, due to the difficulty separating the effects of mass transport and adsorption from measured chromatograms (Natarajan and Cramer, 2000, Kaczmarski et al., 2002, Borg et al., 2013). However, Gerontas et al., (2010) were able to estimate adsorption and mass transport parameters simultaneously using a genetic algorithm combined with derivative based search algorithm to ensure the search algorithm did not become trapped in local optima.

Table 2.3. Correlations for mass transfer parameters (continued on the following page)

| Description | Correlation | Parameters |
|---|---|---|
| The apparent dispersion coefficient (Guiochon et al., 2006). | $D_A = \frac{vL}{2N_p}$ | where $v$ is the superficial velocity, $L$ is the column height and $N_p$is the number of theoretical plates. |
| The axial dispersion for liquid flow in packed beds with spherical particles (Ligny, 1970). | $D_{ax} = 0.7D_m + \frac{5R_p u}{1 + 4.4D_m/(R_p u)}$ | where $D_m$ is the molecular diffusivity, $R_p$ is the particle radius and $u$ is the interstitial velocity. |
| Axial dispersion coefficient (van Deemter 1956) | $D_{ax} = \gamma_1 D_m + \gamma_2 d_p \frac{u}{\varepsilon_b}$ | where $\gamma_1$ and $\gamma_2$are empirical constants, $D_m$ is the molecular diffusivity, $d_p$ is the particle diameter, $u$ is the interstitial velocity and $\varepsilon_b$ is the bed porosity. |
| Axial dispersion (Chung and Wen, 1968). | $D_{ax} = \frac{2R_p u \varepsilon_b}{0.2 + 0.011Re^{0.48}}$ $(10^{-8} < Re < 10^3)$ | where $R_p$ is the particle radius, $u$ is the interstitial velocity, $\varepsilon_b$ is the bed porosity and Re is the Reynolds number |
| Molecular diffusivity (Polson, 1950). | $D_m = 2.74 \times 10^{-5}(MW)^{-1/3}$ | where $D_m$ is the molecular diffusivity ($cm^2/s$) and $MW$is the molecular weight of the solute. |
| Molecular diffusivity (Young et al., 1980). | $D_m = 8.34 \times 10^{-8} \times \frac{T}{\eta MW^{1/3}}$ | where $T$ is the column temperature, $\eta$ is the kinematic viscosity, and $MW$is the molecular weight of the solute. |

Table 2.4. Correlations for mass transfer parameters (continued)

| Description | Correlation | Parameters |
|---|---|---|
| Intraparticle diffusivity (Striegel et al., 2009). | $D_m = \frac{D_{mol}\left[1 - 2.104\left(\frac{d_m}{d_p}\right) + 2.09\left(\frac{d_m}{d_p}\right)^3 - 0.95\left(\frac{d_m}{d_p}\right)^5\right]}{\tau_{tor}}$ | where $d_m$ is the molecular diameter (Å), $d_p$ is the average particle macropore diameter (Å), $D_{mol}$ is the molecular coefficient, and $\tau_{tor}$ is the particle tortuosity (usually unavailable so assumed around 2-6 for commercial porous solids). |
| Molecular diameter for proteins in water (Gu et al., 1999). | $d_m = 1.44(MW)^{1/3}$ | where $MW$ is the molecular weight of the solute. |
| Film mass transfer coefficient (Wilson and Geankoplis, 1966). | $k = 0.687u^{1/3}\left(\varepsilon_b R_p/D_m\right)^{-2/3}$ (0.0016 < Re < 55) | where $u$ is the interstitial velocity, $R_p$ is the particle radius, and $D_m$ is the molecular diffusivity (cm$^2$/s). |
| Film mass transfer coefficient (Kataoka et al., 1972). | $k = 1.165u^{1/3}\left(R_p/D_m\right)^{-2/3}((1-\varepsilon_b)/\varepsilon_b)^{1/3}$ $(Re < 100)$ | where $u$ is the interstitial velocity, $R_p$ is the particle radius, and $D_m$ is the molecular diffusivity (cm$^2$/s). |

#### *2.3.1.3. Experimental techniques*

A useful approach to estimating mass transfer parameters is to relate experimental data to empirical equations defining known relationships between experimental measurements and mass transfer parameters (Boyer and Hsu, 1992, Natarajan and Cramer, 2000, Persson et al., 2006). This involves correlating the height equivalent to a theoretical plate (HETP) to the hydrodynamic properties of a column through the plate height equation (Gritti and Guiochon, 2010). In this methodology, pulse injections of the molecule of interest are conducted at linear adsorption conditions, and the retention time, $t_R$, and the peak width at half peak height, $w_{0.5}$, are recorded as a function of superficial velocity and mobile phase conditions. This data is used to calculate the HETP using the following equation:

$$\text{HETP} = \frac{L}{5.54} \cdot \left(\frac{w_{0.5}}{t_R}\right)^2 \qquad [2.1]$$

where $L$ is the column length. The HETP is plotted against the superficial velocity. The HETP vs velocity data is compared with a plate height equation which is derived from moment analysis of the rate model being used. The derived equations are complex, and the derivation is tedious, involving successive differentiations of the Laplace transform solution of the chromatography model used (Guiochon et al., 2006). However, once the plate height equation has been formulated, it is straightforward to relate mass transfer parameters to the experimental data (Muller – Spath et al., 2011, Ng et al., 2012, Gétaz et al., 2013).

### 2.3.2. **Methods to determine adsorption isotherms**

Adsorption isotherms are used in chromatography models to describe the relationship between a component's concentration in the mobile phase and in the stationary phase. The complexity of protein adsorption means that adsorption isotherm parameters must usually be fitted to experimental data. Methods that are used to generate suitable data can be grouped into static experimental methods, dynamic experimental methods, the inverse method, and the retention time method. A summary of the key features of each method is presented in Table 2.5 .

#### *2.3.2.1. Static experimental methods*

In static methods, the equilibrium state of adsorption is measured in multiple experiments conducted over a range of material compositions and protein concentrations (Seidel-Morgenstern, 2004). The data is combined to create an experimental adsorption isotherm to which the isotherm model is fit. The most popular static method is ultra-scale down batch adsorption, where solutions of the component under investigation are brought to equilibrium

in closed lots of low volumes of resin (< 1 ml). The mobile phase can be analysed and the concentration of protein bound to the resin determined by mass balance. Alternatively, the bound protein can be eluted and analysed directly.

Ultra-scale down batch adsorption can be tedious, requiring labour intensive experiments, and can give inaccurate results. However, it only requires small amounts of protein and can be conducted in high throughput mode. In addition, automation by robotic liquid handling can greatly decrease the amount of time required whilst increasing accuracy due to better precision (Seidel-Morgenstern, 2004). The method has been used successfully in the development of models for a range of systems (Susanto et al., 2006, Sun and Yang, 2007, Susanto et al., 2008, Gu et al. 2013), including with crude feed material (Bak et al., 2007).

Another static method involves completely equilibrating a column with feed solution of known protein concentration. Again, the amount of bound protein can be determined either by mass balance, or by eluting all bound protein and measuring the amount directly. However, unless the column volume used is very small, completely equilibrating the column at multiple compositions and concentrations is very material and labour intensive. Therefore, this method has been used in only very few studies, and only with widely available products such as pure IgG (Ng et al., 2012) and BSA (Gu et al. 2013).

#### *2.3.2.2. Dynamic experimental methods*

Dynamic methods are based upon the analysis of the dynamic response to defined changes in column inlet protein concentrations (Seidel-Morgenstern, 2004). It is assumed that the only source of mass transfer in the column is convection. The adsorption isotherm is then directly related to the shape of elution profiles and breakthrough curves. Although the data analysis in dynamic experimental methods is more complex that static experimental methods, dynamic experimental methods are popular as all experiments can be conducted on one column. The magnitude of the changes to column inlet concentration can be small, intermediate or large, and dictates the exact method to determine the adsorption isotherm i.e. the perturbation method, elution by characteristic points and frontal analysis, respectively (Lisec et al., 2001, Seidel-Morgenstern, 2004). Frontal analysis is commonly used due to its relative simplicity, and possible automation, although it requires large amounts of material. There are examples of the methods use for all major retention mechanisms, i.e. anion exchange (Kaczmarski et al., 2001, Jakobsson et al., 2005, Gallant, 2004, Osberghaus et al., 2012a), cation exchange (Melter et al. 2008, Muller – Spath et al., 2011), hydrophobic interaction (Nagrath et al., 2011), and affinity separations (Ng et al., 2012). The perturbation method and elution by characteristic points method are described in the literature (Seidel-

Morgenstern, 2004), but are rarely used as they are difficult to apply to systems with multiple components.

#### *2.3.2.3. The inverse method*

The inverse method involves using an algorithm to minimize the error between the measured elution profile from an experiment, and the profile calculated from the full chromatography model by varying isotherm parameters, thus determining best fit. Advancements in numerical methods used to solve parameter estimation problems have resulted in a large increase in the use of the inverse method over the past decade (Teoh et al., 2001, Chan et al., 2008, Melter et al. 2008, Lienqueo et al., 2009, Westerberg et al., 2010, Gerontas et al. 2010, Muller – Spath et al., 2011, Osberghaus et al., 2012a, Gétaz et al., 2012), although problems have been reported where significant differences are observed in estimated parameter values depending on the choice of axial discretisation domain (Kaczmarski, 2007). Also, uncertain experimental data can result in large uncertainties in estimated parameter values (Borg et al., 2013).

#### *2.3.2.4. Retention time methods*

Retention time methods use the retention time of components of interest under linear conditions to determine the initial slope of isotherms (Mollerup, 2008). The method is particularly useful as pulse injections of components onto columns are straightforward to conduct, and can be used to explore the impact of mobile phase conditions on the isotherm quickly and efficiently. The advantage of using this methodology is that the influence of pH and counter ion concentration are captured without having to generate the complete isotherm at each unique operating point. In addition, detailed thermodynamic information may be determined via comprehensive analysis of the results, which can aid the development of isotherms derived from fundamental thermodynamic principles such as the association models (Mollerup et al, 2008a, Mollerup, 2008b). However, the method does not give any indication of the maximum saturation capacity, and therefore further experiments must also be completed in order to complete the calibration of the adsorption isotherm. In addition, the methodology requires many experiments with different buffer compositions. In recent years, retention time methods have emerged as a popular tool and are now applied regularly in the literature because complex chromatographic problems are now being considered where the effect of mobile phase composition on adsorption is of key importance (Mollerup et al., 2007, Melter et al. 2008, Muller – Spath et al., 2011, Nagrath et al., 2011, Nfor et al. 2011, Gétaz et al., 2012).

Table 2.5. Features of the different methods available for measuring adsorption isotherms, adapted from Seidel – Morgenstern, (2004).

| Method | Type | Material requirements | Favourable features | Unfavourable features | Applicable to one solute | Applicable to two solutes | Applicable to more than two solutes |
|---|---|---|---|---|---|---|---|
| Batch | Static | Small | Automation | Tedious, not accurate | Yes | Yes | Yes |
| Adsorption – desorption | Static | Small | Accurate, automation | Tedious | Yes | Yes | Yes |
| Frontal analysis | Dynamic | Large | Easy automation | High material requirements | Yes | Yes | Yes |
| Perturbation | Dynamic | Small | No detector calibration required | Isotherm model required | Yes | Yes | Difficult |
| Dispersed front analysis | Dynamic | Intermediate | Small number of experiments | High column efficiency required | Yes | No | No |
| Chromatogram fitting | Dynamic | Intermediate | Small number of experiments | Models for isotherm and mass transfer required | Yes | Yes | Difficult |
| Retention time method | Dynamic | Small | Straightforward to apply to systems with variable mobile phase conditions | Only applied at linear section of adsorption isotherm | Yes | Yes | Yes |

### 2.3.3. **Methods to measure void volumes**

Bed voidage, particle porosity and total column porosity are important parameters that are related to the bed and particle structure and they can be obtained experimentally by measuring the retention time of suitably sized unretained molecules. Molecules with very large molecular weight that do not penetrate particle pores, such as dextran blue, can be used to determine the bed voidage. Smaller molecules, such as sodium chloride or acetone, can be used to determine the total column porosity. With these values, a simple relation can be used to calculate the particle porosity.

The bed voidage has been determined for many different resins and systems and is commonly around 0.37. Particle porosities are more varied (0.55 – 0.8), and are often specified by the resin manufacturer. The effective void volume experienced by the specific component may vary depending on the component size, and amendments to models that account for this effect have been suggested (de Neuville et al., 2013). The effective porosity can be characterised experimentally by conducting inverse size exclusion chromatography (iSEC), where dextran standards of known size are used as probe molecules. The fraction of the total particle porosity available as a function of molecule size can then be determined from the retention time of the dextran standards. Alternatively, the void volumes of a large number of commercially available resins have been studied and published in the literature (dePhillips and Lenhoff, 2000, Yao and Lenhoff, 2006), which can be used directly in models, or as a means of checking measured parameters.

## 2.4. Model applications

Models of chromatography can be applied to complete important process development tasks such as process optimisation, design space identification, robustness and sensitivity analysis, and scale up. In the following section the state of the art in the open literature in these areas is reviewed.

### 2.4.1. **Resin selection**

Many different chromatographic resins are now available. The most suitable resin must be identified from hundreds of potential candidates early in the development process to leave time for optimisation and validation studies. The identification is usually achieved via experimental high throughput screening methodologies. Model based approaches have been proposed which may provide advantageous as resins can be evaluated at their optimal operating conditions with minimal experimentation required (Nfor et al., 2011).

### 2.4.2. **Purification process synthesis**

Purification process synthesis refers to the task of selecting the optimal sequence of chromatography unit operations to purify the clarified crude material following fermentation and primary recovery. This is nontrivial as a large number of process alternatives are usually possible, especially when the process does not utilize affinity chromatography. Nfor et al., (2013) recently demonstrated a methodology for selecting the most optimal process scheme for the purification of a monoclonal antibody from a crude mixture, employing a systematic cycle of flow sheet synthesis, optimisation, evaluation and rational elimination of the least feasible options at each purification step based on the specific needs of that step. The process evaluation was based on the performance of optimized mechanistic models for each step, and thus provided a more accurate indication of the most favourable sequence when compared to alternate approaches.

### 2.4.3. **Process optimisation**

There are useful examples of mathematical optimisation of the chromatographic purification of therapeutic proteins using mechanistic models of chromatography, where mathematical optimisation refers to minimising or maximising an objective function by varying decision variables subject to constraints (Degerman et al., 2006, 2007, Ng et al., 2012, Osberghaus et al., 2012b). Common factors to consider in the objective function include the yield and productivity of the chromatographic separation, and the purity of the product. When considering multiple objectives, cost functions have been used which define the relative importance of each factor when optimising a particular process (Lienqueo et al., 2009). Alternatively, multiple optimisations can be completed where the objective function is changed each time so that each factor is weighted differently. The resulting optimal values can then be used to generate a Pareto front useful for exploring the trade-off between the different factors (Degerman et al., 2009, Gétaz et al., 2012).

If the yield, productivity and purity are not included in the objective function, then they are usually included as a constraint. A wide range of decision variables are usually available in chromatographic separations. Column length, flow rate, volumes (wash, load and elution), buffer composition (e.g. ionic strength, pH) have all been considered. A recent study by Osberghaus et al. (2012a) compared mechanistic and empirical model based approaches for the optimisation of a three component separation, and concluded that for processes with low robustness, the performance of a DOE approach was significantly inferior to the performance of a mechanistic model, resulting in inaccurate predictions and a sub optimal process. However, discussion of the advantages and disadvantages revealed useful synergies between the two approaches, which suggested process optimisation should start with the

traditional DOE approach in order to comfortably and quickly reveal important factors which will generate a basic understanding of the chromatography. Then the outcomes from this study can be used to direct the development of a mechanistic model, using data from DOE experiments for model calibration and validation. The mechanistic model can then be used for detailed process optimisation, as well as other development tasks which are discussed in this section.

Despite the examples seen in the literature, mathematical optimisation of the sort described above does not see regular use in industry due to the large and frequent variance of inlet material, uncertainties in controlled process parameters, and frequency of non-ideal phenomena such as resin fouling which promotes a focus on identifying the most robust operating conditions, rather than optimising for particular scenarios.

#### 2.4.4. **Design space identification**

Mechanistic models are ideally suited to design space identification as they can explore different operating conditions and design parameters with greater efficiency and speed than an experimental approach, although few examples have been published in the literature. Degerman et al., (2009), used a mechanistic model to identify the design space for the purification of IgG from BSA by gradient elution using hydrophobic interaction chromatography. The method used was based on Pareto optimisation assuming that the process should only be run at optimal operating points, with Pareto fronts developed for different magnitudes of process disturbances which provide information that are used to determine a suitable design space. The method combines both process optimisation and design space determination whilst accounting for parameter uncertainty and operating point sensitivity. Although it requires a large number of simulations to be performed and does not provide information for non-optimal operating conditions, it is a very useful example of a model based approach to design space determination.

Gétaz et al., (2013), use a similar approach to determine the design space for the purification of a 4.3 kDa polypeptide crude mixture via gradient elution using a Kromasil 100 A 10 $\mu$m C8 (hydrophobic interaction) high performance liquid chromatography (HPLC) column. Optimal operating conditions were determined by Pareto optimisation, and then the response of product critical quality attributes to variations in process parameters was plotted as a function of loading and elution volume in order to indicate the design space borders. Both examples highlight the importance of accounting for process variability in order to assure the registered design space is robust. In addition, although ideally the design space should

contain a dimension for every process parameter, in practice due to the complexity of such a multi-dimensional design spaces, the number of parameters considered is limited to two.

The issue of how to communicate multidimensional design spaces is a wider challenge associated with design space identification that is not just limited to model based approaches, but is also a key challenge for experimental approaches, as it limits operating parameter ranges defined in regulatory submissions to linear combinations of process parameters, limiting design space size and excluding many feasible points of interest.

### 2.4.5. **Robustness and sensitivity analysis**

An important task in the development of a chromatographic step for purification of a therapeutic protein is concerned with ensuring that the process can cope with bioprocess variability (Rathore, 2009). Maximising process robustness, and minimising sensitivity to disturbances, are key aspects of this effort. Model based approaches to these tasks have been considered in the literature (Jakobsson et al., 2005, Degerman et al., 2009, Westerberg et al., 2012, and Gétaz et al., 2013).

Jakobsson et al. (2005), conducted a full factorial study of six factors on the purity and yield of the ion exchange purification of BSA, myoglobin and IgG. Using the results the relative importance and effect of each process parameter was determined. Degerman et al. (2009) used a model based approach to determine which process parameters were critical to control in order to assure process robustness for three case studies: (i) purification of IgG from BSA with hydrophobic interaction chromatography, (ii) purification of insulin from desamido insulin with reversed phase chromatography, and (iii) purification of IgG from BSA and myoglobin with hydrophobic interaction chromatography. Parameters were ranked according to importance, and risk of batch failure was determined for each case study accounting for uncertainty in a selection of process parameters. Gétaz et al. (2013) varied both process parameters (flowrate, loading, column length, feed concentrations, and buffer compositions) and model parameters (mass transfer coefficient and saturation capacity) around the standard operating conditions that had been found via process optimisation. The results were used to determine critical process parameters depending on the position of operation within the design space, and to determine correlated effects. All studies described found that process disturbances significantly decrease design space size, and illustrate the importance of process robustness in order to assure product quality.

### 2.4.6. **Process scale up**

Scale up strategies currently employed in industry are based on keeping the bed height and linear velocity constant. Process development experiments must therefore be conducted whilst keeping the bed height constant. This limits the minimum column volume that can be used for these experiments. Compared to a shorter bed height, the extra length of column means that experiments are more time consuming, and the extra volume means that larger amounts of material are required. As the mechanistic models of chromatography capture the underlying phenomena which are driving purification processes, they can provide useful information on alternative approaches to process scale up (Mollerup et al. 2007). Gerontas et al. (2010) were able to demonstrate how a mechanistic model can be developed using scale down columns with reduced bed heights (and thus volumes), and then the validated mechanistic model can be used to predict process operation in columns at full bed height, thus achieving significant savings in terms of time and material. Despite the simplified composition of the feed material considered (BSA and lactoferrin were selected due to the difficulty in procuring the very large amounts of protein required to load the manufacturing scale columns), the study demonstrated how a relatively simple application of a mechanistic model can be of enormous value for industry where time and material constraints are of great importance.

## 2.5. Concluding remarks

In order for first principles modelling approaches to be applied in industry for the design and development of chromatographic processes for the purification of proteins, a large body of evidence and best practices must be developed in the literature. The literature review considered three key areas, model formulation, model calibration and model applications. The key findings are summarised in this section, and in Appendix A, which details the referenced studies, indicating the mode of chromatography, retention mechanism, molecule of interest, load material composition, adsorption model, mass transfer model, and any subsequent model applications.

A large number of well understood options are available for modelling the movement of solutes through the packed bed of porous particles via mass transport mechanisms. The exact choice of model depends on the specific objectives of the modelling project. The most frequently used model is the general rate model, which describes convection, axial dispersion, diffusion through an external film surrounding resin particles, and intraparticlar diffusion through the stagnant mobile phase within particle pores (Guiochon et al., 2006). This is usually sufficiently accurate for most chromatographic separations. More complex

models are available if required, which include equations describing surface diffusion (Kaczmarski et al., 2002, 2003, Sun and Yang, 2007), pore shrinkage (de Neuville et al., 2013), and heterogeneity in particle and packed bed structure (Gerontas et al., 2013). Alternatively, simpler models such as the lumped pore model, lumped kinetic model, and equilibrium dispersive model are available for circumstances where high computational efficiency or fast model development is important (Kaczmarski et al., 2001).

Mass conservation equations are linked with equations describing adsorption to complete the chromatography model. Despite the wide range of options available, in practice, adsorption models are generally restricted to what is experimentally measurable, and the ability to distinguish between different adsorption phenomena is limited and difficult. In addition, it is desirable to keep the number of adjustable parameters to a minimum, as a higher complexity of model degrades the validity of the mechanistic meaning of the models parameters, i.e. the mechanistic model becomes more like a statistical model. As a result, the application of adsorption models has mainly been limited to simpler expressions, such as the Langmuir isotherm. Additional complexity is often described mathematically by extending simpler isotherms to account for competition, mobile phase modulators, and kinetic effects. In recent years, increasingly complex chromatographic systems have been considered (i.e. Osberghaus et al., 2012a, Guélat et al. 2012, Borg et al., 2013 etc), which has seen the utilisation of greater adsorption isotherm complexity such as the steric mass action (Bak et al., 2007), and association isotherms (Mollerup et al., 2008). However, the modelling of complex industrial systems is still extremely difficult because of the lack of options and approaches for describing heterogeneous, multi-component load material.

One area that has so far seen little consideration in the chromatography modelling literature are aging effects such as resin fouling and ligand leaching, and undesirable reactions between material components during separations such as aggregation. These phenomena can seriously impact process performance (Staby et al, 1998, Jin et al., 2009). If first principles modelling approaches are to provide a true alternative to existing experimental approaches, mathematical descriptions must be formulated and integrated into chromatography models, otherwise there is a risk of dangerously optimistic performance predictions. In addition, the lack of discussion and emphasis on these undesirable phenomena in the modelling literature may result in many experimentalists disregarding and dismissing mechanistic modelling, without considering the benefits such an approach may bring.

Model calibration involves determining values for model parameters. There are three main approaches for determining mass transfer parameters. The first involves the use of literature

correlations. The second is known as the inverse method, where an algorithm is used to minimise the error between experimental measurements and model predictions by changing the mass transfer parameter in question. The third approach involves relating experimental data to empirical equations defining known relationships between experimental measurements and mass transfer parameters. All are well understood, have been used extensively, and are often used together to increase confidence in estimated parameter values.

Similarly, adsorption isotherm parameters can be determined using a range of approaches. Static experimental methods include batch adsorption experiments conducted using scale down and laboratory scale systems. Dynamic experimental methods include frontal analysis, perturbation analysis and elution by characteristic points (Seidel-Morgenstern, 2004). Other methods include the inverse method where isotherm parameters are fit to chromatograms from column runs (Teoh et al., 2001, Kaczmarski, 2007), and retention time methods which can quickly determine the isotherm at linear adsorption conditions over a range of mobile phase conditions (Mollerup et al, 2008a). As with the estimation of mass transfer parameters, although each method can be applied on its own, (Susanto et al., 2008, Gerontas et al. 2010, Ng et al., 2012), the complexity of protein adsorption means that in practice, multiple methods are often used together to ensure accurate isotherm parameters (i.e. Jakobsson et al., 2005, Nfor et al. 2011, Muller – Spath et al., 2011, Osberghaus et al., 2012a).

Void volumes are usually determined experimentally by measuring the retention time of suitably sized unretained molecules, or taken from the published literature. Care must be taken when the experimental approach is used, but in general it is straightforward to complete. However, assuming uniformly porous resin structure can result in prediction errors due to dynamic phenomena such as hindered diffusion. In this case, it may be necessary to use inverse size exclusion to characterise the pore size distribution.

The application of chromatography models for process purification development has seen less consideration in the literature than model formulation and calibration, although the introduction of quality by design has seen a sharp increase in interest in recent years. There have been publications demonstrating the use of models for a wide range of development tasks, such as resin selection, whole process synthesis, process optimisation, design space formulation and analysis, robustness and sensitivity analysis, and process scale up. All of these studies show the great potential for first principles modelling approaches. However, only a few consider real industrial systems where crude feed material is purified rather than

well-known model proteins, and many proposed approaches require similar or greater time and material than alternative experimental approaches.

In summary, the key areas that need addressing before first principles modelling approaches are accepted by industry as a feasible aid or alternative to experimental approaches are all related to the practical implementation of modelling approaches in industry. There is a fundamental lack of mathematical descriptions and approaches to characterise and calibrate relevant model parameters for describing the non-ideal phenomena and the challenging feed material compositions that are commonplace in industry. In addition, more often than not, little consideration is given to how to apply the relevant mathematical and experimental techniques described in this chapter in an industrial environment with limited time, material and money. More needs to be done to demonstrate how the advantages of a model based approach can be leveraged in an industrial environment to generate value, when there remains an established experimental alternative that is well understood by regulators and biopharmaceutical companies alike, which has been proven with many examples in the past.

## 2.6. Aims of the thesis

The aim of this thesis is to derive fundamental process understanding of specific industrial chromatographic separations currently in development or operation at Pfizer, via the development and application of mechanistic models chromatography, in order to accelerate the development and increase the robustness of *industrial* protein purification processes, whilst following guidance regarding the implementation of Quality by Design. A range of experimental and mathematical methods are used to achieve a number of objectives related to specific chromatography processes currently in development or operation at Pfizer:

### 2.6.1. **Chapter 3 - Weak partitioning chromatography**

Pfizer utilise an anion exchange chromatography step operated in weak partitioning mode as part of their two - step platform monoclonal antibody purification process (Kelley et al., 2008a). The step has consistently provided excellent clearance of impurities whilst maintaining high step yields (> 90 %) for numerous proteins (Kelley et al., 2008, Iskra et al, 2013). However, feed material with high levels of product aggregates can occasionally pose a purification challenge, where operating conditions need to be carefully chosen in order to assure impurity clearance. In extreme cases, additional chromatography columns may be required. The current experimental procedure used to identify operating conditions (high throughput batch binding studies (HTS) followed by scale down column studies), requires a

significant amount of time and material for challenging feed material compositions, contrary to industrial objectives at an early stage of process development.

Developing an exhaustive chromatographic rate model is unlikely to be feasible at an early stage of process development due to limited time, material and analytics. Therefore, a simplistic 'platform' model of the WPC system that can be applied irrespective of the particular molecule will be developed. The aim is to aid the existing experimental process development procedure by providing a link between HTS and scale down column studies. The model will provide a more informative means for exploring how process parameters can be controlled in order to raise product recovery to acceptable levels and maintain impurity clearance. Stochastic simulation will be used to increase understanding of process robustness, and to identify prospective operating conditions for further development that can assure product quality when purifying material with challenging compositions.

### 2.6.2. **Chapter 4 - Resin fouling**

Resin aging/fouling during process operation can significantly decrease anion exchange chromatographic performance (Staby et al, 1998, Jin et al., 2009). There is a lack of fundamental knowledge and mechanistic understanding of fouling in industrial chromatographic processes. Therefore, the application of mechanistic models to industrial chromatographic processes is problematic, because model predictions are restricted to columns containing clean/new resin. Resin fouling of the anion exchange weak partitioning chromatography step considered in chapter three had been observed during purification process development of a monoclonal antibody. Significantly earlier breakthrough of impurities and premature loss of capacity was observed during experimental studies conducted by Iskra et al. (2013). The fouling was attributed to a unique quality of the particular feed stream.

In this thesis, the location of the foulant will be revealed, and the effect of fouling on protein uptake kinetics and resin capacity will be determined. The knowledge gained can increase process understanding, and thus provide for better informed process development and model formulation.

### 2.6.3. **Chapter 5 - Resin lot variability**

Serious performance issues were observed in a hydrophobic interaction chromatography (HIC) step at a late stage of development, which were attributed to resin lot variability. (Note that the HIC is part of a different process to the one considered in chapters three and four of this thesis). The HIC provides impurity clearance whilst producing a complex final

product composed of six closely related variants of a *dimer* protein therapeutic (~30 kDa), with their *monomer* subunits in a specific ratio. Impurity removal is well understood, however, achieving the correct monomer subunit ratio poses a purification challenge. An extended range of resin lots had been obtained from the supplier for testing within normal process operating ranges. All resin lots were within the manufacturers' specifications for ligand density and chloride capacity. Despite this, many resins failed to meet product quality specifications during testing, and would have incurred significant losses if used for the large scale manufacture of the product.

A model is developed and used in a process scenario to allow specific variables critical to product quality to be studied. Stochastic simulation is used in order to identify robust operating conditions, and the level of control required on uncertain process parameters/variables to bring process robustness to an acceptable level.

# Chapter 3. Weak Partitioning Chromatography

*A model based approach for linking experimental high throughput batch bind screens (HTS) and scouting runs traditionally conducted during process development is proposed. The approach is specific to a weak partitioning chromatography (WPC) anion exchange (AEX) polishing step that is part of Pfizer's two-step platform monoclonal antibody purification process. The approach involves the development of a simplistic 'platform' model that can be applied to new candidate molecules based on the results of a standard HTS. This is achieved by characterising the equilibrium isotherms of three critical components (monomer, dimer and multimer) of the WPC separation, as a function of the product partition coefficient, rather than the conventional approach of pH and counterion concentration. Use of the model is limited to an early stage of process development. This reduces the impact of inaccuracies due to simplifications made when formulating the model. Important advantages are realised by harnessing the models' predictive power when (1) there are maximum degrees of freedom available for bioseparation design, and (2) minimal investment has been made in the product. The model can quickly identify operating parameter ranges that are of interest for the purification of load material with challenging compositions. When combined with stochastic simulation, the model can explore the impact of process variability on product quality and process performance. This approach enables the purification of previously impossible to purify feed streams using the two-step platform monoclonal antibody purification process. It also identifies promising parameter ranges to explore experimentally, thus accelerating process development and helping optimise column performance.*

# 3.1. Introduction

A typical platform for the purification of monoclonal antibodies (mAb) derived from recombinant cell culture employs three chromatographic steps. Protein A capture is followed by two polishing steps, usually anion exchange (AEX) chromatography in flowthrough mode, and one of either cation exchange, ceramic hydroxyapatite or hydrophobic interaction chromatography. The Protein A capture step removes the bulk of the impurities, and the two polishing steps ensure clearance of host cell protein, DNA, high molecular mass species (HMMS - also known as aggregated product), virus and leached Protein A.

Weak partitioning chromatography (WPC) is an isocratic mode of protein purification that enables a two column purification process (e.g. Protein A affinity and AEX weak partitioning chromatography), rather than the established three column process (e.g. Protein A affinity, AEX and HIC chromatography). By reducing the number of chromatographic steps, process development is accelerated, and development and manufacturing costs are reduced. Although similar to flowthrough (FT) mode where impurities bind to the resin and the protein of interest flows through to be collected as product, WPC is distinct, as it is performed under mobile phase conditions where in addition to impurities a significant amount of product also binds to the resin. The more stringent binding conditions improve removal of impurities such that a third column is no longer required to assure impurity clearance, and any loss in yield due to adsorption of the product can be restored by extending the load challenge and conducting a wash step at the end of the load phase to recover the product.

The weak partitioning mode is defined by the product partition coefficient, $K_p$, falling between 0.1 and 20, which is distinct from bind and elute ($K_p > 100$) and flowthrough ($K_p < 0.1$) modes of chromatography. The product partition coefficient is defined as the ratio between the concentration of bound and unbound product in equilibrium in the linear region of the adsorption isotherm. In AEX, the product partition coefficient is modulated by the mobile phase pH and counterion concentration. Figure 3.1 overlays chromatograms from column runs at WPC ($K_p = 2$) and FT ($K_p < 0.1$) conditions. The chromatograms show that product breaks through later under WPC conditions, indicating higher protein adsorption during the load phase. The additional bound protein is recovered during the wash, without reducing impurity removal as illustrated by the larger WPC strip peak.

WPC operating conditions can be rapidly determined using high throughput batch binding studies (HTS), where resin is brought to equilibrium with small amounts of protein solutions

(< 5 g/L) at unique combinations of pH and counterion concentration. The protein concentration in the supernatant is measured and a mass balance is used to calculate the bound concentration and thus the partition coefficient. A response surface can be generated from the HTS data that plots the partition coefficient as a function of pH and counterion concentration. The response surface forms the basis for the development of a design space which provides sufficient clearance of impurities (e.g. host cell protein, DNA, HMMS, virus and leached Protein A). Initial ranges of pH and counterion concentration are defined for further characterisation by factorial design of experiment (DOE) studies on qualified scale down columns.

Several clinical current good manufacturing practice cGMP processes at Pfizer have utilised AEX in WPC mode, which has consistently provided excellent clearance of impurities whilst maintaining high step yields (> 90 %). Studies have shown that WPC is a robust polishing step over a wide range of operating conditions. However, feed material with high levels of high molecular mass species (especially product dimer) can occasionally pose a purification challenge, where operating conditions (e.g. pH, counterion concentration) need to be carefully chosen in order to assure impurity clearance. In extreme cases, a third chromatography column may be required. Scale down design of experiment studies in order to identify robust operating conditions for these challenging material compositions require a significant amount of time and material, contrary to industrial objectives.

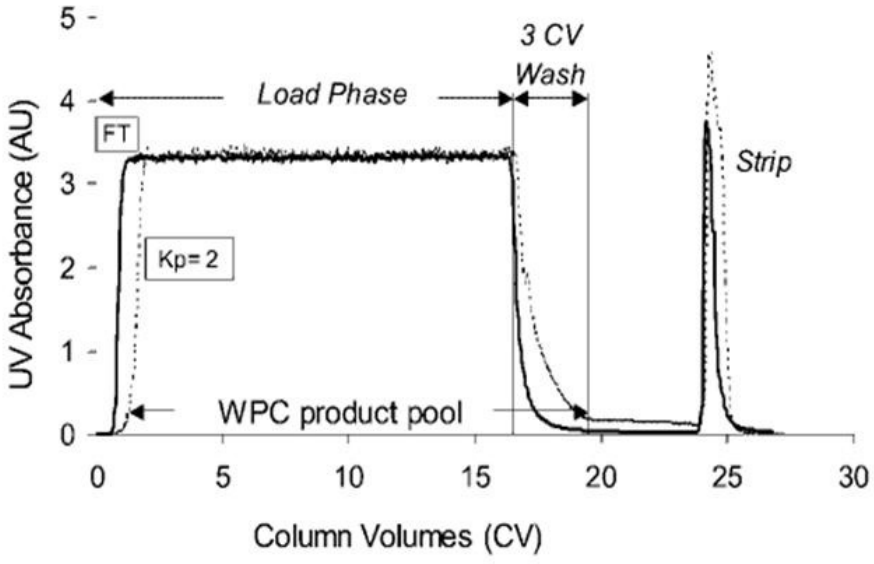


Figure 3.1. Overlay of chromatograms at flowthrough conditions (Solid line - $\mathbf{K_p}$ < 0.1) and weak partitioning conditions (dotted line - $\mathbf{K_p}$= 2) adapted from Kelley et al., 2008a.

A model based approach for application at an early stage of process development is proposed to provide a link between HTS and scale-down column studies. The objective is to enhance experimental efficiency, reduce the number of column studies necessary for process definition, and increase process understanding. The approach involves formulating a simplistic 'platform' model of the WPC containing a basic mass balance and a description of adsorption equilibrium. The key feature of the approach is that once the model has been developed, it can be applied to new candidate molecules based on the results of the standard HTS experiment conducted at the start of process development. This is achieved by prior characterisation of the equilibrium isotherms of three critical components of the WPC separation, namely the product monomer, dimer and multimer, as a function of the product partition coefficient, $K_p$, rather than pH and counterion concentration.

The approach is distinct, but complementary, to developing an exhaustive chromatographic rate model for each molecule, which may not be feasible at an early stage of process development due to limited time, material and analytics. The ability to quickly and efficiently explore potential operating conditions is particularly useful for scenarios where challenging feed material compositions pose problems for an experimental approach to process development. The approach is equally useful for increasing understanding of weak partitioning chromatography, and can indicate where enhancements to the WPC platform can be made. The difference between traditional development and the proposed approach is illustrated in Figure 3.2.

In this chapter, the platform model is developed and then tested. Ultra-scale down batch adsorption experiments are used to collect the data required to fit model parameters. Existing platform knowledge of how WPC operates, and molecule specific information provided by Pfizer, is used to choose relevant mobile phase conditions to characterise the equilibrium isotherms of the three critical components (monomer, dimer and multimer). The model is applied to two case studies to demonstrate how the model can be applied during early process development. In addition, an in-depth analysis of monomer – dimer selectivity, maximum load challenge, recovery, and the impact of uncertainty in the AEX WPC system is conducted, supported by relevant experimental studies. The results show how a model based approach based on fundamental process understanding can be used at an early stage of process development for exploring how process parameters (e.g. partition coefficient, load challenge and load concentration) can be controlled in order to raise product recovery to acceptable levels, whilst maintaining robust impurity clearance.

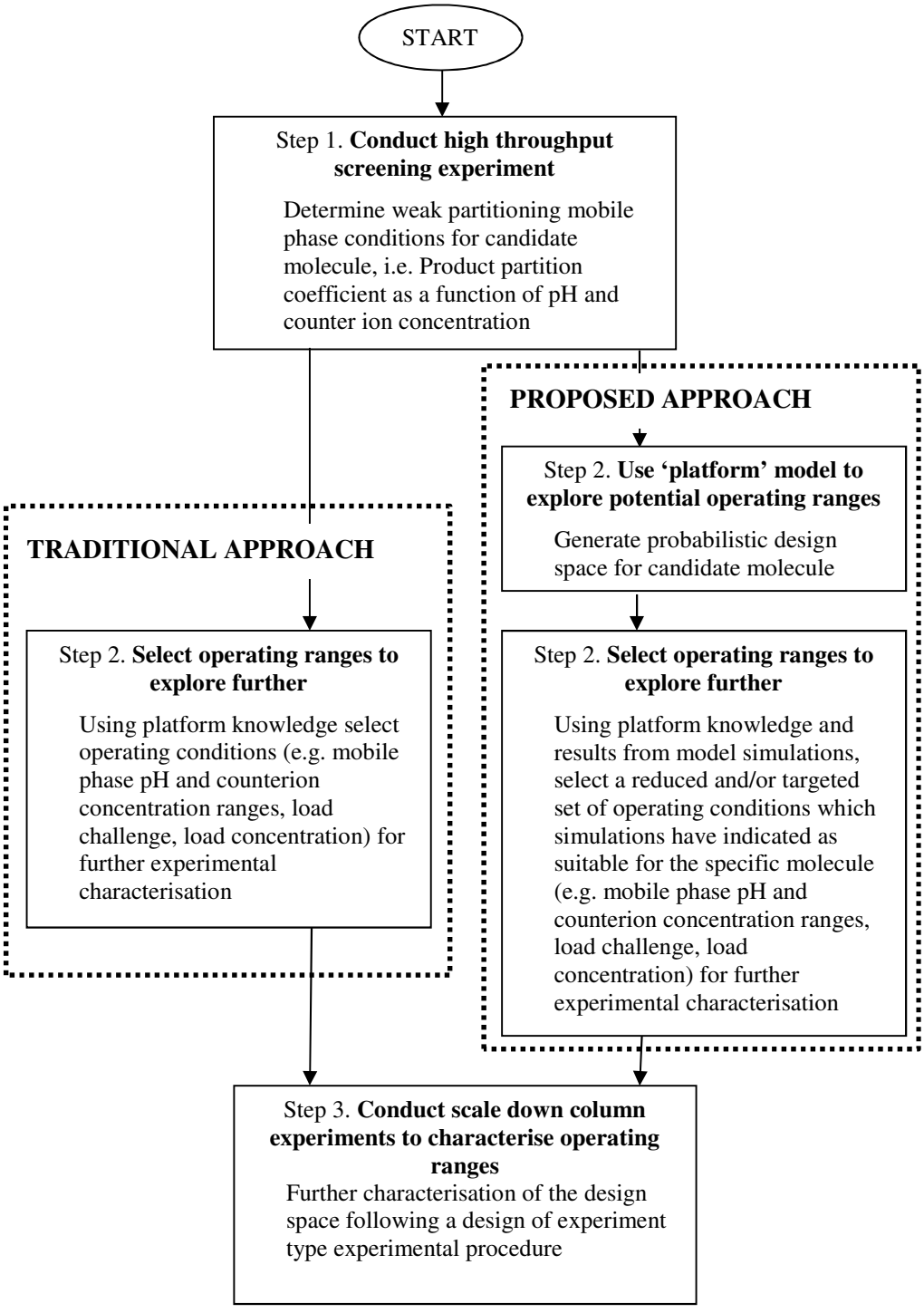


Figure 3.2. The difference between a traditional and the proposed early stage development approach utilising simplistic 'platform' model of WPC to provide a link between high throughput screening experiments and scale down column studies

## 3.2. Experimental Materials and methods

### 3.2.1. **Materials**

***Therapeutic protein and feed material***

Two different humanized IgG1monoclonal antibodies (mAb A and B) are used in this chapter. Both were produced in recombinant chinese hamster ovary (CHO) cells grown in serum free medium. Downstream processing prior to AEX WPC consisted of centrifugation and depth filtration, followed by Protein A chromatography. Load material used in experiments was derived from Protein A peak pools generated during either scale down process development or pilot plant studies. The correct pH and counterion concentration was achieved in load material by buffer exchange and dilution/concentration. Protein A peak pool material typically contained the product of interest, host cell proteins, DNA, residual Protein A which had leached from the affinity capture resin, and high molecular mass species (HMMS) comprised of dimer and multimer.

***Chromatography resin***

Fractogel® EMD TMAE HiCap (M) anion exch*a*nge resin was obtained from EMD Merck (Darmstadt, Germany).

***Equipment***

All preparative scale laboratory experiments were carried out using an ÄKTA FPLC chromatography system from GE Healthcare (Uppsala, Sweden). Laboratory columns used for WPC were 0.5 cm in diameter and 15 cm in height. A Tosoh TSK – GEL G3000SW$_{XL}$ high performance liquid chromatography (HPLC) column was used for analytics.

### 3.2.2. **Experimental methods**

***Depth filtration***

Depth filtration was used to reduce the amount of negatively charged species that were not considered in the model (HCP, DNA and leached Protein A) in neutralised Protein A peak pool material, prior to batch adsorption experiments. A XOHC depth filter was obtained from EMD Millipore (Billerica, MA). 26 cm$^2$ µPOD format filters were used for all experiments. The depth filter is based upon diatomaceous earth and is positively charged. It was used to reduce the amount of negatively charged species (HCP, DNA and leached Protein A) in neutralised Protein A peak pool material, prior to batch adsorption experiments. Before loading, the filters were flushed with 100 L/m$^2$ RO water to remove

preservative followed by 50 L/m$^2$ of equilibration buffer. Filters were loaded up to 200 L/m$^2$ at 200 LMH. After loading, any remaining protein was blown out of the filter with air.

### *High throughput screening for $K_p$ contours*

High throughput screening had been conducted prior to this work by Pfizer for the two different candidate monoclonal antibodies, A and B. The data was used to estimate parameters of response surface models of the partition coefficient, $K_p$, as a function of pH and counterion concentration for each mAb. The response surface model was used to help choose relevant mobile phase conditions to characterise the equilibrium isotherms of the three critical components (monomer, dimer and multimer). The high throughput screening methodology is presented in detail in the literature (Kelley et al., 2008a), showing the excellent fit ($r^2 > 0.985$), and high significance of parameters ($p < 0.01$), typically achieved during parameter estimation. The regression equations for mAbs A and B are presented in Table 3.1 and Table 3.2. Figure 3.3 shows the product partition coefficient as a function of pH and counterion concentration for monoclonal antibodies A and B generated using the response surface models (RSM) provided by Pfizer.

Table 3.1. Monoclonal antibody A regression equation terms and estimate

| Term | Estimate |
|---|---|
| Intercept | -6.99 |
| Total Cl | - 0.015 |
| pH | 0.90 |
| $(\mathrm{pH} - 8.3) \times (\mathrm{pH} - 8.3)$ | 0.47 |
| $(\mathrm{Cl} - 45.23) \times (\mathrm{Cl} - 45.23)$ | 0.00013 |
| $(\mathrm{pH} - 8.3) \times (\mathrm{Cl} - 45.23)$ | - 0.018 |

Regression Equation:

$$\log \mathrm{K_p} = -6.99 + (\text{Total Cl} \times -0.015) + (\mathrm{pH} \times 0.90) + \big((\mathrm{pH} - 8.3) \times (\mathrm{pH} - 8.3) \times 0.47\big) + \big((\mathrm{Cl} - 45.23) \times (\mathrm{Cl} - 45.23) \times 0.00013\big) + ((\mathrm{pH} - 8.3) \times (\mathrm{Cl} - 45.23) \times -0.018))$$

Table 3.2. Monoclonal antibody B regression equation terms and estimate

| Term | Estimate |
|---|---|
| Intercept | - 6.37 |
| Total Cl | -0.013 |
| pH | 0.91 |
| $(\mathrm{pH} - 7.74) \times (\mathrm{pH} - 7.74)$ | 0.38 |
| $(\mathrm{Cl} - 50.25) \times (\mathrm{Cl} - 50.25)$ | 0.000058 |
| $(\mathrm{pH} - 7.74) \times (\mathrm{Cl} - 50.25)$ | - 0.020 |

Regression Equation:

$$\log \mathrm{K_p} = -6.37 + (\text{Total Cl} \times -0.013) + (\mathrm{pH} \times 0.91) + \big((\mathrm{pH} - 8.3) \times (\mathrm{pH} - 8.3) \times 0.38\big) + \big((\mathrm{Cl} - 45.23) \times (\mathrm{Cl} - 45.23) \times 0.000058\big) + ((\mathrm{pH} - 8.3) \times (\mathrm{Cl} - 45.23) \times -0.02))$$

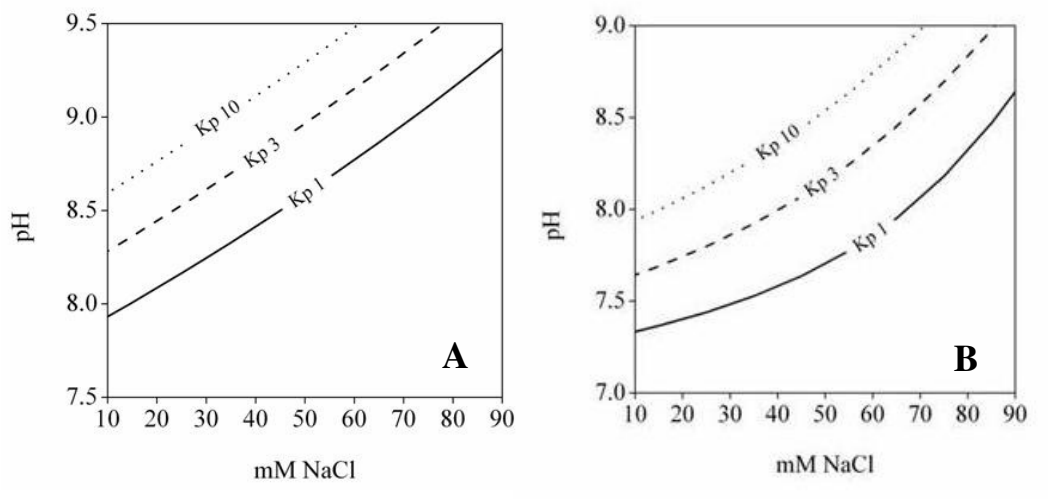


Figure 3.3. Monoclonal antibody A and B product partition coefficient, $K_p$, contours as a function of pH and counterion concentration. The contour plots were generated using response surface models generated from high throughput screening studies conducted prior to this work at Pfizer.

***Batch adsorption experiments***

Batch adsorption experiments were conducted using mAbs A and B to generate data for estimating isotherm parameters for monomer, dimer and multimer adsorption in the WPC AEX system. HCP, DNA and leached Protein A was removed prior to batch adsorption studies via depth filtration (mAb A) or WPC (mAb B). MAb A material contained 89% monomer, 8% dimer and 3% multimer. MAb B material contained 89% monomer, 2% dimer and 9% multimer. Response surface models (Table 3.1 and Table 3.2) provided by Pfizer were used to select pH and counterion concentrations (Table 3.3) for batch adsorption experiments. The experiments were designed in order to ensure broad coverage of the mobile phase conditions typically explored during process development. Figure 3.4 illustrates the breakdown of the experimental study. The concentration of monomer, dimer and multimer in the solid and liquid phase was determined for three product partition coefficients ($K_p$ = 1, 3 and 10), at three unique counterion/pH combinations for each product partition coefficient, and 5 different load concentrations ($[C_0]$ = 0.2, 0.5, 1, 1.5 and 2 mg/ml), with all experiments repeated in triplicate.

The experiments were based on the work of Coffman et al. (2008), conducted in a 96-well 800µl were round-well filterplates with 0.45 µm pore-size polypropylene membrane, and repeated in triplicate. 25µl of resin was taken from a bulk reservoir and dispensed by the robotic liquid handler into the individual wells as 25% (v/v) slurry in the appropriate

equilibration buffer. The plate was then centrifuged to evacuate excess liquid and leave damp resin. Subsequently, load material was added into wells containing the resin. The initial concentrations for each filter plate well were produced by mixing together protein from bulk solutions of known concentrations and compositions, with the appropriate amount of equilibration buffer from a bulk solution in order that the total volume of liquid dispensed into each well was 275µL ($V_{tot}$). The resin and solutions were then agitated on a platform shaker for 120 minutes. Studies have indicated that this incubation time was suitable for this system (Kelley et al. 2008a). Foil adhesive tape was used on the underside of the filter-plate to prevent liquid loss during shaking.

Table 3.3. Mobile phase conditions used in batch adsorption isotherm experiments

| **Target $K_p$** | **Condition identifier** | **Ionic strength (mM)** | **pH** |
|---|---|---|---|
| 1 | A1 | 15 | 8.00 |
| 1 | A2 | 30 | 8.24 |
| 1 | A3 | 50 | 8.58 |
| 1 | B1 | 35 | 7.52 |
| 1 | B2 | 50 | 7.70 |
| 1 | B3 | 70 | 8.05 |
| 3 | A1 | 15 | 8.36 |
| 3 | A2 | 30 | 8.61 |
| 3 | A3 | 50 | 8.96 |
| 3 | B1 | 70 | 8.56 |
| 10 | A1 | 15 | 8.67 |
| 10 | A2 | 30 | 8.93 |
| 10 | A3 | 50 | 9.29 |
| 10 | B1 | 30 | 8.19 |
| 10 | B2 | 50 | 8.53 |
| 10 | B3 | 65 | 8.85 |

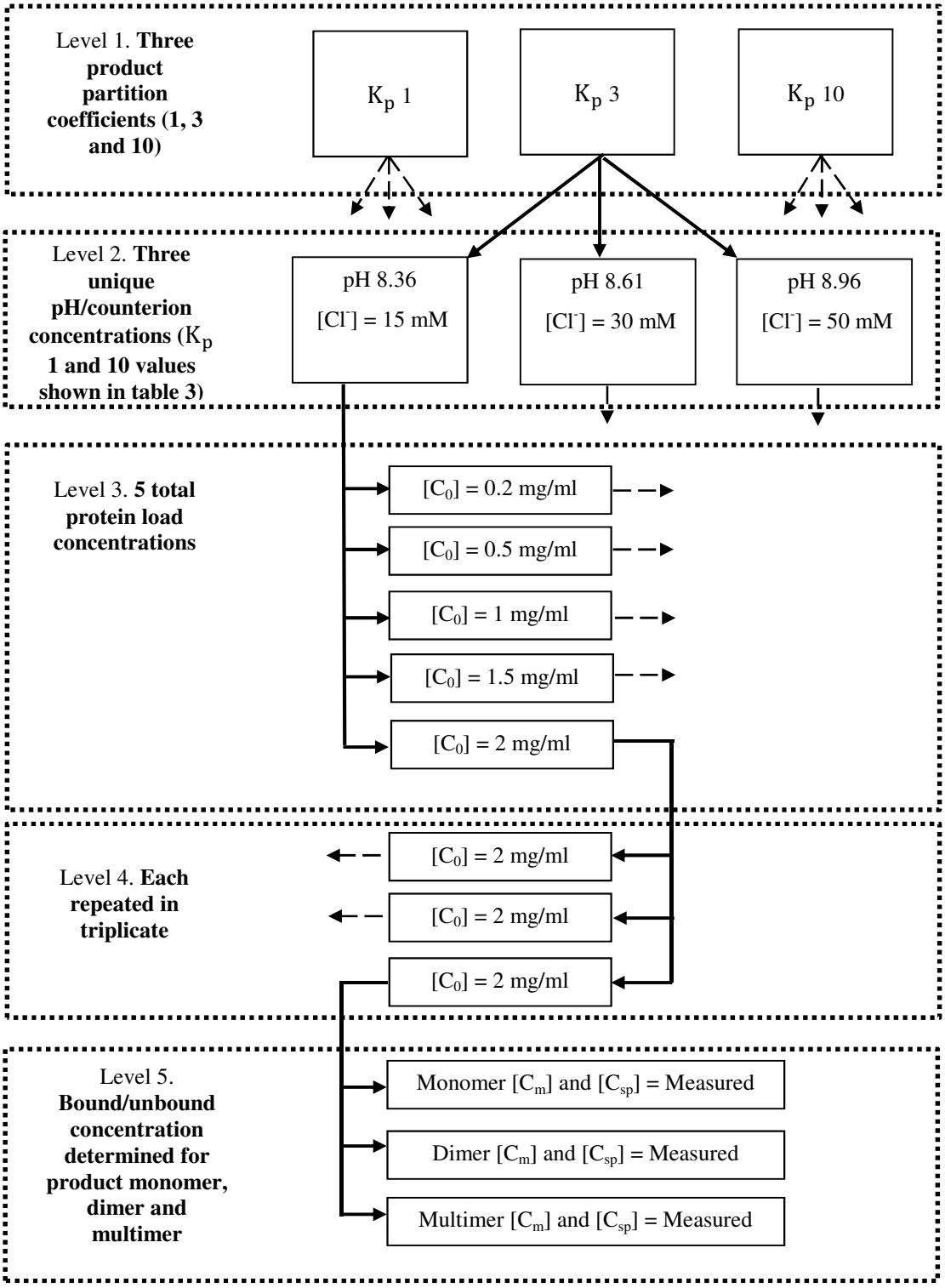


Figure 3.4. Breakdown of experimental batch adsorption studies used to characterise the adsorption equilibria of monomer, dimer and multimer

After incubation, a centrifuge evacuated the supernatant into a UV-transparent 96 well micro plate which was stacked beneath the filter plate for analysis. The supernatant was then analyzed by a 96-well UV spectrophotometer (SpectraMax 250, Molecular Devices, Sunnyvale, CA) to determine the concentration of protein in the supernatant, $C_i^m$. Size exclusion chromatography (SEC) high performance liquid chromatography (HPLC) was used to determine the percentage of each component in the supernatant, $P_i^m$. The concentration of the protein in the mobile phase is then calculated from Eq 3.1:

$$C_i^m = \frac{C_{equil} \cdot P_i^m}{100} \qquad [3.1]$$

where $C_i^m$ is the concentration of component $i$ in the mobile phase in mg/ml, $C_{equil}$ is the measured concentration in the supernatant of the micro well determined by UV spectroscopy, and $P_i^m$ is the percentage of component $i$ in the mobile phase as determined by SEC HPLC.

An elution cycle was then conducted following the same methodology as the load cycle, where 275 µL of elution buffer was added to each well, the plate agitated on a platform shaker for 120 minutes and the supernatant subsequently collected as described previously and analysed using the spectrophotometer and SEC HPLC. The amount of protein adsorbed per unit volume settled resin, $q_i$, was calculated using Eq 3.2:

$$q_i = \left(\frac{V_{elution}}{V_{resin}}\right) \cdot C_{elution} \cdot \left(\frac{P_i^{elution}}{100}\right) \qquad [3.2]$$

where $C_{elution}$ is the concentration of the elution supernatant (mg/ml) determined by UV spectroscopy, $P_i^{elution}$ is the percentage of component $i$ in the elution phase as determined by SEC HPLC, $V_{elution}$ is the volume of the elution supernatant (275 µl in this work), and $V_{resin}$ is the settled volume of resin in the microwell (25 µl in this work).

***Size exclusion HPLC***

Size exclusion HPLC was used to determine the relative percentages of monomer, dimer and multimer in samples (taken from both batch adsorption experiments and column runs). The size exclusion (SEC) HPLC assay utilises a Tosoh TSK – GEL G3000SW$_{XL}$ stainless steel column, 7.8 mm ID × 30 cm length, 5 $\mu$m mean particle size. After equilibrating the column with 10 mM Sodium Phosphate, 500 mM Sodium Chloride at pH 7.3 for 90 minutes or until a stable baseline is established, 50 µl samples at approximately 3 mg/ml are injected onto a column at a flowrate of 0.5 ml/min. The separation is isocratic. Molecules are

separated by their hydrodynamic volume, and elute in order of molecular size (largest first). Absorbance at 280 nm is measured at the column exit. Integration of the resulting chromatogram and analysis of the relative percentage area of each peak indicates the percentage of each component in the sample. The total time to run each sample is 30 minutes.

***Weak partitioning chromatography***

Column runs were conducted to validate model predictions. During all experiments the columns were first equilibrated with buffer at the desired pH and counterion concentration. Load material at the desired pH and counterion concentration was then applied to the column at 150 cm/hr. In certain experiments the load was followed by a wash of the equilibration buffer. The load eluate (and wash if present) was collected as the process pool, and any remaining bound protein was removed using a 2 M NaCl strip buffer. The columns were sanitized with 2 M NaCl, 0.5 M NaOH and stored in 16% ethanol, 150 mM NaCl, 50 mM TRIS, pH 7.5.

***Summary***

In order to characterise the adsorption equilibria of the two monoclonal antibodies on Pfizer's WPC AEX platform process, material was generated via column experiments, and prepared for batch adsorption studies by depth filtration, followed by buffer exchange and dilution/concentration. High throughput batch adsorption studies were then conducted. A robotic liquid handler deposited resin into 96 well plates, and protein was added to each well by hand. The liquid supernatant was collected for analysis via centrifugation following resin equilibration and resin strip. The total concentration and percentage of each species in the material were measured using UV spectroscopy and size exclusion high performance liquid chromatography, respectively. All experiments were repeated in triplicate, and the resulting data was used for estimating adsorption isotherm model parameters. In order to validate the model and test the proposed approach, multiple column studies were conducted. In all studies, material was prepared by buffer exchange and dilution/concentration, and the analytical techniques used for characterising flowthrough, wash and strip fractions collected during experiments were identical to those used in the batch adsorption studies.

# 3.3. Mathematical methods

### 3.3.1. **Chromatography model**

***Adsorption isotherm***

Single component Langmuir isotherms were used to describe the adsorption of the monomer, dimer and multimer species in the AEX WPC system. The model assumes monolayer adsorption at a finite number of equivalent and identical binding sites, with no lateral interactions, steric hindrance, migration of adsorbed molecules on the adsorption surface, or competition for binding sites between species. In particular, assuming no competition for binding sites is unrealistic in the multicomponent AEX WPC system. However, the experimental effort required to elucidate competitive phenomena is prohibitive at an early stage of process development. The impact of this erroneous, but necessary, assumption on model predictions was minimised by: (i) fitting model parameters to data collected under competitive conditions typically experienced in the industrial process, where monomer accounts for 85-90 % of the load material, and (ii) restricting the application of the final model to an early stage of process development. The single component Langmuir adsorption isotherm was extended to cover the mobile phase conditions considered in experimental studies by writing the adsorption isotherm parameters, $a_i$ and $b_i$, as a function of the product partition coefficient, $\mathrm{K_p}$, for monomer and dimer, and constant for multimer:

$$q_i = \frac{a_i \cdot C_i}{1 + b_i \cdot C_i} \qquad \forall i = \text{Monomer, dimer, multimer} \qquad [3.3]$$

$$a_{\text{monomer}} = \alpha_{\text{monomer}} \cdot \mathrm{K_p} \qquad [3.4]$$

$$a_{\text{dimer}} = \alpha_{\text{dimer}} \cdot \mathrm{K_p} \qquad [3.5]$$

$$a_{\text{multimer}} = \alpha_{\text{multimer}} \qquad [3.6]$$

$$b_{\text{product}} = \beta_{\text{dimer}} \cdot \mathrm{K_p} \qquad [3.7]$$

$$b_{\text{dimer}} = \beta_{\text{dimer}} \cdot \mathrm{K_p} + \gamma \qquad [3.8]$$

$$b_{\text{multimer}} = \beta_{\text{multimer}} \qquad [3.9]$$

where

$q_i$ = Bound concentration of component i [mg/ml]

$C_i$ = Mobile phase concentration of component i [mg/ml]

$a_i$ = Adsorption constant of component i

$b_i$ = Adsorption constant of component i

$\alpha_i$ = Adsorption constant of component i

$\beta_{\mathrm{i}}$ = Adsorption constant of component i

$\gamma$ = Adsorption constant

$\mathrm{K_p}$ = Product partition coefficient

***Mass conservation***

A simple mass balance is used to predict the amount of each species collected in the flowthrough during column runs, i.e. the capacity of the column for each species (as predicted by the adsorption isotherm model) is subtracted from the amount of each species loaded onto the column. The flowthrough amounts can then be used to predict column performance such as product recovery and purity.

### 3.3.2. **Adsorption isotherm parameter estimation**

The 'parameter estimation' entity in gPROMS™ is based on the SRQPD sequential quadratic programming code, and was used to estimate parameters, $\alpha_{\mathrm{i}}$ and $\beta_{\mathrm{i}}$, from the empirical equations, which link the Langmuir adsorption isotherm parameters, $a_i$ and $b_i$, to the product partition coefficient, $\mathrm{K_p}$. Parameter estimation was based on the maximum likelihood formulation, which determines values for the uncertain physical and variance model parameters that maximise the probability that the model will predict measured values from development experiments (Process Systems Enterprise, 2013). Parameters were estimated by fitting the single component Langmuir isotherm model to batch adsorption experimental data (section 3.3.2).

### 3.3.3. **Stochastic simulations**

Stochastic simulations were conducted to explore the impact of uncertainty/variability on process performance. Uncertainty in process parameters of interest is accounted for by specifying a probability distribution function with appropriate arguments (e.g. a normal distribution defined by the average and standard deviation). During stochastic simulations, a built in function within gPROMS is used that returns a random value sampled from the probability distribution function. Each time a simulation is run, a different value is picked for the uncertain variable/parameter of interest. Multiple simulations are conducted (> 5000). Process performance parameters (e.g. recovery) and/or critical product attributes or interest (e.g. purity) are recorded. The data is used to generate process performance mean and variance as a function of process parameter/variable mean and variance. The performance parameters considered in this chapter are the monomer recovery and purity in the flowthrough material. The sequence of calculations is illustrated in an example shown in Figure 3.5.

Table 3.4. Uncertain process parameters

| Process parameter | Uncertainty | Notes |
|---|---|---|
| Equilibration buffer pH | ± 0.05 pH | Neutralised Protein A peak pool is brought to correct pH by titration. If TRIS is used, note it has a pI temperature dependence. |
| Equilibration buffer counterion concentration (mM) | ± 5 mM | Counterion concentration from Protein A elution buffer. |
| Bed height (cm) | ± 0.5 cm | - |
| Compression factor | 1.15 – 1.25 | - |
| Load volume (ml) | ± 1 ml | Usually ± 5% for a large scale column. The uncertainty for experimental studies conducted in this work was ± 1ml using a 50 ml super loop. |
| Total load concentration (mg/ml) | ± 0.2 mg/ml | Measured using A280 reading of the neutralised Protein A peak pool, and includes contributions from all protein species in load. |
| Load monomer, dimer and multimer composition (on a mass fraction basis) | ± 0.05 | Not usually measured prior to AEX WPC but general range will be known from process development studies. |

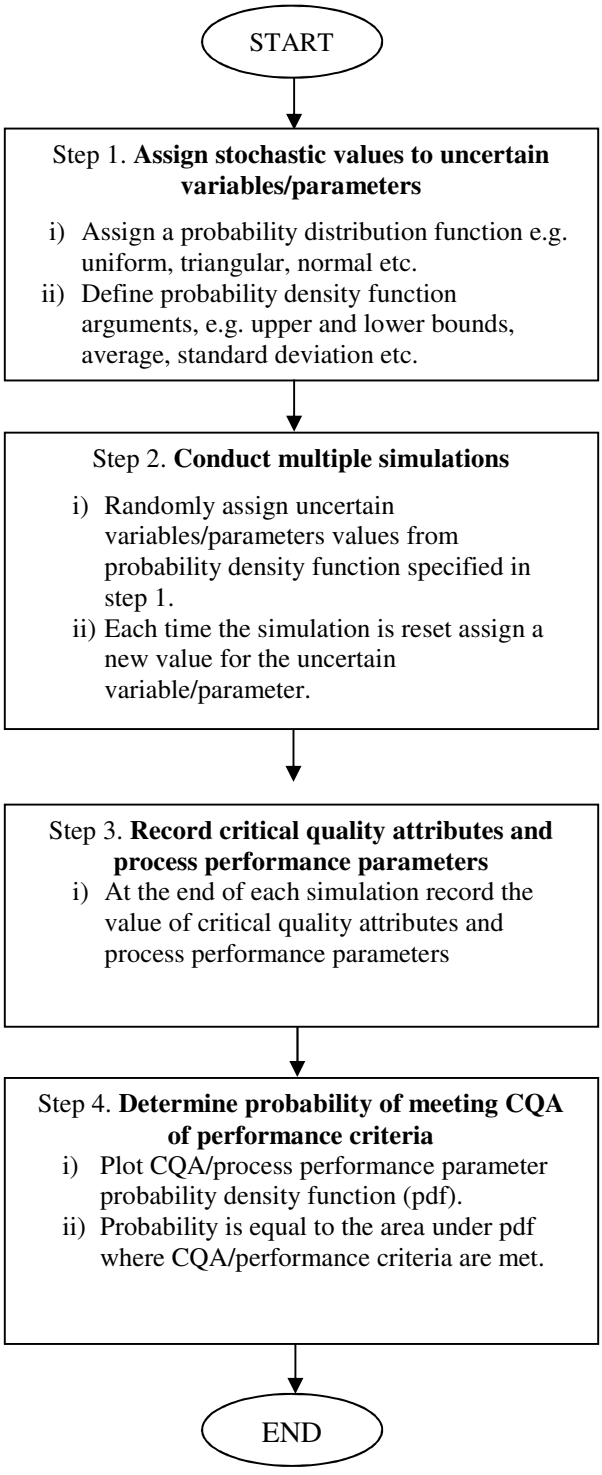


Figure 3.5. The sequence of calculations used for the stochastic simulations conducted in this work.

The stochastic simulations considered uncertainty in multiple process variables and parameters as shown in Table 3.4. They include: (i) equilibration buffer ionic strength, (ii) equilibration buffer pH, (iii) total load material concentration, (iv) load material monomer, dimer and multimer composition, (v) resin compression factor for the packed bed, (vi) load volume and (vi) column volume. Uncertainty in the load material concentration and composition can be attributed to the biological source of load material, and the desire to minimise the use of analytics on process intermediates. The practical challenges of operating chromatographic equipment results in uncertain bed heights, resin compression, and volumes of material applied to the column. The pH and counterion concentration can only be controlled to the precision of measurement devices. Note that the uncertainty in the load volume is due to practical inaccuracies when applying the desired volume to the column, i.e. not due to uncertainty in the total load concentration and column volume, which are both assumed correct when calculating the load volume in the model. Further details are provided alongside simulation results.

## 3.4. Model calibration

The WPC AEX model developed in this work is based upon characterisation of the equilibrium isotherms of three critical components of the WPC separation (monomer, dimer and multimer), as a function of the product (monomer) partition coefficient, $K_p$. This was achieved using batch adsorption experiments (sections 1.2.2.1 to 1.2.2.4). In the following section, the experimental adsorption isotherm data collected from the batch adsorption experiments is presented and discussed. The data is then used to fit the adsorption isotherm model parameters described in section 1.2.3 using parameter estimation in gPROMS (section 1.2.4).

### 3.4.1. **Experimental adsorption isotherms**

Adsorption isotherms are shown for monomer in Figure 3.6, dimer in Figure 3.7, and multimer in Figure 3.8, at the mobile phase conditions described in Table 3.3. The initial slopes of all monomer isotherms (Figure 3.6) matched the target product partition coefficients, and confirming suitable mobile phase conditions were achieved in the batch adsorption experiments. The data scatter is due to experimental inaccuracies in the batch adsorption method. A robot was used to ensure high precision when dispensing resin solutions. However, all protein dispensing was completed by hand which introduced variability, especially during series dilution of the equilibration and elution supernatant, which was required for measurement of protein concentration by UV spectroscopy. It was also difficult to control the pH and counterion concentration of the mobile phase, which is

important as the partition coefficient and thus the binding strength is sensitive to small changes in these parameters. The pH was sensitive to temperature change as TRIS is used for buffering, and the RSM predictions used to identify operating conditions contain uncertainty themselves. Despite the scatter, the data was deemed adequate for early process development objectives where an exact process representation is unnecessary.

Adsorption isotherms (monomer in Figure 3.6, dimer in Figure 3.7, and multimer in Figure 3.8) at a constant product partition coefficient were similar regardless of the molecule or exact mobile phase conditions, suggesting that the adsorption isotherms can be approximated exclusively as a function of the product partition coefficient. This facilitates a generic model to be formulated for this system which can be applied irrespective of molecule, providing the unique relationship between the product partition coefficient and mobile phase conditions is determined using the traditional high throughput screening methodology, presented in detail in the literature (Kelley et al., 2008a).

As the product partition coefficient increases, the monomer and dimer adsorption isotherms become increasingly nonlinear, and the bound concentrations increase (Figure 3.6 and Figure 3.7). It is interesting to consider dimer removal implications for a typical batch of load material which contains 3% dimer and 90% monomer at a total concentration of 8 mg/ml, corresponding to 0.24 mg/ml dimer and 7.2 mg/ml monomer. At these industrially relevant concentrations, the amount of dimer that binds to the resin (Figure 3.7) is typically an order of magnitude lower than monomer (Figure 3.6), regardless of partition coefficient. The example illustrates the difficulty of developing a process which can achieve adequate dimer removal whilst maintaining monomer recovery without fundamental knowledge of the adsorption isotherms. The relative shapes of the monomer and dimer isotherms (Figure 3.6 and Figure 3.7, respectively) suggest a reduction in load concentration may reduce monomer binding and thus increase monomer recovery, with minimal impact on dimer removal.

The multimer batch adsorption data suggests multimer isotherms remain unchanged regardless of the partition coefficient (Figure 3.8). Matching isotherms were observed at partition coefficients of 1 and 3. A multimer capacity of 11 mg/ml ± 1 mg/ml was found, which is in agreement with understanding of the WPC AEX system at Pfizer. Experimental discrepancies found in SEC analytics indicated that insufficient multimer was present in the load material used for partition coefficient of 10 to reach a bound concentration of 11 mg/ml, thus an isotherm could not be generated. Because of the very nonlinear isotherms at partition coefficients at 1 and 3, a conservative assumption is that the multimer isotherm at a partition coefficient of 10 is similar.

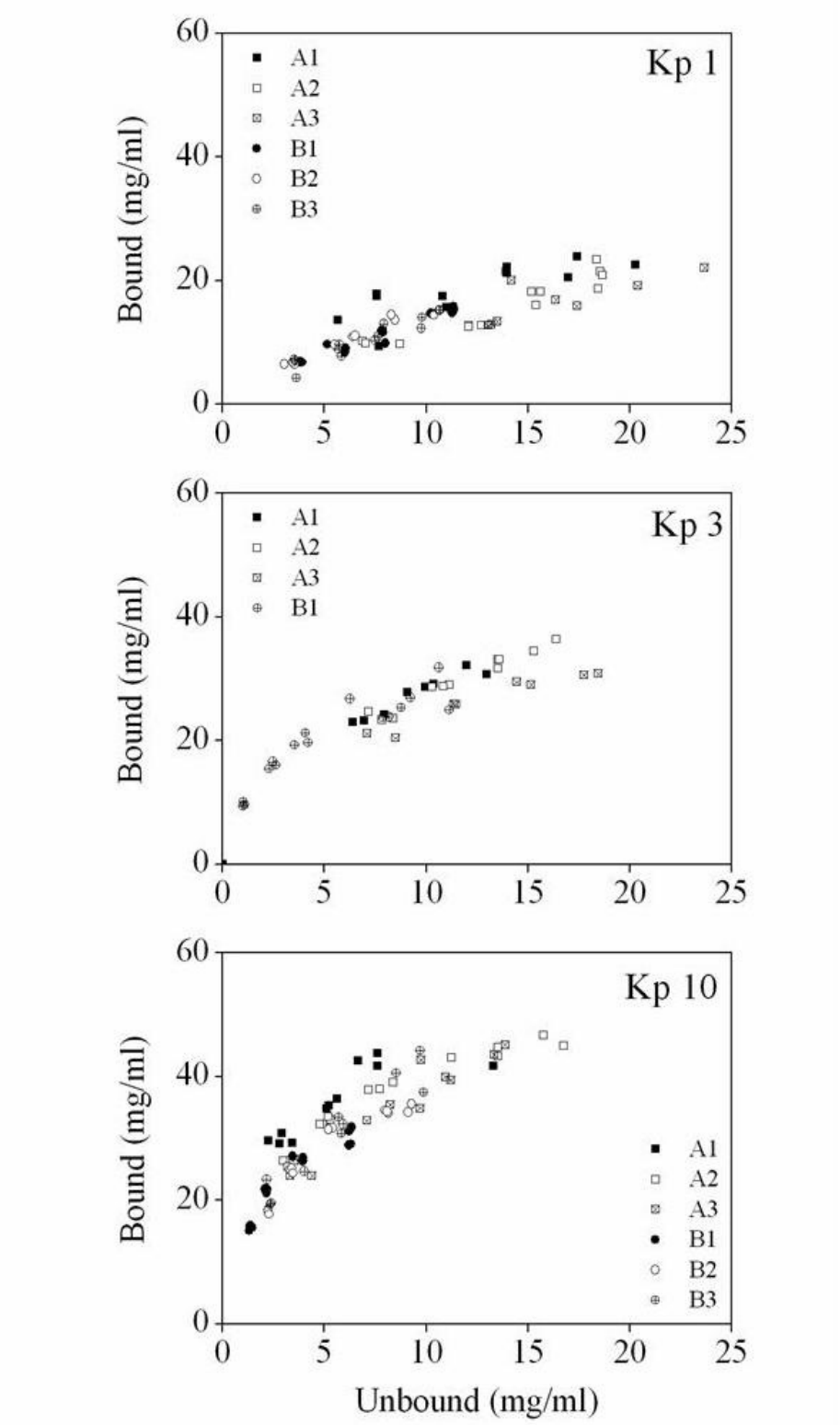


Figure 3.6. Monomer adsorption isotherm data from batch adsorption experiments at product partition coefficients, $K_p$, of 1, 3 and 10.

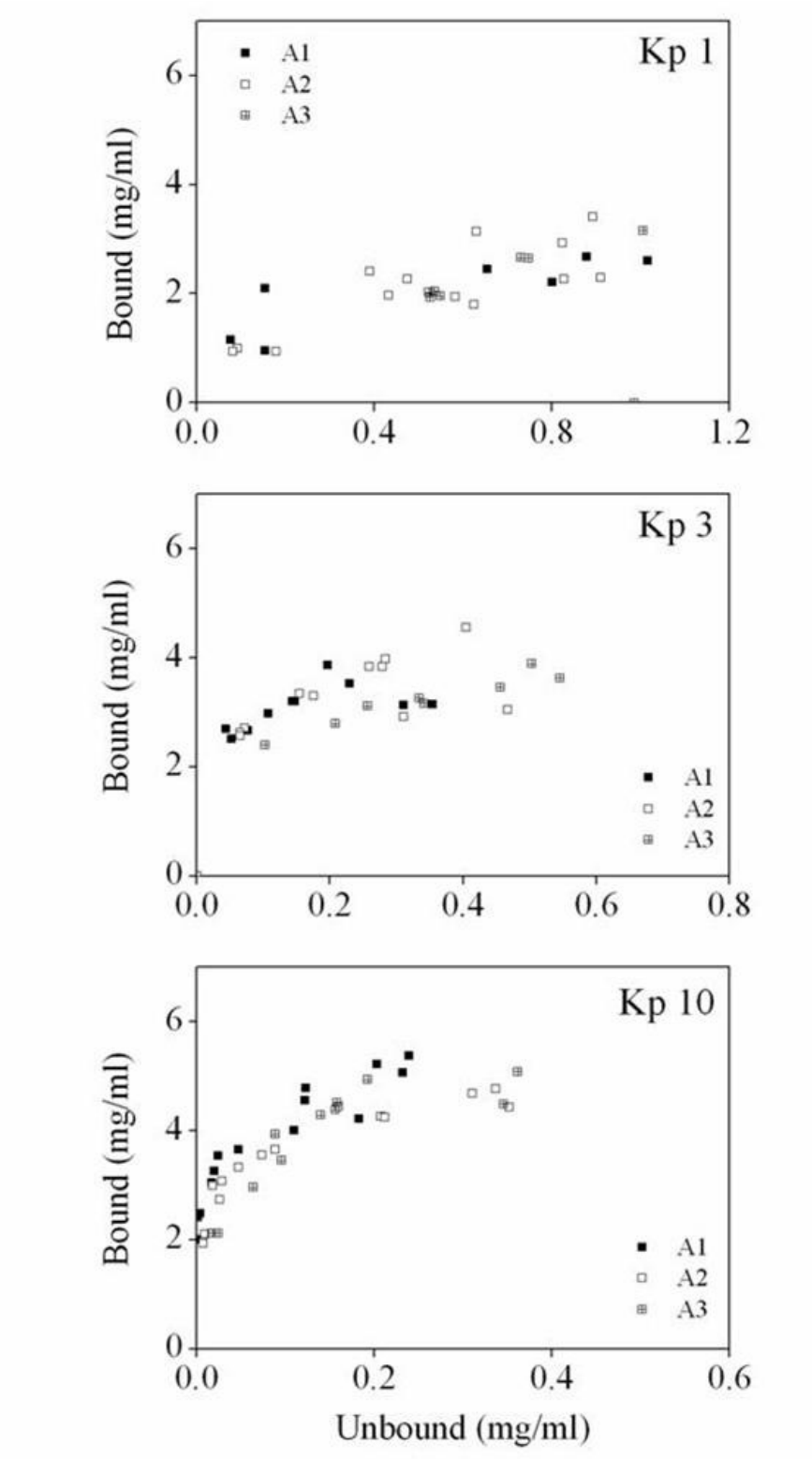


Figure 3.7. Dimer adsorption isotherm data from batch adsorption experiments at product partition coefficients, $K_p$, of 1, 3 and 10.

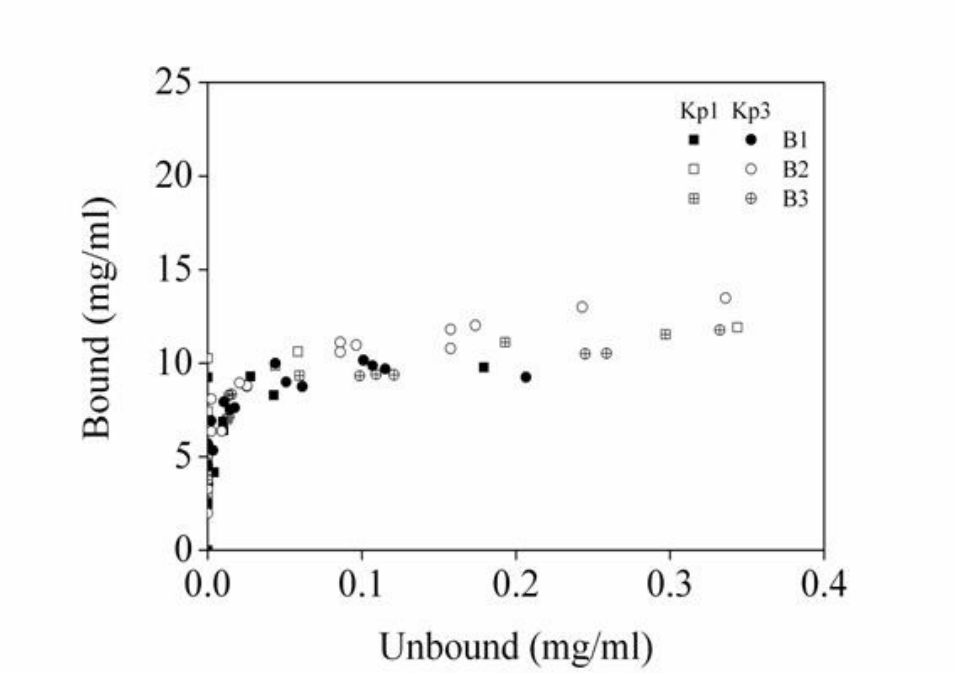


Figure 3.8. Multimer adsorption isotherm data from batch adsorption experiments at product partition coefficients, $K_p$, of 1 and 10.

Clearly the AEX WPC system provides extremely robust multimer removal provided the column is not over challenged. The data shown in Figure 3.8 suggests that even large changes in the pH and counterion concentration have no effect on the multimer isotherms within the WPC operating region considered ($1 < K_p < 10$), and the concentration of multimer in typical load material will seldom fall to levels where the resin capacity falls below 11 mg/ml (±0.05 mg/ml).

Table 3.5. Values of estimated isotherm parameters in Equation 3.3 to 3.7

| **Species** | $\alpha$ | **StDev** | $\beta$ | **StDev** | $\gamma$ | **StDev** |
|---|---|---|---|---|---|---|
| Monomer | 1.67782 | 0.056 | 0.031065 | 0.0019 | - | - |
| Dimer | 23.4248 | 1.8 | 4.28984 | 0.44 | 3.7612 | 0.53 |
| Multimer | 2035.64 | 290 | 183.224 | 29 | - | - |

### 3.4.2. **Adsorption isotherm model fit**

The adsorption isotherm models were fit to averaged batch adsorption data as shown in Figure 3.9. Estimated parameter values are shown in Table 3.5. The model gave excellent predictions which was interesting given the simplistic nature of the empirical equations used to link the product partition coefficient, $K_p$, to the isotherm parameters, $a_i$ and $b_i$. Values for classical Langmuir parameters (i.e. saturation capacity and equilibrium constant) can be determined from the estimated parameters. The data suggest the saturation capacity of the monomer is constant regardless of the partition coefficient at 59 mg/ml settled resin. The saturation capacity of the dimer increases between partition coefficients of 0 – 4 and then levels off. At a partition coefficient of 4, the dimer saturation capacity has already reached 90% of the saturation capacity at a partition coefficient of 10. Although this suggests that increasing the partition coefficient past 4 may not be helpful for increasing impurity removal whilst maintaining recovery, dimer removal at partition coefficients higher than 4 will be more robust because the adsorption isotherm will be less sensitive to changes in pH and counterion concentration. The estimated parameters suggest the multimer saturation capacity is constant at 11 mg/ml. As discussed previously, this is in agreement with understanding of the WPC AEX system at Pfizer.

## 3.5. Model applications

A model of the weak partitioning anion exchange chromatography process has been developed. The model consists of a basic mass balance and a description of adsorption equilibrium (section 1.2.3) which was calibrated using batch adsorption experimental data. The application of the model at an early stage of process development is now considered. The model is combined with stochastic simulation (section 1.2.5) and used to explore operating conditions for two case studies by generating probabilistic design spaces for molecules A and B. The stochastic calculations generate probability density functions of process performance parameters (flowthrough recovery) and critical quality attributes (product purity), as a function of the variability experienced in process variables (e.g. total load concentration and load composition) and process parameters (e.g. buffer pH, buffer counterion concentration, load volume, bed height, resin compression) shown in Table 3.4. The probabilistic design spaces are used to select promising operating conditions for providing robust impurity clearance whilst maintaining product recovery, which are subsequently tested experimentally via column runs. An in-depth analysis of monomer – dimer selectivity, maximum load challenge, recovery, and the impact of uncertainty in the process is then conducted, supported by relevant experimental studies.

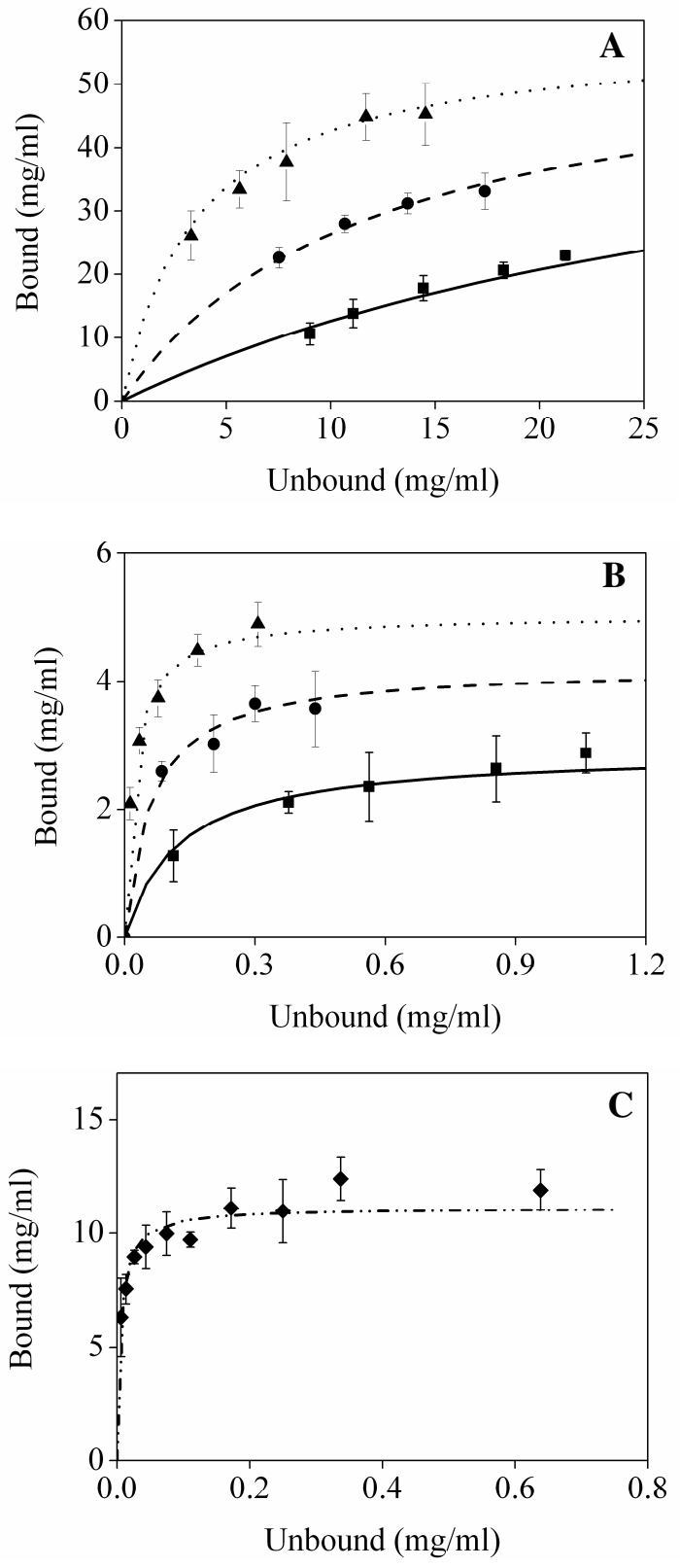


Figure 3.9. Adsorption isotherm model (lines) fit to batch adsorption experiments, data points showing 1 standard deviation. A. Monomer and B. Dimer: ■ $\mathbf{K_p}1$, ● $\mathbf{K_p}3$, ▲ $\mathbf{K_p}10$. C. Multimer: ♦ $\mathbf{K_p}$ 1-10.

### 3.5.1. **Case studies**

Case study 1 considers monoclonal antibody A. The load material contains 89% monomer, 9% dimer, and 2% multimer. Traditionally this composition would represent too great of a purification challenge for a two column process due to the high percentage of dimer. As a result, a third chromatography column would be required with an associated increase in costs. In this study, the model is used to explore whether there are conditions available in the design space which would achieve sufficient impurity removal with satisfactory product recovery to facilitate a two column process. Stochastic simulations were conducted to calculate the probability of meeting the desired product purity (> 0.98 monomer) across a knowledge space encompassing parameter ranges shown in Table 3.6.

Case study 2 considers monoclonal antibody B. The load material contains 89% monomer, 2% dimer and 9% multimer. The purification should be straightforward because the load material contains only small amounts of dimer. However, it is important to ensure that the load challenge is carefully selected so that no breakthrough of multimer occurs. In this study, the model is used to find conditions which achieve robust impurity removal whilst maximising product recovery. Stochastic simulations were conducted to calculate the probability of meeting the desired product purity (> 0.98 monomer) across a knowledge space encompassing parameter ranges shown in Table 3.6.

Table 3.6. Parameter ranges explored during model simulations.

| **Parameter** | **Lowest value considered** | | **Highest value considered** | |
|---|---|---|---|---|
| | MAb A | MAb B | MAb A | MAb B |
| Total load concentration | 2 mg/ml | 2 mg/ml | 11 mg/ml | 11 mg/ml |
| Load challenge | 40 mg/ml resin | 60 mg/ml resin | 120 mg/ml resin | 140 mg/ml resin |
| Product partition coefficient, $K_p$ | 1 | 1 | 10 | 10 |

Figure 3.10 shows the knowledge space explored at a partition coefficient of 3 and 1 for Case studies 1 and 2, respectively. The shaded areas show the region where the predicted probability of assuring that flowthrough material purity is greater than 98% is 1.0 (red), 0.9 (purple) and 0.8 (pink). The contour lines show the predicted recovery mean. Interestingly, the probability of meeting the purity objective drops very sharply for case study 1 compared to a much more gradual drop in case study 2. This is reflecting the impact of uncertain process parameters on the resin's capacity for binding dimer and multimer. Figure 3.10 shows that multimer removal is extremely robust in this AEX WPC system regardless of uncertainty in pH and counterion concentration, however, dimer removal is not. Reasons for this will become clear when considered in depth in section 3.5.2.

The probabilistic design spaces were used to select promising operating conditions. For case study 1, a total load concentration of 3.3 mg/ml and a load challenge of 50 mg/ml resin was selected for testing experimentally. For case study 2, a total load concentration of 7.2 mg/ml and a load challenge of 102 mg/ml resin was chose for testing experimentally. In both studies, a two column volume wash was collected separately from the flow though material. The wash phase is a normal part of the AEX WPC process, and so it was interesting to examine what impact the wash had on the final product recovery and purity.

Figure 3.11 shows the resulting chromatograms from the experimental studies conducted to test the operating conditions selected using the probabilistic design spaces, showing UV absorption at 280 nm of the material exiting the column during the experiment. Table 3.7 shows the predicted and experimental flowthrough recovery and purity, and the final recovery and purity when the material collected during the wash phase is included. For both studies, model recovery predictions were good, and the desired purity was met. The results for case study 1 were particularly exciting, as a recovery of 82% was achieved when the wash material was included. Although lower than usually achieved in the AEX WPC platform step, it is equivalent to recoveries of approximately 90% for the second and third columns in the alternative 3 step process (i.e. 90% × 90% = 81%), but without the extra time and cost of developing and operating the third column. The reasons for the success of the experimental studies will be explored and discussed in detail in the following section.

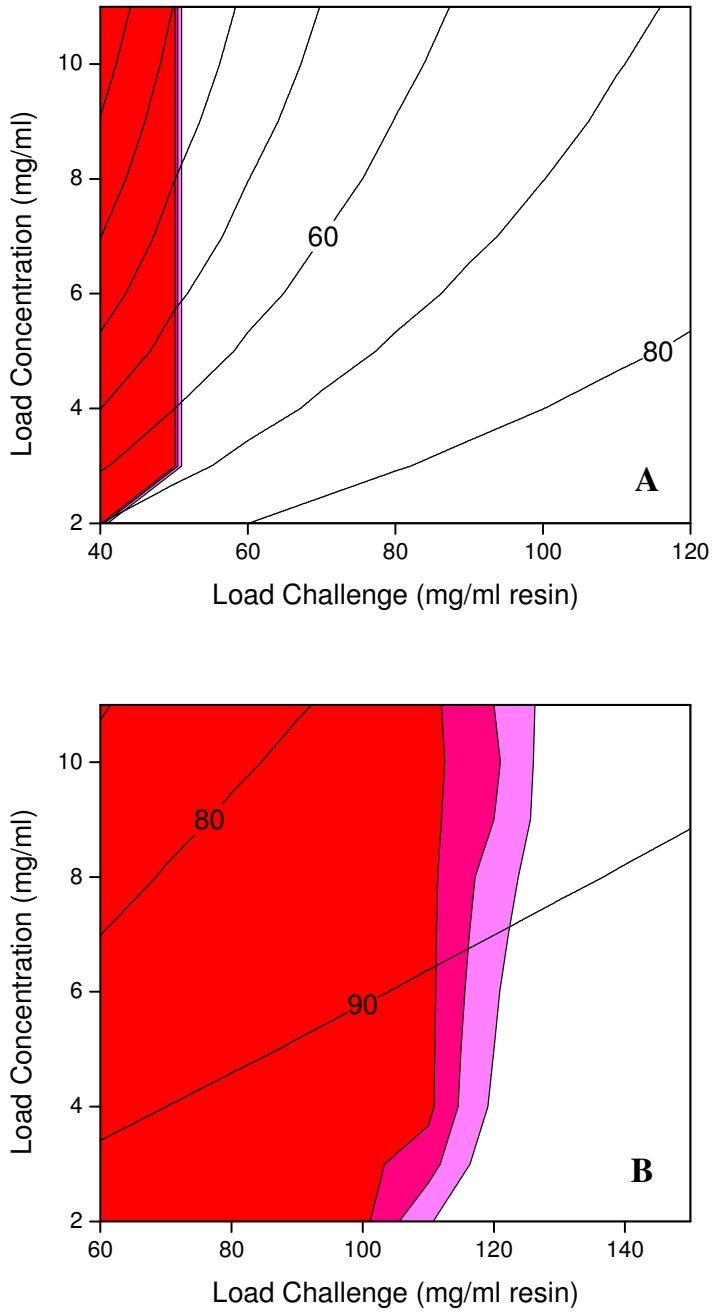


Figure 3.10. **A**. Knowledge space explored at $\mathbf{K_p}$ = 3 for case study 1. **B**. Knowledge space explored at $\mathbf{K_p}$ 1 for case study 2. The shaded areas show the region where the predicted probability of assuring that flowthrough material purity is greater than 98% is 1.0 (red), 0.9 (purple) and 0.8 (pink). Contour lines show predicted product recovery.

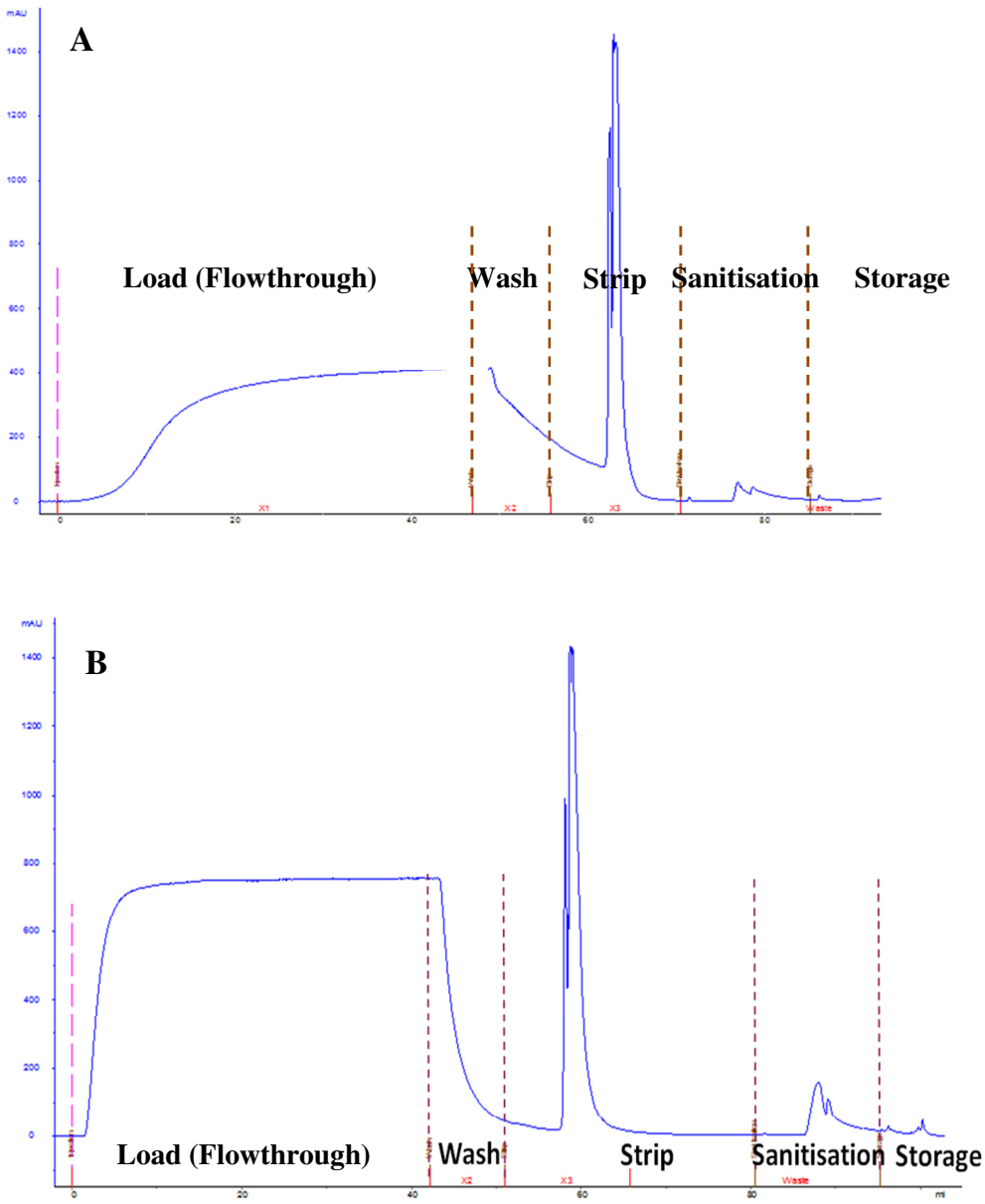


Figure 3.11. Experimental chromatograms from A. case study 1, total load concentration = 3.3 mg/ml, load challenge = 50 mg/ml and $\mathbf{K_p}$ = 3. B. case study 2, total load concentration = 7.2 mg/ml, load challenge = 102 mg/ml and $\mathbf{K_p}$ = 1.

Table 3.7. Showing model predictions and experimental results from Case study 1 (total load concentration = 3.3 mg/ml, load challenge = 50 mg/ml and $\mathbf{K_p}$ = 3), and Case study 2, (total load concentration = 7.2 mg/ml, load challenge = 102 mg/ml and $\mathbf{K_p}$ = 1).

| Case study | Data source | Flowthrough purity | Flowthrough recovery | Final purity | Final recovery |
|---|---|---|---|---|---|
| 1 | Model | 99.4% | 64.1% | - | - |
| | Experimental | 98.1% | 68.1% | 98% | 82% |
| 2 | Model | 99.7% | 88.0% | - | - |
| | Experimental | 98.9% | 93.3% | 99% | 100% |

***Conclusion***

Operating conditions for the two case studies were chosen by manual exploration of model predictions. A systematic method for identifying optimal, robust operating conditions is desirable, but was beyond the scope of this work. Due to the complexity of the relationships between key process parameters and variables, and noting that each operating condition has a different robustness, it is clear that it is that exploration of the design space generated by the model by an inexperienced process developer will not be able to find the optimal operating space. Despite providing a more sophisticated methodology than the traditional experimentation only approach, an experienced process developer is required to analyse the data and identify optimal operating conditions in terms of any objective function, be it maximising purity, recovery, throughput or robustness. New tools and workflows such as incorporating mathematical optimisation studies into the development process are required to assist experienced process developers, and should enable them to spend more time making decisions based on their knowledge and understanding, rather than spending time generating data.

### 3.5.2. **In depth analysis of WPC**

In the following section, an in-depth analysis of monomer – dimer selectivity, maximum load challenge, recovery, and the impact of uncertainty in the AEX WPC system is conducted, supported by relevant experimental studies.

***Selectivity***

Selectivity is the driving force of chromatographic separations, and is traditionally calculated by dividing the monomer partition coefficient (the product) by the dimer partition coefficient (the impurity). The partition coefficient is defined as the ratio between the concentration of bound and unbound protein in equilibrium in the linear region of the adsorption isotherm (Kelley et al. 2008a). However, in industrial separations, the load concentrations are rarely low enough for binding to occur in the linear region of the adsorption isotherm, and so selectivity in its traditional definition is misleading. In this work, we calculate a similar selectivity parameter that is useful for studying monomer and dimer binding in a column system. The selectivity is calculated using Eq 3.10, where q is the bound concentration (mg/ml) and C is the unbound concentration (mg/ml):

$$\text{Selectivity} = \frac{{}^{q_{monomer}}/_{C_{monomer}}}{{}^{q_{impurity}}/_{C_{impurity}}} \qquad [3.10]$$

A high selectivity is desirable as it leads to a better separation between monomer and dimer. The model can be used to calculate the selectivity as a function of load material dimer composition and total load concentration at partition coefficients of 1, 3 and 10 (Figure 3.12). Figure 3.12 shows that in general, a decrease in load concentration results in higher selectivity. The capacity of dimer decreases as the load concentration decreases (as shown in the dimer adsorption isotherms in Figure 3.9), thus, the increase in selectivity is a result of an increase in monomer recovery. The impact of decreasing the load concentration is specific to the exact dimer composition in the load material. Although operating at a partition coefficient of 10 may give the highest selectivity, the high selectivity occurs at industrially irrelevant compositions and concentrations. A partition coefficient of 1 gives the highest selectivity at industrially relevant load material compositions. However, it is important to note that although the selectivity is high, this isn't conveying greater dimer removal, only higher monomer recovery, as the increase in selectivity is due to increasing monomer recovery.

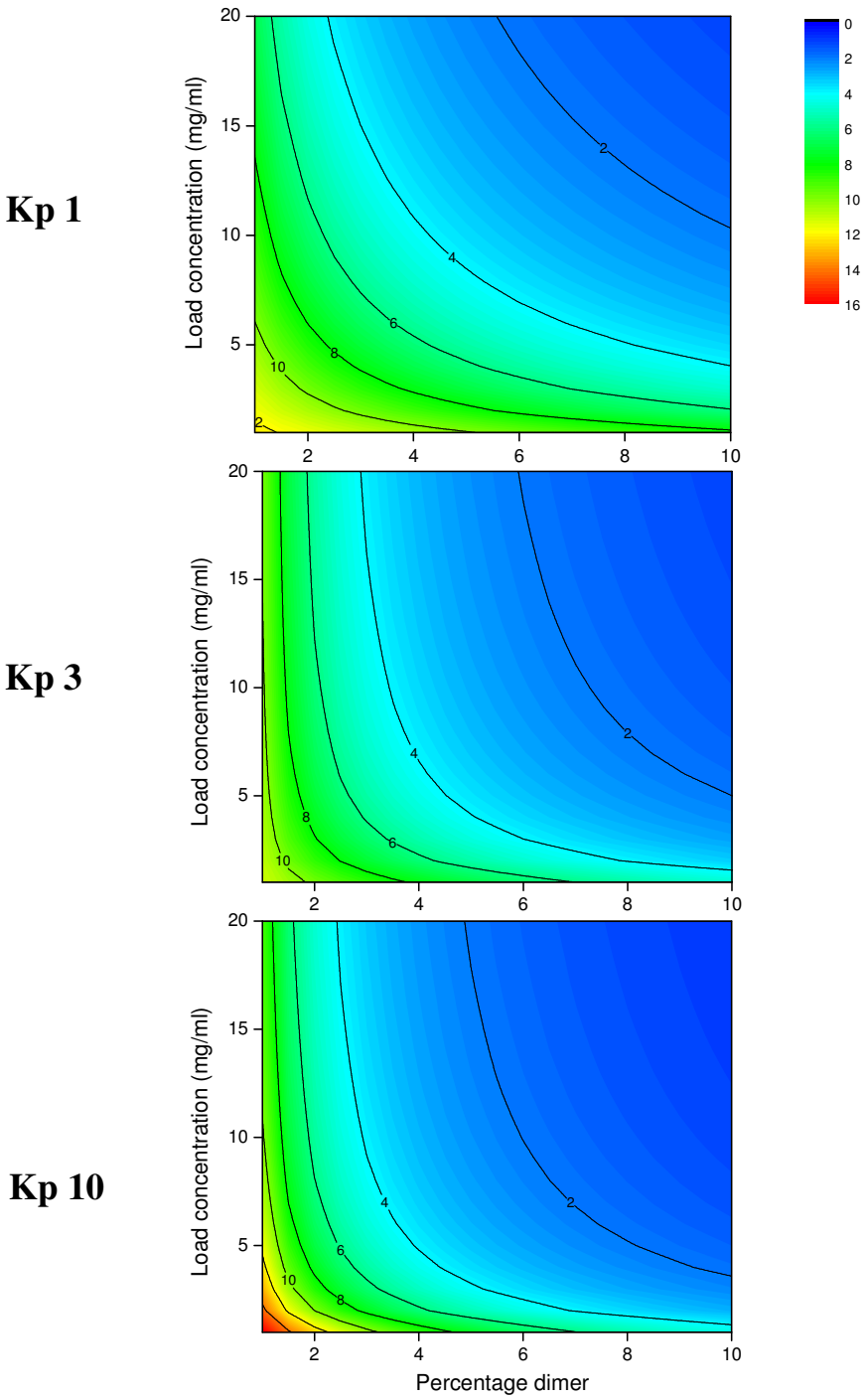


Figure 3.12. Monomer - dimer selectivity (contours and colours) at product partition coefficients, $K_p$, of 1, 3 and 10.

***Load challenge***

In practice, it is desirable to maximise the load challenge in order to increase throughput. Contour plots are shown in Figure 3.13 which show the (theoretical) maximum load challenge that enable full removal of dimer in the load material for partition coefficients of 1, 3 and 10. The corresponding monomer recovery is shown in Figure 3.14. The nonlinear behaviour of the mass challenge and recovery contours is due to the nonlinear nature of the adsorption isotherms (Figure 3.9), in particular the dimer isotherms. As expected, the maximum allowable load challenges increase as the partition coefficient increases (Figure 3.13). However, an increasingly lower load concentration must be used to reach an industrially acceptable recovery as the partition coefficient increases (Figure 3.14). The plots are particularly useful for showing the limitations of AEX WPC system for dimer removal. Notice that even at a partition coefficient of 10, once the dimer load composition increases above 6% the maximum load challenge becomes less than 100 mg/ml (Figure 3.13, bottom).

***Recovery***

Figure 3.14 shows that reducing the total load concentration is predicted to improve monomer recovery whilst maintaining impurity removal in the flowthrough material. Experimental column studies were conducted at partition coefficients of 1, 3 and 10, to test model flowthrough purity and recovery predictions. Depth filtered load material was used, therefore, the material contained negligible amounts of HCP, DNA and leached Protein A. Process parameters that were held constant during column studies are described in Table 3.8. An overlay of model predictions and experimental data is shown in Figure 3.15, and values are reported in Table 3.10. Model predictions in Table 3.10 are shown with associated uncertainty due to uncertain process parameters and variables. The stochastic simulation parameters used to calculate these are shown in Table 3.9.

Table 3.8. Process parameters held constant during column studies to test model predictions

| **Process parameter** | $K_p$ **1** | $K_p$ **3** | $K_p$ **10** |
|---|---|---|---|
| Load challenge (mg/ml resin) | 42 | 66 | 70 |
| Superficial velocity (cm/hr) | 150 | 150 | 150 |
| Load monomer composition | 0.9 | 0.895 | 0.9 |
| Load dimer composition | 0.075 | 0.08 | 0.075 |
| Load multimer composition | 0.025 | 0.025 | 0.025 |

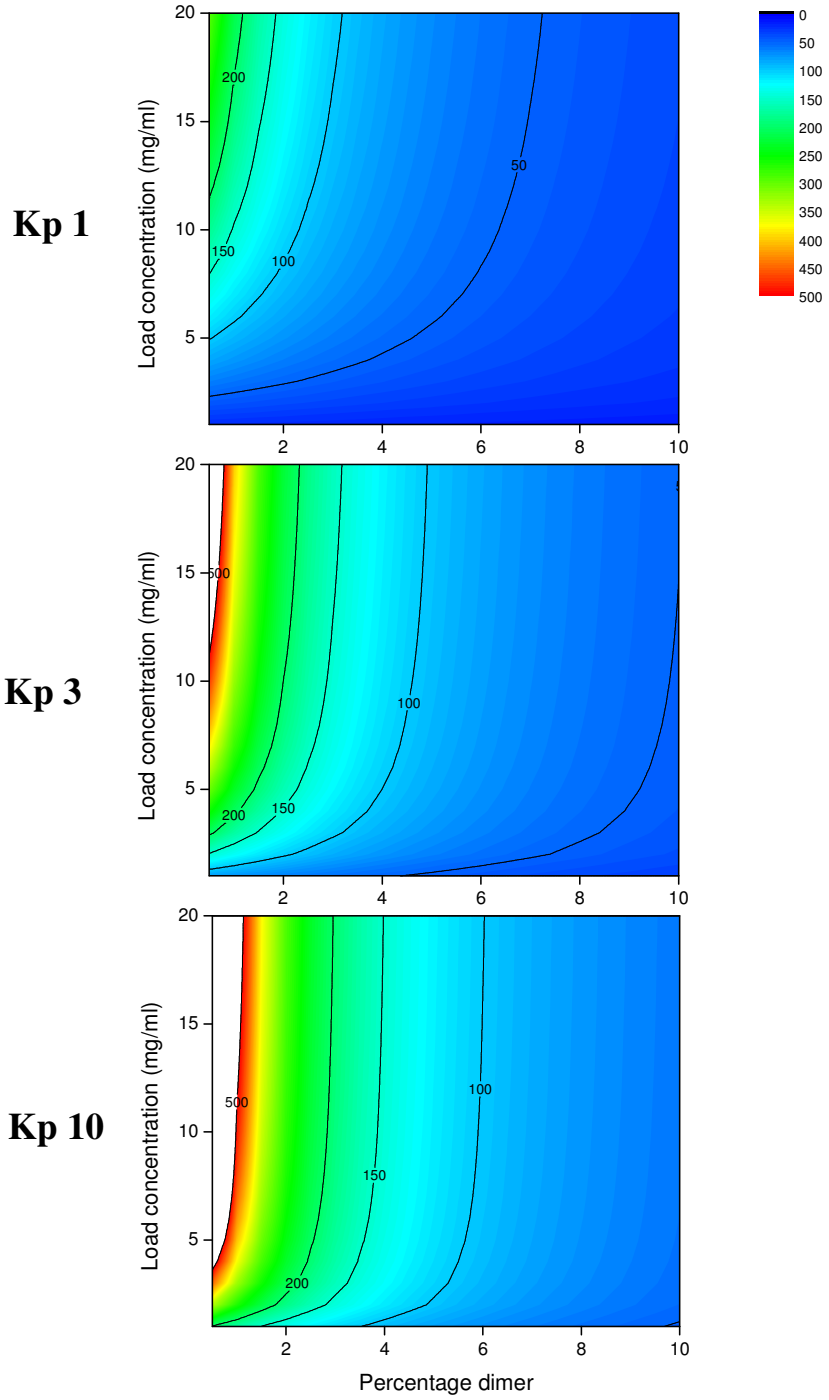


Figure 3.13. Maximum load challenge possible whist providing full removal of dimer in the load material (contours and colours) at product partition coefficients, $K_p$, of 1, 3 and 10.

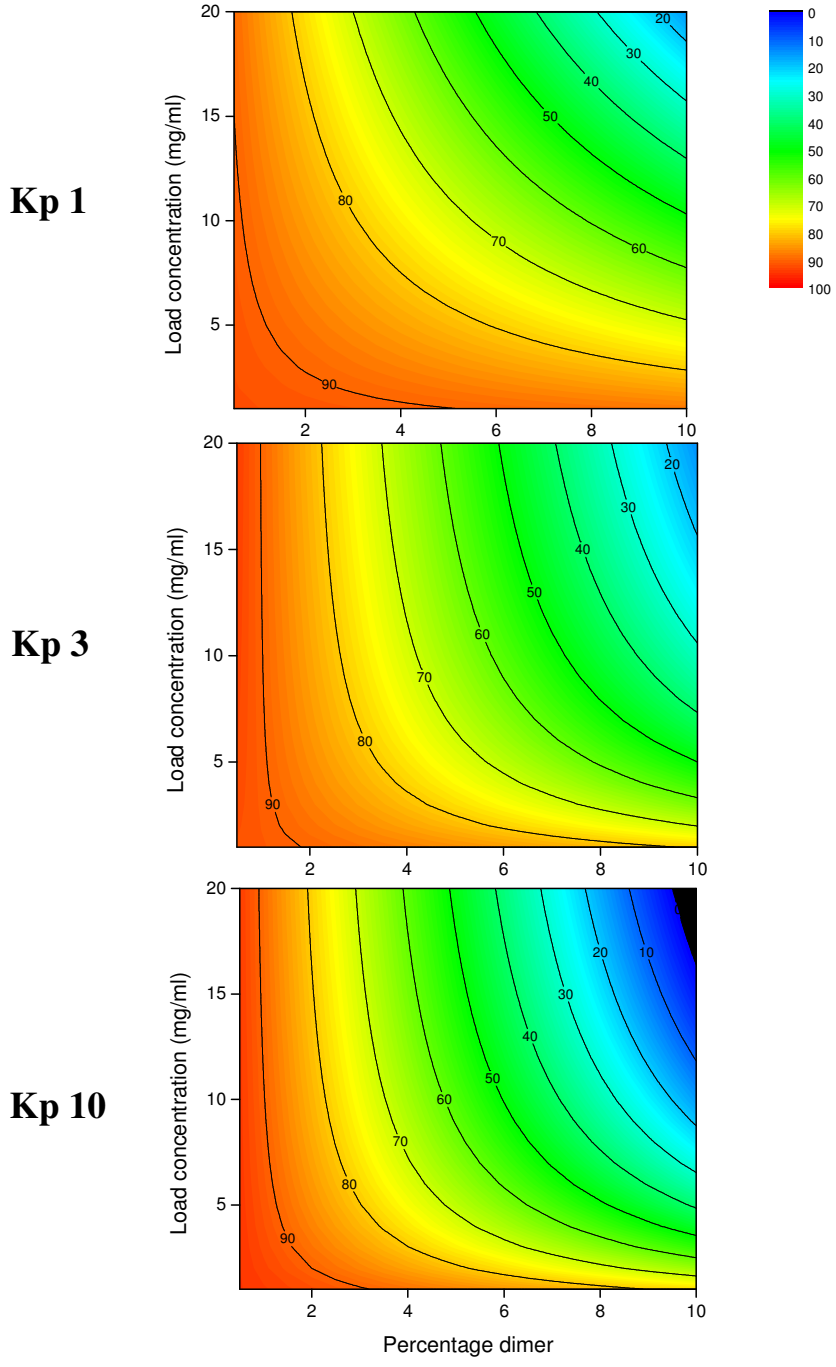


Figure 3.14. Predicted monomer recovery (contours and colours) when using the maximum load challenge possible whist providing full removal of dimer in the load material, at product partition coefficients, $K_p$, of 1, 3 and 10.

Model recovery predictions (Table 3.10) were satisfactory at all partition coefficients. The experimental recovery was consistently within one standard deviation of predicted recovery. Purity predictions were good for a partition coefficient of 3 and 10, but partition coefficient 1 purity predictions were inaccurate, outside of the predicted variance in model predictions. Monomer recovery predictions at a partition coefficient of 1 were good, which supports the hypothesis that experimental error was not the cause of the discrepancy. The data suggests the column dimer capacity is less than experimental batch adsorption isotherms at $K_p = 1$. The model does not account for dynamic phenomena occurring in the column, and therefore the disagreement may have been mass transfer related, although it is unusual that the partition coefficient 3 and 10 column studies would be unaffected by this.

Despite the unsatisfactory predictions at a partition coefficient of 1, the experimental results were very encouraging as they revealed scope for previously unidentified process improvements. Both simulations and experiments were in agreement that reducing the total load concentration increases the monomer recovery in the flowthrough (Figure 3.15). The rate of increase in monomer recovery increases as concentration decreases for partition coefficients. Higher partition coefficients experience a greater increase in monomer recovery over the concentration range considered (4 – 12 mg/ml). However, higher partition coefficients have much lower recoveries at the high load concentrations than the lower partition coefficients, which mean that product recovery in the flowthrough material is not at industrially relevant levels until the load concentration is low.

The result that reducing the total load concentration increases the monomer recovery in the flowthrough is exciting because reducing the load concentration may enable higher partition coefficients to be utilised for improved dimer removal. In the past, the low recovery at higher partition coefficients using conventional load concentrations (e.g. 7-10 mg/ml) may well have rendered a two column process infeasible. The data from studies at partition coefficients of 3 and 10 show that a reduction in load concentration from 12 mg/ml to 4 mg/ml increased the product recovery from 50% to 72% for a partition coefficient of 3, and a reduction in load concentration from 8 mg/ml to 4 mg/ml increased product flowthrough recovery from 32% to 57% (Table 3.10). For both partition coefficients, dimer removal was not affected. The disadvantage of reducing the load concentration and the low load challenges is that the throughput of the AEX WPC step is reduced. However, the savings achieved by not requiring a third chromatography step may offset such losses, so this is an option worth exploring further.

Table 3.9. Stochastic simulation parameters (number of simulations = 1000)

| Factor | Distribution | Distribution type | Average | Standard deviation | Upper | Lower |
|---|---|---|---|---|---|---|
| Equilibration buffer pH | Random | Uniform | Depends on partition coefficient | - | Average + 0.05 | Average – 0.05 |
| Equilibration buffer counterion concentration (mM) | Random | Uniform | 30 | - | 35 | 25 |
| Column volume (ml) | Random | Uniform | 2.95 | - | 3.04 | 2.85 |
| Compression factor | Random | Uniform | 1.2 | - | 1.25 | 1.15 |
| Load volume (ml) | Random | Normal | Depends on load concentration | 1 | - | - |
| Total load concentration (mg/ml) | Random | Normal | Varied during column studies | 0.2 | - | - |
| Load monomer, dimer and multimer composition | Random | Uniform | Depends on partition coefficient | - | Average + 0.05 | Average – 0.05 |

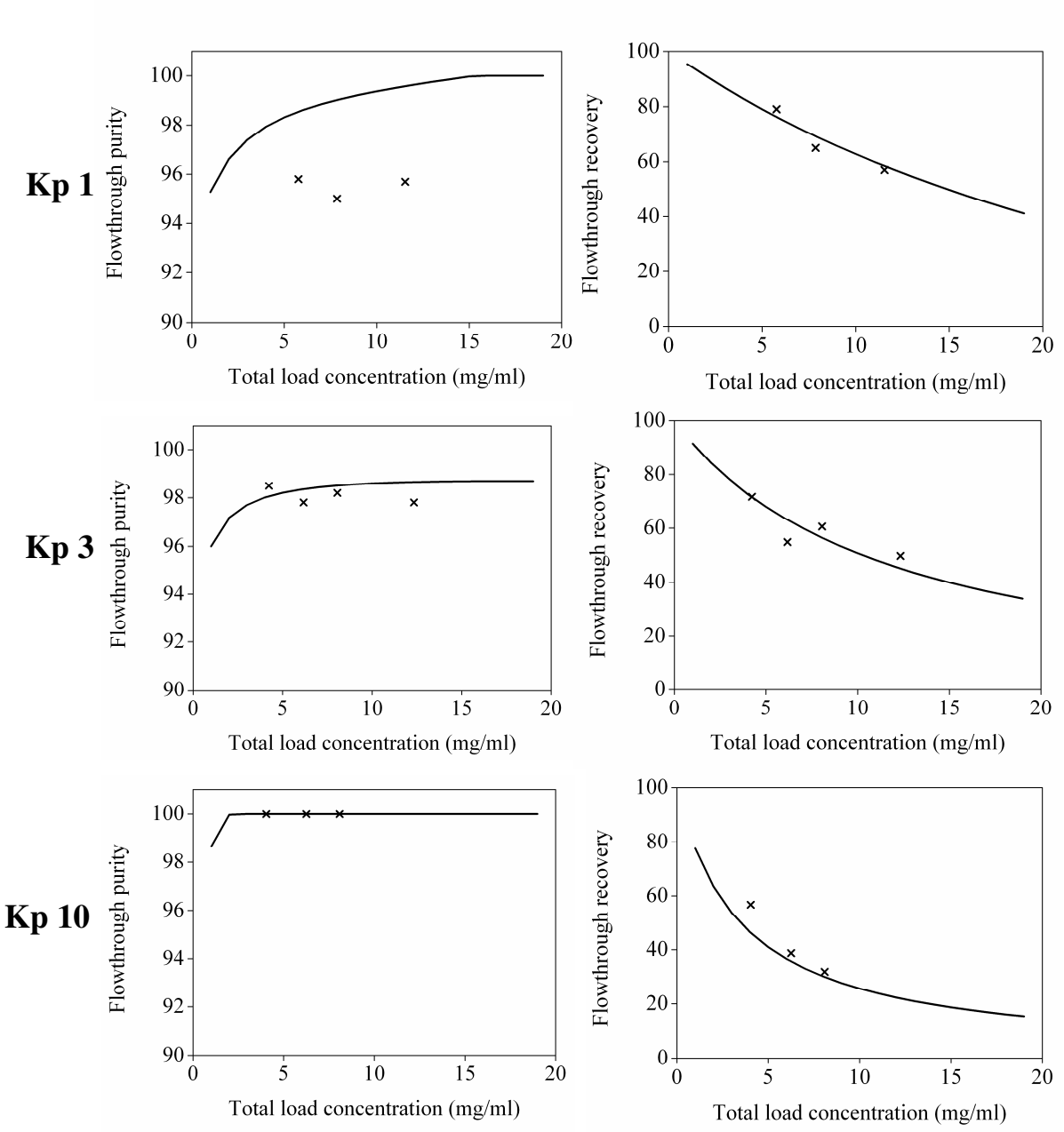


Figure 3.15. Overlay of model flowthrough recovery and purity predictions (lines) and experimental data from column studies (data points) at product partition coefficients, $K_p$, of 1, 3 and 10.

Table 3.10. Predicted and experimental flowthrough recovery and purity (the standard deviation of model predictions are calculated as a result of process uncertainty), model predictions within standard deviations are shown in italic bold

| **Partition coefficient** | **Total load concentration** | **Experimental purity** | **Purity mean and stdev** | **Experimental recovery** | **Recovery mean and stdev** | **Probability purity > 98%** |
|---|---|---|---|---|---|---|
| 1 | 12.8 | 95.7 | 98.8 ± 0.8 | ***57*** | 53 ± 7.3 | 0.93 |
| | 7.9 | 95.0 | 99.6 ± 0.8 | ***65*** | 68 ± 4.4 | 0.94 |
| | 5.8 | 95.8 | 99.4 ± 0.8 | ***79*** | 75 ± 3.4 | 0.86 |
| 3 | 12.3 | ***97.8*** | 98.2 ± 1.2 | ***50*** | 46 ± 6.3 | 0.67 |
| | 8.1 | ***98.2*** | 98.2± 1.0 | ***61*** | 56 ± 5.4 | 0.71 |
| | 6.2 | ***97.8*** | 98.1 ± 0.9 | ***55*** | 63 ± 4.9 | 0.69 |
| | 4.2 | ***95.8*** | 97.9 ± 0.8 | ***72*** | 71± 4.1 | 0.57 |
| 10 | 8.1 | ***100*** | 100 ± 0.2 | ***32*** | 30 ± 6.8 | 1.0 |
| | 6.3 | ***100*** | 99.9 ± 0.3 | ***39*** | 36 ± 6.9 | 1.0 |
| | 4.0 | ***100*** | 99.9 ± 0.3 | ***57*** | 46 ± 7.0 | 1.0 |

***Uncertainty***

The impact of uncertain process parameters and variables was considered in more detail for the studies conducted at a total load concentration of approximately 8 mg/ml. A total load concentration of 8 mg/ml is the most industrially relevant of the concentrations used in the column studies. Table 3.11, Table 3.12 and Table 3.13 show the mean, average and quartiles of the partition coefficient, monomer capacity, dimer capacity, load challenge, monomer loaded, dimer loaded, recovery and purity when the partition coefficient is 1, 3 and 10 respectively.

The stochastic simulations revealed the uncertainty in the partition coefficient as a function of uncertainty in the pH (± 0.05) and the counterion concentration (± 5mM) of the equilibration buffer. The product partition coefficient means and standard deviations were 1 ± 0.15, 3.1 ± 0.58 and 10.2 ± 2.39, respectively. As expected, higher product partition coefficients were more uncertain, as smaller changes in counterion concentration and pH have a larger effect on the product partition coefficients (Figure 3.3). However, the associated means and standard deviations in the dimer capacity were 8.9 ± 0.74, 13.6 ± 0.85 and 17.1 ± 0.68, respectively. The standard deviations of dimer capacity are similar regardless of partition coefficient, because changes in the buffer conditions have smaller impact on dimer adsorption isotherms at higher partition coefficients. The implication for process development is that the impact of increased uncertainty of higher partition coefficients on impurity removal can be considered negligible for the AEX WPC system.

For desired product partition coefficients of 1, 3 and 10, the highest and lowest values observed as a function of pH and counterion uncertainty were 0.74 – 1.44, 1.9 – 4.7 and 5.8 – 17.3, respectively, which are surprisingly large The highest observed values were consistently further from the mean than the lowest observed values. This is preferable to the lowest observed values being further from the mean, because a lower than desired partition coefficient value reduces product purity, which can potentially mean the batch must be discarded, whereas a higher than desired partition coefficient will reduce recovery, but the material may still be used. Uncertainty in the dimer capacity (8.9 mg ± 0.74, 13.6 mg ± 0.85 and 17.1 ± 0.68, respectively) was similar to the uncertainty in the dimer loaded (9.3 mg ± 0.74, 15.6 ± 0.91 and 15.3 mg ± 0.81, respectively) which is reassuring, considering that the dimer capacity is a function of uncertainty in the pH, counterion concentration, total load concentration, load composition, column volume and compression factor.

Uncertainty in the load challenge was due to uncertainty in the total load concentration (normal distribution, average = 8 mg/ml, standard deviation = 0.2 mg/ml), column volume (2.85 to 3.04 ml based on a bed height of 15 cm ± 0.5 cm), and load volume (normal distribution, average = dependent on load challenge, standard deviation 1 ml). The load challenge means and standard deviations were 42 ± 2.95 mg/ml resin, 66.1 ± 3.29 mg/ml resin and 70.2 ± 3.53 mg/ml resin for studies conducted at partition coefficients of 1, 3 and 10, respectively. The corresponding maximum and minimum load challenges at each partition coefficient were 51.4 to 32.6 mg/ml resin, 76.0 to 56.9 mg/ml resin, and 81.5 to 59.3 mg/ml resin, respectively. The large ranges and standard deviations in the load challenge show the importance of conservative use of the column capacity, in case the column becomes over challenged, resulting in impurities eluting into the flowthrough material. The data also illustrates how higher load challenges are more uncertain than lower load challenges. When the total load concentration is decreased but the load challenge remains constant, the uncertainty in load challenge increases further due to the larger impact of load concentration uncertainty.

The important implications of the stochastic simulations for purification process development can be illustrated by model predictions at a partition coefficient of 3. Although the model predicts that the purity will be 97.8%, as shown by the mean (which is close to acceptable product quality), the median of 97.8% shows that approximately 50% of experimental studies will result in a purity that is lower due to uncertainty in process parameters. Clearly this is why safety margins are built into processes. These studies illustrate that models can be especially useful for uncertain processes such as bioseparations, because stochastic simulations can be used to help select conditions for which the uncertainty is allowed. In this case, the model can ensure that the lowest impurity capacity due to normal process uncertainty is always greater than the highest amount of impurity loaded due to process uncertainty. By incorporating process uncertainty into process models, and then designing the process around understanding of the impact of that uncertainty on process performance, greater assurance of product quality can be obtained, compared to the traditional approach where process robustness as designed by empirical rules of thumb and tested by repeated experiments.

Table 3.11. Statistics from stochastic simulation of column studies where the partition coefficient = 1, and the total load concentration = 7.86 mg/ml data

| **Statistical parameters** | | | $K_p$ | **Monomer capacity (mg)** | **Dimer Capacity (mg)** | **Load challenge (mg/ml resin)** | **Monomer loaded (mg)** | **Dimer loaded (mg)** | **Recovery** | **Purity** |
|---|---|---|---|---|---|---|---|---|---|---|
| Mean | | | 1.0 | 37 | 8.9 | 42.0 | 114.4 | 9.3 | 67.4 | 99.3 |
| Standard Deviation | | | 0.15 | 4.50 | 0.74 | 2.95 | 7.70 | 0.74 | 4.39 | 0.78 |
| | 100 | Maximum | 1.44 | 71 | 10.8 | 51.4 | 137.9 | 11.4 | 77.9 | 100.0 |
| | 99.5 | | 1.40 | 69 | 10.6 | 49.6 | 135.8 | 11.1 | 76.2 | 100.0 |
| | 97.5 | | 1.35 | 65 | 10.3 | 47.6 | 129.4 | 10.7 | 74.7 | 100.0 |
| | 90 | | 1.24 | 62 | 9.9 | 45.8 | 124.3 | 10.2 | 72.9 | 100.0 |
| | 75 | Quartile | 1.14 | 59 | 9.5 | 44.1 | 119.7 | 9.8 | 70.8 | 100.0 |
| Quartiles | 50 | Median | 1.01 | 54 | 8.9 | 42.1 | 114.3 | 9.3 | 67.6 | 99.5 |
| | 25 | Quartile | 0.91 | 50 | 8.3 | 39.9 | 108.8 | 8.7 | 64.4 | 98.7 |
| | 10 | | 0.84 | 47 | 7.9 | 38.2 | 104.8 | 8.3 | 61.4 | 98.1 |
| | 2.5 | | 0.79 | 44 | 7.6 | 36.8 | 100.2 | 7.9 | 58.3 | 97.6 |
| | 0.5 | | 0.76 | 43 | 7.4 | 34.8 | 95.9 | 7.6 | 55.6 | 97.1 |
| | 0 | Minimum | 0.74 | 42 | 7.2 | 32.6 | 90.8 | 7.0 | 52.2 | 96.9 |

Table 3.12. Statistics from stochastic simulation of column studies where the partition coefficient = 3, and the total load concentration = 8.06 mg/ml data

| **Statistical parameters** | | | $K_p$ | **Monomer capacity (mg)** | **Dimer Capacity (mg)** | **Load challenge (mg/ml resin)** | **Monomer loaded (mg)** | **Dimer loaded (mg)** | **Recovery** | **Purity** |
|---|---|---|---|---|---|---|---|---|---|---|
| Mean | | | 3.1 | 78 | 13.6 | 66.1 | 179.9 | 15.6 | 56.2 | 97.9 |
| Standard Deviation | | | 0.58 | 9.07 | 0.85 | 3.29 | 8.44 | 0.91 | 5.41 | 0.81 |
| Quartiles | 100 | Maximum | 4.7 | 106 | 16.2 | 76.0 | 203.8 | 18.4 | 70.4 | 100.0 |
| | 99.5 | | 4.6 | 100 | 15.6 | 74.3 | 198.8 | 17.7 | 67.7 | 100.0 |
| | 97.5 | | 4.3 | 96 | 15.2 | 72.2 | 195.2 | 17.3 | 65.5 | 99.7 |
| | 90 | | 3.9 | 91 | 14.7 | 70.3 | 189.9 | 16.8 | 63.2 | 98.9 |
| | 75 | Quartile | 3.5 | 85 | 14.3 | 68.4 | 184.7 | 16.2 | 60.5 | 98.4 |
| | 50 | Median | 3.0 | 78 | 13.6 | 66.1 | 179.0 | 15.6 | 56.4 | 97.8 |
| | 25 | Quartile | 2.6 | 71 | 13.0 | 63.8 | 173.0 | 14.9 | 52.3 | 97.3 |
| | 10 | | 2.3 | 67 | 12.5 | 61.7 | 168.3 | 14.4 | 49.0 | 96.8 |
| | 2.5 | | 2.1 | 62 | 12.0 | 59.6 | 161.8 | 13.8 | 45.9 | 96.4 |
| | 0.5 | | 2.0 | 60 | 11.7 | 57.9 | 157.2 | 13.3 | 42.8 | 96.0 |
| | 0 | Minimum | 1.9 | 55 | 11.2 | 56.9 | 155.5 | 12.9 | 37.5 | 95.7 |

Table 3.13. Statistics from stochastic simulation of column studies where the partition coefficient = 10, and the total load concentration = 8.09 mg/ml data

| **Statistical parameters** | | | $K_p$ | **Monomer capacity (mg)** | **Dimer Capacity (mg)** | **Load challenge (mg/ml resin)** | **Monomer loaded (mg)** | **Dimer loaded (mg)** | **Recovery** | **Purity** |
|---|---|---|---|---|---|---|---|---|---|---|
| Mean | | | 10.2 | 133 | 17.1 | 70.2 | 190.8 | 15.3 | 30.3 | 100 |
| Standard Deviation | | | 2.39 | 10.14 | 0.68 | 3.53 | 8.64 | 0.9 | 6.1 | 0.2 |
| Quartiles | 100 | Maximum | 17.3 | 71 | 19.0 | 81.5 | 216.2 | 18.3 | 48.2 | 100.0 |
| | 99.5 | | 16.6 | 162 | 18.8 | 78.7 | 211.2 | 17.6 | 44.6 | 100.0 |
| | 97.5 | | 15.4 | 157 | 18.4 | 77.0 | 207.5 | 17.2 | 41.2 | 100.0 |
| | 90 | | 13.6 | 152 | 18.0 | 74.9 | 202.0 | 16.7 | 38.1 | 100.0 |
| | 75 | Quartile | 11.9 | 146 | 17.6 | 72.6 | 196.7 | 16.1 | 34.6 | 100.0 |
| | 50 | Median | 10.0 | 140 | 17.1 | 70.1 | 190.9 | 15.5 | 30.3 | 100.0 |
| | 25 | Quartile | 8.4 | 133 | 16.6 | 67.8 | 184.8 | 14.8 | 25.9 | 100.0 |
| | 10 | | 7.3 | 125 | 16.2 | 65.6 | 179.8 | 14.3 | 22.3 | 100.0 |
| | 2.5 | | 6.6 | 119 | 15.8 | 63.7 | 173.5 | 13.8 | 18.7 | 99.3 |
| | 0.5 | | 6.2 | 113 | 15.5 | 61.4 | 168.7 | 13.3 | 15.9 | 98.7 |
| | 0 | Minimum | 5.8 | 110 | 15.0 | 59.3 | 166.7 | 12.9 | 8.9 | 98.1 |

## 3.6. Conclusion

A model based approach for linking experimental high throughput batch bind screens (HTS) and scouting runs, traditionally conducted during process development of a weak partitioning chromatography (WPC) anion exchange (AEX) polishing step (part of Pfizer's two-step platform monoclonal antibody purification process), has been proposed. The approach involves formulating a simplistic 'platform' model, which once developed, can be applied to new candidate molecules based on the results of a standard high throughput screen. This is achieved by characterising the equilibrium isotherms of three critical components of the WPC separation, namely the product monomer, dimer and multimer, as a function of the product partition coefficient (rather than the conventional approach of pH and counterion concentration) via ultra-scale down batch adsorption experimentation. Use of the model is limited to an early stage of process development. This reduces the impact of inaccuracies due to simplifications made when formulating the model. Important advantages are realised by harnessing the models predictive power when (1) there are maximum degrees of freedom available for bioseparation design, and (2) minimal investment has been made in the product.

It has been shown how the model based approach is useful for: (1) Increasing process understanding, by providing a more informative method for exploring how process parameters can be controlled in order to raise product recovery to acceptable levels, whilst maintaining impurity clearance, and (2) assisting process development, by providing a link between high throughput screen and scale down column studies. The model can quickly identify operating parameter ranges that are of interest for the purification of feed streams with challenging compositions. When combined with stochastic simulation, the model can explore the impact of process variability on product quality and process performance. This approach enables the purification of previously impossible to purify feed streams using the two-step platform monoclonal antibody purification process. It also identifies promising parameter ranges to explore experimentally, thus accelerating process development and helping optimise column performance.

One of the problems with existing work on modelling chromatographic processes in industry is a lack of understanding as to how these models fit into industrial workflows which are dominated by significant time and material constraints, and a high risk of candidate failure. The proposed approach of using models at an early stage of process development can form part of a wider modelling approach, where the isotherms developed at this early stage are built upon as molecules move through the development pipeline. The necessary column

experiments required to determine mass transfer parameters are already conducted as part of the existing development approach. All that may be required is a fractionation of the flowthrough material and a greater analytical burden to determine the composition of samples. The number of parameters that need to be estimated depends on the complexity of the selected mass transfer model, so one possible approach is to increase model complexity as the development process proceeds. For example, a simple mathematical description (e.g. neglecting resin particles) of the mass transfer at standard processing conditions is developed during phase 3, and then more detailed descriptions of particle kinetics and or competitive adsorption can be developed post approval.

An understanding of the mass transfer occurring in the AEX WPC system is particularly interesting as it would enable the wash phase to be studied. If the length of the wash phase is not an issue, then the implications for process development around use of the wash phase are intriguing. The current 1 CV wash phase is very successful at increasing monomer recovery whilst maintaining impurity removal at low partition coefficients. As the dimer isotherms become more nonlinear as the partition coefficient increases, it follows that the wash phase will be even more successful at separating dimer from monomer as the partition coefficient increases. An increase in the washlength can be leveraged to offset any loss in recovery incurred by higher partition coefficients. The model has shown that a decrease in load material concentration can increase recovery, however, this also decreases productivity. One possible approach is to load at high partition coefficients and a high load concentration to maximise the load challenge, productivity and capacity for impurities, but recover the extra bound monomer by washing for longer. Determining the washlength is very challenging experimentally, but is simple using a model. In addition, the model can predict how a non-isocratic weak partitioning process, i.e. changing the product partition coefficient either during the load or the wash phase. An experimental effort to determine how to do this is extensive, but with the model developed in this work, the design space can be mapped quickly and efficiently.

Clearly there are exciting opportunities for applying the model for elucidating a range of very interesting design and development questions. There is scope for a number of improvements to the AEX WPC platform. The problem with the model is that it assumes an ideal column system, which is rarely the case in industry where resin fouling and aging is commonplace. This will be considered in the following chapter (Chapter 4).

# Chapter 4. Resin Fouling

*Resin fouling over a chromatography column's lifetime can cause significant (undesired) changes in process performance. A lack of fundamental knowledge and mechanistic understanding of fouling in industrial bioseparations limits the application of mechanistic models in industry. Scanning electron microscopy (SEM), batch uptake experiments, confocal laser scanning microscopy (CLSM) and small-scale column studies are applied to characterize fouling observed during process development of the AEX WPC considered in the first results chapter. Fouled resin samples analyzed by SEM and batch uptake experiments indicated that after successive batch cycles, significant blockage of the pores at the resin surface occurred, thereby decreasing the protein uptake rate. Further studies were performed using CLSM to allow temporal and spatial measurements of protein adsorption within the resin, for clean, partially fouled and extensively fouled resin samples. These samples were packed within a miniaturized flowcell and challenged with fluorescently labeled bovine serum albumin (BSA) that enabled in situ measurements. The results indicated that the foulant has a significant impact on the kinetics of adsorption, severely decreasing the protein uptake rate, but does not cause a decrease in saturation capacity. The impact of the foulant on the kinetics of adsorption was further investigated by loading BSA onto fouled resin over an extended range of flow rates. By decreasing the flow rate during column loading, the capacity of the resin was recovered. The data supports the hypothesis that the foulant is located on the particle surface, only penetrating the particle to a limited degree. The increased understanding of resin fouling can direct future efforts to mitigate this detrimental phenomenon and maintain process performance, whilst providing a basis for the development of new fouling models.*

# 4.1. Introduction

Fouling of chromatographic resin over operational lifetimes is a serious issue associated with industrial separations, attributed to repeated or prolonged exposure to the complex mix of components commonly seen in feed streams. Despite this, there have been very few (mainly experimental) studies conducted on this subject (Boushaba et al., 2011; Bracewell et al., 2008; Chau et al., 2006; Shepard et al., 2000; McCue et al., 2008). The lack of fundamental knowledge and mechanistic understanding of fouling in industrial bioseparations limits the application of mechanistic models in industry, and must be addressed in order for mechanistic models to be applied to industrial separations without giving increasingly unrealistic model predictions over the lifetime of a chromatographic separation.

In this work, we consider a case study where resin fouling had been observed during process development; that of an industrial anion exchange polishing step following a protein A affinity capture step in a process for the purification of a monoclonal antibody. The anion-exchange chromatography, which operates in weak-partitioning mode (Kelley et al., 2008), was characterized through high throughput screening experiments (Coffman et al., 2008; Kelley et al., 2008), as well as in-house cycling studies performed on qualified scale-down models, and large-scale manufacturing runs.

The anion exchange resin has been successfully used as part of a two column platform process for the purification of numerous monoclonal antibodies in the past (Kelley et al., 2008), with no significant fouling phenomena observed. Hence it was surprising that for this protein as column lifetime increased, when protein A elution pool material was loaded onto the AEX resin, significantly earlier breakthrough of impurities and premature loss of capacity was observed. Interestingly, it was found that the lifetime of the AEX resin was linked to the Protein A cycle number such that as Protein A cycle number increased, there was a consequent increase in capacity of the AEX polishing step. The data suggested a unique quality of the particular feed stream resulted in the fouling. Iskra et al. (2013) also found that the fouling could be accelerated by overloading the AEX resin well beyond normal operating conditions.

Different control strategies were considered for preventing impurity breakthrough and improving resin lifetimes. An investigation using small-scale chromatography, dynamic light scattering, mass spectroscopy and fourier transform infrared spectroscopy (FTIR), indicated that the most likely hypothesis was that resin was being fouled by a combination of product

and host cell proteins. A detailed account has been presented in the literature (Iskra et al., 2013). In this work, the objective is to elucidate on this resin fouling case study, by revealing the location of the foulant, and determining the mechanistic effects fouling has on protein uptake kinetics and resin capacity.

Scanning Electron Microscopy (SEM), batch uptake experiments, Confocal Laser Scanning Microscopy (CLSM) on a miniaturised packed bed, and small scale column experiments are conducted on samples of fouled resin derived from the industrial process using the worst case feed stream and overloading conditions. SEM and batch uptake experiments are used to give initial indications of foulant location and resin performance as fouling progresses, before CLSM is used to conduct a more detailed investigation. TexasRed labelled BSA is used as a reporter molecule for protein uptake kinetics. The technique uses a flowcell to measure changes at various stages of fouling in resin capacity and uptake kinetics, at a particle level. The time and space distribution of the labelled BSA within the resin particles is recorded in situ in order to facilitate a comparison between clean, partially fouled and extensively fouled resin. Finally, column studies are conducted to investigate the effect of the foulant on protein uptake and breakthrough performance of a column system. Together these techniques (summarised in Table 4.1) enable us to determine the spatial location of the foulant and its effect on the process during protein uptake.

## 4.2. Experimental materials and methods

### 4.2.1. **Chemicals**

All chemicals were purchased from Sigma-Aldrich (Dorset, UK) and were of analytical grade unless stated otherwise.

### 4.2.2. **Chromatography resin and equipment**

MabSelect Protein A affinity chromatography resin was obtained from GE Healthcare (Uppsala, Sweden). Fractogel® EMD TMAE HiCap (M) anion exchange resin was obtained from EMD Merck (Darmstadt, Germany). All laboratory experiments were carried out using an ÄKTA FPLC chromatography system from GE Healthcare (Uppsala, Sweden).

Table 4.1. Experimental methodology for investigating clean, partially found and extensively fouled resin samples.

| **Experiment** | **Results** | **Purpose** |
|---|---|---|
| Batch experiments | Uptake curves | Initial indication of impact of fouling on uptake rate and saturation capacity |
| Scanning electron microscopy | Images of particle surfaces | Morphology of resin surface |
| Confocal laser scanning microscopy (CLSM) during live uptake experiments | Radial light intensity profiles of a BSA reporter molecule during uptake in a miniature column | Fouling effect on intraparticle profiles of bound BSA reporter molecule during uptake |
| Column lifetime studies investigating load flowrate | BSA reporter molecule breakthrough curves and dynamic binding capacities | Fouling effect on BSA reporter molecule breakthrough and dynamic binding capacity at different loading flowrates |

### 4.2.3. **Proteins**

The monoclonal antibody (mAb) used in these studies was humanized IgG1 produced in recombinant Chinese hamster ovary (CHO) cells grown in serum free medium. Downstream processing prior to the anion exchange step considered in this work consisted of centrifugation and depth filtration, followed by Protein A chromatography. Bovine serum albumin (BSA) - Texas Red(R) conjugate was purchased from Invitrogen, Paisley, UK.

### 4.2.4. **Protein A Chromatography**

The column used in protein A chromatography was 1.6 cm in diameter and 30 cm in height. The column was equilibrated with 0.15 M sodium chloride at pH 7.5 prior to loading. Clarified condition media was then applied followed by a two column volumes (CV) wash of the equilibration buffer. This was followed by 5 CV's of 1.8 M calcium chloride at pH 7.5. The elution pool consisted of material collected from start in UV rise, to a total of 2.5 CV's, collected as the process pool. The remaining bound protein was removed using an additional 5 CV's of low pH followed by sanitisation with 50 mM NaOH, 0.5 M Sodium Sulfate, and stored in 16% ethanol, 150 mM NaCl, 50 mM TRIS, pH 7.5.

### 4.2.5. **Anion exchange chromatography**

The anion exchange columns used in this study were 0.5 cm in diameter and either 5 or 15 cm in height, and were operated in weak partitioning mode (Kelley et al., 2008, Iskra et al., 2013). The columns were equilibrated with 50 mM TRIS, 10 mM NaCl at pH 8.1. Protein A peak pools were applied to the column at 150 cm/hr followed by a 3 CV wash of the equilibration buffer. Protein A peak pools contained the product of interest, host cell protein, DNA and residual Protein A which had leached from the affinity capture resin, and approximately 3.5% high molecular mass species (HMMS). The turbidity of the Protein A pool was 28.1 NTU (Iskra et al., 2013). The load eluate and wash volumes were collected together as the process pool, and any remaining bound protein was removed using a 2 M NaCl strip buffer. The columns were sanitized with 2 M NaCl, 0.5 M NaOH and stored in 16% ethanol, 150 mM NaCl, 50 mM TRIS, pH 7.5. The loading conditions used during column runs (50 mM TRIS, 10 mM NaCl at pH 8.1) had been determined by high-throughput screening (HTS) under batch binding conditions, and were confirmed using scale – down column chromatography experiments to provide sufficient clearance of impurities (residual HMMS < 1.5%, HCP clearance > 3.0 LRV, and leached Protein A clearance > 3.0 LRV), while maintaining yield > 90%, prior to resin fouling. These conditions would be expected to produce the desired product quality in large scale manufacturing (Iskra et al., 2013).

### 4.2.6. **Generation of fouled resin samples**

Three resin samples were used in subsequent experimental studies to characterise the fouling. These were generated by conducting multiple cycles of the anion exchange chromatography on a column 0.5 cm in diameter and 15 cm in height, using the worst case feed stream and overloading conditions (Iskra et al., 2013), according to the standard operating procedure set out previously. The three resin samples are classified as follows: unused clean resin, fully fouled resin representative of resin at the end of the column's lifetime (hereon referred to as extensively fouled resin), and partially fouled resin, representative of an intermediate state of fouling.

### 4.2.7. **Batch uptake experiments**

A set amount of TMAE HiCAP (M) resin was allowed to settle by gravity. After measuring the settled volume, the resin was washed with ultra-pure Millipore water to remove the storage ethanol solution and then equilibrated with 0.05 M TRIS Base pH 9.0 HCl adjusted buffer, giving a final concentration of 50% (v/v). 50 µl of this slurry was then aliquoted to a 2 mL eppindorf tube. Adsorption was started by adding 2 mL of Texas Red labelled BSA to the resin sample (Overall BSA concentration: 5 mg/mL, dye to protein (D/P) ratio: 0.01). The eppindorf was kept under constant agitation, except at fixed times when the eppindorf tube was quickly centrifuged for 10 s at 1200 g, before a 50 µl sample was taken from the supernatant and collected for subsequent UV analysis at 280 nm and 593 nm by a Nanodrop. The sedimented resin particles were quickly resuspended by resuming agitation. For the duration of the experiment resuspension was ensured by placing the eppendorf tube onto an orbital shaker rotating at 2000rpm, and confirmed by visual inspection.

### 4.2.8. **Scanning Electron Microscopy (SEM)**

Sample preparation for SEM consisted of sample drying followed by gold coating. A thin layer of resin slurry was pipetted onto a glass slide which had been pre-coated in gold and mounted onto a copper block. Excess liquid was carefully adsorbed on filter paper without contacting the resin particles, before the sample was left for 30 minutes to allow any remaining ethanol to evaporate. The dried sample was thereafter transferred to a high resolution ion beam coater (Gatan Model 681, Oxford, UK), and ion sputtered with gold at an angle of $45^{o}$ in order to form a 2-3 nm gold layer on the surface of the resin particles. The ion beam coater was operated at 6mA at an acceleration voltage of 10 keV. Coated surfaces were subsequently imaged with a JEOL JSM-7401F scanning electron microscope (JEOL Ltd., Tokyo, Japan) at 1 keV accelerating voltage.

4.2.9. **Live uptake imaging by Confocal Laser Scanning Microscopy**

Image acquisition was performed on an inverted confocal laser scanning microscope (Leica TCS SPEinv, Leica Microsystems GmbH, Mannheim, Germany) equipped with krypton/argon ($\lambda$ = 488 nm and $\lambda$ = 568 nm) and helium/neon ($\lambda$ = 633 nm) lasers. Using a 40x oil immersion objective, images (512×512) were captured (3 averages) through the Leica Application Suite (LAS) software (Version 2.0) (Leica Microsystems GmbH, Mannheim, Germany). Optimal laser settings, including laser intensity, signal gain, offset and emission detection range were determined to ensure that there were no auto fluorescence effects, and that even at full particle saturation the detected emitted light intensity stayed within the confocal laser scanning microscope's detection range. The settings were then kept constant for the duration of the study.

In order for BSA to be detected by the confocal laser scanning microscope, it must be labelled by a suitable fluorescent dye molecule (Ljunglöf and Thömmes, 1998). There are many different dye molecules currently available for this purpose. However, it has been reported that the attachment of dye molecules can significantly change the adsorption behaviour of the BSA and therefore must be carefully selected (Hubbuch and Kula, 2008; Teske et al., 2006). BSA conjugated to TexasRed, AlexaFluoro488, Cy3 and Cy5 on a strong anion exchanger chromatographic system, similar to that considered in this work, has previously been screened to determine which was most suitable for CLSM (Susanto et al., 2006). The elution profiles of the conjugates were compared with native BSA in relation to retention time and peak shape. BSA TexasRed conjugate showed the least deviation from the native BSA, and was therefore selected in this work. The ratio between native and TexasRed conjugated BSA was tested by measuring UV adsorption at 280 nm and 593 nm throughout the batch uptake experiments. The constant ratio during protein uptake over 1 hour confirmed that there were minimal competitive effects in our system.

In order to minimise the readsorption of emitted fluorescence by other dye molecules, a dye to protein ratio (D/P) of 0.01 was used for the feed solution following recommended literature D/P ratios (Hubbuch and Kula, 2008). At this D/P ratio we were able to assume that the contribution of emitted fluorescence readsorption to light attenuation could be neglected.

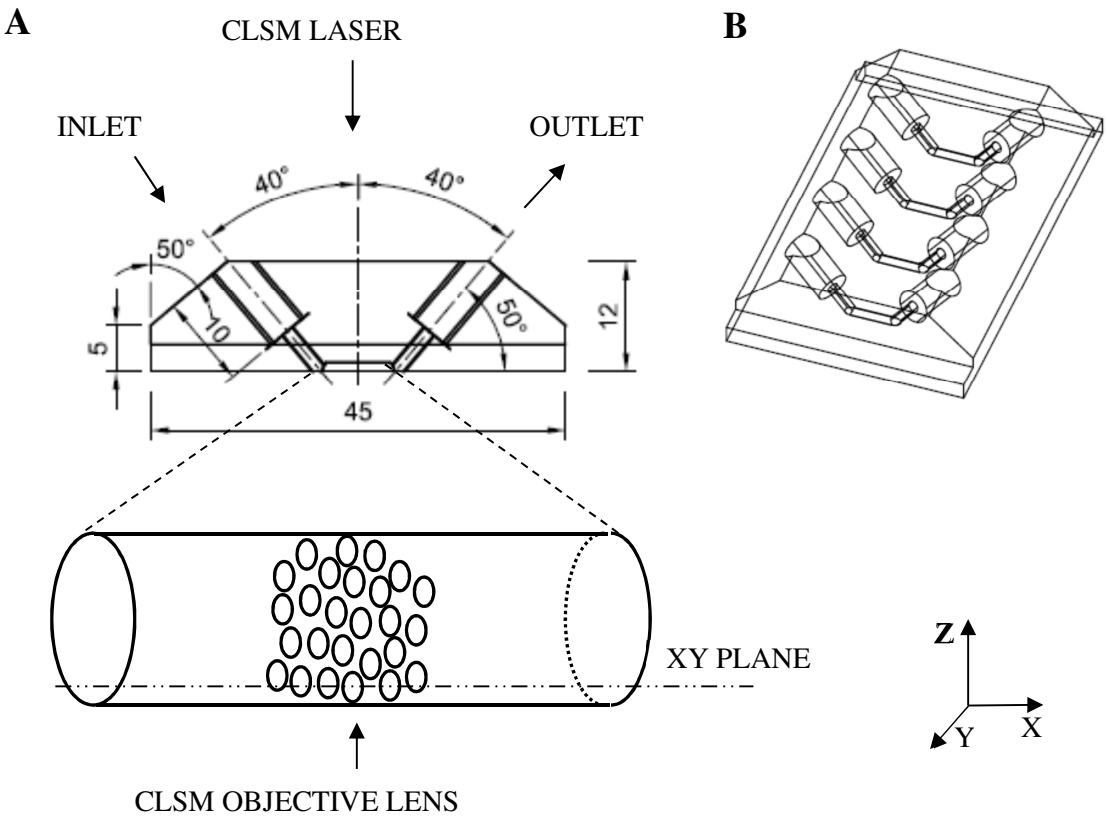


Figure 4.1. **A.** Side elevation of the miniaturized flowcells setting within the confocal laser scanning microscope. XY image acquisition plane shown on diagram. **B.** Three dimensional representation of the miniaturized flowcell used for live imaging of the intra-particle uptake within a packed bed.

Control experiments investigating fluorophore bleaching upon repeated use were completed, and confirmed that bleaching could be neglected for the purposes of this work. A range of precautions were taken to minimise fluorophore bleaching throughout the experimental work: the use of low laser powers, minimised exposure times and wrapping all samples in aluminium foil in order to minimise exposure to light during transition and storage.

A miniaturized flowcell was fabricated similar in design to that used by Hubbuch and Kula (2008). Four horizontal channels (10mm length, 1mm diameter) were drilled into a Pyrex block with $45^{O}$ inlets on both sides. A viewing window was then created by fixing a cover slip onto the open face of the block with epoxy glue Araldite® (Huntsman Advanced Materials, Cambridge, UK) in order to seal each channel. The resulting effective column volume was 0.02 mL. A schematic of the flowcell is shown in Figure 4.1.

Flowcell channels were packed by manually administering resin slurry (50% (v/v)) from a syringe. Great care was taken to ensure that the resin was not over or under packed. Frits were placed at either end of the channel, which was then connected to a syringe pump. The resin was washed with ultra-pure Millipore water to remove the storage ethanol solution (2 mL, 150 cm/hr), before equilibration with 0.05 M TRIS Base pH 9.0 HCl adjusted equilibration buffer (2 mL, 150 cm/hr).

Texas Red labelled BSA feed was adjusted to the required pH and salt concentration in the running buffer, and loaded onto the resin bed within the flowcell channel at 150 cm/hr for 90 minutes. Images were recorded using a Confocal Laser Scanning Microscope at set time intervals with excitation at 568 nm and emission detection in the range 550 nm – 701 nm. The setting of the flowcell within the laser scanning confocal microscope is shown in Figure 4.1 .

### 4.2.10. **Live uptake data processing**

The large number of confocal images from the flowcell experiments were processed to generate a reliable set of radial light intensity profiles. This was done in order to allow a direct comparison of the spatial location of BSA within resin particles during protein uptake between the clean, partially fouled and extensively fouled samples over the 90 minute experiments. For each experimental data set 5 particles were selected for data processing from the area of the flowcell imaged. We found that using more than 5 particles gave negligible benefits in terms of the reliability of our data. The appropriate XY image where the focal plane intersected with the centre of each particle was then selected at each time interval, as illustrated in Figure 4.2A. This was possible because at each time interval throughout the 90 minute flowcell experiments, images of XY planes of the flowcell bed area under scrutiny were taken over a range of z values at 5 µm intervals. The selection of 5 particles from those available (up to 14) also helped us to ensure this centre cross-section positioning, as we were able to only select particles where the focal plane exactly intersected with the centre of each particle.

The next step was to generate radial profiles of the emitted light intensity. This is typically done by a simple linear profile evaluation through the central cross section of a scanned particle (Hubbuch and Kula, 2008). However, this method neglects the inhomogeneous nature of protein uptake due to effects such as particle contact points and fouling. In this work, the emitted fluorescence intensity was measured as a function of the radial coordinate and subsequently averaged over particle circumference in order to account for this inhomogeneous uptake (Figure 4.2C). We utilized ImageJ v1.31 for this purpose, which is

an imaging software developed by the Research Services Branch of the National Institute of Mental Health in Bethesda, Md, USA and is freely available in the public domain (Abramoff, 2004; Rasband, 2011).

The radial profiles of each particle were then normalised by dividing the radial dimension by the appropriate particle diameter. In this work the particle - fluid phase boundary was identified by the highest emitted light intensity across the radial profile, and subsequently used to calculate the particle diameter. It was found that the emitted light intensity values outside the determined particle - fluid phase boundary consistently dropped to an insignificant value within 4 µm of the particle diameter over the range of particle diameters analysed (50 - 90 µm), for all resin samples. This is in agreement with the literature, where lengths of this region typically fall between 2 - 10µm (Dziennik et al., 2005; Susanto et al., 2006). All emitted light intensity data was corrected for light attenuation effects following the methodology set out by Susanto at al. (2006). Lastly, the corrected emitted light intensity radial profiles (normalised by particle diameter and averaged over particle circumference) were averaged over the 5 particles per resin sample. The resulting set of data thus describes the average time and space distribution of the BSA in the resin samples throughout the 90 minute flowcell experiment.

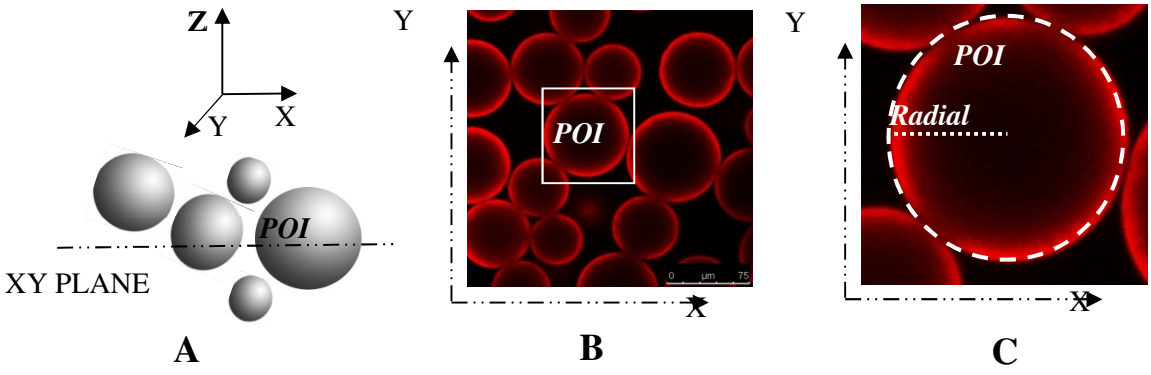


Figure 4.2. **A.** The XY plane intersecting with centre of the particle of interest (POI) is selected. **B**. The POI's centre XY plane image from CLSM, also showing all available particles in the flowcell area imaged. **C.** Illustrating how the emitted fluorescence intensity is measured as a function of radial coordinates (dotted line), and is averaged over particle circumference (dashed line).

#### 4.2.11. **Column studies**

An iterative procedure where a column 0.5 cm in diameter and 5 cm in height was subjected to multiple anion exchange chromatography cycles using representative load material and a scheme of over challenge was performed, until the cumulative amount of protein from protein A peak pools that had been challenged onto the resin reached predefined amounts (1, 2, 3, 4, and 5 g/ml). Each time the cumulative load challenge reached one of the predefined amounts, the cycle in progress was allowed to run to completion, i.e. the column washed, eluted, sanitized and placed into storage buffer according to the methodology set out previously (Section 4.2.5), and the anion exchange cycling paused. The effect of resin fouling that had occurred during the anion exchange cycling was then measured via full breakthrough of BSA at different flowrates (0.49, 0.33, 0.16, 0.08 ml/min). BSA breakthrough was conducted as follows: The column was equilibrated with 50 mM TRIS, 10 mM NaCl at pH 9.0. BSA was then applied to the column at the specified flowrate (load concentration 10 mg/ml, load challenge 300 mg/ml). Any bound BSA was then removed using a 50 mM TRIS, 2 M NaCl, pH 7.5 elution buffer. The column was further cleaned with 2 M NaCl, 0.5 M NaOH, and then placed in storage buffer (16% ethanol, 150 mM NaCl, 50 mM TRIS, pH 7.5). Once the breakthrough of BSA had been recorded at each flowrate, the column was returned to anion exchange chromatography cycling.

## 4.3. Results and Discussion

The overall objective of this work was to determine the location of fouling on resin particles and the effect of this fouling on protein kinetics and resin capacity in an anion exchange polishing step from an industrial purification process. In the following, the results from SEM imaging and batch uptake experiments are presented which give initial indication of the foulant location and the progressive nature of the effect with cycle number. Following this, the results from a detailed CLSM investigation are presented. This includes the intra-particle radial adsorption profiles during protein uptake within the miniaturized flowcell bed, accompanied by corresponding uptake curves. Finally, the results from column studies which include BSA breakthrough profiles and dynamic binding capacities over a range of flowrates with increasing cycle number and hence also increasing fouling.

#### 4.3.1. **Batch Experiments**

The batch experiments were designed to give an initial indication of the effect that the foulant had on protein uptake, and to confirm that there were no competitive effects in the system due to modification of BSA binding characteristics when conjugated with the TexasRed flurophore, in preparation for the CLSM study. Figure 4.3 shows the batch uptake

curves of BSA with clean, partially fouled and extensively fouled resin samples. For all samples the batch adsorption kinetics were consistant with previous literature results on tentacle exchangers (Almodóvar et al., 2011; Urmann et al., 2010). However, a clear difference in the initial uptake rates was observed with clean resin having the fastest uptake, followed by partially fouled resin, then extensively fouled resin. More detailed analysis of the data indicated that the initial uptake of BSA by clean resin was roughly twice as fast as uptake by extensively fouled resin, indicating fouling significantly impacts mass transfer.

Figure 4.3 shows that by the end of the experiment equilibrium had not been reached by any of the resin samples. Although the amount of BSA bound to the extensively fouled resin was lower than the amount bound to the clean resin (partially fouled resin ~87% amount bound to clean resin, extensively fouled resin ~ 82% amount bound to clean resin), uptake was still ongoing. Firm conclusions regarding the effect that the foulant had on the saturation capacity of the resin could therefore not be made. As there was a constant ratio between conjugated and non-conjugated BSA in the supernatant throughout uptake, confirmation that there were no competitive adsorption effects in the system was achieved (not shown).

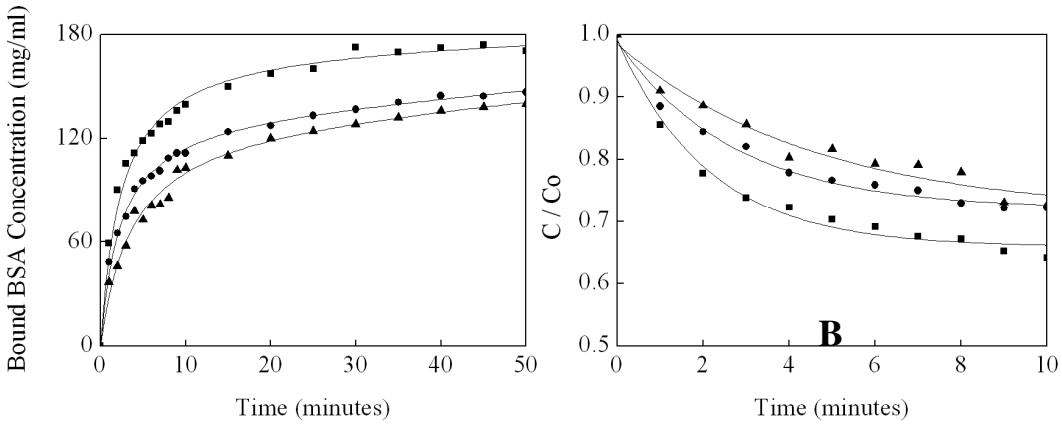


Figure 4.3. Batch uptake curves of 5mg/ml BSA at 0.05M TRIS Base pH 9.0, by clean ■, partially fouled ●, and extensively fouled ▲ Fractogel® EMD TMAE HiCap (M) resin particles during batch experiments. (Feed to resin volume ratio 80:1 (80×)). **A.** Bound BSA concentration as a function of time. **B.** Bulk mobile phase BSA concentration as a function of time.

### 4.3.2. **Scanning Electron Microscope Imaging**

Figure 4.4 shows high resolution SEM images of clean, partially fouled and extensively fouled resin particles at progressively higher magnifications. The area of the particle under analysis was kept constant for each sample. The images show distinct differences in the particle surface morphology between the three samples. In the clean resin (Figure 4.4A), the surface is well-defined, homogenous, and the pores are clearly accessible. By comparison, the extensively fouled resin (Figure 4.4C) shows a high amount of pore blockage by a material covering much of the surface. This is particularly clear on the highest magnification image (10000x for A3/B3/C3). In Figure 4.4, images CX and CY illustrate the magnitude of the fouling, with many particles showing completely clogged pore entrances over a significant percentage of particle surface area. Fouling on partially fouled resin surface is not as obvious, but does show an intermediate level of pore blockage (Figure 4.4B).

Interestingly, circular patches were found on the extensively fouled resin which were comparable in surface morphology to that seen in the clean resin images in Figure 4.4C. These are regions where particle – particle contact occurs within the packed bed, and show little or no fouling. Previous studies have also shown such areas, clearly distinguishable from the rest of the particle surface, and have reported localised external mass transfer resistance through these regions (Hubbuch et al., 2002; Jin, 2010; Siu et al., 2007). In addition to the pore blocking, images CX and CY show larger pieces of clumped material on the particle surface that were common throughout fouled and partially fouled particles. The SEM imaging suggests a mechanism where the foulant blocks pore entrances but does not penetrate a significant distance into the particle, instead continuously growing outwards over successive cycles. This is in agreement with results by Jin et al. (2010) who reported the progressive build-up of lipid based foulant on the surface of Sepharose® Butyl-S 6 Fast Flow resin over successive cycles.

### 4.3.3. **Live uptake experiments**

The purpose of the live uptake experiments was to conduct a direct comparison between the clean, partially fouled, and extensively fouled resin based on their intra-particle radial light intensity profiles, during uptake of a BSA reporter molecule in a packed bed using confocal laser scanning microscopy (CLSM). The light intensity is proportional to the concentration of bound protein, and therefore can be used to estimate differences in the intra-particular mass transfer and adsorption (Figure 4.5). Integrating the area underneath the radial light intensity profiles, and correcting for the spherical nature of resin particles, indicates the relative amount of BSA bound to the different resin samples throughout uptake (Figure 4.6).

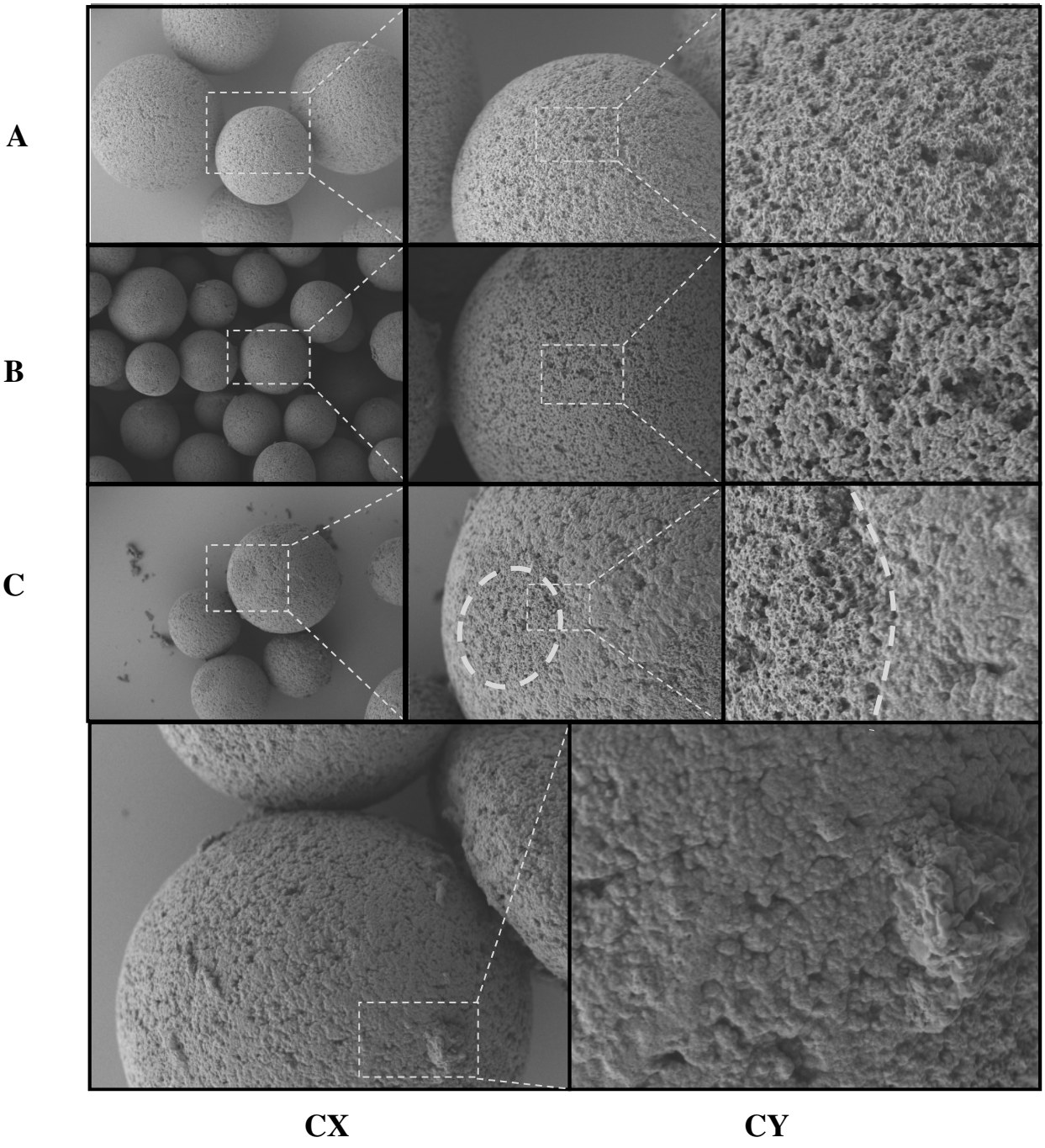


Figure 4.4. Scanning electron microscopy images of **A**. Clean **B.** Partially fouled. **C.** Extensively fouled Fractogel® EMD TMAE HiCap (M) resin particles. **A1.** x1000 **B1**. x450 **C1.** x750 **A2/C2.** x3000 **B2.** x2000 **A3/B3/C3.** x10000. **CY.** x2,000. **CY.** x7,000.

Figure 4.5 and Figure 4.6 show a dramatic difference was found in the protein uptake rate of the different samples. Clean resin had the fastest uptake, followed by partially fouled, then extensively fouled resin. Partially fouled resin took approximately twice as long as the clean resin to reach the highest light intensity seen in the experiments, and fouled resin still had not reached this value after 85 minutes of loading. However, the amount of BSA bound to the partially and extensively fouled resin samples was approaching that of the clean resin at the end of the experiment. Partially fouled resin was at 98%, and extensively fouled resin at 83%, of the clean resin's capacity, and adsorption was still ongoing. This suggests that if the partially fouled or extensively fouled resin is challenged for long enough, it will eventually reach the capacity of the clean resin, or somewhere near this.

For all three resin samples there was minimal difference between the shape of the intra-particle binding profiles. Some differences would have expected, either localized or in general, between the different resin samples had foulant been irreversibly binding to intra-particular binding sites, but this was not the case. In Figure 4.5, the peak close to the exterior boundary of the particle does become marginally wider and less defined with fouling, but this effect is minimal. This flattened region of the profiles in the fouled resin samples is approximately 3 μm in length, and may indicate that slightly less protein may be binding to this region as fouling worsens. These results are all in agreement with the hypothesis that the foulant forms a layer on the surface of the resin and does not significantly penetrate into the particles. It appears that as the foulant blocks access to the pore entrances, the available surface area where protein can diffuse freely into the particle therefore decreases, which introduces increased resistance to mass transfer. This causes the dramatic differences in uptake, but minimal differences in capacity which we saw between the resin samples. Intra-particle mass transfer thus does not appear to be a limiting step.

### 4.3.4. **Column studies**

Column breakthrough experiments were used for studying the effect of the foulant on resin performance. Scale down cycling studies provided fouled samples to measure BSA breakthrough over an extended range of flow rates. The use of BSA for breakthrough studies was not intended to replicate industrial process behaviour. Instead, the BSA was used as an analytical tool to test the pore blockage hypothesis where resin fouling would hinder mass transfer into the resin, only allowing capacity of the resin to be recovered at high residence times.

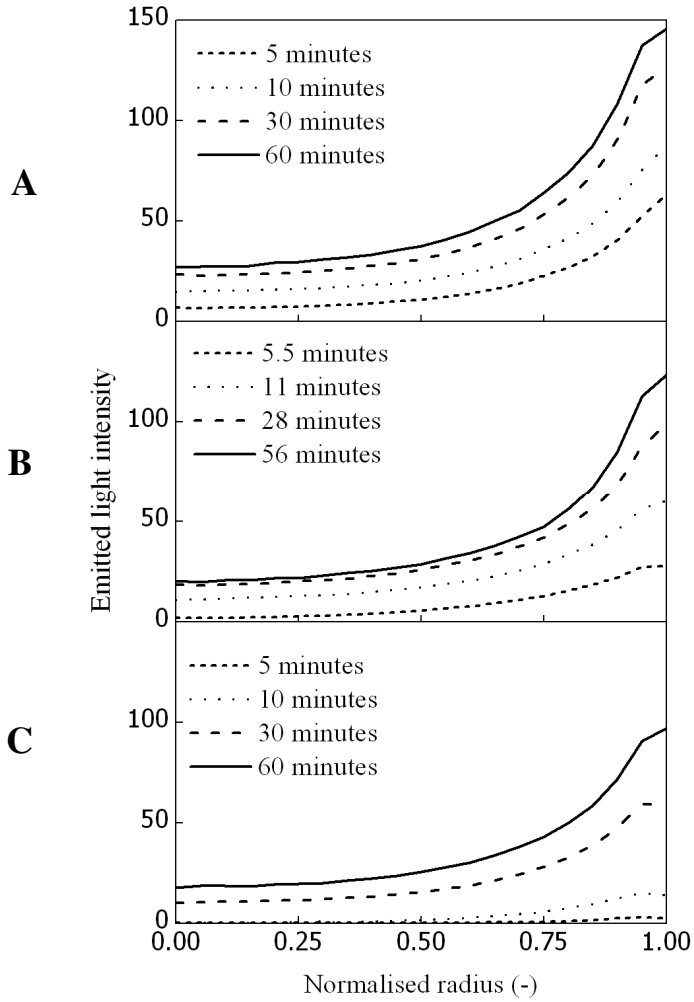


Figure 4.5. Average radial emitted light intensity of BSA (stationary phase: **A.** Clean. **B.** Partially fouled. **C.** Extensively fouled Fractogel® EMD TMAE HiCap (M) resin particles) over time (0, 5, 10, 30, 60mins), during the uptake of Texas Red labelled BSA from the process feed (5mg/ml BSA, D/P ratio = 0.01, 0.05M TRIS Base pH 9.0 HCl adjusted, 150cm/hr), during flowcell experiments.

Figure 4.7 shows that over the course of the column studies, both the shape and the position of BSA breakthrough changed drastically as cycle number increased. Figure 4.8 illustrates the corresponding decrease in dynamic binding capacity (DBC), which for the normal operating flowrate of 0.49 ml/min (~150 cm/hr), dropped by 71% over the course of the study. At this flowrate, Figure 4.7 shows that for clean resin, breakthrough begun after approximately 10 CV of material had been applied to the column. In contrast, when the resin was extensively fouled, onset of breakthrough was rapid, beginning after less than 1 CV, similar to what would be expected during operation in flow through mode with minimal protein binding.

The shape of the breakthrough went from sharp to diffuse as fouling progressed (Figure 4.7), and indicated that the loss in capacity and rapid breakthrough observed at the end of the study was due to severe mass transfer resistance, rather than a decrease in capacity due to foulant binding in place of the protein molecule of interest. Breakthrough would have been expected to remain sharp if the mass transfer was not affected by fouling, which was not the case.

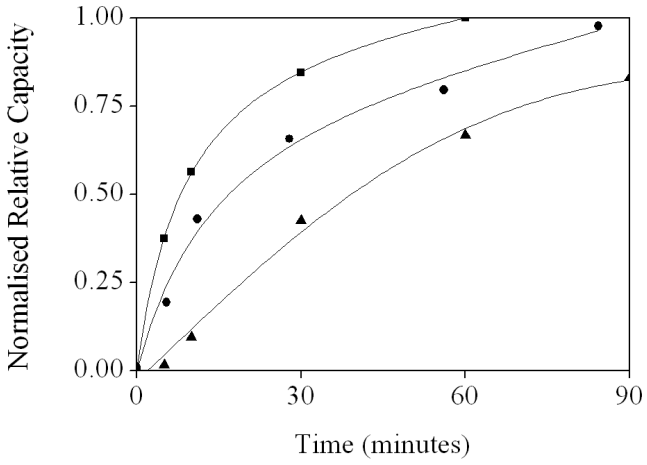


Figure 4.6. Relative uptake curves of clean ■, partially fouled ●, and extensively fouled ▲ Fractogel® EMD TMAE HiCap (M) resin calculated from integrating under intra-particle labelled BSA profiles during uptake in a packed bed in Figure 5, and correcting for the spherical nature of resin particles.

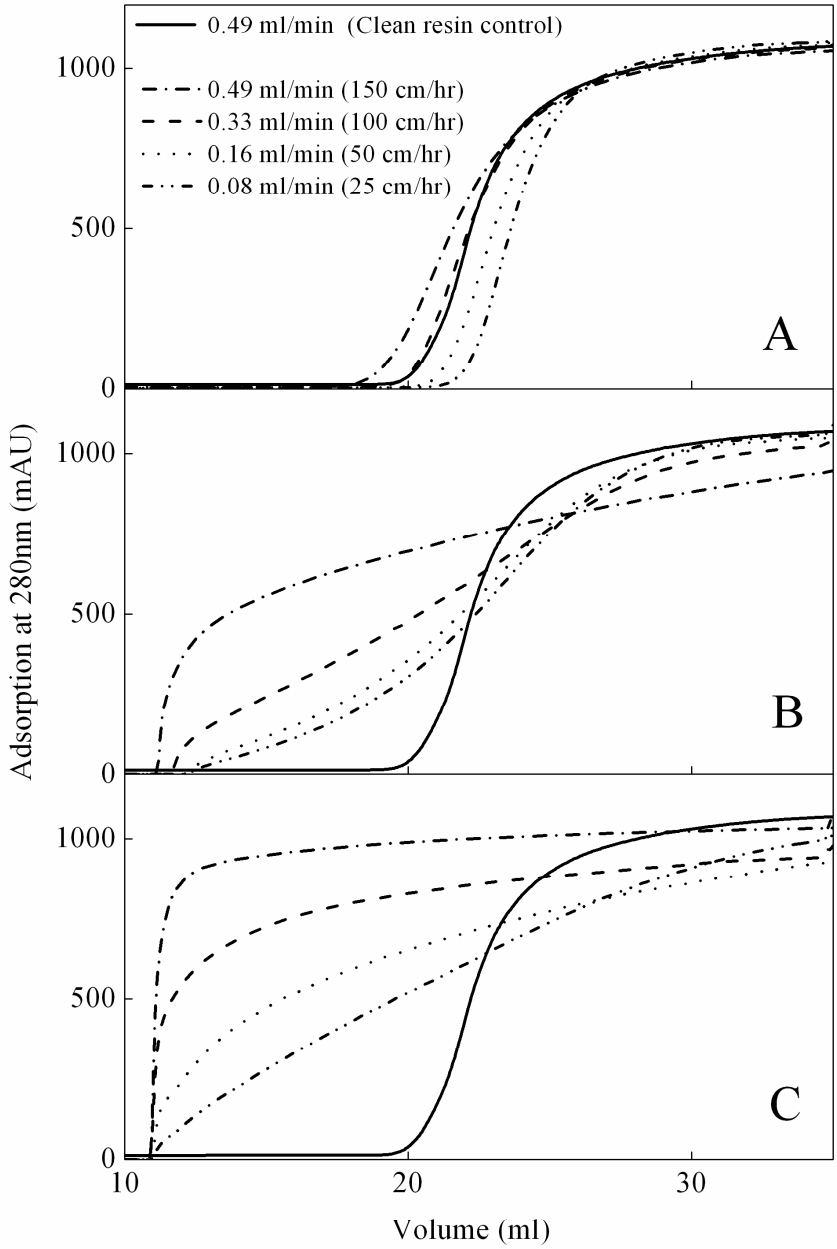


Figure 4.7. Breakthrough curves of 10 (mg/ml) BSA load in 0.05M TRIS Base pH 9.0 at different flow rates on a 0.98ml TMAE HiCap (M) column, 5cm in length. Load phase begins at 10ml. The column had been previously challenged with Protein A peak containing 1g (**A**), 3g (**B**) and 5g (**C**) of mAb. The control experiment using clean resin at 0.49 ml/min (~150 cm/hr) is shown for reference on each graph.

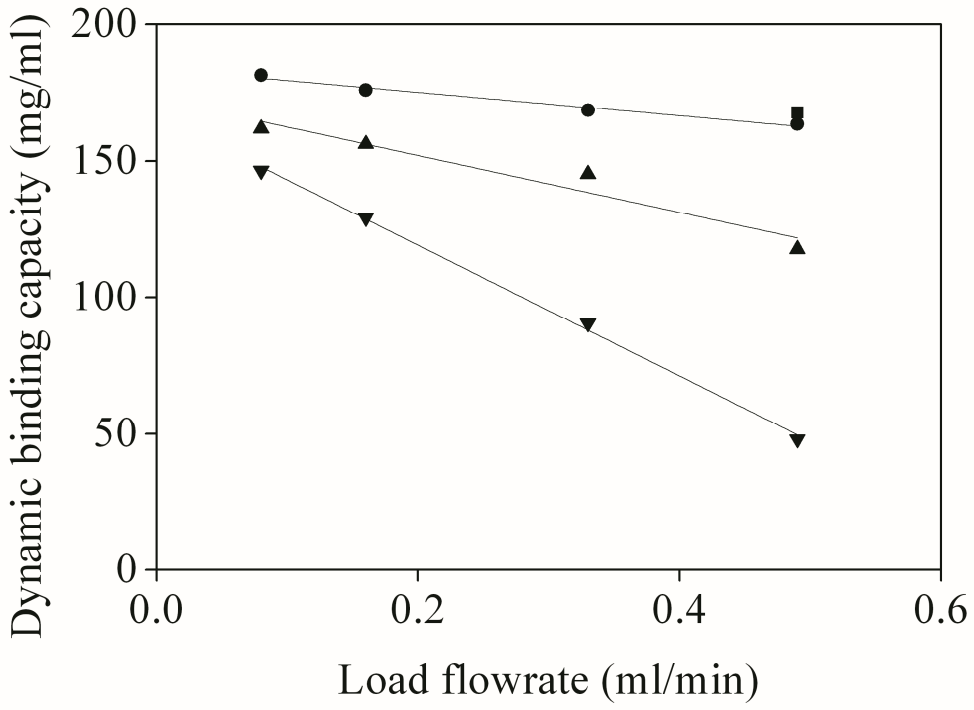


Figure 4.8. Fractogel® EMD TMAE HiCap (M) resin BSA dynamic binding capacity (at 90% breakthrough) as a function of load flow rate on a 0.98ml TMAE HiCap (M) column, 5cm in length. The column had been previously challenged with Protein A peak containing 0g ■, 1g ●, 3g ▲, 5g ▼of mAb. The load concentration of BSA was 10mg/ml in 0.05M TRIS Base pH 9.0. Data arrived at from Figure 7.

The data shows that by decreasing the flow rate, the dynamic binding capacity (DBC) lost due to fouling can be recovered (Figure 4.8). Reducing the flow rate from 0.49 ml/min (~150 cm/hr) to 0.08 ml/min (~25 cm/hr) at the highest level of fouling (after 5g of feed material had been challenged), resulted in the DBC increasing from 47 mg/ml to 146 mg/ml resin, a 3 fold increase. A linear equation with an $r^2$ value of 0.997 was fit to the data from Figure 4.8. The y intercept of this equation showed that with the fouling levels experienced at the end of the study, the theoretical maximum DBC was 167 mg/ml resin, the same DBC as the control run conducted at the start of the study using clean resin. This further supports the hypothesis that the foulant is located on the particle surface, only penetrating the particle to a limited degree. The increase in time that particles are exposed to BSA at lower flow rates, enables the BSA to overcome the mass transfer limitations as a result of the fouling, thus restoring DBC to pre fouled levels.

## 4.4. Conclusion

Batch experiments, Scanning Electron Microscopy (SEM) and Confocal Laser Scanning Microscopy (CLSM) and small scale column experiments are useful tools for characterizing fouling in chromatographic resin. In this study the foulant was shown to progressively build up on the particle surface using SEM. The batch and CLSM live uptake experiments were in agreement that the foulant reduced the uptake rate of the BSA reporter molecule, with little or no change in saturation capacity. The column study confirmed that binding capacity lost due to the foulant could be restored by decreasing the flow rate, providing further evidence to support the conclusion that the foulant is located on the particle surface, only penetrating the particle to a limited degree. The results suggest that progressive fouling of resin can severely impact the performance of chromatography columns. The knowledge and understanding of resin fouling gained can direct future efforts to mitigate this detrimental phenomenon and maintain process performance, whilst providing a basis for the development of new fouling models.

# Chapter 5. Resin Lot Variability

*A model based approach is used to identify robust operating conditions for an industrial hydrophobic interaction chromatography at a late stage of process development. Resin lot and load material variability was resulting in serious performance issues during the purification of a multi component therapeutic protein from crude material. An equilibrium dispersive model is developed of the HIC. Stochastic simulations are conducted to generate probabilistic design spaces for resins that gave the highest and lowest protein recoveries during testing. The design spaces show the probability of meeting product quality specifications for a key critical quality attribute, over a range of possible operating conditions. The simulations account for historical variability experienced in the load material composition and concentration. The results are used to determine operating conditions that assure product quality despite the process variability. With normal process variability, no operating condition was found where the probability of meeting product quality specifications remained > 0.95 for all resin lots. The stochastic methodology is extended to identify the level of control required on the load material composition and concentration to bring process robustness to an acceptable level. This is not possible using an experimental method due to the impractical amount of resources that would be required. The results indicated that adopting an adaptive design space, where operating conditions are changed according to which resin lot is in use, was the favourable option for ensuring process robustness, which is a step change concept for bioprocessing.*

# 5.1. Introduction

Chapter 3 and 4 considered the use of mechanistic chromatography models to derive fundamental process understanding of specific industrial chromatographic separations currently in development or operation at Pfizer, at an *early stage of development*. The goal was to accelerate the development and increase the robustness of industrial protein purification processes, whilst following guidance regarding the implementation of Quality by Design. In this chapter, the same objectives are considered for a chromatographic separation at a *late stage of development*.

Chapter 5 focuses on an industrial chromatographic separation where resin lot variability, combined with a variable feed stream, had resulted in serious performance issues during the purification of a therapeutic protein from crude feed material. The resin lot variability occurred on a hydrophobic interaction chromatography (HIC) that produces a complex final product composed of six closely related variants of a *dimer* protein therapeutic (~30 kDa), with their *monomer* subunits in a specific ratio. The desired ratio of *monomer* subunits must be met by this unit operation, and is a defined CQA of the final product. An extended range of resin lots were obtained from the supplier for testing within normal process operating ranges. All resin lots were within the manufacturers' specifications for ligand density and chloride capacity. Despite this, many failed to meet product quality specifications during testing and would have incurred significant losses if used for the large scale manufacture of the product. No link between resin lot specifications and successfully meeting process objectives was found.

The traditional approach to identifying an operating region where the product quality remains within the defined product specification is to conduct an extensive experimental effort directed by factorial design of experiments. The data would be used to generate a response surface model which functions as a deterministic design space. The approach is extremely time consuming and costly. The outcome the DOE is a fixed, inflexible manufacturing process, with a control strategy based on reproducibility rather than robustness. The experimental results are unlikely to bring any fundamental understanding of the source of performance issue, which means analysing and understanding reasons for further batch failures would be extremely difficult. In addition, the experimental approach provides no contingency in case suitable operating conditions cannot be found, and the response surface model is limited to the data used to generate it.

In this chapter, a model based approach is used to identify robust operating conditions that ensure the desired product quality is met, despite the resin lot and inherent bioprocess variability. The HIC was at a late stage of process development and had predefined mobile phase conditions, flow rate and column dimensions that had been fixed prior to this work. The mass challenge and wash length were the only manipulated variables available for adjustment. An equilibrium dispersive model with competitive Langmuir adsorption is developed for the two most extreme resin lots which gave the highest (designated high binding resin) and lowest (designated low binding resin) protein recoveries at normal operating conditions (not shown for confidentiality purposes). Micro well batch adsorption and scale down column experiments are used for model calibration, and the model is validated against multiple scale down column experiments over an extended range of inlet variables and process parameters.

Stochastic simulations are conducted using the validated models to generate probabilistic process design spaces for each resin lot. These show the probability of meeting product quality specifications (i.e. the product CQA), over a range of possible operating conditions, whilst accounting for historical variability experienced in the load material composition and concentration. The data is used to determine if operating conditions exist that are eligible for all resin lots, by assuming that the operating conditions that assure product quality for the polar extreme high and low resin lots are suitable for all other resin lots. The stochastic methodology used to generate probabilistic design spaces is then extended, demonstrating how stochastic simulation can be used to identify the level of control required on uncertain variables to bring process robustness to an acceptable level, when current uncertainty results in an unsatisfactory design space. In this work, the control required on the load material composition and concentration is determined. The presented approach can be used with any validated mechanistic model with parameters that are variable or uncertain, and enables the rapid exploration of the trade-off between control of process parameters and the robustness of the design space, which is not possible using DOE experimental methods due to the impractical amount of resources that would be required.

FDA guidance encourages the application of mechanistic models to improve process understanding, based on fundamental knowledge of the underlying causes linking process parameters to product CQA's. The methodology demonstrates how useful mechanistic models can be for this task, for as well as determining the functional relationship between process parameter values and the resulting value of the CQA, the use of models can quickly and efficiently determine the relationship between process parameter and CQA variances, a key aspect of providing assurance of product quality.

## 5.2. Experimental materials and methods

### 5.2.1. **Materials**

#### *5.2.1.1. Therapeutic protein and feed material*

The product of interest is a disulphide linked dimer protein molecule (MW = 30 kDa), comprised of two monomer subunits. Three variations of the monomer subunit exist due to slight variations in the amino acid sequence, here denoted $A$, $\bar{A}$ and $B$. This results in six possible isoforms of the dimer ($AA, \bar{A}\bar{A}, A\bar{A}, \bar{A}B, AB$ and $BB$) as illustrated in Figure 5.1. The corresponding analytical chromatogram is shown in Figure 5.2 (Top). Each form is an active component of the final product which must contain a specific ratio of the monomer subunits, $(A + \bar{A}) : B$, i.e. not just one product form at a given total amount is required, but six closely related dimer variants, with a specific ratio of their monomer subunits. Specifically, subunit $B$ must account for between 25 – 45 % of all monomer subunits in the product, i.e. $0.25 < B < 0.45$. In addition to the product, the HIC feed material contains several product related impurities accounting for up to 25% by mass of the feed material, including the individual monomer subunits ($A$, $\bar{A}$ and $B$), incorrectly formed product species (MW = 42, 60, 80 and 100 kDa), and host cell related contaminants consisting of mainly host cell protein (HCP) and DNA. The analytical chromatogram used to distinguish between the different product and impurity species is shown in Figure 5.2 (Bottom).

#### *5.2.1.2. Chromatography resin*

Multiple (>20) Butyl Sepharose 4B fast flow hydrophobic interaction resin lots were obtained from GE Healthcare (Uppsala, Sweden). The two most extreme resin lots were selected for use in this work based on protein recovery in process development experiments conducted at standard operating conditions (not shown). The resins are designated high and low binding resin, e.g. the high binding resin gave high protein recoveries and the low binding resin gave low protein recoveries.

#### *5.2.1.3. Equipment*

All preparative scale laboratory experiments were carried out using an ÄKTA FPLC chromatography system from GE Healthcare (Uppsala, Sweden). Laboratory columns were 1.1 – 3.2 cm in diameter and 7.4 cm in bed height. A GE Healthcare Mono S column (5.0mm x 50mm) high performance liquid chromatography (HPLC) column was used for analytics, and a a TSK-Phenyl reversed phase column was used for the phenyl reverse phase assay.

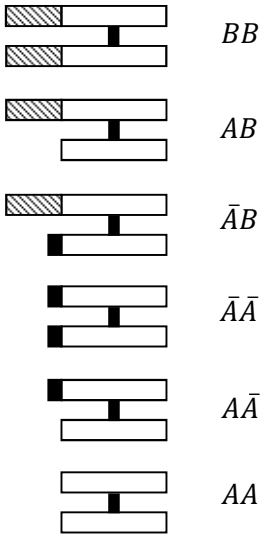


Figure 5.1. The product is a disulphide linked dimer protein therapeutic (MW ≈ 30 kDa), comprised of two monomer subunits. Three variations of the monomer subunit exist due to slight variations in the amino acid sequence, here denoted $A$, $\bar{A}$ and $B$. This results in six possible forms of the dimer, all of which are active components of the final product and that must be present in the elution peak in a specific distribution.

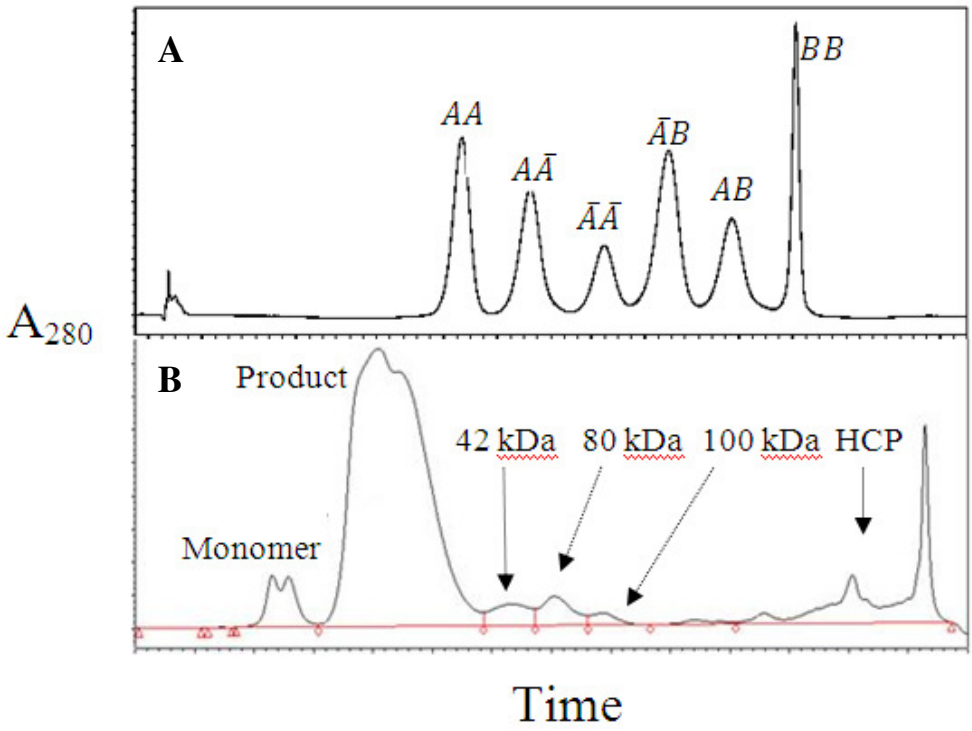


Figure 5.2. Analytical chromatogram of **A.** the product and **B.** the feed material. (Axis values deliberately removed for confidentiality purposes)

.

5.2.2. **Methods**

***5.2.2.1. Hydrophobic Interaction Chromatography***

During all runs, the columns were first equilibrated with 50 mM Tris, 1.0 M NaC1, 0.50 M Arg-HC1, pH 7 equilibration buffer. The elution peak from a preceding pseudo affinity capture chromatography was brought to the correct NaCl concentration and applied to the column at 4.2 CV/hr, followed by a wash step using the equilibration buffer. Elution buffer consisting of 20% Propylene Glycol, 50 mM Tris, 0.50 M Arg-HCl, pH 7 was then applied and the product peak collected. The pooling policy was fixed for all runs. Any remaining bound protein was removed in a strip step using 0.1 M Sodium Acetate, pH 4 sanitization buffer, and the column was stored in storage buffer when not in use. The efficacy of the elution stage is well understood, and was experimentally validated during process development. Negligible amounts of protein remain in the column after the elution stage and all mass balances were satisfactory during experimental runs. All experiments were conducted between 4 and 8 $^{o}$C.

#### *5.2.2.2. Cation Exchange HPLC Assay*

The Cation Exchange (CEX) HPLC assay utilises a Mono S column and a gradient of sodium acetate, acetonitrile and sodium chloride at pH 5.0 in order to determine the relative percentages of the six dimer isoforms of the product in the sample. After equilibrating the column for 30 minutes, 100 µl samples at 0.5 mg/ml are injected onto a column at a flowrate of 1 ml/min. Over the course of the gradient, separation of the isoforms is accomplished based upon competitive ionic exchange of the sample ions with a counter ion in the mobile phase, for fixed cationic functional groups on the column resin. Absorbance at 280 nm is measured at the column exit. Integration of the resulting chromatogram and analysis of the relative percentage area of each peak indicates the percentage of each isoform in the sample. The total time to run each sample is 30 minutes (Figure 5.2. Top).

#### *5.2.2.3. Phenyl Reverse Phase HPLC Assay*

The Phenyl Reversed Phase (RP) HPLC assay utilises a TSK-Phenyl reversed phase column and a water/acetonitrile/trifluoroacetic acid gradient system to determine the relative amount of product and product related impurities in samples. After equilibrating the column for 30 minutes, 100 µl samples at 1 mg/ml are injected onto a column equilibrated with a low percentage of acetonitrile mobile phase at a flowrate of 1 ml/min. As the organic modifier (acetonitrile) is increased over the course of the gradient, separation of the product related species and impurities is accomplished. Absorbance at 214 nm is measured at the column exit. Integration of the resulting chromatogram and analysis of the relative percentage area of each peak indicates the percentage of each species in the sample. The total time to run each sample is 80 minutes (Figure 5.2. Bottom).

#### *5.2.2.4. Generating purified product*

Protein solutions for model development experiments were generated from crude feed material, i.e. for batch adsorption experiments and impurity/no-impurity column experiments. Following initial purification by pseudo affinity capture, the material contained the 6 product forms of interest, as well as a range of product related impurities and host cell proteins (HCP's). The product forms were further purified and isolated from impurities over multiple runs on the HIC considered in this work. Multiple runs were required as it was particularly challenging to separate the product isoform BB from similar product related impurities. Fractions were taken every column volume (CV) and analysed by CEX HPLC in order to determine the isoform distribution of the sample. Multiple samples with a range of isoform distributions were generated in this way, and later pooled in order to generate material with desired isoform distributions for development experiments. Removal of product related impurities and HCP's was confirmed by phenyl RP HPLC.

#### *5.2.2.5. Impurity/no-impurity column experiments*

To confirm that the product related impurities and HCP's in the load material had a negligible impact on the separation of the product of interest, HIC column experiments were conducted with and without impurities in the load material. Experiments were identical in all other aspects i.e. load challenge, product concentration, product composition and washlength. In order to ensure that the product in the load material was the same for impurity and no-impurity experiments, material only containing impurities was combined with pure product.

#### *5.2.2.6. Batch adsorption experiments*

Batch adsorption experiments were required to generate data for calibrating the equilibrium adsorption isotherm parameters. Batch binding studies based on the work of Coffman et al. were conducted in a 96-well filter plate and were repeated in triplicate (Coffman et al., 2008). The filter plates used throughout the experiments were round-well 800 µl plates with 0.45 µm pore-size polypropylene membrane. 25 µl of resin was taken from a bulk reservoir and dispensed by the robotic liquid handler into the individual wells as 25% (v/v) slurry in the appropriate equilibration buffer. The plate was then centrifuged to evacuate excess liquid and leave damp resin. Subsequently, solutions composed of pure product, having various total protein concentrations (0.5 – 1 mg/ml) and isoform distributions (each component was varied between 20 – 60%) were added into wells containing the resin. The desired initial concentration and component distribution for each filter plate well was achieved by mixing together protein from bulk solutions of known component distributions and concentrations, with the appropriate amount of equilibration buffer from a bulk solution in order that the total volume of liquid dispensed into each well was 275µL ($V_{tot}$). The resin and solutions were then agitated on a platform shaker for 120 minutes. Separate batch uptake studies indicated that equilibrium was reached in less than 30 minutes (not shown), and therefore that this incubation time was suitable. Foil adhesive tape was used on the underside of the filter- plate to prevent liquid loss during shaking. After incubation, a centrifuge evacuated the supernatant into a UV-transparent 96 well micro plate which was stacked beneath the filter plate for analysis. The supernatant was then analyzed by a 96-well UV spectrophotometer (SpectraMax 250, Molecular Devices, Sunnyvale, CA) to determine the concentration of protein in the supernatant, $C_i^m$. CEX HPLC was used to determine the percentage of each component in the supernatant, $P_i^m$. The concentration of the protein in the mobile phase is then calculated from Eq 1:

$$C_i^m = \frac{C_{equil} \cdot P_i^m}{100} \quad [5.1]$$

where $C_{equil}$ is the measured concentration in the supernatant of the micro well (mg/ml), determined by UV spectroscopy. An elution cycle was then conducted following the same methodology as the load cycle, where 275 µL of elution buffer was added to each well, the plate agitated on a platform shaker for 120 minutes and the supernatant subsequently collected as described previously and analysed using the spectrophotometer and CEX HPLC. The total amount of protein added to each micro well was then determined by Eq 2:

$$M_t = \frac{C_{elution}}{V_{elution}} + \frac{C_{equil}}{V_{equil}} \quad [5.2]$$

where $M_t$ is the total amount of protein added to the micro well (mg), $C_{elution}$ is the concentration of the elution supernatant (mg/ml), $V_{elution}$is the volume of the elution supernatant (ml), $C_{equil}$ is the concentration of the equil supernatant (mg/ml), and $V_{equil}$ is the volume of the equil supernatant. The amount of protein adsorbed per unit volume settled resin, $q_i$, is calculated using Eq 3:

$$q_i = \frac{\left(\frac{M_t \cdot P_i^{load}}{100} - C_i^m \cdot V_{equil}\right)}{V_{resin}} \quad [5.3]$$

where $P_i^{load}$is the percentage of component $i$ in the load material and $V_{resin}$is the settled volume of resin in the microwell (25 µl in this work).

### *5.2.2.7. Pulse injection experiments*

Pulse injection experiments were required to determine the total column porosity, $\epsilon_T$. Pulses of NaCl were injected onto the column system and the retention time measured, accounting for dead time in the system. All experiments were performed in triplicate. The total column porosity, $\epsilon_T$, was calculated by the following equation:

$$\epsilon_T = \frac{t_0 F}{V_C} \quad [5.4]$$

where $t_0$ is the retention time of the unretained molecule, $F$ is the mobile phase flowrate and $V_C$ is the column volume.

## 5.3. Mathematical methods

### 5.3.1. **Process assumptions**

The similar amino acid sequence of two of the monomer subunits ($A$ and $\bar{A}$) results in similar separation properties of the product isoforms $AA, \bar{A}\bar{A}, A\bar{A}$ and of the product isoforms $\bar{A}B, AB$ . In order to simplify the modeling problem, the six product isotherms were reduced in the model to three species: $AA, AB,$ and $BB$. Because all product isoforms that remain bound to the column after the load and wash steps are subsequently collected in the elution step, only the load and wash stages of the separation are simulated and the elution peak composition calculated by mass balance.

### 5.3.2. **Model**

An equilibrium dispersive model was chosen to simulate the HIC (Guiochon et al., 1994, Kaczmarski et al., 2001) as it is faster to solve than the general rate model, which was important for reducing simulation time, and because fewer model parameters need to be determined, whilst still predicting the product CQA sufficiently well (as will be shown in section 4). The model is discussed in detail in the literature review section of this work and so is not repeated here. Model equations are summarised in Table 5.1 and described in detail in Appendix B. It is important to note that when the adsorption isotherm is linked with the mass conservation equation, the amount of protein adsorbed per unit volume of settled resin, $q_i$, is converted to the amount of protein adsorbed per unit volume of stationary phase in the packed bed, $C_i^{sp}$. Dividing $q_i$ by $(1-\epsilon_T)$ accounts for the phase ratio (Mollerup, 2008), and multiplying $q_i$ by a compression factor, $CF$, defined as the ratio between settled bed volume and packed bed volume, accounts for bed compression (Gerontas et al., 2010). The necessary compression had been determined experimentally during process development in order to prevent the formation of column headspace under flow conditions. All model equations were implemented and solved using the dynamic simulation tool gPROMS™ (Process Systems Enterprise, 2013). Discretisation of the column in the axial coordinate is done using the built-in orthogonal collocation on finite element method.

### 5.3.3. **Parameter estimation**

The 'parameter estimation' entity in gPROMS™ is based on the SRQPD sequential quadratic programming code and was used to fit adsorption isotherm parameters ($q_s, k_{a,i}$) and the apparent axial dispersion coefficient ($D_A$). Parameter estimation was based on the maximum likelihood formulation, which determines values for the uncertain physical and variance model parameters that maximise the probability that the model will predict

measured values from development experiments (Process Systems Enterprise, 2013). First the adsorption isotherm parameters are estimated by fitting the competitive Langmuir isotherm model to the three component competitive adsorption data from the micro well batch adsorption experiments (section 5.2.2.6). For estimation of the apparent axial dispersion coefficient, the full equilibrium dispersive model with competitive Langmuir adsorption is fitted to experimental product form distributions in samples taken every CV during the wash of a scale down column run (section 5.2.2.1).

Table 5.1. Summary of equiliubrium dispersive model used in this chapter. For a detailed description of the model and variables please refer to Appendix B

**Equilibrium dispersive model with competitive Langmuir adsorption**

Mass conservation

$$\frac{\partial C_i^m}{\partial t} + \frac{(1-\epsilon_T)}{\epsilon_T} \cdot \frac{\partial C_i^{sp}}{\partial t} + u \cdot \frac{\partial C_i^m}{\partial z} = D_A \cdot \frac{\partial^2 C_i^m}{\partial z^2} \qquad \forall i = 1, 2, \dots, N_C \qquad z \in (0, L)$$

Boundary conditions

$$\left[ u C_i^m - D_A \frac{\partial C_i^m}{\partial z} \right]|_{z=0} = u C_{i,0}^m \qquad \forall i = 1, 2, \dots, N_C$$

$$\frac{\partial C_i^m}{\partial z}|_{z=L} = 0 \qquad \forall i = 1, 2, \dots, N_C$$

Initial condition

$$\frac{\partial C_i^m}{\partial t} = 0 \qquad 0 < z < L \qquad \forall i = 1, 2, \dots, N_C$$

Adsorption isotherm

$$q_i = \frac{q_s \cdot k_{a,i} \cdot C_i^m}{1 + \sum k_{a,i} \cdot C_i^m} \qquad \forall i = 1, 2, \dots, N_C \qquad z \in (0, L)$$

$$C_i^{sp} = \frac{CF \cdot q_i}{(1 - \epsilon_T)} \qquad \forall i = 1, 2, \dots, N_C \qquad z \in (0, L)$$

where

| | |
|---|---|
| $C^m$ | Extra particular mobile phase concentration [mg/ml] |
| $C^{sp}$ | Stationary phase concentration [mg/ml] |
| $CF$ | Compression factor [-] |
| $D_A$ | Apparent axial dispersion coefficient [cm$^2$/s] |
| $i$ | Component identifier [-] |
| $k_a$ | Equilibrium constant [-] |
| $L$ | Column length [cm] |
| $N_C$ | Number of components [-] |
| $q_s$ | Saturation capacity [mg/ml] |
| $q$ | Concentration per unit volume settled resin [mg/ml] |
| $t$ | Time [s] |
| $u$ | Interstitial velocity [cm/s] |
| $z$ | Axial coordinate [cm] |
| $\epsilon_T$ | Total column porosity [-] |

Table 5.2. Historical average and standard deviations of product form inlet concentrations.

| Variable name | Variable notation | Average (mg/ml) | Standard deviation |
|---|---|---|---|
| ***AA*** inlet concentration | $C_{1,0}^{m}$ | 0.108 | 0.024 |
| ***AB*** inlet concentration | $C_{2,0}^{m}$ | 0.127 | 0.023 |
| ***BB*** inlet concentration | $C_{3,0}^{m}$ | 0.104 | 0.023 |

### 5.3.4. **Stochastic simulation**

Stochastic simulations were conducted following the same procedure as described in Chapter 3, Section 3.3.3. In this chapter, the impact of variability in the load material concentration and composition on the ratio of the monomer subunits, $(A + \bar{A}):B$ in the elution pool (a defined CQA for the HIC process) was considered. The impact of errors in model predictions, as well as uncertainty in controlled variables such as ionic strength, bed height etc. was not considered. The rational for this is discussed later. The exact parameter varied in the mechanistic model was the inlet concentrations of the load material, $C_{i,0}^{m}$. Historical averages and standard deviations from manufacturing data were used to generate probabilistic design spaces for current process variability (Table 5.2).

In this chapter, the stochastic simulation approach is extended to explore the impact of reducing variability in the load material on the design space. The aim is to identify the level of control required on uncertain variables to bring process robustness to an acceptable level when current uncertainty results in an unsatisfactory design space. Standard deviations in model simulations are manually assigned assuming that better control would result in less variability, and therefore a reduced standard deviation. Manually changing the load concentration average is also possible, and may be of interest as feed dilution is trivial, but this was not considered in this work.

## 5.4. Results and discussion

### 5.4.1. **Impurities**

The FDA requires that the removal of various contaminants in the final drug product is validated (Lightfoot and Moscariello, 2004). The complexity and variety of these contaminants result in a range of issues when developing a mechanistic model that can accurately simulate their separation and thus fulfil this requirement. Impurities are often at levels on the lower detection limit of available assays, which require a large amount of material, time and resources in order to analyse.

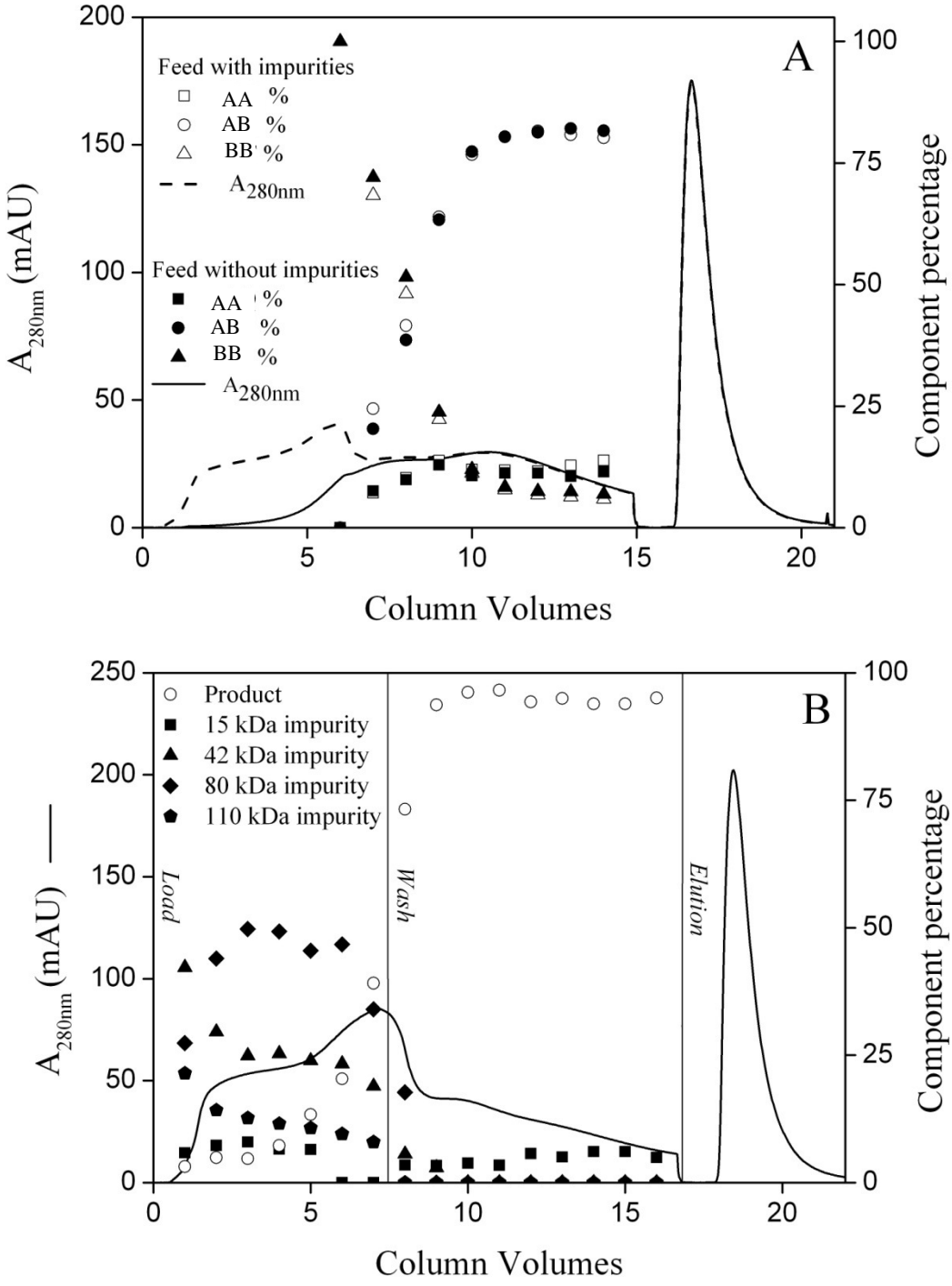


Figure 5.3. **A**. Experimental comparison between column runs using feed material with and without impurities (7 ml CV, 7.3 cm bed height, 5.7 CV/hr, inlet concentration = 0.34 mg/ml, load challenge = 2 mg/ml). Similar product form percentages and overlapping A280nm trace during wash and elution indicates that impurities have minimal impact on separation of product forms and can be neglected in the model. **B**. Chromatogram showing the A280nm trace and the percentage of product related impurities and product in samples taken every CV during a standard HIC run, determined by phenyl RP HPLC. The figure shows that the majority of impurities in the feed material elute from the column during the load phase, product forms begin to elute from the column at the end of the load phase and continue throughout the wash.

In this work, it was impractical in terms of time and material requirements to generate samples in high enough volumes and concentrations of impurities in order to develop a mechanistic model for simulating these components. From an industrial perspective, the experimental design of experiment (DOE) approach to developing and validating the removal of impurities during the chromatography is preferable to a mechanistic modelling approach. Therefore, the effect of impurities was not included in the model. Instead, it was assumed that the product related impurities and HCP's in the feed stream had a negligible impact on the separation of the product of interest, as the impurities are observed to flow through during the load phase of the chromatographic cycle (Figure 5.3B). This assumption was confirmed by comparing the product form distributions in fractions collected every CV during HIC runs with and without impurities in the feed material. Runs were identical in all other aspects e.g. load challenge, product form concentrations and washlength. The results indicated that the impurities had no effect on the product distributions (Figure 5.3A). In addition, by comparing the UV traces in Figure 5.3A, one can clearly see where the impurities are flowing through during the load step, before the two UV traces merge and are in exact agreement.

### 5.4.2. **Model development**

Micro well batch adsorption experiments (3.2.2) were utilized to generate data for estimating the adsorption isotherm parameters, $q_s$, $k_{a,i}$. Figure 5.4 shows the multi-component competitive adsorption data from the micro well experiments for the high and low binding resin lots, at four different load material product distributions shown on the graphs in the ratio $AA\ \% : AB\ \% : BB\ \%$. The product form distribution in the load material was varied to ensure that the competition between the closely related product forms was captured in the isotherm model. Note that although the graphs show the bound concentration of the product form as a function of its mobile phase concentration, the mobile phase concentration of the other two product forms are also affecting the bound concentration.

The estimated isotherm parameter values are shown in Table 5.3. The standard deviations of the estimated parameters are approximately ten percent, indicating there is still some uncertainty in the parameter values. The coefficient of determination, $r^2$, for the model fit to experimental data was 0.93 for the high resin and 0.96 for the low resin. This was found to be sufficient for satisfactory agreement between model predictions and experimental data given the inherent uncertainties of the batch adsorption experiments. Interestingly, the estimated saturation capacity of the Langmuir isotherm, $q_s$, were similar for both resins, however, the equilibrium constants differed for all three components. This indicated that the source of the resin lot variability was associated with protein adsorption-desorption kinetics

and not the maximum saturation capacity. A detailed investigation into the exact mechanism behind this variability was beyond the scope of this work.

Both resin lots showed significant competition between product forms, with component $BB$ particularly vulnerable to displacement by the more strongly binding $AA$ and $AB$ forms. In Figure 5.4C, the $BB$ stationary phase concentrations are significantly higher compared to Figure 5.4B. This is due to the favourable product distribution in the load material resulting in fewer competing components, allowing more $BB$ to bind (Figure 5.4C load material 25% $AA$ : 20% $AB$ : 55% $BB$, Figure 5.4B load material 28% $AA$ : 59% $AB$ : 13% $BB$). It was found that the low binding resin had lower binding capacities than the high binding resin. This was especially clear for the $BB$ component as shown in Figure 5.4C where the low binding resin $BB$ stationary phase concentration is approximately half that of the high binding resin.

Pulse injections onto scale down columns (section 5.2.2.7) using an unretained molecule (NaCl) found that both resin lots had the same total column porosity, 0.9 +/- 0.02, which was in agreement with previous literature estimations for this resin (McCue et al., 2007). The apparent axial dispersion coefficient, $D_A$, was first estimated from the number of theoretical plates of the column, $N_p$, according to the following correlation (Guiochon et al., 1994):

$$D_A = \frac{vL}{2N_p} \qquad [5.5]$$

Table 5.3. Model parameter values obtained for low and high binding resins based on batch adsorption and scale down column experiments, fitted using parameter estimation in gPROMS. Figure 5.5 gives an illustration of the fit between experimental data and simulations achieved by estimated parameters.

| **Parameter name** | **Parameter notation** | **Low** | **High** |
|---|---|---|---|
| ***AA* equilibrium constant** | $k_{a,1}$ | 4.33 | 6.33 |
| ***AB* equilibrium constant** | $k_{a,2}$ | 1.49 | 2.30 |
| ***BB* equilibrium constant** | $k_{a,3}$ | 0.52 | 1.01 |
| Saturation capacity | $q_s$ | 6.45 | 6.39 |
| Total column porosity | $\epsilon_T$ | 0.9 | 0.89 |
| Apparent axial dispersion coefficient | $D_A$ | 0.0029 | 0.003 |

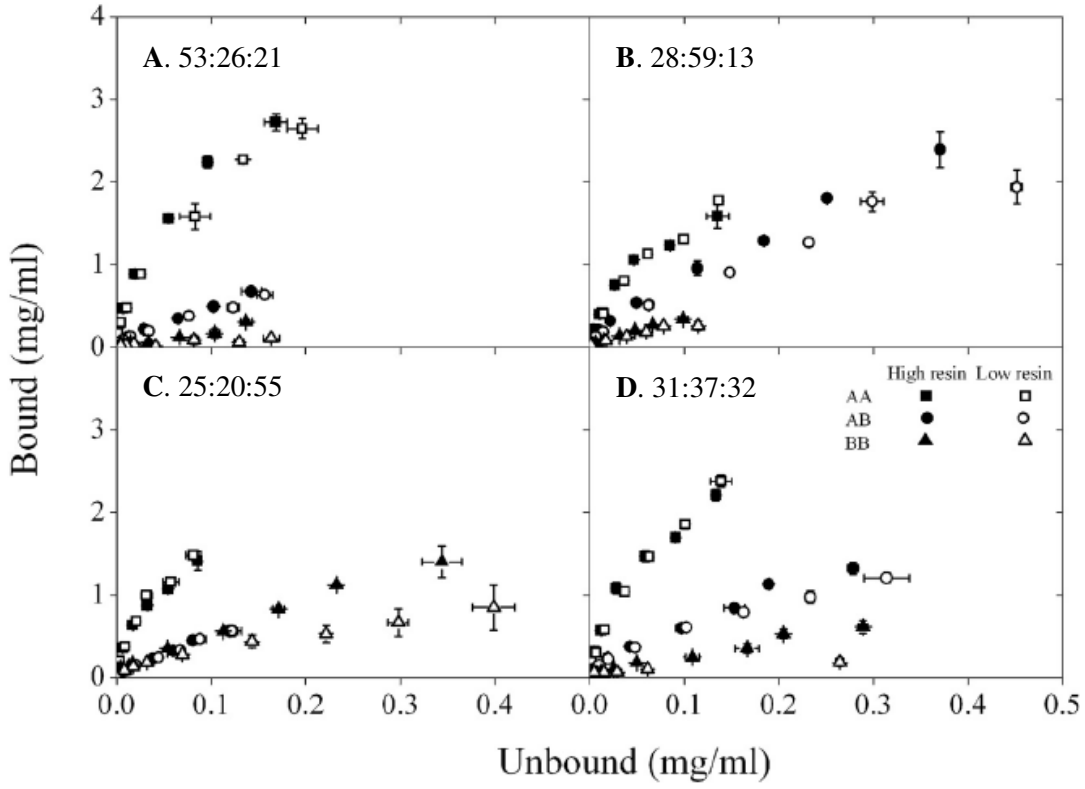


Figure 5.4. High and low resin multicomponent competitive adsorption isotherms at a range of load material product distributions, as shown on the graphs in the order AA% : AB% : BB%. The experimental data is from micro well plate batch adsorption followed by CEX HPLC analysis. All experimental points were repeated in triplicate and standard error is shown on graphs.

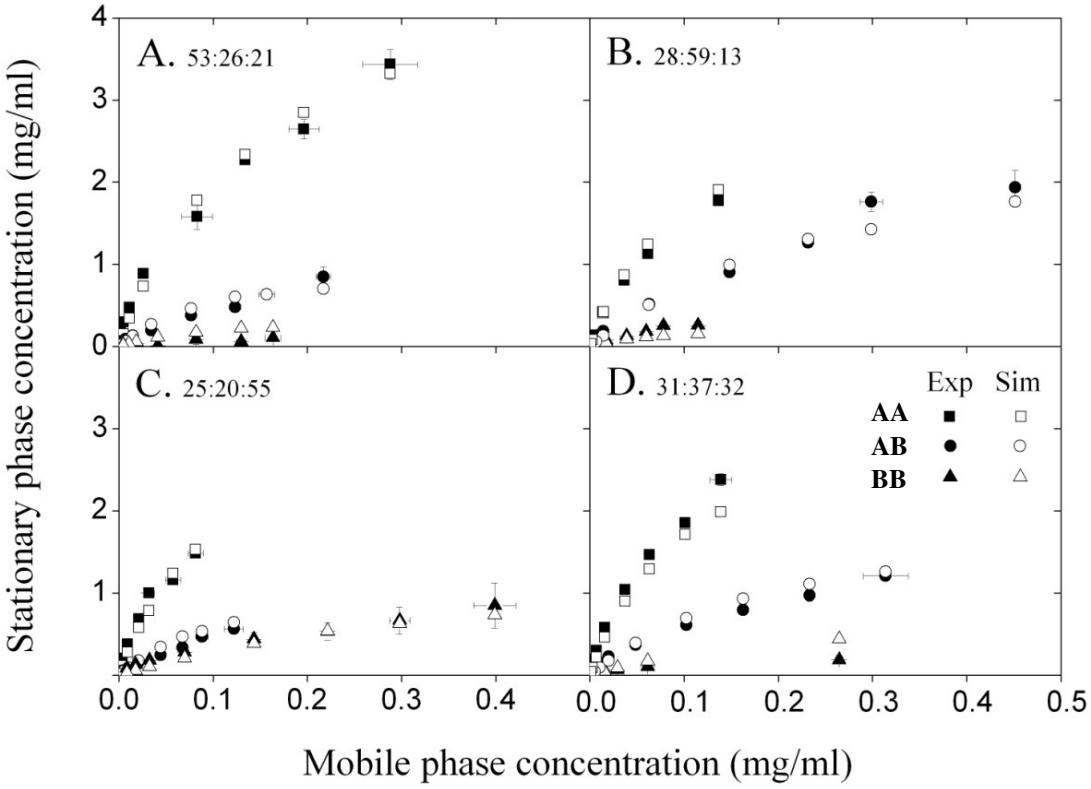


Figure 5.5. Experimental and simulated multicomponent competitive adsorption isotherms for the high binding resin at a range of load material product distributions, as shown on the graphs in the order AA% : AB% : BB%. The experimental data is from micro well plate batch adsorption followed by CEX HPLC analysis. All experimental points were repeated in triplicate and standard error is shown on graphs. The competitive Langmuir isotherm model (Equation 9) was fitted to the experimental data, and simulations showed good agreement with experiments.

However, the model was unable to give satisfactory predictions of the chromatographic process using the value estimated from this correlation Figure 5.6. This was not unexpected, as the lumped mass transfer coefficient value was determined using the residence time of an unretained molecule (NaCl) that was significantly smaller than the protein, and thus would be expected to experience faster mass transfer. The apparent axial dispersion coefficient was therefore estimated by fitting the full equilibrium dispersive model to experimental product form distributions in samples taken every CV during the wash of a scale down column run. The value calculated by the correlation was used as the initial guess. We found that the estimated apparent axial dispersion coefficients for high and low binding resin lots were very similar (high resin = 0.029 and low resin = 0.03), indicating that mass transfer was not responsible for differences between the resin lots.

### 5.4.3. **Model validation**

Multiple scale down column runs were conducted for each resin lot in order to provide a rigorous test of model predictive capacity, where the product form distribution was measured across the wash phase and in the elution peak. An extensive experimental validation of model predictive capability across the complete design space to be explored was unfeasible due to industrial time and material constraints. However, the isoform distribution in the load material, total load concentration and load challenge were carefully selected (Table 5.3) to provide wide ranging coverage of the envisaged design space, and model predictions were also compared with existing elution peak product data from scale down experiments which had been conducted previously by Pfizer purification process development (Table 5.4), at load concentrations, load challenges and wash lengths considerably different from those conducted by the authors of this work. The flowrate, $F$, wash length, and bed height, $L$, were kept constant throughout all runs and a range of column volumes were used (7, 15 and 60 ml). For both resins, the model was able to successfully predict the product form distribution across the wash and in elution peaks in all scale down model validation column runs, both from this work, and those conducted separately by Pfizer. Figure 5.7 shows examples where model predictions are compared with experiments. Model elution peak composition was consistently within +/- 5% of experimentally measured values (Table 5.5), which was similar to the accuracy seen in design of experiment driven statistical response surface models of this process at Pfizer. This is significant, as it demonstrates that despite the complex feed stream and wide range of conditions tested, a relatively simplistic equilibrium dispersive model can provide similar accuracy predictions to a DOE type approach to design space generation, often used in industry.

Table 5.4. Model validation runs: Product percentage in load, load concentration, and load challenge.

| **Run identifier** | **Load Challenge (mg/ml resin)** | **Load Concentration (mg/ml)** | ***% AA*** | ***% AB*** | ***% BB*** |
|---|---|---|---|---|---|
| A | 1.5 | 0.26 | 35 | 35 | 30 |
| B | 2.2 | 0.35 | 40 | 44 | 16 |
| C | 2.4 | 0.44 | 14 | 38 | 48 |

Table 5.5. Model validation runs: Experimental vs simulated percentage ***A*** and ***B*** in elution peaks

| **Resin identifier** | **Run identifier** | **Exp *% A*** | **Sim *% A*** | **Difference** | **Exp *% B*** | **Sim *% B*** | **Difference** |
|---|---|---|---|---|---|---|---|
| | A | 81 | 79 | -3 | 19 | 21 | +3 |
| High | B | 85 | 82 | -3 | 15 | 18 | +3 |
| | C | 71 | 68 | -3 | 29 | 32 | +3 |
| | A | 90 | 90 | 0 | 10 | 10 | 0 |
| Low | B | 93 | 93 | 0 | 7 | 7 | 0 |
| | C | 86 | 81 | -5 | 14 | 19 | +5 |

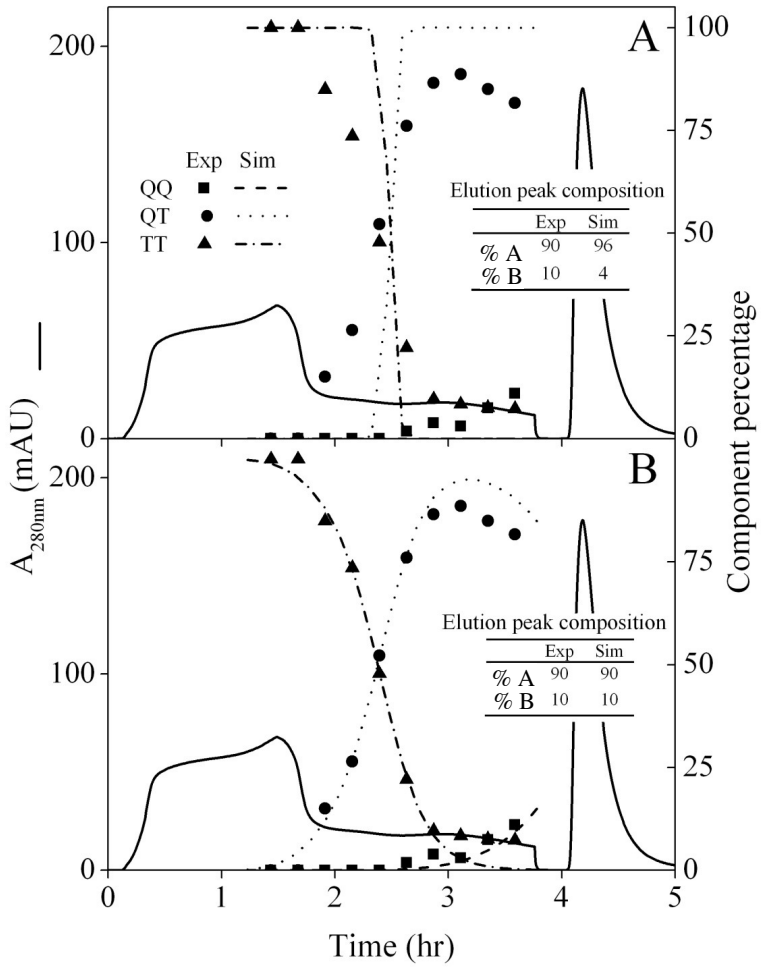


Figure 5.6. Experimental and simulated product form distributions for the low binding resin lot during load, wash and in final elution peak. **A**. Before model refinement. **B**. After model refinement. The apparent axial dispersion coefficient and the *AA* adsorption constant were modified from 0.0001 $cm^2/s$ to 0.003 $cm^2/s$, and 5.31 to 3.5 respectively.

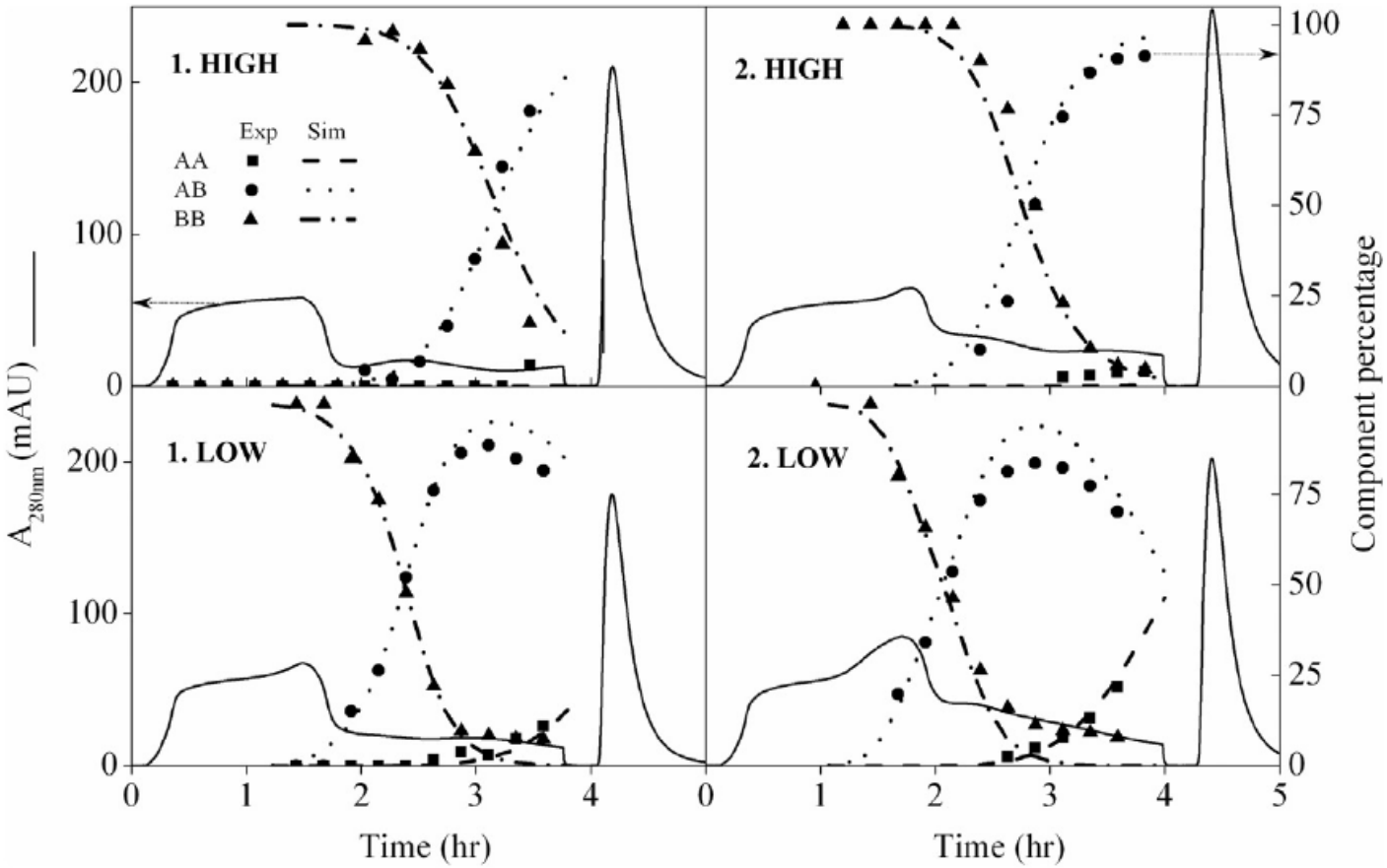


Figure 5.7. Experimental and simulated product form distributions for the high (top) and low (bottom) resin lots during load, wash and in final elution peak in model validation runs A (right) and B (left). (7 ml CV, 7.4 cm bed height, 4.2 CV/hr, load details shown in Table 5.4). Experiments and simulations were in good agreement.

### 5.4.4. **Stochastic simulations**

The mechanistic models developed for the high and low resin lots can determine the operating conditions where product quality specifications will be met for a known inlet concentration and composition. However, in practice, for industrial chromatographic separations the feed material is often uncharacterised prior to column loading, and will vary from batch to batch depending on upstream operations. In this work, a model based approach combining the validated mechanistic model with stochastic simulation is used to account for the inherent variability of inlet concentration and composition when determining the ability of a resin lot to meet the process objectives (or conversely the risk of batch failure).

The methodology is illustrated in an example which shows the data generated at one potential mass challenge – wash length combination. The component inlet concentration distributions were generated from historical data, and are shown in Figure 5.8A. Averages and standard deviations are shown in Table 5.2. For illustrative purposes the first 1000 randomly generated inlet concentrations of product form AA is shown in Figure 5.8B, and the corresponding value of the product CQA (i.e. subunit B must account for between 25 – 45 % of all monomer subunits in the product, i.e. $0.25 < B < 0.45$) is shown in Figure 5.8C.

It is a straightforward procedure to generate useful statistical information with this data regarding CQA variance at each operating point, such as moments and quartiles, as shown in Figure 5.9 for the low binding resin. The statistical data can be conveniently displayed using a box and whisker plot. The bottom and top of the box are the first and third quartiles, and the band inside the box is the median. The end of the lower whisker represents the datum still within 1.5 interquartile range (IQR) of the lower quartile, and the end of the upper whisker represents the datum still within 1.5 IQR of the upper quartile. The minimum and maximum of the data is indicated in the whiskers by a straight line, and the 1% and 99% quartiles are represented by crosses. Outliers are plotted as dots. More sophisticated statistical techniques can be employed to analyse multivariate interactions and CQA dependencies. The derived data can play a key role in the quality risk assessments recommended by FDA guidance when developing quality products (ICH, 2005). The data was transformed into probability density functions which were used to calculate the probability of meeting the product CQA as a function of inlet uncertainty, as also shown in Figure 5.9. Probabilistic design spaces were then generated by plotting the probability of meeting the product CQA (%B) as a function of available manipulated variables, e.g. mass challenge and wash length.

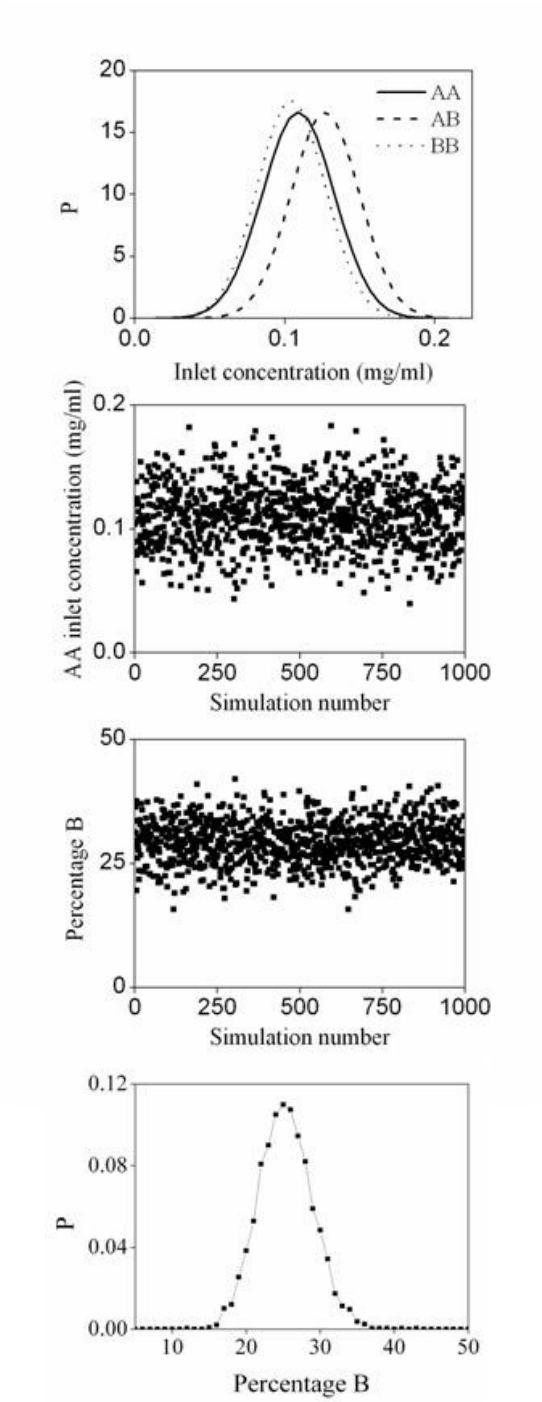


Figure 5.8. Example of the stochastic modeling technique used in this work. **A** Normal distribution of inlet concentration of example product form from historical operating data. **B**. Example of randomly selected inlet concentrations of product form *AA* during the first 1000 stochastic simulations. **C.** Percentage *B* in elution peak over the first 1000 simulations. (Mass challenge 2 mg/ml, 5 CV wash length). **D.** Probability density function of product CQA.

Accounting for uncertainty in controlled variables such as ionic strength was beyond the scope of this work, but can be integrated into simulations if desired. In this case, a suitable isotherm with a parameter that can be assigned uncertainty concerning ionic strength, such as the steric mass action (SMA) isotherm, would be required (Brooks and Cramer, 1992). In addition, the impact of model uncertainty on stochastic predictions can be included, although this was neglected in this work as the CQA variance (e.g. 10% - 42% in the example shown in Figure 5.9) was typically much larger than the largest model error found during model validation studies (+/- 5%). Despite this, the uncertainty in model predictions cannot be easily neglected and care must be taken to ensure that robust operating areas identified by model predictions are tested experimentally.

| MOMENTS | |
|---|---|
| Standard deviation | 3.74 |
| Mean | 23 |

| QUARTILES | | |
|---|---|---|
| 100 | Maximum | 42 |
| 99.5 | | 34 |
| 97.5 | | 31 |
| 90 | | 28 |
| 75 | Quartile | 26 |
| 50 | Median | 23 |
| 25 | Quartile | 21 |
| 10 | | 19 |
| 2.5 | | 16 |
| 0.5 | | 14 |
| 0 | Minimum | 10 |

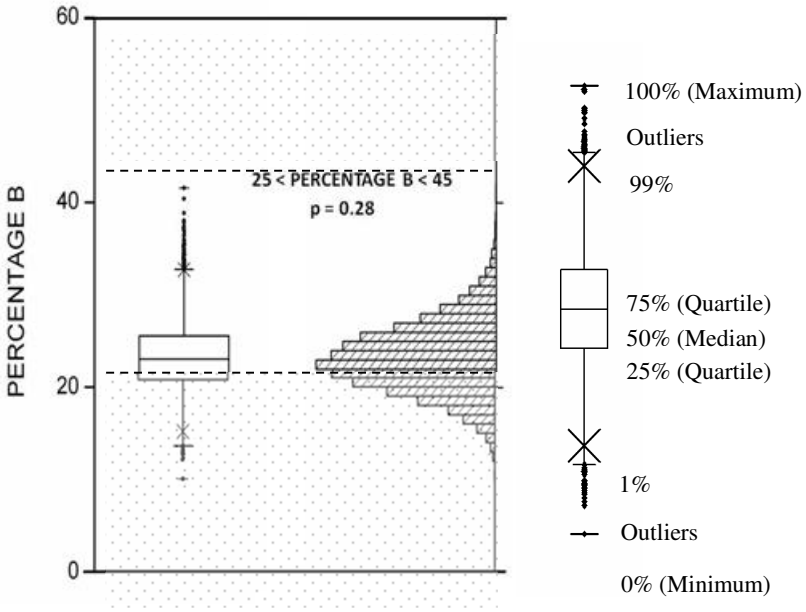


Figure 5.9. CQA data from stochastic simulation at mass challenge = 2 mg/ml, washlength = 5 CV in box plot and probability distribution form with associated moments and quartiles.low resin

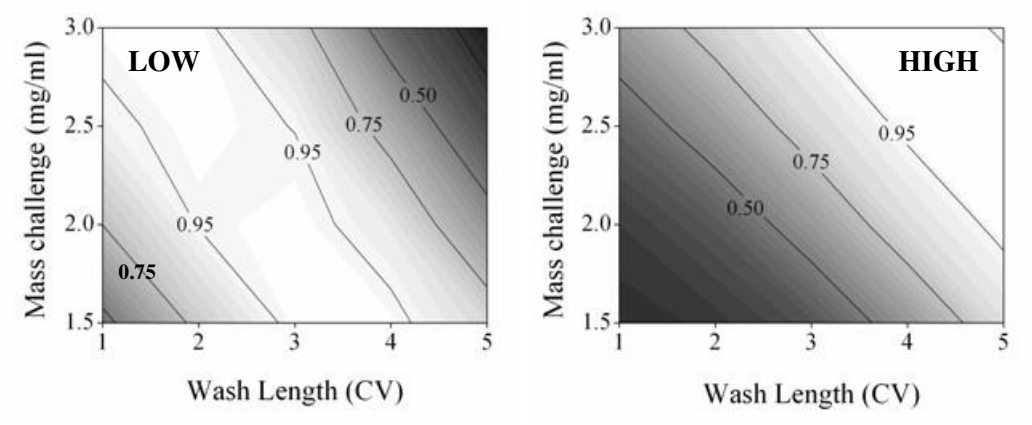


Figure 5.10. Probabilistic design spaces for low binding (left) and high binding (right) resin lots, showing the probability that the resin will achieve the correct product form distribution in the elution peak over a ranges of possible mass challenges and wash lengths.

Probabilistic design spaces for the low and high resin lots are shown in Figure 5.10. The design space is defined as the multidimensional combination and interaction of input variables and process parameters that have been demonstrated to provide assurance of product quality, i.e. that product CQA's are met. The key characteristic of probabilistic design spaces is that they provide quantitative information on the assurance of quality, accounting for both the mean and the variance of uncertain process parameters and variables. No combination of mass challenge and wash length was found for either resin lot which had a probability of 1.0 for the historical variability experienced in the load material, i.e. that would guarantee the CQA is always met. However, the large size of regions where the probability < 0.95 meant that rarely would the process fail to meet its objectives if the operating condition was specific to the resin lot in use. The large difference between operating conditions that give p > 0.95 for each resin are somewhat surprising given the small difference between the adsorption isotherm parameters, but are due to the very challenging CQA constraint, combined with the mean and variance of the inlet composition and concentration.

When the design space must be eligible for all resin lots, then the probability of achieving the correct product form distribution in the elution peak should be high for both resin lots. Figure 5.11 shows an overlay of the two resins' probabilistic design spaces. Critically, there was no operating region where the probability of both the low and high resin lots remained > 0.95, i.e. risk of batch failure < 5%. Even at the optimum operating condition where the two

curves intersect (e.g. mass challenge 2 mg/ml, wash length 4 CV), the probability only reaches 0.84. As a result, the operating parameter ranges available for manufacturing are small, and at best, 16 % of batches are still predicted to fail product quality specifications. In addition, the product form distribution will vary within the full allowable range (0.25 < B < 0.45), which is undesirable when the objective is to produce a consistent product.

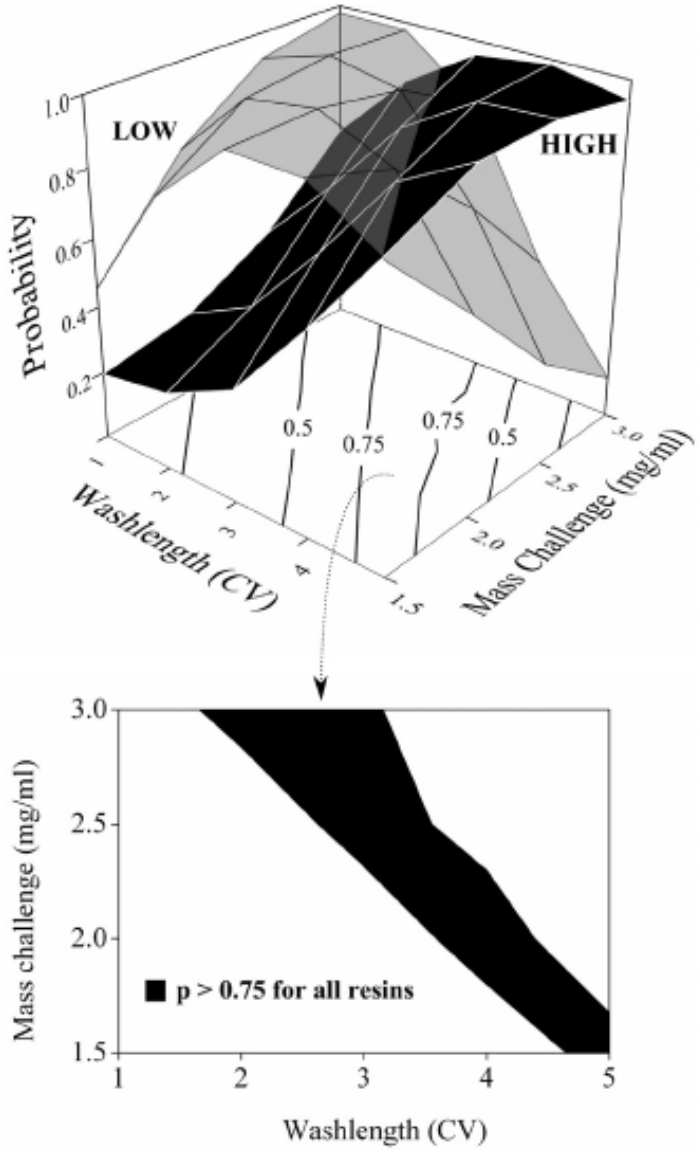


Figure 5.11. Overlay of high and low resin probabilistic design spaces showing the operating parameter ranges where product quality is assured with p > 0.75 for all resins.

Selecting operating conditions that are eligible for all resin lots also means that high risk regions are selected, where deviations from usual inlet stream composition can result in further performance issues. For this case study, significant increases in process robustness can be made by adapting the design space based on the resin lot in use, rather than fixing the design space for all resin lots. In practice, this would involve varying the length of the wash length based on the resin lot in use. This adaptive approach significantly increases the size of potential operating regions, improves flexibility to variations in process inputs, provides a more consistent product composition, and enables operation further away from high risk regions. This conclusion, that adaptive operation can bring significant benefits is in agreement with literature (Gétaz et al., 2013), and is a viable mode of operation under FDA Quality by Design guidance (ICH, 2008a).

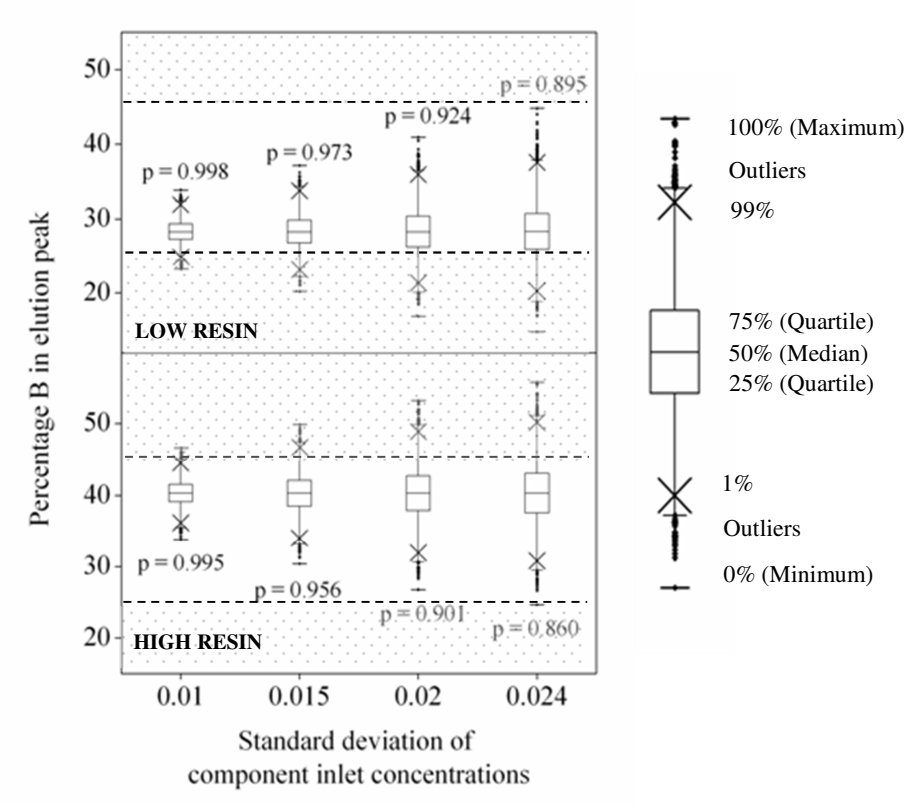


Figure 5.12. Box plots showing variability of percentage *B* in elution peak as a function of variability in component inlet concentration, with probability of meeting quality specifications indicated next to each box plot, for a mass challenge of 2 mg/ml and wash length 4 CV.

The probabilistic design spaces presented are particularly useful as they provide a quantitative measure of the assurance of product quality, which either validates the robustness of potential operating regions, or indicates a need for process improvement. The stochastic methodology can be easily extended to identify the level of control required on uncertain parameters/variables to achieve adequate assurance of quality, by systematically reducing the variance of uncertain parameters, and measuring the quality response. Alternatively, when parameter variability is reduced due to improvements and optimisation by process operators as experience is built over a process lifetime, the method can identify how operating ranges can be expanded to give greater flexibility to process operators during manufacturing.

For this case study, the data indicates that if the operating parameter ranges must be fixed for all resin lots, then process improvements are needed. Without process improvements, operating regions that provide assurance of product quality are small and are not robust. We now consider how decreasing variability in the product form inlet concentrations via increased control of upstream unit operations can improve the assurance of quality when using an operating region fixed for all resins. Better control was assumed to result in less variability, and therefore a reduced standard deviation. A detailed description of how this can be achieved in practice is beyond the scope of this work, but could include modifications to upstream processes such as optimising the elution stage of preceding affinity chromatographic separations. In any case, the study is a useful exercise for illustrating how stochastic simulation and mechanistic models can be used not only for quantifying risk associated with uncertainty, but for exploring the relationship between parameter and CQA variance, a key consideration when validating quality assurance.

Figure 5.12 shows box plots indicating predicted variability of the product CQA (percentage B in the elution peak) as a function of the variability in the product form inlet concentrations. The mass challenge was 2 mg/ml and wash length 4 CV, previously identified as one of the optimal operating points for a fixed design space. The standard deviations considered include: 0.01, 0.015, 0.02 and 0.024. The probability of meeting the CQA specification is indicated next to each box plot (e.g. $p = 0.998$). As expected, reducing feed stream uncertainty (i.e. going from 0.024 towards 0.01) results in a reduction in product CQA variability, which translates into increases in the probability of meeting quality specifications (i.e. for low resin, $p = 0.0895$ to $p = 0.998$).

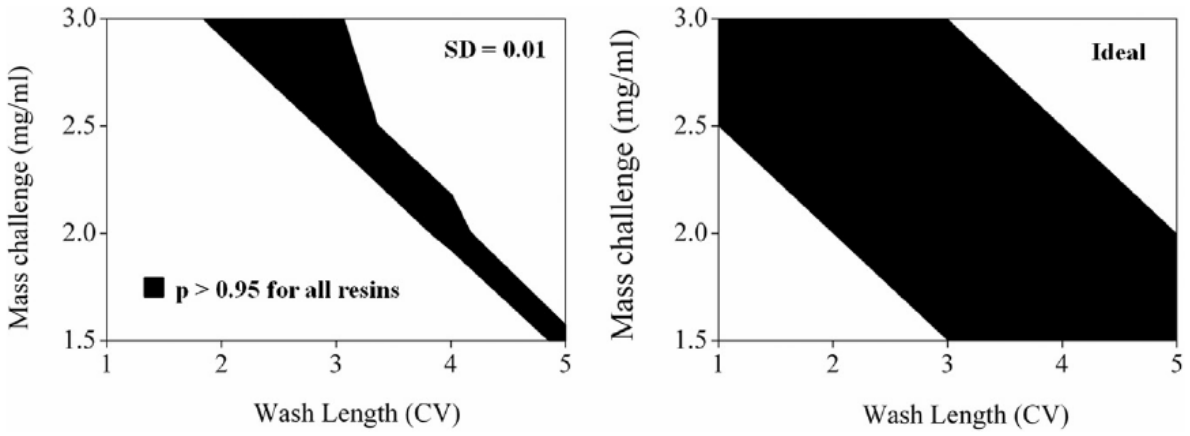


Figure 5.13. Fixed design space with highest level of feed stream control considered in this work, SD = 0.01, (left), and ideal design space assuming no feed stream variability (right).

When this is completed for all operating conditions, the size of regions with $p > 0.95$ (i.e. <5% failure) increases. Figure 5.13A shows the region where $p > 0.95$ for both resins at the lowest inlet variability considered (SD = 0.01). Even with this high level of control over the feed material, operating regions where $p > 0.95$ were significantly smaller than those available if the operating conditions were adapted according to the resin lot in use under normal inlet variability (Figure 5.10). Figure 5.13B shows the design space which assures product quality for all resins in an ideal (but unrealistic) system with no inlet variability. The large difference in size between Figure 5.13A (ideal system with no inlet variability) and Figure 5.13B (lowest inlet variability considered, SD = 0.01), provides a stark demonstration of the importance of considering parameter variances when designing chromatography processes. If this is not accounted for, then the result may be unrealistically good expectations and in turn high failure rates.

## 5.5. Conclusion

A model based approach was used to identify robust operating conditions for an industrial hydrophobic interaction chromatography where resin lot variability, combined with a variable feed stream, was resulting in serious performance issues during the purification of a multi component therapeutic protein from crude feed material. FDA guidance encourages the application of mechanistic models to improve process understanding, based on fundamental knowledge of the underlying causes linking process parameters to product CQA's. The methodology presented in this work demonstrates that mechanistic models can be very useful for this task, for as well as determining the functional relationship between process parameter values and the resulting value of the CQA, they can quickly and

efficiently determine the relationship between process parameter and CQA variances, a key aspect of providing assurance of product quality. This was not possible using a design of experiment type of approach for the HIC considered in this work, due to the impractical amount of resources that would be required.

The model based approach combines mechanistic models and stochastic simulation, and was used to predict a key product CQA as function of mass challenge and wash length for two polar extreme resin lots, designated high and low binding resin, whilst accounting for uncertainty in feed stream composition and concentration. With normal process variability, no operating condition was found where the probability of both the low and high resin lots meeting product quality specifications remained > 0.95. The risk of batch failure when operating at the most favourable conditions found in this work was 16%, and selecting operating conditions that were eligible for both resin lots meant that operating conditions were not robust. Increasing control on the inlet concentration and composition was predicted to improve fixed design space robustness, but we found that using an adaptive design space, where operating conditions are changed according to which resin lot is in use, was the favorable option.

# Chapter 6. Conclusions and Future Work

*The overall aim of this thesis was to derive fundamental process understanding of specific industrial chromatographic separations currently in development or operation at Pfizer, via the development and application of mechanistic chromatography models. The thesis contains three distinct contributions: (1) A platform model of weak partitioning anion exchange chromatography was developed to provide a link between high throughput screening (HTS) and scouting runs conducted during early process development. (2) An experimental investigation was conducted into fouling of the anion exchange weak partitioning chromatography, providing a basis for addressing a lack of fundamental knowledge and mechanistic understanding of fouling in industrial bioseparations. (3) A mechanistic model was used to identify robust operating parameter ranges for an industrial hydrophobic interaction chromatography, at a late stage of development, experiencing performance issues due to resin lot variability. The key outcome of the work is that there are significant advantages to be gained by the use of mechanistic models of chromatography in industry. The recommendation for future work is to develop a platform that brings the various models, tools, procedures and expert guidance together to allow industrial users to efficiently and quickly implement mechanistic models within industrial constraints. The key areas that need addressing are discussed related to the modelling framework, model parameters and physical properties, model calibration and model applications.*

## 6.1. Review of Project Objectives

The overall aim of this thesis was to derive fundamental process understanding of specific industrial chromatographic separations currently in development or operation at Pfizer, via the development and application of mechanistic chromatography models. The goal was to accelerate the development and increase the robustness of *industrial* protein purification processes, whilst following guidance regarding the implementation of Quality by Design.

### 6.1.1. **Weak partitioning chromatography**

Chapter 3 looked at developing and applying mechanistic models of chromatography at an early stage of process development, focusing on the platform anion exchange weak partitioning process. This key step in the purification process of monoclonal antibodies experienced difficulty delivering the required level of impurity removal, whilst maintaining product recovery, when facing challenging load material compositions. In addition, there was an overreliance on experimental process development and a lack of fundamental process understanding.

A platform model was developed that was applicable at an early stage of process development. This was achieved by characterising the equilibrium adsorption isotherms of the three key species involved in the separation: the product (monomer) and two product related impurities (dimer and multimer) which were not previously known. In addition, a new approach was taken where the adsorption was characterised as a function of the product partition coefficient, enabling the model to be applied to new candidate monoclonal antibodies without additional experimental effort. A simple high throughput screening experiment, which can be automated and conducted in a few hours by a trained scientist, was all that was needed to calibrate the model to the particular molecule. This experiment is routinely conducted as part of the existing experimental approach to process development, and as such, does not comprise any additional effort.

The model was applied in concert with stochastic simulation to generate probabilistic design spaces which predict the probability of achieving certain purity and recovery as a function of operating variables. In the first of two case studies, it was possible to select robust operating conditions using the probabilistic design spaces that enabled the purification of previously impossible to purify load material with extremely challenging composition. In the second case study, it was shown that the probabilistic design spaces could enable the required purity to be reached for material with a more standard load composition with very high product recovery.

The detailed analysis of the model simulations increased fundamental knowledge and understanding of weak partitioning chromatography, revealing the complex multidimensional design space. The impact of the mean and variance of load concentration, load challenge, pH, counterion concentration, and product partition coefficient among others, on the mean and variance of purity and recovery will allow for significantly better informed process development at Pfizer.

### 6.1.2. **Resin fouling**

Chapter 4 considered a key aspect of industrial chromatographic separations, which in the author's opinion, has not been given sufficient consideration in the mechanistic modelling literature: resin fouling. The platform anion exchange weak partitioning chromatography process considered in chapter 3 had experienced performance issues due to suspected resin fouling. In chapter 4, the location of the fouling on the resin particles, and the mechanistic effect of the resin fouling on the chromatographic separation over the lifetime of a column, was elucidated. The foulant was found to be located on the resin surface through the use of a number of orthogonal experimental techniques. Thus, the primary effect of the fouling was to limit mass transfer into the resin particle, rather than reduce the binding capacity of the resin itself, which was shown to be recoverable by reducing the flowrate of material during column loading. The increased understanding of resin fouling is an important step to characterising this important phenomenon mathematically, in order that model predictions are more applicable in an industrial setting where column aging is commonplace.

### 6.1.3. **Resin variability**

Chapter 5 considered the development and application of mechanistic models of chromatography at a late stage of process development. The chapter considered a hydrophobic interaction chromatography process used in the purification of a complex multicomponent therapeutic protein. The drug substance produced by the downstream processing section of the manufacturing process had to contain a specific ratio of the different forms of the protein, but was experiencing serious performance issues due to suspected resin lot variability. Prior to this work, an extended range of resin lots were obtained from the supplier for testing within normal process operating ranges. All resin lots were within the manufacturers specifications for ligand density and chloride capacity. Despite this, many failed to meet product quality specifications during testing and would have incurred significant losses if used for the large scale manufacture of the product.

In chapter 5, a mechanistic chromatography model of the step was developed for the two most extreme resin lots which gave the highest (designated high binding resin) and lowest (designated low binding resin) protein recoveries at normal operating conditions, in the experimental study conducted prior to this work. Model development revealed that the resin lot variability manifested itself in the equilibrium adsorption isotherms of the different therapeutic protein variants, bringing increased understanding of the issue at hand. The model was applied with stochastic simulation to generate probabilistic design spaces for the two resin lots which were designated high and low resins. These design spaces showed the probability of the final product meeting product specification criteria as a function of the load challenge and washlength, the only two operating conditions that were available for manipulation because the process was in late stage development. The probabilistic design spaces revealed that the optimum solution for a robust process was to vary the washlength based on the particular resin lot in use, which is a step change concept for bioprocessing that has not been considered before. Model predictions shows that limiting the operating space to conditions that gave the highest probability of meeting the product specification for all resins, may result in an unacceptable number of batch failures, and a variable final product.

## 6.2. Recommendations for future work

It is clear from this thesis that there are significant advantages to be gained by the use of mechanistic models of chromatography in industry. However, there is still much work to be done before models are used in practice. In the following section, potential directions for future work related to use of mechanistic chromatography models in industry are discussed.

The foremost need in order for mechanistic models of chromatography to be used in industry is the development of an expert driven software environment that provides users with: (1) a library of rigorous mathematical models based upon a chromatography modelling framework containing descriptions of all the key phenomena occurring in chromatography and supporting unit operations, (2) a database containing physical properties and parameters of existing process models, where values for new products and processes can easily be added, (3) recommended workflows and experimental standard operating procedures for calibrating model parameters for new chromatography processes, including guidelines on how to integrate model based approaches for development, design and operation of chromatographic processes with current industry procedures, and (4) recommended workflows and examples of key model applications such as optimisation, experimental design, global sensitivity analysis and automated design space generation.

### 6.2.1. **Modelling framework**

***Mass transfer***

As regards to the availability and quality of models of the various phenomena, the mathematical description of mass transport is currently the strongest part of the framework. This thesis has shown how even simplistic mathematical models such as the equilibrium dispersive model can describe complex multicomponent chromatographic separations as seen in the hydrophobic interaction process. More detailed descriptions of mass transport are available if required, such as the lumped kinetic and general rate models which account for intraparticlar diffusion. Greater understanding of particle level phenomena may be useful, especially regarding the impact of localised variations in pH and counterion concentration which may prove important when modelling non–isocratic separations. This extension would be useful if the mass transfer of the weak partitioning anion exchange system was characterised and salt gradients considered, but in general, this section of the framework is satisfactory.

***Adsorption***

Continued consideration needs to be given to developing fundamental understanding and mathematical descriptions of protein adsorption. Although progress has been made in recent years (Mollerup et al., 2008), a fundamental description based on thermodynamics of protein adsorption has not yet been achieved, and there is reliance on empirical and semi-empirical models with parameters fitted to experimental data. In addition, the complexity of feed streams and low concentrations of many species in process material means that often a great many simplifications and dubious assumptions must be made, as (1) there are limited options for modelling the adsorption equilibria seen in this type of system, and (2) accurately measuring the very low concentrations of species in heterogeneous material is an extremely difficult analytical challenge. In this work, the model of the anion exchange weak partitioning chromatography did not account for the impact of process related impurities in the load material, such as host cell protein, leached protein A, and virus, all of which would be expected to bind strongly to an anion exchange resin. It was assumed that the impact of these species would be minimal as they are typically present in very small quantities compared to the product related impurities which were considered in the model. This was acceptable because the model was for use at an early stage of development, and the impact of this assumption was leveraged by platform knowledge and subsequent experimental studies. However, in the future, approaches for incorporating these species will need to be found as their removal from the final drug substance is considered critical to product quality.

***Reaction***

A description of the various reactions that occur in chromatographic separations is a critical area of weakness that needs to be addressed. As most of the reactions produce undesired species, it is important that they are understood and characterised to ideally prevent them from happening, but more realistically limit the impact when they occur. The work conducted on the fouling of chromatography resin demonstrated the importance of accounting for non-ideal reaction phenomena. Although it was determined that the foulant itself was composed of primarily protein, thought to have been a complex including protein A, product, product related impurities and host cell proteins, there was little understanding of the reactions involved in its creation. In particular, the reactions occurring between different product forms and species in the load material are of great interest, as it is generally understood that these reactions are reversible. If it was possible to describe these reactions mathematically, an envisaged extension of the model would be to determine operating conditions favourable for the formation of product rather than impurity.

***Ionic equilibria***

A further extension to the model framework which would be of great interest is characterising the chemical equilibria in the mobile phase. Ionic reactions involving the product may play an important role in the chemical reactions as charge plays a large role in protein aggregation. However, more importantly, this addition would enable the model to accurately assess non-isocratic separations during the load and the wash phases. In relation to this thesis, this would enable operating models such as partition coefficient gradients in the load and/or wash to be examined for the weak partitioning chromatography process, and the buffer conductivity to be considered as an extra manipulated variable in the hydrophobic interaction chromatography process.

***Chromatography system***

One element of mechanistic modelling of chromatography that is rarely considered, but has a large impact on separations, is the chromatography system itself. Most often, system parameters such as column length and porosity are measured and assumed to stay constant thereafter. However, in practice these parameters will change over a chromatography column's lifetime, and in some cases will differ during each phase of a separation (e.g. load, wash, elution etc). Resin particles of the weak partitioning chromatography are known to swell and shrink based upon the buffer composition, and column packing is variable, especially when moving from laboratory scale to manufacturing scale. This work considered the impact of non-ideal, variable chromatography systems in the form of resin fouling of the weak partitioning anion exchange process, and the resin lot-to-lot variability of the

hydrophobic interaction chromatography. Deriving a mathematical description of the resin fouling in the weak partitioning chromatography system is the next logical step. Further experimental work is needed to understand the mechanistic effect of the other non-ideal phenomenon mentioned above, before mathematical descriptions can be developed.

### 6.2.2. **Physical properties and model parameters**

One of the challenges with developing mechanistic models of industrial chromatographic separations is that model parameters have to be determined for each process. The perceived experimental effort needed for finding these parameters dissuade the application of model based approaches in industry, as there is little guarantee that values will be found that give satisfactory model predictions, and it is difficult to conduct the required experiments without expert guidance. The makes the investment in a model based approach risky. This work has gone further than the usual approach to determining model parameters by developing a "platform" model of the anion exchange weak partitioning chromatography, utilising an adsorption isotherm model that is based upon the product partition coefficient, and can thus be reused for new molecules with minimal experimentation. The idea of reusing models is very powerful and one that should be explored further. In the weak partitioning anion exchange chromatography process, the next step is to validate the adsorption model by applying it to other monoclonal antibodies. However, in general there is a need for new approaches to reduce the experimental workload. One of the most important steps could be the creation of a physical properties package, containing a database where values for parameters of existing process models are stored, and where values for new processes can be calculated/added. In addition, emerging fields such as molecular dynamics simulations are of great interest for *in silico* calculation of model parameters. In particular, a relevant area for research in relation to this thesis is the use of a molecular model to estimate product partition contours, which would theoretically enable completely *in silico* process development of anion exchange weak partitioning chromatographic processes.

### 6.2.3. **Model calibration**

Although there are many different approaches for model calibration that have been published, there is a lack of guidance or comparisons on which approach to take in specific scenarios. In addition, not enough consideration has been given to how to incorporate model calibration approaches into existing industrial experimental development workflows and process development timelines. This work showed how it is possible to closely integrate a model based approach into the existing the weak partitioning anion exchange experimental development process. The next step for the anion exchange process is to extend the mass

transfer description and calibrate mass transfer parameters so that the wash phase may be modelled.

### 6.2.4. **Model applications**

***Probabilistic design spaces***

The work conducted on the hydrophobic interaction chromatographic separation in this thesis has many areas of future work that can be considered relatively easy to complete. Similar to the weak partitioning simulations, there are a range of simple simulation studies that can be run with the existing model to evaluate the impact of uncertainty in many of the different factors by generating further probabilistic design spaces. The stochastic methodology can be easily extended to examine the impact of uncertainty in load challenge, column volume, compression factor etc. An interesting study would be to examine and compare the contribution from variability in the resin or the load material on the probability of meeting product quality specifications. An alternative approach to changing the wash length based on the resin lot in use would be to change the operating condition based upon the load material composition and concentration. This approach is possible in a Quality by Design paradigm. The other thing that is of interest is determining what the impact of relaxing or tightening constraints would be. In the case of the hydrophobic interaction chromatography, the recovery constraint did not play a role in choosing operating conditions as a recovery as low as 52% was still satisfactory. It would be of interest to tighten this constraint and determine how different the conclusions would be based on the probabilistic design spaces.

Another interesting study would be to use stochastic simulations to determine an allowable standard deviation of resin characteristics to fit into a defined design space. In this workflow, each new resin would be put through a set of experiments to characterise the adsorption equilibria, and then its suitability for use would be determined based on its fit to validated ranges.

The difficulty with the probabilistic design space methodology is that it currently requires many simulations to be conducted and managing the generated data is very time consuming. The time to complete the necessary simulations was reduced by utilising multiple computers for the simulations, with each computer considering at a single operating condition, and the results imported manually to a central file. Future research into automating this process and possible utilisation of multi-core machines, is of great interest.

In this work, the statistical analysis of the results from the stochastic simulations was limited to determining basic parameters such as probabilities, means and standard deviations of critical process parameters etc. The next step in both the anion exchange weak partitioning chromatography process and the hydrophobic interaction chromatography process is to conduct detailed global sensitivity analysis calculations. A very interesting application of this would be to examine interactions between different variables in order to determine where additional time and effort in process development should be targeted for the greatest increase in process robustness. In addition, another related area of research is to determine the actual variability and uncertainty experienced in industrial manufacturing processes, which can indicate where to focus future work (i.e. model development in order to gain better description of chromatographic processes, or model application to improve process robustness).

***Evaluation of continuous processing***

One area of great interest that has seen some work, but will require more, is using mechanistic models of chromatography to evaluate the move to continuous processing. It is relatively straightforward to extend a model that has been developed for a batch chromatography process to modelling a continuous process. Of interest with relation to this thesis, is evaluating how to convert the batch weak partitioning anion exchange chromatography process to a continuous one. In particular, it will be useful to understand the benefits with relation to different objectives at different stages in the drug development lifecycle, as it is possible that the process may switch from batch to continuous as the candidate molecule moves through the various development phases in order to leverage the advantages of each approach.

***Regulatory considerations***

Regulatory guidance regarding the implementation of Quality by Design has proposed greater use of mechanistic models (ICH, 2008a). However, there is no guidance on *how* this should be achieved in practice. Unless this is addressed, it is likely that the use of mechanistic models in industry will remain ad hoc and only as a worst case scenario to solve a particular problem or scenario. One of the most important areas of future work, if modelling approaches are to be used in industry, is that the regulator authorities are approached and discussion initiated into how models should, and should not, be applied. Formal model validation procedures need to be developed and guidance should be issued on how to communicate models and results in filings, in addition to the publication of exemplary modelling case studies and examples by the regulatory authorities.

***Process optimisation***

Rigorous process optimisation has been used extensively for many years in traditional chemical engineering sectors such as oil and gas, and is a proven approach for gaining maximum value out of a process. However, despite optimisation of chromatographic processes being a topic that is often revisited in the literature, there is little uptake in industry. This is because the primary objective in industry is the production of a product of consistent quality in amounts satisfying demand, and as a year's supply can be produced in a single manufacturing campaign lasting only a few weeks for many products, most optimisation examples, such as maximising the recovery or minimising the cost of a particular piece of equipment, are just not relevant. There is a real need for examples of optimisation where the objective function is more relevant, such as maximising process robustness. In addition, chromatographic processes often experience lots of variability and uncertainty (e.g. most have variable and unknown feed material compositions and concentrations), and since the solution to optimisation studies is heavily dependent on the input variables, most solutions are easy to write off as irrelevant in all practical sense. There is a need for new optimisation studies which demonstrate how to account for this uncertainty whilst searching for a solution.

### 6.2.5. **Summary**

Future work should focus on (1) reducing the required effort to implement a model based approach in industry, (2) demonstrating the value of the approach using case studies and exemplary examples, and (3) providing relevant regulatory guidance on its implementation. The current state of the art in mechanistic modelling of chromatographic separations should be brought together into a single software tool, to create a platform that enables more straightforward application in the biopharmaceutical industry. The tool should contain a library of mathematical models and physical properties, as well as guidance on model calibration, validation and application. In parallel to the development of such a tool, further work should be conducted on mathematical models of adsorption, reaction, ionic equilibria and column systems to increase the applicability of models in industry. Further work should also be conducted to demonstrate the industrial relevance of model applications such as design space generation, global sensitivity analysis and process optimisation. Lastly, and probably most importantly, regulators, biopharmaceutical companies, and modelling experts need to come together to develop formal guidance on good modelling practices which describe how models must be used in industry.

# Chapter 7. References

*The following chapter contains references used in this thesis.*

Abia, J.A., Mriziq, K.S., Guiochon, G.A., 2009, Radial heterogeneity of some analytical columns used in high-performance liquid chromatography, J Chromatogr A, 1216: 3185–3191.

Abramoff, M.D., Magelhaes P.J., Ram, S.J, 2004, Image processing with ImageJ. Biophotonics Int., 11: 36–21.

Aldington, S., Bonnerjea, J., 2007, Review: Scale – up of monoclonal antibody purification processes. J Chromatogr B, 848: 64-78.

Almodóvar, E.X.P., Tao, Y., Carta, G. Protein adsorption and transport in cation exchangers with a rigid backbone matrix with and without polymeric surface extenders. Biotechnol Prog, 27: 1264-1272.

Ayyar, B.V., Arora, S., Murphy, C., O'Kennedy, R., 2012, Affinity chromatography as a tool for antibody purification, Methods, 56: 116-129

Avraam, M.P., Shah, N., Pantelides, C.C., 1998, Modelling .and optimisation of general hybrid systems in the continuous time domain, Computers & chemical engineering, 22: 221-228.

Bak, H., Thomas, O.R.T., Abildskov, J., 2007, Lumped parameter model for prediction of initial breakthrough profiles for the chromatographic capture of antibodies from a complex feedstock, J Chromatogr B, 848: 131 – 141.

Bhambure, R., Kumar, K., Rathore, A.S., 2011, High-throughput process development for biopharmaceutical drug substances, Trends in Biotechnology, 29: 127-135.

Bohart, G.S., Adams, E.Q., 1920, Journal of American Science, 40: 523.

Boushaba, R., Baldascini, H., Gerontas, S., Titchener-Hooker, N.J., Bracewell, D.G., 2011, Demonstration of the use of windows of operation to visualise the effects of fouling on the performance of a chromatographic step. Biotechnol Prog, 100: 941-949.

Borg, N., Westerberg, K., Andersson, N., von Lieres, E., Nilsson, N., 2013, Effects of uncertainties in experimental conditions on the estimation of adsorption model parameters in preparative chromatography, Compute. Chem. Eng, 55: 148 – 157.

Boyer, P.M., Hsu, J.T., 1992, Experimental studies of restricted protein diffusion in an agarose matrix. AIChE journal, 38: 259-272.

Bracewell, D., Boychyn, M., Baldascini, M., Storey, S.A., Bulmer, M., More, J., Hoare, M. 2008, Impact of clarification strategy on chromatographic separations: processing of cell homogenates. Biotech Bioeng, 100: 941-949.

Brooks, C.A., Cramer, S.M., Steric mass action ion exchange: displacement profiles and induced salt gradients, AIChE Journal, 38: 1969-1978.

Carter, P.J., 2011, Review: Introduction to current and future protein therapeutics: A protein engineering perspective, Experimental Cell Research, 317: 1261-1269.

Chan, S., Titchener-Hooker, N., Bracewell, D. G. and Sørensen, E. 2008a, A systematic approach for modeling chromatographic processes—Application to protein purification. AIChE J., 54: 965–977.

Chan, S., Titchener-Hooker, N., Sorensen, E., 2008b, Optimal economic design and operation of single and multicolumn chromatographic processes, Biotechnol Prog, 24: 389-401.

Charton, F., Bailly, M., Guiochon, G. 1994. Recycling in preparative liquid chromatography. Journal of Chromatography A, 687: 13-31.

Chau, S., Baldascini, H., Hearle, D., Hoare, M., Titchener-Hooker, N.J. 2006. Effect of fouling on the capacity and breakthrough characteristics of a packed bed ion exchange chromatography column. Bioprocess Biosys Eng, 28: 405-414.

Chhatre, S., Titchener-Hooker, N.J. 2009, Review: Microscale methods for high-throughput chromatography development in the pharmaceutical industry. Chem. Technol. Biotechnol, 84: 927-940.

Chhatre, S., Francis, R., Newcombe, A. R., Zhou, Y., Titchener-Hooker, N., King, J., Keshavarz-Moore, E. 2008, Global sensitivity analysis for the determination of parameter importance in the chromatographic purification of polyclonal antibodies. Chem. Technol. Biotechnol., 83: 201-208.

Chung, S.F., Wen, C.Y., 1968, Longitudinal dispersion of liquid flowing through fixed and fluidized beds, AIChE J. 14: 857–866.

Chu, L., Robinson, D.K., 2001, Industrial choices for protein production by large-scale cell culture, Current Opinion in Biotechnology, 12: 180-187.

Close, E.J., Salm. J.R., Bracewell, D.G., Sorensen, E, 2014, Modelling of industrial biopharmaceutical multicomponent chromatography, Chemical Engineering Research and Design, 92: 1304 – 1314.

Coffman, J.L., Kramarczyk, J.F., Kelley, B.D., 2008. High – throughput screening of chromatographic seperations: 1. Method development and column modeling. Biotechnol. Bioeng. 100, 605 - 618.

Costa, R., Rodrigues, M.E., Henriques, M., Azeredo, J., Oliveira, R., 2010, Guidelines to cell engineering for monoclonal antibody production, European Journal of Pharmaceutics and Biopharmaceutics, 74: 127-138.

van Deemter, J.J., Zuiderweg, F.Z., Klinkenberg, A., 1956, Chem. Eng. Sci, 5: 271.

Degerman, M., Jakobsson, N., Nilsson, B., 2007. Modeling and optimization of preperative reversed – phase liquid chromatography for insulin purification. J. Chromatogr. A. 1162: 41 - 49.

Degerman, M., Westerberg, K., Nilsson, N., 2009. A Determining critical process parameters and process robustness in preparative chromatography – a model based approach. Chem. Eng. Technol. 2009, 32: 903–911.

Degerman, M., Westerberg, K., Nilsson, N., 2009. A model based approach to determine the design space of preparative chromatography. Chem. Eng. Technol. 2009, 32: 1195–1202.

Degerman, M., Jakobsson, N., Nilsson, N., 2006. Constrained optimization of a preparative ion-exchange step for antibody purification. J Chromatogr A, 1113: 92–100.

Dejaegher, B., Heyden, Y.V., 2011, Experimental designs and their recent advances in set-up, data interpretation, and analytical applications, Journal of Pharmaceutical and Biomedical Analysis, 56: 141-158.

Di Masi, J.A., Hansen, R.W., Grabowski, H.G., 2003, The price of innovation: new estimates of drug development costs, Journal of Health Economics, 22: 151-185.

Di Masi, J.A., Grabowski, H.G. 2007, The cost of biopharmaceutical R&D: is biotech different? Manage. Decis. Econ., 28: 469–479.

Downey, W., 2013, Contract manufacturing, Trends in Biopharmaceutical Contract Manufacturing, Chemistry Today, 31: 19-24.

de Assis, A.J., Filho, R.B., 2000, Soft sensors development for on-line bioreactor state estimation, Computers & Chemical Engineering, 24: 1099-1103.

DeVault, D., 1943, Journal of the American Chemical Society, 65: 532.

de Ligny, C.L., 1970, Coupling between diffusion and convection in radial dispersion of matter by fluid flow through packed beds, Chem. Eng. Sci. 25, 1177 – 1181.

dePhillips, P., Lenhoff, A.M., 2000, Pore size distributions of cation-exchange adsorbents determined by inverse size-exclusion chromatography, J Chromatogr A, 883: 39-54.

Farkas, T., Sepanlak, M.J., Guiochon, G., 1996, Column radial homogeneity in high-performance liquid chromatography, J Chromatogr A, 740: 169 –181.

Ferreira, S.L.C., Bruns, R.E., da Silva, E.G.P., dos Santos, W.N.L., Quintella, C.M., David, J.M., de Andrade, J.B., Breitkreitz, M.C., Jardim, I.C.S.F., Neto, B.B., 2007, Statistical designs and response surface techniques for the optimization of chromatographic systems, Journal of Chromatography A, 1158: 2-14.

Foo, K.Y., Hameed, B.H., 2010, Review: Insights into the modeling of adsorption isotherm systems, Chemical Engineering Journal, 156: 2 – 10.

Fornstedt, T., 2010, Review: Characterization of adsorption processes in analytical liquid–solid chromatography. J Chromatogr A, 1217: 792 – 812.

Gallant, S. R., 2004. Modeling ion-exchange adsorption of proteins in a spherical particle. Journal of Chromatography A, 1028: 189-195.

Gerontas, S., Asplund, M., Hjorth, R., Bracewell, D.G., 2010. Integration of scale – down experimentation and general rate modelling to predict manufacturing scale chromatographic seperations. J. Chromatogr. A. 1217, 6917 - 6926.

Gétaz, D., Butté, A., Morbidelli, 2013. Model-based design space determination of peptide chromatographic purification processes. J. Chromatogr. A. 1284, 80 - 87.

Gétaz, D., Stroehleina, G., Butté, A., Morbidelli, 2013. Model-based design of peptide chromatographic purification processes. J. Chromatogr. A. 1284, 69 - 79.

Gétaz, D., Hariharan, S. B., Butté, A., Morbidelli, M. 2012. Modeling of ion-pairing effect in peptide reversed-phase chromatography. J. Chromatogr. A., 1249: 92-102.

Gétaz, D., Stroehleina, G., Butté, A., Morbidelli, 2013. Model-based design of peptide chromatographic purification processes. J. Chromatogr. A. 1284: 69 - 79.

Gu, T., Tsao, G.T., Tsai, G.J., Ladisch, M.R. 1990. Displacement effect in multicomponent chromatography. AIChE Journal, 36: 1156-1162.

Gu, T., Tsai, G.J., Tsao, G.T. 1991. Some considerations for optimization of desorption chromatography. Biotechnology and bioengineering, 37: 65-70.

Gu, T., Zheng, Y., 1999, A study of the scale-up of reversed-phase liquid chromatography, Sep. Purif. Technol. 15: 41–58.

Gu, T., Iyer, G., Cheng, K.S.C., 2013, Parameter estimation and rate model simulation of partial breakthrough of bovine serum albumin on a column packed with large Q Sepharose anion-exchange particles. Separation and Purification Technology, 116: 319–326.

Guiochon, G., Goldshan-Shirazi, S., Katti, A.M., 1994. Fundamentals of preperative and non-linear chromatography. Boston: Academic Press.

Guiochon, G., Felinger, A., Shirazi, D.G., Katti, A.M., Fundamentals of Preparative and Nonlinear Chromatography, 2nd ed., Academic Press, San Diego, 2006.

Guélat, B., Ströhlein, G., Lattuada, M., Delegrange, L., Valax, P., Morbidelli, M. 2012. Simulation model for overloaded monoclonal antibody variants separations in ion-exchange chromatography. J. Chromatogr. A 1253: 32– 43.

Gritti, F., Guiochon, G., 2007, Consequences of the radial heterogeneity of the column temperature at high mobile phase velocity, J. Chromatogr. A., 1166: 47–60

Gritti, F., Guiochon, G., 2010, A protocol for the measurement of all the parameters of the mass transfer kinetics in columns used in liquid chromatography. J Chromatogr A, 1217: 5137 – 5151.

Gritti, F., Guiochon, G. 2011. Importance of sample intraparticle diffusivity in investigations of the mass transfer mechanism in liquid chromatography. AIChE journal, 57: 346-358.

Harms, J., Wang, X., Kim, T., Yang, X. and Rathore, A. S. 2008. Defining Process Design Space for Biotech Products: Case Study of *Pichia pastoris* Fermentation. Biotechnol Progress 24, 655–662.

Hibbert, B.D., 2012, Experimental design in chromatography: A tutorial review, Journal of Chromatography B, 910: 2-13.

Hubbuch, J., Kula, M.R. 2008. Confocal laser scanning microscopy as an analytical tool in chromatographic research. Bioprocess Biosys Eng, 31: 241-59.

Hubbuch, J., Linden, T., Knieps, E., Thömmes, J., Kula, M.R. 2002, Dynamics of protein uptake within the adsorbent particle during packed bed chromatography. Biotech Bioeng, 80: 359-68.

International Conference of Harmonisation, 2005, ICH Harmonised Tripartite Guideline: Q9 Quality Risk Management

International Conference of Harmonisation, 2008a, ICH Harmonised Tripartite Guideline: Q8 Pharmaceutical Development

International Conference of Harmonisation, 2008b, ICH Harmonised Tripartite Guideline: Q10 Pharmaceutical Quality Systems

Iskra, T., Bolton, G.R., Coffman, J.L., Godavarti, R. 2013. The effect of protein A cycle number on the performance and lifetime of an anion exchange polishing step. Biotech Bioeng, 110:1142–1152.

Jakobsson, N., Degerman, M., Nilsson, B., 2005. Optimization and robustness analysis of a hydrophobic interaction chromatography step. J. Chromatogr. A., 1063: 99 – 109.

Jakobsson, N., Karlsson, D., Axelsson, J. P., Zacchi, G., Nilsson, B. 2005. Using computer simulation to assist in the robustness analysis of an ion-exchange chromatography step. J. Chromatogr. A., 1063: 99-109.

Jiang, C., Liu, J., Rubacha, M., Shukla, A.A., 2009. A mechanistic study of Protein A chromatography resin lifetime. J Chromatogr A, 1216: 5849-5855.

Jiang, C., Flansburg, L., Ghose, S., Jorjorian, P., Shukla, A., 2010. Defining process design space for a hydrophobic interaction chromatography (HIC) purification step: Application of quality by design (QbD) principles. Biotechnol. Bioeng, 107: 985 - 97.

Jin, J., Chhatre, S., Titchener-Hooker, N.J., Bracewell, D.G. 2009. Evaluation of the impact of lipid fouling during the chromatographic purification of virus-like particles from Saccharomyces cerevisiae. Chem Tech Biotech, 85: 209-215.

Jin, J. 2010. Lipid foulant interactions during the chromatographic purification of virus like particles from *Saccharomyces Cerevisiae*. PhD thesis, University College London.

Kaczmarski, K., Cavazzini, A., Szabelski, P., Zhou, D., Liu, X., Guiochon, G. 2002. Application of the general rate model and the generalized Maxwell–Stefan equation to the study of the mass transfer kinetics of a pair of enantiomers. Journal of Chromatography A, 962, 57-67.

Kaczmarski, K., Antos, D., Sajonz, H., Sajonz, P., Guiochon, G., 2001. Comparitive modeling of breakthrough curves of bovine serum albumin in anion – exchange chromatography. J. Chromatogr. A. 925, 1 – 17.

Kaczmarski, K., Gubernak, M., Zhou, D., Guiochon, G. 2003. Application of the general rate model with the Maxwell–Stefan equations for the prediction of the band profiles of the 1-indanol enantiomers. Chemical Engineering Science, 58: 2325 – 2338.

Kaczmarski, K., Cavazzini, A., Szabelski, P., Zhou, D., Liu, X., Guiochon, G. 2002. Application of the general rate model and the generalized Maxwell–Stefan equation to the study of the mass transfer kinetics of a pair of enantiomers. J Chromatogr A, 962: 57 – 67.

Kaczmarski, K., 2007, Estimation of adsorption isotherm parameters with inverse method – Possible problems. J. Chromatogr. A. 1176, 57 - 68.

Karlsson, D., Jakobsson, N., Axelsson, A., & Nilsson, B. 2004. Model-based optimization of a preparative ion-exchange step for antibody purification. Journal of Chromatography A, 1055: 29-39.

Kataoka, T., Yoshida, H., Ueyama, K., 1972, Mass transfer in laminar region between liquid and packing material surface in the packed bed, J. Chem. Eng. Jpn. 5: 132–136.

Kelley, B.D., 2009. Industrialization of mAb production technology. Mabs, 1, 443 - 452.

Kelley, B., Tobler, S., Brown, P., Coffman, J.L., Godavarti, R., Iskra, T., Switzer, M., Vunnum, S. 2008a. Weak partitioning chromatography for anion exchange purification of monoclonal antibodies. Biotech Bioeng,101:553–566.

Kelley, B. 2007. Very large scale monoclonal antibody purification: the case for conventional unit operations. Biotechnol Prog, 23: 995-1008.

Kelley, B.D., 2007, Review: Very large scale monoclonal antibody purification: the case for conventional unit operations. Biotech Prog, 23: 995-1008.

Kelley, B.D., Switzer, M., Bastek, P., Kramarczyk, J.F., Molnar, K., Yu, T., Coffman, J., 2008, High-throughput screening of chromatographic separations: IV. Ion-exchange, Biotechnology and bioengineering, 100: 950-963.

Khanna, I., 2012, Drug discovery in pharmaceutical industry: productivity challenges and trends, Drug Discovery Today, 17: 1088-1102.

Kramarczyk, J.F., Kelley, B.D., Coffman, J.L., 2008, High-throughput screening of chromatographic separations: II. Hydrophobic interaction, Biotechnology and bioengineering, 100: 707-720.

Lapidus, L., Amundson, N.L., 1952, Journal of Physical Chemistry, 56: 984.

Lau, E.C., Kong, S., McNulty, S., Entwisle, C., Mcilgorm, A., Dalton, K.A., Hoare, M. 2013, An ultra scale-down characterization of low shear stress primary recovery stages to enhance selectivity of fusion protein recovery from its molecular variants. Biotechnol. Bioeng, 110: 1973–1983.

Leader, B., Baca, Q.J., Golan, D.E., 2008, Protein therapeutics: a summary and pharmacological classification. Nat Rev Drug Discov, 7: 21 -39.

Lienqueo, E.M., Shene, C., Asenjo, J., 2009. Optimization of hydrophobic interaction chromatography using a mathematical model of elution curves of a protein mixture. J. Mol. Recognit, 22: 110–120.

Lisec, O., Hugo, P., Seidel-Morgenstern, A., 2001, Frontal analysis method to determine competitive adsorption isotherms, J Chromatogr A 908, 19-34.

Linden, T., Ljunglöf, A., Kula, M., Thömmes, J. 1999. Visualizing two-component protein diffusion in porous adsorbents by confocal scanning laser microscopy. Biotech Bioeng 65: 622-30.

Li, Z., Gu, Y., & Gu, T. 1998. Mathematical modeling and scale-up of size-exclusion chromatography. Biochemical engineering journal, 22: 145-155.

Lightfoot, E.N., Moscariello, J.S. 2004, Bioseparations. Biotech and Bioeng, 87: 259 – 273.

Li, Q., Aucamp, J.P., Tang, A., Chatel, A., Hoare, M., 2012, Use of focused acoustics for cell disruption to provide ultra scale-down insights of microbial homogenization and its

bioprocess impact—recovery of antibody fragments from rec *E. coli*. Biotechnol. Bioeng., 109: 2059–2069.

Ljunglöf, A., Hjorth, R. 1996. Confocal microscopy as a tool for studying protein adsorption to chromatographic matrices. Aperture 743:75-83.

Ljunglöf, A., Thömmes, J. 1998. Visualising intraparticle protein transport in porous adsorbents by confocal microscopy. J of Chromatogr A, 813:387-395.

McCue, J.T., Engel, P., Ng, A., Macniven, R., Thömmes, J., 2008. Modeling of protein/aggregate purification and separation using hydrophobic interaction chromatography. Bioprocess. Biosyst. Eng. 31, 261 - 275.

McCue, J.T., Cecchini, D., Chu, C., Liu, W.H., Spann, A., 2007, Application of a two dimensional model for predicting the pressure flow and compression properties during column packing scale up, J. Chromatogr. A. 1145: 89– 101.

McCue, J.T., Engel, P., Thömmes, J., 2009. Effect of phenyl sepharose ligand density on protein monomer/aggregate purification and separation using hydrophobic interaction chromatography, J Chromatogr A, 1216: 902 – 909.

Melter, L., Butte, A., Morbidelli, M., 2008. Preperative weak cation - exchange chromatography of monoclonal antibody variants: 1. Single component adsorption. J. Chromatogr. A. 1200, 156 - 165.

Mollerup, J.M., 2008, A review of the thermodynamics of protein association to ligands, protein adsorption, and adsorption isotherms. Chem Eng Technol, 31: 864 – 874.

Mollerup, J.M., Hansen, T.B., Kidal, S., Staby, A., Quality by design—Thermodynamic modelling of chromatographic separation of proteins. J. Chromatogr. A 1177: 200–206.

Mollerup, J.M., Hansen, T.B., Kidal, S., Sejergaard, L., Hansen, E., Staby, A., 2007. Development, modelling, optimisation and scale – up of chromatographic purification of a therapeutic protein. Fluid. Phase. Equilibr. 261, 133 – 139.

Müller-Späth, T., Ströhlein, G., Aumann, L., Kornmann, H., Valax, P., Delegrange, L., Charbaut, E., Baer, G., Lamproye, A., Jöhnck, M., Schulte, M., Morbidelli, M., 2011. Model simulation and experimental verification of a cation-exchange IgG capture step in batch and continuous chromatography. J. Chromatogr. A, 1218: 5195– 5204.

Muller-Spath T., Aumann, L., Morbidelli, M. 2009. Role of Cleaning-in-Place in the Purification of mAb Supernatants Using Continuous Cation Exchange Chromatography. Separ Sci Technol, 44:1-26.

Nagrath, D., Xia, F., Cramer, S.M., 2011. Characterization and modeling of nonlinear hydrophobic interaction chromatographic systems. J. Chromatogr. A. 1218, 1219 - 1226.

Natarajan, V., Cramer, S. 2000. A methodology for the characterization of ion-exchange resins. Separation Science and Technology, 35, 1719-1742.

Nfor, B.K., Verhaert, P.D.E.M., van der Wielen, L.A.M., Hubbuch, J., Ottens, M., 2009, Rational and systematic protein purification process development: the next generation. Trends in Biotechnology, 27: 673 – 679.

Nfor, B.K., Zuluaga, D.S., Verheijen, P.J.T., Verhaert, P.D.E.M., van der Wielen, L.A.M., Ottens, M., 2011. Model-based rational strategy for chromatographic resin selection, Biotechnol. Prog. 27: 1629 – 164.

Nfor, B.K., Ahamed, T., van Dedem, G.W.K., Verhaert, P.D.E.M., van der Wielen, L.A.M., Eppink, L.H.M., de Sandt, E.J.A.X., Ottens, M., 2013. Model-based rational methodology for protein purification process synthesis. Chemical Engineering Science 89: 185–195.

Nfor, B.K., Ahamed, T., Pinkse, M.W.H., van der Wielen, L.A.M., Verhaert, P.D.E.M., van Dedem, G.W.K., Eppink, M.H.M., van de Sandt, E.J.A.X., Ottens, M., 2012. Multi-Dimensional Fractionation and Characterization of Crude Protein Mixtures: Toward Establishment of a Database of Protein Purification Process Development Parameters, Biotech and Bioeng, 109: 3070 – 3083.

Ng, C.K.S., Osuna-Sanchez, H., Valery, E., Sørensen, E., Bracewell, D.G., 2012. Design of high productivity antibody capture by protein A chromatography using an integrated experimental and modeling approach. J Chromatogr. B. 899, 116 - 126.

Norde, W., 1996, Driving forces for protein adsorption at solid surfaces, Macromol. Symp 10: 5-18.

Norling, L., Lute, S., Emery, R., Khuu, W., Voisard, M., Xu, Y., Chen, Q., Blank, G., Brorson, K. 2005. Impact of multiple re-use of anion-exchange chromatography media on virus removal. J Chromatogr A, 1069:79-89.

Osberghaus, A., Drechsel, K., Hansen, S., Hepbildikler, S.K., Nath, S., Haindl, M., vonLieres, E., Hubbuch, J., 2012a. Model – integrated process development demonstrated on the optimization of a robotic cation exchange step. Chem. Eng. Sci. 76, 129 – 139.

Osberghaus, A., Hepbildikler, S., Nath, S., Haindl, M., von Lieres, E., Hubbuch, J., 2012b. Optimizing a chromatographic three component separation: A comparison of mechanistic and empiric modeling approaches. J. Chromatogr. A. 1237, 86 – 95.

Osberghaus, A, Hepbildikler, S, Nath, S, Haindl, M, von Lieres, E, Hubbuch, J, 2012c. Determination of parameters for the steric mass action model—A comparison between two approaches. J. Chromatogr. A 1233: 54– 65.

Pantelides, C.C., Urban, Z.E., 2004, Process modelling technology: A critical review of recent developments. In Proc. Int. Conf. on Foundations of Process Design, FOCAPD, 69-83.

Persson, P., Gustavsson, P. E., Zacchi, G., Nilsson, B. 2006. Aspects of estimating parameter dependencies in a detailed chromatography model based on frontal experiments. Process Biochemistry, 41, 1812-1821.

Pollock, J., Bolton, G., Coffman, J., Ho, S.V., Bracewell, D.G., Farid, S.S., 2013, Optimising the design and operation of semi-continuous affinity chromatography for clinical and commercial manufacture, J. Chromatogr. A 1284: 17– 27.

Polson, A., 1950, Some aspects of diffusion in solution and a definition of a colloidal particle, J. Phys. Chem. 54: 649–652.

Process Systems Enterprise, 2014, gPROMS, www.psenterprise.com/gproms.

Rabe, M., Verdes, D., Seeger, S., 2011, Understanding protein adsorption phenomena at solid surfaces, Advances in colloid and interface science 162: 87 – 106.

Rathore, A.S., and Winkle, H., 2009. Quality by design for pharmaceuticals: regulatory perspective and approach. Nat. Biotechnol. 27, 26–34.

Rathore, A.S., 2009. Roadmap for implementation of quality by design (QbD) for Biotechnology products. Trends in Biotechnology 27, 546–55.

Rasband, W.S., ImageJ, U. S. National Institutes of Health, Bethesda, Maryland, USA, http://imagej.nih.gov/ij/, 1997-2011.

Regnier, F.E., Mazsaroff, I., 1987, A theoretical examination of adsorption processes in preparative liquid chromatography of proteins, Biotechnol. Prog 3: 22.

Rounds, M.A., Regnier, F.E., 1984, Evaluation of a retention model for high-performance ion-exchange chromatography using two different displacing salts, J. Chromatogr 283: 37.

Roush, D.J., Lu, L, Review: Advances in primary recovery: Centrifugation and membrane technology, Biotech Progress, 24: 488 – 495.

Sandoval, G., Andrews, B.A., Asenjo, J.A., 2012. Elution relationships to model affinity chromatography using a general rate model. J. Mol. Recognit. 25: 571–579.

Seidel-Morgenstern, A., 2004. Review: Experimental determination of single solute and competitive adsorption isotherms. J. Chromatogr. A. 1037, 255 – 272.

Shepard S.R., Brickman-stone, C., Schrimsher J.L., Koch, G. 2000. Discoloration of ceramic hydroxyapatite used for protein chromatography. Science, 891: 93-98.

Siu S.C., Boushaba, R., Topoyassakul, V., Graham, A., Choudhury, S., Moss, G., Titchener-Hooker, N.J. 2006. Visualising fouling of a chromatographic matrix using confocal scanning laser microscopy. Biotech Bioeng, 95: 714–723.

Siu, S.C., Boushaba, R., Liau, J., Hjorth. R., Titchener-Hooker, N.J. 2007. Confocal imaging of chromatographic fouling under flow conditions. J Chem Technol Biot, 82:871-881

Shalliker, R. A., Scott Broyles, B., Guiochon, G. 2003. Axial and radial diffusion coefficients in a liquid chromatography column and bed heterogeneity. Journal of Chromatography A, 994, 1-12.

Shukla, A.A., Hubbard, B., Tressel, T., Guhan, S., Low, D., 2007. Downstream processing of monoclonal antibodies – Appliation of platform approaches. J. Chromatogr. B. 848, 28 - 39.

Shukla, A.A., Thömmes, J., 2010, Recent advances in large-scale production of monoclonal antibodies and related proteins, Trends in Biotechnology, 28: 253-261.

Sun, Y., Yang, K. 2008. Analysis of mass transport models based on Maxwell–Stefan theory and Fick's law for protein uptake to porous anion exchanger. Separation and Purification Technology, 60: 180-189.

Susanto, A., Herrmann, T., Hubbuch, J. 2006. Short-cut method for the correction of light attenuation influences in the experimental data obtained from confocal laser scanning microscopy. J Chromatogr A, 1136: 29-38.

Susanto, A., Wekenborg, K., Hubbuch, J., Schmidt-Traub, H. 2006. Developing a chromatographic column model for bovine serum albumin on strong anion-exchanger Source30Q using data from confocal laser scanning microscopy. J Chromatogr A, 1137:63-75

Susanto, A., Knieps-Grünhagen, E., von Lieres, E., Hubbuch, J. 2008. High throughput screening for the design and optimization of chromatographic processes: assessment of model parameter determination from high throughput compatible data. Chemical engineering & technology, 31: 1846-1855.

Susanto, A., Herrmann, T., von Lieres, E., Hubbuch J., 2007, Investigation of pore diffusion hindrance of monoclonal antibody in hydrophobic interaction chromatography using confocal laser scanning microscopy. J Chromatogr A, 1149:178-88.

Staby, A., Johansen, N., Wahlstrøm, H., Mollerup, I. 1998. Comparison of loading capacities of various proteins and peptides in culture medium and in pure state. J Chromatogr A, 827:311–318.

Steinmeyer, D.E., McCormick, E.L., 2008, The art of antibody process development. Drug Discovery Today, 13: 613 – 618.

Striegel, A., Yau, W.W., Kirkland, J.J., Bly, D.D., Modern size-exclusion liquid chromatography: practice of gel permeation and gel filtration chromatography, Wiley, New York, 2009.

Teeters, M., Benner, T., Bezila, D., Shen, H., Velayudhan, A., Alred, P., 2009. Predictive chromatographic simulations for the optimization of recovery and aggregate clearance during the capture of monoclonal antibodies. J. Chromatogr. A 1216, 6134–6140.

Teoh, H.K., Turner, M., Titchener-Hooker, N., Sorensen, E. 2001. Experimental verification and optimisation of a detailed dynamic high performance liquid chromatography column model. Computers & Chemical Engineering, 25, 893-903.

Teske, C.A., Lieres, E., Schröder, M., Ladiwala, A., Cramer, S.M., Hubbuch, J.J. 2006. Competitive adsorption of labeled and native protein in confocal laser scanning microscopy. Biotech Bioeng, 95: 58–66.

Theil, K,A, 2004, Biomanufacturing, from bust to boom…to bubble? Nature Biotechnology, 22: 1365 – 1372.

Thomas, H., de Neuville, B.C., Storti, G., Morbidelli, M., Joehnck, M., Schulte, M., 2013, Role of tentacles and protein loading on pore accessibility and mass transfer in cation exchange materials for proteins. J. Chromatogr. A. 1285: 48– 56.

To, B.C.S., Lenhoff, A.M., 2007a, Hydrophobic interaction chromatography of proteins: I. The effects of protein and adsorbent properties on retention and recovery, Journal of Chromatography A, 1141: 191-205.

To, B.C.S., Lenhoff, A.M., 2007b, Hydrophobic interaction chromatography of proteins: II. Solution thermodynamic properties as a determinant of retention, Journal of Chromatography A, 1141: 235-243

To, B.C.S., Lenhoff, A.M., 2008, Hydrophobic interaction chromatography of proteins III. Transport and kinetic parameters in isocratic elution, J Chromatogr A, 1205: 46–59.

Urmann, M., Graalfs, H., Joehnk, M., Jacob, L.R., Frech, C. 2010. Cation exchange chromatography of monoclonal antibodies: Characterization of novel stationary phase designed for production-scale purification. mAbs 2: 395-404.

Velayudhan, A., Horvath, C.S., 1988, Preparative chromatography of proteins analysis of the multivariant ion-exchange formalism, J Chromarogr 443: 13.

Vermeulen, T., LeVan, M.D., Herister, N.K., Klein, G., 1984. Adsorption and Ion exchange in Chemical Engineers Handbook, 6th Ed, Perry, R.H., Green, DW, Maloney, JA, (eds) McGraw-Hill, New York.

van Deemter, J.J., Zuiderweg, F.J., Klinkenberg, A., 1956, Journal of Chemical Engineering Science, 5: 271.

Waldman, T.A., 2003, Immunotherapy: Past, present and future, Nature Medicine, 9: 269 – 277.

Walsh, G., 2010, Biopharmaceutical benchmarks 2010, Nature Biotechnology, 28: 917 – 924.

Westerberg, K., Borg, N., Andersson, N., Nilsson, B. (2012). Supporting Design and Control of a Reversed-Phase Chromatography Step by Mechanistic Modeling. Chemical Engineering & Technology, 35, 169-175.

Westerberg, K., Hansen, E.B., Degerman, D., Hansen, T.B., Nilsson, B., 2012. Model-Based Process Challenge of an Industrial Ion-Exchange Chromatography Step. Chem. Eng. Technol. 35: 183 – 190.

Westerberg, K., Broberg-Hansen, E., Sejergaard, L., Nilsson, B. 2013. Model-based risk analysis of coupled process steps. Biotechnology and bioengineering, 110, 2462-2470.

Wensel, D.L., Kelley, B.D., Coffman, J.L., 2008, High-throughput screening of chromatographic separations: III. Monoclonal antibodies on ceramic hydroxyapatite, Biotechnology and bioengineering, 100, 839-854

Wilson, E.J., Geankoplis, C.J., 1966, Liquid mass transfer at very low Reynolds Numbers in packed beds, Ind. Eng. Chem. Fund. 5: 9–14.

Wicke, E., 1939, Kolloid Z, 86: 295.

Wicke, E., 1940, Kolliod Z, 90: 156.

Wilson, J.N., 1940, Journal of the American Chemial Society, 62: 1583.

Woodcock, J., 2005, Pharmaceutical quality in the 21st century – an integrated systems approach. In AAPS Workshop on Pharmaceutical Quality Assessment – A Science and Risk-Based CMC Approach in the 21st Century

Wurm, F.M., 2004, Production of recombinant protein therapeutics in cultivated mammalian cells, Nature Biotechnology 22: 1393 – 1398.

Xia, F., Nagrath, D., Cramer, S.M., 2003, Modeling of adsorption in hydrophobic interaction chromatography systems using a preferential interaction quadratic isotherm, J. Chromatogr. A 989: 47–54.

Yamamoto, S., Nakanishi, K., Matuno, R., 1988, Ion exchange chromatography of proteins, Marcel Dekker, New York.

Young, M.E., Carroad, P.A., Bell, R.L., 1980, Biotechnol. Bioeng. 22: 947.

Yao, Y., Lenhoff, A. M. 2006. Pore size distributions of ion exchangers and relation to protein binding capacity. Journal of Chromatography A, 1126: 107-119.

# Chapter 8. Appendix A

*The following appendix contains a table summarising the literature reviewed in chapter 2 with regard to the mode of chromatography, the retention mechanism, the molecules of interest, the impurities considered, the mass transfer model, and the adsorption model, in addition to brief notes on each study.*

Table 8.1. Studies using mechanistic models of chromatography for studies related to the purification of therapeutic proteins (part 1)

| Reference | Mode | Retention mechanism | Molecules of interest | Impurities | Mass transfer model | Adsorption model | Notes |
|---|---|---|---|---|---|---|---|
| Charton et al., 1994 | Elution | cellulose based | Ketoprofen enantiomers | N/A | Equilibrium dispersive | Bi-Langmuir | Explored recycling |
| Boyer and Hsu, 1992 | Pulse injections | None- sepharose matrix, size exclusion | Myoglobin, Beta-Lactoglobulin, Ovalbumin, Albumin, Hexokinase, Immunoglobin G, Catalase | N/A | General Rate model | N/A | Restricted protein diffusion in agarose matrix. Looked at mass transfer correlations. |
| Li et al., 1998 | elution | Size exclusion | Myoglobin, Ovalbumin | N/A | General Rate model | N/A | Scale up and sensitivity of mass transfer parameters |
| Gu et al., 1990 | frontal, elution and displacement | N/A | Not specific | N/A | General Rate model | Multicomponent Langmuir | Displacement phenomena in multicomponent systems |
| Gu et al., 1990 | elution | N/A | Not specific | N/A | General rate model | Langmuir | Considerations of desorption chromatography |
| Natarajan and Cramer, 2000 | N/A | Cation exchange | alpha chymotrypsinogen A, ribonuclease A, nyomysin sulphate | N/A | Lumped rate model | Steric mass action | Method for identifying appropriate mass transport models |

Table 8.2. Studies using mechanistic models of chromatography for studies related to the purification of therapeutic proteins (part 2)

| Reference | Mode | Retention mechanism | Molecules of interest | Impurities | Mass transfer model | Adsorption model | Notes |
|---|---|---|---|---|---|---|---|
| Kaczmarski et al., 2001 | elution | Anion exchange | Bovine Serum Albumin | N/A | General rate, lumped pore, equilibrium dispersive, transport dispersive | modified bi-Langmuir | Comparing breakthrough curves from different models of chromatography |
| Teoh et al., 2001 | isocractic elution | size exclusion | nitrobenzene, naphthalene, flourene, fluoranthene | N/A | Equilibrium dispersive | Langmuir | simulation and optimisation of a closed loop recycling HPLC |
| Charton et al., 1994 | Elution | cellulose based | Ketoprofen enantiomers | N/A | Equilibrium dispersive | Bi-Langmuir | Explored recycling |
| Kaczmarski et al., 2002 | isocractic elution | cellulose tribenzoate | 1-phenyl-1-propanol enantiomers | N/A | General rate model with the generalised maxwell stefan equation | competitive toth | Developing a extremely detailed model of the enantiomer separation where mass transpot is relatively slow |
| Gallant,2004 | N/A | ion exchange | alpha - Chymotrypsinogen, Cytochroma C | N/A | Particle model | SMA | Developing understanding of adsorption of protesin in spherical particles |
| Persson et al., 2006 | N/A | N/A | BSA | N/A | General rate model | N/A | To derive methods and understanding of flow rate and bead size dependency of mass transfer coefficients |

Table 8.3. Studies using mechanistic models of chromatography for studies related to the purification of therapeutic proteins (part 3)

| Reference | Mode | Retention mechanism | Molecules of interest | Impurities | Mass transfer model | Adsorption model | Notes |
|---|---|---|---|---|---|---|---|
| Susanto et al., 2006 | Flowthroug h | Anion exchange | BSA | N/A | General rate model | Steric mass action | Used insights from confocal microscopy for developing the particle model |
| Bak et al., 2007 | Bind/Elute | Affinity | Clarified rabbit antiserum | HCP, DNA | Ideal | Lumped parameter approach with Langmuir kinetics | Interesting as the study considered crude feed material |
| Sun and Yang, 2007 | Batch uptake | anion exchange | Bsa and gamma globulin | N/A | Maxwell stefan | langmuir | compared fickian diffusion with maxwelll stefan diffusion |
| Chan et al., 2008 | isocratic and gradient elution | ion exchange | Many model proteins | N/A | equilibrium dispersive and general rate model | linear | Proposed approach for estimating model parameters using inverse method when feed material is unknown |
| McCue et al., 2008 | Bind/Elute | Hydrophobic interaction | Fusion protein | Aggregated fusion protein | Lumped pore model | Competitive langmuir binary | Included a term in the model for irreversible binding |
| To and Lenhoff, 2008 | Isocratic elution | Hydrophobic interaction | Ribonuclease A, lysozome, lactalbumin, ovalbumin, BSA | N/A | General rate model | Kinetic expression including conformational change on the resin surface | The elution profiles of five model proteins were investigated in eight hydrophobic interaction resins |
| Melter et al. 2008 | Isocratic elution | Cation exchange | Monoclonal antibody variants | N/A | General rate model | Langmuir with mobile phase modifiers | characterisation of mAb varaints |

Table 8.4. Studies using mechanistic models of chromatography for studies related to the purification of therapeutic proteins (part 4)

| Reference | Mode | Retention mechanism | Molecules of interest | Impurities | Mass transfer model | Adsorption model | Notes |
|---|---|---|---|---|---|---|---|
| Muller – Spath et al., 2011 | Bind/Elute | Cation exchange | Monoclonal Antibody | Aggregate, HCP, DNA | Lumped kinetic model | Competitive Langmuir | - |
| Nagrath et al., 2011 | displacement and gradient | Hydrophobic interaction | lysozyme and lectin | N/A | general rate model | preferential interaction quadratic adsorption | characteriosation and mdoelling of HIC using the PIQ isotherm |
| Sandoval et al. 2012 | Gradient elution | Affinity | IgG, BSA, Haemoglobin | N/A | General rate model | Second order kinetic binding expression | Power law and exponential elution relationships were used to simulation gradient elution |
| Guélat et al. 2012 | Bind/Elute (isocratc and gradient elution) | Cation exchange | Monoclonal antibody variants | N/A | General rate model | competitive multi component Langmuir | Henry constants were calculated using a statistical thermodynamic model based on properties of the proteins. |
| Borg et al., 2013 | Isocratic elution | reversed phase | insulin | n/A | Equilibrium dispersive model | Langmuir with mobile phase modulators | analyse effects of uncertainty in estimation of model paramerers |
| Gu et al. 2013 | Bind/elute | Anion exchange | BSA | N/A | General rate model | Langmuir | - |

Table 8.5. Studies using mechanistic models of chromatography for studies related to the purification of therapeutic proteins (part 5)

| Reference | Mode | Retention mechanism | Molecules of interest | Impurities | Mass transfer model | Adsorption model | Notes |
|---|---|---|---|---|---|---|---|
| Karlsson et al., 2004 | Gradient elution | Ion exchange | IgG and BSA | N/A | General rate model | Langmuir with mobile phase modifiers | Optimisation |
| Jakobsson et al., 2005 | Isocratic elution | Ion exchange | IgG, BSA and myoglobin | - | Equilibrium dispersive | Steric mass action | Robustness |
| Degerman et al., 2006 | Gradient elution | Ion exchange | IgG and BSA | - | General rate model | Langmuir with mobile phase modifiers | Optimisation |
| Mollerup et al., 2007 | isocratic elution | ion exchange | BSA, Beta lactoglobulin A and B, and alpha lactalnumin | N/A | Reactive dispersive | Association model | optimistaion and scale up |
| Degerman et al., 2007 | Isocratic elution | Reversed phase | Insulin | Desamido insulin | Equilibrium dispersive | Kinetic Langmuir | Optimisation |
| Susanto et al., 2008 | Isocratic elution | cation exchnage | lysozyme | N/A | Equilibrium dispersive | Kinetic langmur | optmisation using high throughput screening development methods |
| Chan et al., 2008 | Isocratic elution | N/A | N/A | N/A | kinetic dispersive | linear | Optimisation and understanding of HIC |

Table 8.6. Studies using mechanistic models of chromatography for studies related to the purification of therapeutic proteins (part 6)

| Reference | Mode | Retention mechanism | Molecules of interest | Impurities | Mass transfer model | Adsorption model | Notes |
|---|---|---|---|---|---|---|---|
| Teeters et al., 2009 | Elution | Protein A | Monomer and dimer mAb | N/A | Kinetic dispersice | N/A | optmisation of recovery and clearance during protein A elution |
| Degerman et al., 2009 | Isocratic elution | Ion exchange, hydrophobic interaction and reversed phase | IgG and insulin | BSA, Desamido insulin, myoglobin | Kinetic dispersive and general rate | Langmuir with mobile phase modifiers | Robustness |
| Westerberg et al., 2010 | Isocratic elution | Reversed phase | | human insulin | kinetic dispersive | Langmuir with mobile phase modifiers | design and control |
| Gerontas et al. 2010 | Isocratic elution | Ion exchange | BSA and lactoferrin | - | General rate | Langmuir kinetics with phase modifier | Scale up |
| Nfor et al. 2011 | Isocratic elution | Mixed mode | BSA, ovalbumin, amyloglucosidase | - | Lumped kinetic | Multi-component mixed mode formalisation | Resin selection |
| Ng et al., 2012 | Bind/Elute | Affinity | IgG | BSA | Equilibrium dispersive | Langmuir with mobile phase modifiers | Optimisation |
| Westerberg et al., 2012 | Isocratic elution | Ion exchange | Therapeutic protein | A strong and weak impurity | Equilibrium dispersive | Self-association isotherm | Robustness |

Table 8.7. Studies using mechanistic models of chromatography for studies related to the purification of therapeutic proteins (part 7)

| Reference | Mode | Retention mechanism | Molecules of interest | Impurities | Mass transfer model | Adsorption model | Notes |
|---|---|---|---|---|---|---|---|
| Osberghaus et al., 2012a | Gradient elution | Ion exchange | Lysozyme, ribonuclease A and cytochrome C | - | General rate | Steric mass action | Optimisation and scale up |
| Osberghaus et al., 2012b | Gradient elution | Ion exchange | Lysozyme, ribonuclease A and cytochrome C | - | General rate | Steric mass action | Optimisation and scale up |
| Osberghaus et al., 2012c | Gradient elution | Ion exchange | Lysozyme, ribonuclease A and cytochrome C | - | General rate | Steric mass action | Optimisation and scale up |
| Gétaz et al., 2012 | Isocratic elution | Reversed phase | Peptide | Complex mixture of over 20 impurities simplified by classification into 3 groups | Lumped kinetic | Combined a Langmuir with Moreau type isotherm | Design space determination |
| Gétaz et al., 2013 | Isocratic elution | Reversed phase | Peptide | Complex mixture of over 20 impurities simplified by classification into 3 groups | Lumped kinetic | Combined a Langmuir with Moreau type isotherm | Design space determination |
| Nfor et al., 2013 | Isocratic and gradient elution | Ion exchange, hydrophobic and size exclusion | Monoclonal antibody | Full set of impurities from HCCS cell line | Lumped kinetic | Multi-component mixed mode formalisation | Process synthesis |

# Chapter 9. Appendix B

*The following appendix contains a description of the equations used in the general rate model, and the equilibrium dispersive model.*

# 9.1. Equilibrium dispersive model

The differential mass balance in the bulk mobile phase is:

$$\frac{\partial C_i^m}{\partial t} + \frac{(1-\epsilon_T)}{\epsilon_T} \cdot \frac{\partial C_i^{sp}}{\partial t} + u \cdot \frac{\partial C_i^m}{\partial z} = D_A \cdot \frac{\partial^2 C_i^m}{\partial z^2}$$
$$\forall \quad i = 1, 2, \dots, N_C \qquad z \in (0, L) \qquad [9.1]$$

where $C_i^m$ is the concentration of component $i$ in the mobile phase, $t$ is the time, $\epsilon_T$ is the total column porosity, $C_i^{sp}$ is the concentration of component $i$ in the stationary phase, $u$ is the interstitial velocity, $z$ is the axial coordinate, $D_A$ is the apparent axial dispersion coefficient, $N_C$ is the number of components in the system, and $L$ is the column length. $\partial C_i^m/\partial t$ is the rate per unit volume of accumulation of component $i$ in the mobile phase $((1-\epsilon_T)/\epsilon_T) \cdot \left(\partial C_i^{sp}/\partial t\right)$ is the rate per unit volume of accumulation of component $i$ in the stationary phase, $u \cdot (\partial C_i^m/\partial z)$ is the rate per unit volume of mass transfer by convection down the column, and $D_A \cdot (\partial^2 C_i^m/\partial z^2)$ is the rate per unit volume of mass transfer by dispersion and particle mass transfer kinetics lumped into one term. The total column porosity, $\epsilon_T$, is defined as the ratio between the void volume, $V_0$, and the column volume, $V_C$:

$$\epsilon_T = \frac{V_0}{V_C} \qquad [9.2]$$

The boundary conditions for Equation [9.10] are the following (Guiochon, 1994):
At the inlet of the column, i.e. at z = 0, the mobile phase concentration, $C_i^m$, depends on convection and dispersion:

$$\left[uC_i^m - D_A \frac{\partial C_i^m}{\partial z}\right]|_{z=0} = uC_{i,0}^m \qquad \forall \quad i = 1, 2, \dots, N_C \qquad [9.3]$$

where $C_{i,0}^m$ is the inlet concentration.
At the outlet of the column, only convective transport is considered:

$$\frac{\partial C_i^m}{\partial z}|_{z=L} = 0 \qquad \forall i = 1, 2, \dots, N_C \qquad [9.4]$$

An initial condition is also required to solve Equation [9.1] which states that the rate per unit volume of accumulation in the mobile phase of component $i$ at $t = 0$ is zero at all points interior to the column:

$$\frac{\partial C_i^m}{\partial t} = 0 \quad 0 < z < L \ \forall i = 1, 2, \dots, N_C \qquad [9.14]$$

Boundary Condition at $Z = 0$

$$\left[uC_i^m - D_{A,i}\frac{\partial C_i^m}{\partial z}\right]|_{z=0} = uC_{i,0}^m \quad \forall i = 1, 2, \ldots, \mathrm{N_C}$$

Boundary Condition at $Z = L$

$$\frac{\partial C_i^m}{\partial z}|_{z=L} = 0$$

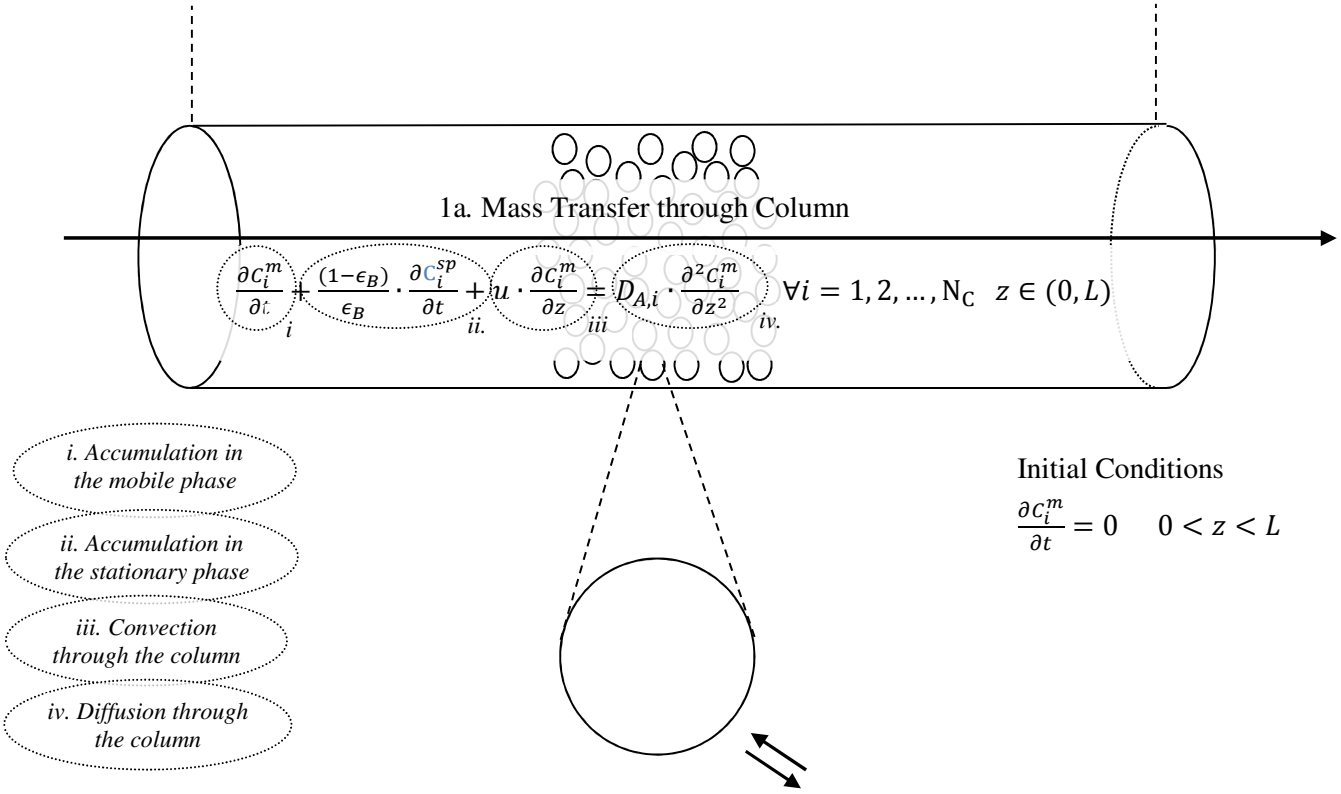


*i. Accumulation in the mobile phase*

*ii. Accumulation in the stationary phase*

*iii. Convection through the column*

*iv. Diffusion through the column*

Initial Conditions

$$\frac{\partial C_i^m}{\partial t} = 0 \quad 0 < z < L$$

Adsorption

$$C_i^{sp} = \frac{a_i \cdot C_i^m}{1 + \sum_{j=1}^{n} b_j C_j^m} \quad \forall i = 1, 2, \ldots, \mathrm{N_C} \quad z \in (0, L)$$

Illustrating the equilibrium dispersive model

## 9.2. General rate model

In the general rate model, a differential mass balance over the packed bed of particles in the column describes convection through the column, axial dispersion and transport through the external film at the particle surface:

$$\frac{\partial C_i^m}{\partial t} + \frac{3k_i(1-\epsilon_B)}{\epsilon_B} \cdot \left(C_i^m - C_i^p|_{r=R_p}\right) + u \cdot \frac{\partial C_i^m}{\partial z} = D_{ax} \cdot \frac{\partial^2 C_i^m}{\partial z^2}$$
$$\forall \quad i = 1, 2, \dots, N_C \quad and \quad z \in (0, L) \qquad [9.6]$$

where $C_i^m$ is the concentration of component $i$ in the extra particular mobile phase, $t$ is the time, $\epsilon_B$ is the bed porosity, $k_i$ is the film mass transfer coefficient of component $i$, $C_i^p$ is the concentration of component $i$ in the intra particular mobile phase, $r$ is the coordinate of the radial dimension through resin particles, $R_p$ is the particle radius, $u$ is the interstitial velocity, $z$ is the coordinate of the axial dimension along the length of the column, $D_{ax}$ is the axial dispersion coefficient, $N_C$ is the number of components in the system, $L$ is the column length. $\partial C_i^m/\partial t$ is the rate per unit volume of accumulation of component $i$ in the extra particular mobile phase, $\frac{3k_i(1-\epsilon_B)}{\epsilon_B} \cdot \left(C_i^m - C_i^p|_{r=R_p}\right)$ is the rate per unit volume of component $i$ transferred from the extra particular mobile phase, through the external film, to the intra particular mobile phase at the surface of the particle, $u \cdot (\partial C_i^m/\partial z)$ is the rate per unit volume of mass transfer by convection down the column, and $D_{ax} \cdot (\partial^2 C_i^m/\partial z^2)$ is the rate per unit volume of mass transfer by dispersion. The bed porosity, $\epsilon_B$, is defined as the ratio between the void volume between resin particles, $V_B$, and the column volume, $V_C$:

$$\epsilon_B = \frac{V_B}{V_C} \qquad [9.7]$$

The boundary conditions for Equation [9.1] are the following (Guiochon, 1994):

At the inlet of the column, i.e. at z = 0, the mobile phase concentration, $C_i^m$, depends on convection and dispersion:

$$\left[uC_i^m - D_A \frac{\partial C_i^m}{\partial z}\right]|_{z=0} = uC_{i,0}^m \qquad \forall \quad i = 1, 2, \dots, N_C \qquad [9.8]$$

where $C_{i,0}^m$ is the inlet concentration.

At the outlet of the column, i.e. at z = column length, only convective transport is considered:

$$\frac{\partial C_i^m}{\partial z}|_{z=L} = 0 \qquad \forall i = 1, 2, \ldots, N_C \qquad [9.4]$$

An initial condition is also required to solve Equation 9.6 which states that the rate per unit volume of accumulation in the extraparticular mobile phase of component $i$ at $t = 0$ is zero at all points interior to the column:

$$\frac{\partial C_i^m}{\partial t} = 0 \quad 0 < z < L \;\; \forall i = 1, 2, \ldots, N_C \qquad [9.10]$$

The differential mass balance over the resin particle pores in the radial dimension describes diffusion of components through the stagnant mobile phase within the resin pores:

$$\epsilon_p \frac{\partial C_i^p}{\partial t} + (1 - \epsilon_p)\frac{\partial q_i}{\partial t} - \epsilon_p D_{m,i}\left[\frac{1}{r^2}\frac{\partial}{\partial r}\left(r^2 \frac{\partial C_i^p}{\partial r}\right)\right] = 0$$
$$\forall i = 1, 2, \ldots, N \quad z \in (0, L) \quad r \in (0, R) \qquad [9.11]$$

where $\epsilon_p$ is the particle porosity, $q_i$ is the concentration of component $i$ per unit volume of the solid adsorbent phase, and $D_{m,i}$ is the molecular diffusivity of component $i$ in the intraparticular mobile phase. The boundary conditions for Equation [9.6] are the following:

At the surface of the particle the mass transport is controlled by film mass transfer:

$$\frac{\partial C_i^p}{\partial r} = \frac{k_i}{\epsilon_P D_{m,i}} \cdot \left(C_i^m - C_i^p|_{r=R_p}\right) \qquad \forall i = 1, 2, \ldots, N_C \qquad r = R_P \qquad [9.12]$$

At the centre of the particle there is no mass transfer due to the symmetrical geometry of the particle:

$$\frac{\partial C_i^p}{\partial r} = 0 \quad \forall i = 1, 2, \ldots, N_C \qquad r = 0 \qquad [9.13]$$

The initial condition required to solve Equation [9.6] states that the rate per unit volume of accumulation in the intraparticular mobile phase of component $i$ at $t = 0$ is zero at all points interior to the column:

$$\frac{\partial C_i^p}{\partial t} = 0 \qquad \forall i = 1, 2, \ldots, N_C \qquad 0 < r < R_p \qquad [9.14]$$

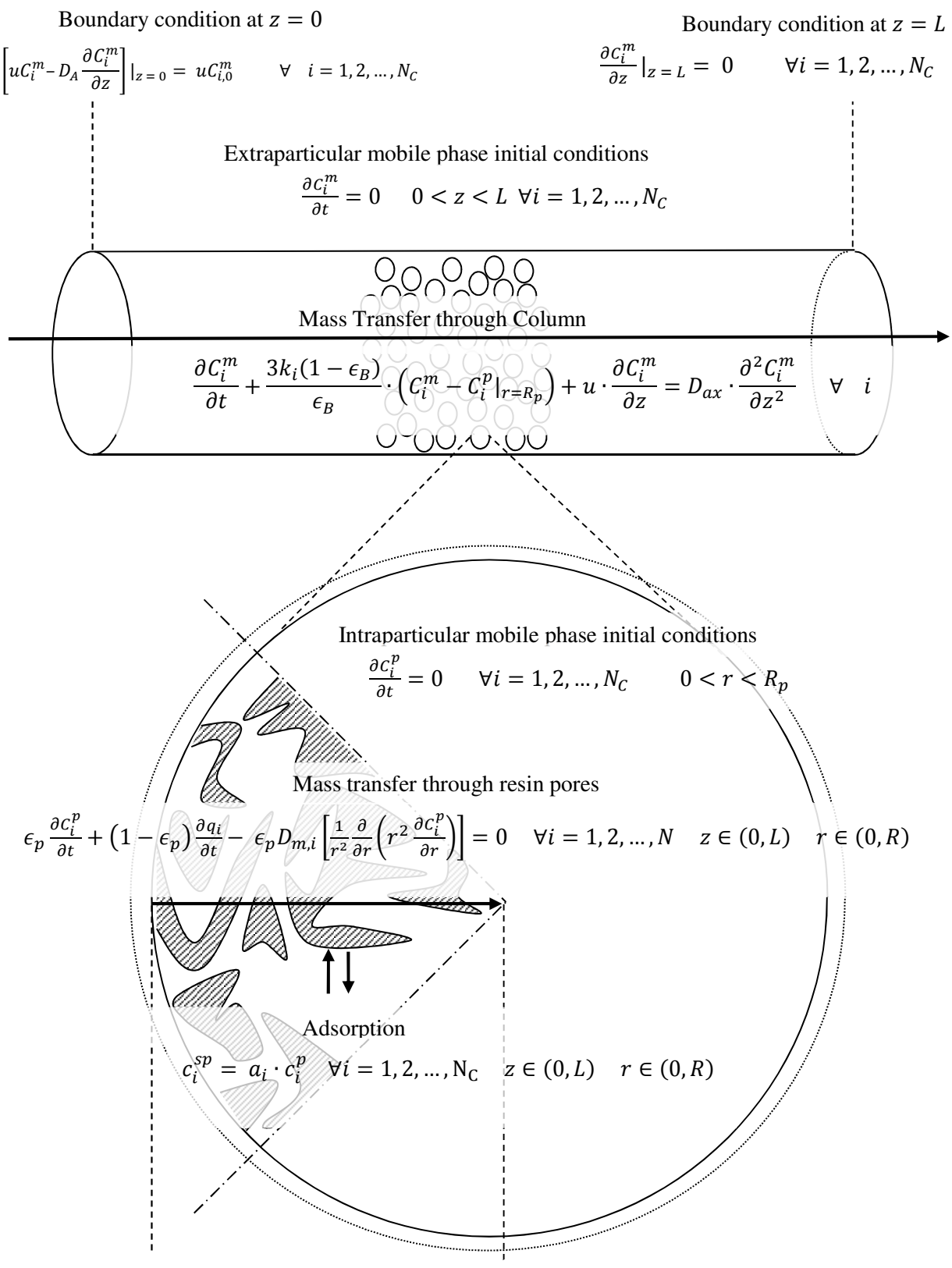


Illustrating the general rate model